

GEOCHEMISTRY AND MINERALIZATION OF BURU  
AND KUGE VOLCANIC CARBONATITE CENTRES,  
WESTERN KENYA

Isaac Oriechi Onuonga

A Thesis Submitted for the Degree of PhD  
at the  
University of St Andrews



1997

Full metadata for this item is available in  
St Andrews Research Repository  
at:

<http://research-repository.st-andrews.ac.uk/>

Please use this identifier to cite or link to this item:

<http://hdl.handle.net/10023/15470>

This item is protected by original copyright

**GEOCHEMISTRY AND MINERALIZATION OF BURU AND KUGE  
VOLCANIC CARBONATITE CENTRES, WESTERN KENYA**

**BY**

**ISAAC ORIECHI ONUONGA**

A thesis submitted for the degree of Doctor of Philosophy in the Faculty of  
Science of the University of St Andrews.



**JULY 1996**

ProQuest Number: 10170807

All rights reserved

INFORMATION TO ALL USERS

The quality of this reproduction is dependent upon the quality of the copy submitted.

In the unlikely event that the author did not send a complete manuscript and there are missing pages, these will be noted. Also, if material had to be removed, a note will indicate the deletion.



ProQuest 10170807

Published by ProQuest LLC (2017). Copyright of the Dissertation is held by the Author.

All rights reserved.

This work is protected against unauthorized copying under Title 17, United States Code  
Microform Edition © ProQuest LLC.

ProQuest LLC.  
789 East Eisenhower Parkway  
P.O. Box 1346  
Ann Arbor, MI 48106 – 1346

TL  
C108

## DECLARATION.

I, Isaac Oriechi Onuong'a, hereby certify that this thesis has been written by myself, that it is a record of my work, and that it has not been accepted in partial or complete fulfilment of any other degree of professional qualification.

Date 16<sup>th</sup> July 1996 Signature of candidate

I was admitted as a research student in November 1992 and as a candidate for the degree of PhD in 1993, the higher study for which this is a record of the work carried out in the University of St Andrews between November 1992 and June 1996.

Date 16<sup>th</sup> July 1996 Signature of candidate

I hereby certify that the candidate has fulfilled the conditions of the Resolution and Regulations appropriate for the degree of PhD in the University of St Andrews and that the candidate is qualified to submit this thesis in application for that degree.

Date 16<sup>th</sup> July 1996 Signature of Supervisor ...

In submitting this thesis to the University of St Andrews I understand that I am giving permission for it to be made available for use in accordance with the regulations of the University Library for the time being in force, subject to any copyright vested in the work not being affected thereby. I also understand that the title and the abstract will be published to any *bona fide* library or research worker.

Date 16<sup>th</sup> July 1996 Signature of candidate

## ABSTRACT

Western Kenya hosts a number of Tertiary and Quaternary alkaline volcanic carbonatite centres, such as Rangwa, the North and South Ruri centres, Kuge, Homa mountain and Legetet which are located along an old Precambrian major shear zone lying within the Nyanza rift, off the main Kenyan (Gregory) rift. The centres consist of agglomerates and breccias with mixed clasts of silicate rocks and carbonatites, interbedded with carbonatitic and nephelinitic tuffs. The volcanic assemblage is transected by high level sheets and dykes of calcite carbonatite and ferrocarnatite which were probably later feeders for the volcanic eruptions.

Carbon, oxygen, and sulphur isotopic compositions were determined for calcite, siderite and barite from the Buru and Kuge carbonatite centres. Wide ranges in the isotopic compositions of the minerals were observed with values for  $\delta^{13}\text{C}$  and  $\delta^{18}\text{O}$  for the Buru calcites ranging from +1.27 to -3.23‰ (PDB) and +11.25 to +26.21‰ (SMOW). The  $\delta^{13}\text{C}$  and  $\delta^{18}\text{O}$  for the Kuge calcites are -3.11 to -8.44‰ (PDB) and +18.09 to +25.73‰ (SMOW). The Buru siderites plot in a narrow and restricted range at -3.07 to -4.39‰ (PDB) and +12.61 to +16.10‰ (SMOW). Data on the sulphur isotopic composition from the Buru hill carbonatite show a fairly widespread variation in  $\delta^{34}\text{S}$  ranging from +4.50 to +12.40‰ (CDT), whereas Kuge hill displays a slightly more homogenous isotopic composition with values ranging from +1.10 to +5.10‰ (CDT).

The carbon and oxygen isotopic compositions from the Buru and Kuge carbonatite centres do not retain the primary isotopic signatures expected for magmatic primary carbonatites. Most of the variations in isotopic composition have been attributed to secondary processes involving low temperature (60° to 144°C) hydrothermal alteration and isotopic exchange between the carbonatites and fluids (meteoric water). Higher  $\delta^{18}\text{O}$  values (+21.91 to +26.21‰) with a significant increase in  $\delta^{13}\text{C}$  values (-1.48 to +1.27‰) shown by the most oxidized samples from the Buru carbonatite may indicate the involvement of supergene exchange with atmospheric  $\text{CO}_2$  at relatively lower temperatures (<50°C). The variations in  $\delta^{34}\text{S}$  shown by the two centres compared to mantle sulphur could be due to either redox processes and/or isotopic fractionations due to loss of volatiles.

The Buru and Kuge carbonatite centres are characterized by enriched rare earth element (REE) values dominated by higher abundances of LREEs with steep chondrite-normalized distribution patterns. The lateritic zone at Buru hill, however, contains the greatest concentrations of REEs, barium, iron and manganese compared to the fresh carbonatite in which calcite and particularly siderite increase in abundance as the influence of supergene processes decrease with depth.

The most common rare earth minerals encountered in the Buru and Kuge carbonatite centres are the fluorocarbonates (bastnäesite, synchysite and parisite), and monazite. The lanthanide fluorocarbonate and monazite control the concentration and bulk distribution of the REEs. The replacement textures of the lanthanide fluorocarbonates and monazite indicate that they are secondary in origin and appear to have been introduced by late stage, low temperature hydrothermal processes. The rare earth minerals are commonly accompanied by fluorite, and barite.

Stable isotope studies suggest that the low temperature mineralogical changes and REE mineralization observed in western Kenyan carbonatites were controlled initially by hydrothermal activity and later by supergene processes. Higher  $\delta^{18}\text{O}$  and  $\delta^{13}\text{C}$  values, especially in the oxidized zones, correspond to higher REE abundances.

## ACKNOWLEDGEMENTS

It was Dr P. Bowden who initiated the idea of carrying my research study at the University of St Andrews to which I am grateful. The writer is indebted to Dr. P. Bowden for his guidance, constant encouragement and critically reviewing early manuscripts and suggesting further improvement. Dr Bowden visited the field area and gave constructive field observations which helped me greatly. Besides this academic nourishment, he has been a source of comfort to myself and my family to which I am grateful.

The scholarship to take up my research work at St Andrews University was awarded by the Overseas Development Administration (ODA), which I gratefully acknowledge. I thank the British Council for the administration of the scholarship. I am grateful to P. Moseley who tirelessly collaborated with the Overseas Development Administration.

The Mines and Geological Department through the Ministry of Environment and Natural Resources granted me permission to carry my research work at St Andrews. The support and assistance accorded to me throughout my research period, particularly during my fieldwork, is appreciated.

The writer is indebted to Dr A. E. Fallick who generously allowed the use of the laboratory facilities at the Scottish Universities Research and Reactor Centre (SURRC). The discussion of the stable isotope results and reviewing of early manuscripts by Dr Fallick is appreciated. I extend my gratitude to Professor J. Gittins, Dr R.E. Harmer and L. Schurmann for their contribution and discussion on various aspects of carbonatite geology during the field trip to western Kenya carbonatites. Appreciation is also extended to Dr. Harmer for reviewing the preliminary manuscript on isotope geochemistry. Constructive discussion of some ideas regarding this thesis by Dr C. Donaldson and Dr. D. Richens is gratefully acknowledged.

I gratefully acknowledge the technical staff for the invaluable expertise. I would like to express my sincere thanks to Lorna Stewart for her help in computing procedures.

Finally, I would like to convey my thanks to my wife Kwamboka and my children Onyangi, Kemunto and Obiti for their love and care. I am indebted to my wife for working devotedly to support the family in the most difficult circumstances.

I dedicate this thesis to my wife Kwamboka and my children, Onyangi, Kemunto and Obiti.

## CONTENTS

Chapter 1. INTRODUCTION TO THE INVESTIGATION OF SECONDARY PROCESSES IN VOLCANIC CARBONATITES	1
1.1 Kenya-Japanese geological cooperation	1
1.2 Aims of the JICA-MMAJ Homa Bay exploration project	1
1.3 Objectives of the present investigation	4
1.4 Carbonatites: Definition and classification	6
1.5 Historical studies of carbonatites	6
1.6 Sedimentary limestone vs Magmatic carbonatite	8
1.7 Nomenclature	9
1.8 Petrogenetic concepts	14
1.9 Conclusion	19
Chapter 2. WESTERN KENYA VOLCANIC CARBONATITES	20
2.1 Introduction	20
2.2 Carbonatite-nephelinite association	22
2.3 Geological evolution of the western Kenya carbonatites	23
2.4 Evolution and geological setting of Kisingiri volcano	25
2.5 The Rangwa carbonatite centre	27
2.6 The Ruri carbonatite centres	31
2.7 The Homa mountain carbonatite centre	39
2.8 Tinderet volcano	41
2.9 Discussion	46
2.10 Conclusion	47
Chapter 3. GEOLOGY OF THE KUGE CARBONATITE COMPLEX	52
3.1 Introduction	52
3.2 Geological setting of the Kuge hill carbonatite	52
3.3 Calcite carbonatite	55
3.4 The ferrocarbonatite breccia	58

3.5 Other rock units in Kuge	62
3.6 Summary	65
Chapter 4. GEOLOGY OF THE BURU HILL CARBONATITE	66
4.1 introduction	66
4.2 Structural setting and basement geology	67
4.3 Geology of the Buru carbonatite	69
4.3.1 Field observations	69
4.3.2 Drill core observations	72
4.3.3 Thin-section studies	81
4.4 Fentization at Buru hill	83
4.4.1 Introduction	83
4.4.2 Fentization at the Buru carbonatite centre	84
4.4.3 Na:K ratios	89
4.5 Conclusion	91
Chapter 5. GENERAL MINERALOGY OF THE BURU AND KUGE CARBONATITE CENTRES	94
5.1 Introduction	94
5.2 Methods of analysis	94
5.3 Selected X-ray diffractometer results	95
5.3.1 The Buru centre - BRL-1	95
5.3.2 The Buru centre - BRL-2	95
5.3.3 The Kuge centre - KG-2	97
5.3.4 Summary of XRD results	97
5.4 Discussion of the mineralogy of the Buru and Kuge carbonatites	99
5.4.1 Introduction	99
5.4.2 Carbonates	101
5.4.3 Barite and fluorite	108

5.4.4 Oxides (magnetite and goethite)	111
5.5.5 Micas (biotite and phlogopite)	112
5.5 Weathering vs hydrothermal processes (mineralogical products)	114
Chapter 6. GENERAL GEOCHEMISTRY OF THE BURU AND KUGE VOLCANIC CARBONATITES	117
6.1 Introduction	117
6.2 Major element geochemistry	118
6.2.1 Buru	118
6.2.2 Kuge	121
6.2.3 Iron and manganese concentrations in Buru and Kuge	121
6.2.4 CaO and P <sub>2</sub> O <sub>5</sub>	125
6.2.5 TiO <sub>2</sub> and total alkalis	125
6.3 Trace elements	127
6.4 Chemical compositions of the Buru and Kuge centres	128
6.4.1 Wolley (1982) and Woolley and Kempe (1989) classification	128
6.4.2 Multi-element variation diagrams	130
6.5 Summary	133
Chapter 7. STABLE ISOTOPE GEOCHEMISTRY	134
7.1 Terminology and standards in use in stable isotope geochemistry	134
7.2 Introduction to the study of carbon and oxygen stable isotopes in carbonatites	136
7.3 Carbon and oxygen isotopic composition from Buru	140
7.3.1 Introduction	140
7.3.2 Results	141
7.4 Variation of $\delta^{13}\text{C}$ and $\delta^{18}\text{O}$ from the Buru carbonatite centre	145
7.4.1 Primary factors	145
7.4.2 Secondary factors	149

7.5 Hydrothermal alteration and isotope exchange	152
7.6 Estimating the equilibration temperature involving carbonatite carbonates and fluids	154
7.7 Weathering and isotopic composition of carbonatites	155
7.8 Carbon and oxygen isotopic composition of siderite from Buru	158
7.9 Carbon and oxygen isotopic composition from the Kuge carbonatite	165
7.10 Variation in $\delta^{13}\text{C}$ and $\delta^{18}\text{O}$ of the Kuge carbonatite - Discussion	167
7.11 Sulphur isotopic composition in carbonatites	169
7.11.1 Introduction	169
7.11.2 Summary of sulphur isotope determinations in carbonatites	171
7.12 Sulphur isotopic composition from the Buru and Kuge centres	172
7.13 Variation of sulphur isotopic data from the Buru and Kuge carbonatite centres	175
7.14 Conclusion	178
<b>Chapter 8. APPLIED MINERALOGY AND GEOCHEMISTRY OF RARE EARTH MINERALS</b>	<b>180</b>
8.1 Classification of rare earth elements (REEs)	180
8.2 Distribution of rare earth elements	183
8.3 Rare earth elements in carbonatites	184
8.4 Rare earth elements from the Buru and Kuge carbonatite centres	185
8.4.1 Introduction	185
8.4.2 Methods of study	185
8.5 Rare earth elements at Buru carbonatite hill carbonatite	186
8.5.1 Introduction	186
8.5.2 Distribution of REEs in the Buru carbonatite	188
8.5.3 REE normalized patterns - the Buru carbonatite	191
8.6 Rare earth elements at the Kuge carbonatite	193
8.6.1 introduction	193

8.6.2 Distribution of REEs in the Kuge carbonatite	195
8.6.3 Normalized REE distribution patterns - the Kuge carbonatite	197
8.7 Discussion of rare earth element abundances and distribution patterns at the Buru and Kuge centres	199
8.7.1 Introduction	199
8.7.2 Factors governing the behaviour and distribution of REEs	200
8.7.3 Transport of REEs	201
8.8 Factors governing the behaviour of rare earth elements during weathering	203
8.9 Rare earth minerals in Buru carbonatite centre	206
8.9.1 Introduction	206
8.9.2 Rare earth bearing minerals in the Buru carbonatite	206
8.9.3 Rare earth bearing minerals from the Buru carbonatite	210
8.9.4 Apatite	214
8.10 The occurrence of rare earth minerals in the Buru and Kuge centres	218
8.10.1 Introduction	218
8.11 Discussion	220
8.12 Rare earth elements in laterites overlying carbonatite complexes	229
8.13 Summary	239
8.14 Conclusion	240
 Chapter 9. CONCLUSION	 243
 Chapter 10 SUGGESTIONS FOR FURTHER WORK	 247
10.1 Isotope studies	247
10.2 Lanthanide mineralization	247
10.3 Industrial applications	248

REFERENCES	249
APPENDICES	266
Appendix 5-1 X-ray diffraction analysis (XRD)	267
Appendix 5-2 Selected diffractograms	268
Appendix 6-1 X-ray fluorescence (XRF)	275
Appendix 6-2 (1-4) Major element and trace element analysis	277
Appendix 7-1 Sample preparation and stable isotope experimental procedures	282
Appendix 8 List of specimens	284

LIST OF FIGURES.	PAGE
Figure 1-1 Location map of homa Bay minreral exploration project	2
Figure 1-2 Carbonatite classification diagram (after Woolley, 1982).	13
Figure 2-1 Location map of wesern Kenya carbonatites in relation to the Nyanza and Kenya rifts.	21
Figure 2-2 General geology of the Rangwa carbonatite including a generalised section of the Kisingiri volcano (after Le Bas, 1977 and King et al., 1972).	28
Figure 2-3 General geological map of the Ruri carbonatite centres (simplified after Le Bas, 1977).	32
Figure 2-4 General geological map of the Homa mountain carbonatite (simplified after Le Bas, 1977).	40
Figure 2-5 General geology of the Legetet carbonatite centre (simplified after Binge, 1962).	42
Figure 2-6 Schematic cross-section of an idealized carbonatite-ijolite-nephelinite volcanic complex and the relative emplacement levels of the Ruri, Homa, Rangwa and Kisingiri lavas.	50
Figure 3-1 The Kuge hill carbonatite centre, viewed northwards from North Ruri. Clear central areas of the hill are composed of Nyanzian metabasalts.	53
Figure 3-2 (a) Geological map of Kuge carbonatite. (b) A cross-section along A - B.	54
Figure 4-1 Geological map of the Buru hill carbonatite centre.	68
Figure 4-2 The Buru hill carbonatite viewed westwards from Muhoroni town.	71
Figure 4-3 Fenite classification on the basis of Na <sub>2</sub> O/ K <sub>2</sub> O variations.	90
Figure 4-4 Schematic cross-section of an idealized carbonatite nephelinite volcanic complex and the relative emplacement levels of Kuge, Buru, Legetet and Tinderet.	92

- Figure 5-1 Plots of carbonate compositions (molecular proportions) from Buru and Kuge centres in the system  $\text{CaCO}_3\text{-MgCO}_3\text{-FeCO}_3$ . The field boundaries are for the sub-solidus system at  $450^\circ\text{C}$  (After Rosenberg, 1967). 107
- Figure 6-1  $\text{SiO}_2\text{-Al}_2\text{O}_3\text{-Fe}_2\text{O}_3$  diagram showing the fields for the laterite and the Buru and Kuge carbonatites (XRF analyses). 120
- Figure 6-2 CaO versus  $\text{P}_2\text{O}_5$  for the laterite, and the Buru and Kuge carbonatites. 126
- Figure 6-3 Carbonatite classification diagram (after Woolley, 1982 and Woolley and Kempe, 1989). (XRF analyses). 129
- Figure 6-4 Carbonatite classification diagram of Buru siderite dyke and ferrocarnatite breccia from Kuge (after Woolley, 1982 and Woolley and Kempe, 1989). Analyses by ICP. 131
- Figure 6-5 Condensed mantle-normalized spider diagram for Buru and Kuge carbonatite centres. Mantle values from Wood et al. (1979). 132
- Figure 7-1 The  $\delta^{13}\text{C}(\text{PDB})$  vs.  $\delta^{18}\text{O}(\text{SMOW})$  from the Buru carbonatite centre. The dashed line is a Rayleigh fractionation line from Pineau et al. (1973) superimposed on the Buru data. 144
- Figure 7-2 Histogram plot of  $\delta^{13}\text{C}$  for calcite and siderite from the Buru carbonatite. 146
- Figure 7-3 Histogram plot of  $\delta^{18}\text{O}$  for calcite and siderite from the Buru carbonatite. 146
- Figure 7-4 Plot of (a)  $\delta^{13}\text{C}$  and (b)  $\delta^{18}\text{O}$  vs. Depth for Buru siderite. Plot of (c)  $\delta^{13}\text{C}$  and (d)  $\delta^{18}\text{O}$  vs depth for Buru calcite. Samples are taken from carbonatite drill hole BRL-1. 159
- Figure 7-5 Plot of  $\delta^{13}\text{C}(\text{PDB})$  vs  $\delta^{18}\text{O}(\text{SMOW})$  for the Buru carbonatite. Tie lines connect calcite-siderite pairs from the same sample. 164
- Figure 7-6 Plot of  $\delta^{13}\text{C}(\text{PDB})$  vs  $\delta^{18}\text{O}(\text{SMOW})$  from the Kuge carbonatite hill carbonatite. 166
- Figure 7-7 Combined plot of  $\delta^{13}\text{C}(\text{PDB})$  vs  $\delta^{18}\text{O}(\text{SMOW})$  showing the two alteration trends (1 and 2) in the Buru and Kuge centres. 170

Figure 7-8 Sulphur isotopic composition of sulphur in barites from the Buru and Kuge carbonatite centres.	174
Figure 7-9 Plot of $\delta^{34}\text{S}(\text{CDT})$ vs $\delta^{13}\text{C}(\text{PDB})$ for Buru and Kuge centres and other carbonatite complexes.	177
Figure 8-1 Chondrite-normalized REE distribution patterns for the Buru carbonatite.	192
Figure 8-2 Chondrite-normalized REE distribution patterns for the Buru carbonatite. Data from unpublished JICA reports, 1988-1990	194
Figure 8-3 Chondrite-normalized REE distribution patterns for the Kuge carbonatite.	198
Figure 8-4 Chondrite-normalized plot of rare earth (RE) minerals from Buru.	211
Figure 8-5 Chondrite-normalized plot of rare earth (RE) minerals from Kuge.	215
Figure 8-6 Energy-dispersive X-ray (EDX) on a coated sample, from the lateritic zone at Buru carbonatite showing rare earth elements	234
Figure 8-7 Energy-dispersive X-ray (EDX) on a coated sample corresponding to Plate 8-10. The spectrum reveals that calcite does contain rare earth elements	235
Figure 8-8 Energy-dispersive X-ray (EDX) of Monazite from Kuge carbonatite centre. The spectrum shows monazite to be cerium selective.	236

LIST OF PLATES.	PAGE
Plate 2-1 Carbonatite pyroclastics (tuffs and agglomerates) cut by high level fine to medium-grained carbonatite dykes in the Rangwa carbonatite complex.	30
Plate 2-2 North Ruri carbonatite centre, viewed southwards from the top of the Kuge hill carbonatite. The photograph shows the prominent inward dipping cone-sheets and dykes of carbonatite.	33
Plate 2-3 South Ruri carbonatite. The lower slopes of the caldera is largely occupied by tuffs and agglomerates. To the north, a ferrocarnatite dyke cuts the pyroclastic deposits. The clear plug to the far north is a phonolitic plug.	33
Plate 2-4 Bedded tuffs and agglomerates within the western side of the South Ruri caldera.	35
Plate 2-5 A fenitized fragment of phonolite within the medium and coarse-grained calcite carbonatite at the South Ruri carbonatite centre.	35
Plate 2-6 Large twinned rhombs of calcite carbonatite from North Ruri with disseminated magnetite. Note also the large euhedral crystal of biotite. Magnification x 20.	36
Plate 2-7 Euhedral crystal of hexagonal apatite and rhombohedral calcite in calcite carbonatite from North Ruri (NR-271) Magnification x 20.	36
Plate 2-8 Plugs of phonolite around the Ruri hills centre. Note the flourishing farming activities which utilize the rich phosphate soils derived from the weathering of carbonatite.	37
Plate 2-9 Phonolitic plug at South Ruri carbonatite. Nepheline (NE), aegirine-augite (AEG) and zoned sphene (SP) occur as phenocryst phases. Groundmass comprises of mainly nepheline and K-feldspar. Magnification x 10.	38
Plate 2-10 Carbonatite tuffs and agglomerates with white rounded and kaolinized basement enclaves.	45
Plate 3-1 Flow-folded calcite carbonatite at the Kuge carbonatite centre.	56

- Plate 3-2 Phlogopite flakes (small reflective mineral) in calcite carbonatite. Note the pitted and grooved texture of carbonatite due to weathering. 56
- Plate 3-3 Magnetite octahedra trails in calcite-carbonatite, Kuge hill. 57
- Plate 3-4 Magnetite aggregates in calcite carbonatite, Kuge hill. 57
- Plate 3-5 Calcite carbonatite (Kuge hill). Note large rhombs of calcite with magnetite and a few flakes of phlogopite. 59
- Plate 3-6 Trails of hematite veins traversing a ferrocarnatite breccia. 59
- Plate 3-7 Recrystallized ferrocarnatite breccia (Kuge hill). Euhedral calcite with magnetite concentrating at the edges of calcite. Flakes of phlogopite are also common. 63
- Plate 3-8 Fenitized Archean (Nyanzian) metabasalt. The section is composed of clinopyroxenes (aegirine) and laths of plagioclase feldspar with minor iron-oxides. Note the prominent cross-cutting dykes of carbonatite. Magnification x 10. 64
- Plate 3-9 Porphyritic phonolite showing phenocrysts of a K-feldspar (Kf) with Carlsbad twinning, nepheline (NE), aegirine augite (AEG) and sphene (SP) in matrix composed of same minerals. Magnification x 10. 64
- Plate 4-1 The Buru basement mylonite shear zone with quartz porphyroclasts in a matrix composed of quartz, feldspar and mica. Magnification x10. 70
- Plate 4-2 Summary (pictorial) of the different lithological units encountered in drill-core BRL-1, Buru carbonatite. 75
- Plate 4-3 Laterite zone in the Buru carbonatite. Goethite (GOE) and barite (BA) are characteristic. Magnification x 20 80
- Plate 4-4 Drill core sample showing a brown and fine-grained siderite carbonatite dyke. Note the dominance of fluorite observed replacing calcite in the Buru cores. The dark vein to the left corner is aegirine (AEG). 80

- Plate 4-5 The Buru carbonatite. Pseudomorphs after calcite (CA) are recognized. Fluorite (F, dark rounded spheres) and barite (BA) are abundant within the section. Magnification x 10. 82
- Plate 4-6 Siderite carbonatite (SID) dyke showing sharp contacts with the Buru carbonatite. The sharp contacts confirms its intrusive nature. Magnification x 10. 82
- Plate 4-7 Fenite from the Buru carbonatite centre. Note the occurrence of thin blue veins of alkali amphibole. 85
- Plate 4-8 Fenitized granitic gneisses, Buru hill. Note the network of granulation channels, now filled by acicular aegirine (AEG). Carbonate (CAB) is also utilizing the existing channels within the feldspar. Magnification x 15. 85
- Plate 4-9 Fine-grained ijolite dyke cross-cutting BRL-1, Buru. The section shown contains tabular and zoned aegirine-augite, carbonate sphene and apatite. Nepheline (NE) appears cloudy and highly altered. Magnification x 20. 87
- Plate 4-10 Fenitized ijolite dyke cross-cutting BRL-2, Buru. Nepheline is extensively altered with aegirine (AEG) veinlets and carbonate (CA) along the fractures. Magnification x 10. 87
- Plate 4-11 Less deformed granitic gneiss from Buru hill. The feldspars and biotite (BT) show sharp contacts. The feldspars show sericite alteration and the quartz appears slightly strained. Magnification x 10. 88
- Plate 7-1 Backscattered electron image showing coexisting calcite(dark grey) and siderite (light grey) carbonate phases and barite (BA) from same sample - Buru carbonatite. Scale bar = 1000  $\mu\text{m}$ . 163
- Plate 8-1 Backscattered electron (BSE) image showing rare earth containing apatite crystals from the North Ruri carbonatite centre. Scale bar = 10  $\mu\text{m}$ . 221
- Plate 8-2 Backscattered electron image of calcite-carbonatite from the North Ruri carbonatite centre with apatite and RE-fluorocarbonates. Scale bar = 10  $\mu\text{m}$ . 222
- Plate 8-3 Backscattered electron image of acicular fluorocarbonates in lateritic zone-Buru carbonatite centre. Scale bar = 10  $\mu\text{m}$ . 224

- Plate 8-4 Backscattered electron image showing fibrous texture, the most common texture encountered in the fluorocarbonates. Scale bar = 10  $\mu\text{m}$ . 225
- Plate 8-5 Backscattered electron image showing fibrous fluorocarbonates. The RE fluorocarbonates are seen exploiting earlier existing cavities within the carbonate phases. Scale bar = 10  $\mu\text{m}$ . 226
- Plate 8-6 Backscattered electron image showing disseminated RE fluorocarbonates in calcite and siderite phases and minor magnetite and barite phases. Scale bar = 1000  $\mu\text{m}$ . 227
- Plate 8-7 Backscattered electron image revealing the cross-cutting relationship of secondary fluorocarbonates at Buru carbonatite. Scale bar = 100  $\mu\text{m}$ . 228
- Plate 8-8 Backscattered electron image of euhedral monazite in calcite from Kuge hill. Scale bar = 10  $\mu\text{m}$ . 230
- Plate 8-9 Scanning electron micrograph (SEM) of RE fluorocarbonates from the laterite zone at Buru hill. Scale bar = 10  $\mu\text{m}$ . 231
- Plate 8-10 Scanning electron micrograph (SEM) of rhombohedral calcite crystals from Buru hill. Scale bar = 10  $\mu\text{m}$ . 232
- Plate 8-11 Scanning electron micrograph (SEM) of supergene monazite from Kuge carbonatite centre. Scale bar = 1.0  $\mu\text{m}$ . 233

LIST OF TABLES.	PAGE
Table 1.1 The Thermal stability of carbonates.	8
Table 1.2 Quantitative composition of carbonatite at 10, 50, and 90% boundaries.	10
Table 2-1 Stratigraphical succession at Legetet and Koru.	43
Table 3-1 Major element contents in ferrocarnonatite breccia and calcite carbonatite from the Kuge hill.	60
Table 3-2 Summary of geology along drill-hole KG-2.	61
Table 4-1 Summary of geology along drill-hole BRL-1.	73
Table 5-1 Minerals identified by XRD from drill hole BRL-1	96
Table 5-2 Minerals identified by XRF from drill hole BRL-2 and KG-2.	98
Table 5-3 (i) Selected electron microprobe analyses of calcite from the Buru hill carbonatite.	101
Table 5-3 (ii) Selected electron microprobe analyses of siderite from the Buru carbonatite.	102
Table 5-3 (iii) Selected electron microprobe analyses of calcite from Kuge hill.	103
Table 5-3 (iv) Selected electron microprobe analyses of accessory carbonate phases, ankerite and strontianite from Buru hill.	104
Table 5-4 Selected electron microprobe analyses of barite and fluorite from the Buru and Kuge carbonatite centres.	109
Table 5-5 Electron microprobe analyses of magnetite and goethite from the Buru and Kuge carbonatites.	111

Table 5-6	Electron microprobe analyses of biotite and phlogopite.	113
Table 6-1	Major and trace elements from the Buru carbonatite Analyses by ICP.	119
Table 6-2	Major and trace elements from the Kuge carbonatite. Analyses by ICP.	122
Table 6-3	Electron microprobe analysis of psilomelane.	124
Table 7-1	The distribution of oxygen and carbon stable isotopes from the Buru and carbonatite centre.	142
Table 7-2	The effect of weathering on the mineralogical composition of the Buru calcites.	150
Table 7-3	Stable isotopic data for calcite and siderite phases.	161
Table 7-4	Carbon and oxygen isotopic data from the Kuge centre.	167
Table 7-5	Sulphur isotope composition of barite from Buru and Kuge.	172
Table 8-1	Names, symbols, atomic number and electron configuration of rare earth elements (after Henderson, 1996).	182
Table 8-2	Major and rare earth elements from the Buru carbonatite.	189
Table 8-3	Major and rare earth elements from the Kuge hill.	196
Table 8-4a	Selected electron microprobe analyses of lanthanide fluorocarbonates from the Buru carbonatite centre.	208
Table 8-4b	A representative electron microprobe analysis of supergene monazite from the Buru carbonatite.	209
Table 8-5	Selected electron microprobe analyses of monazite (Ce) from the Kuge carbonatite centre.	212

Table 8-6	Electron microprobe analyses of lanthanide fluorocarbonates from the Kuge carbonatite.	213
Table 8-7	Selected electron microprobe analyses of unknown mineral from the Buru and Kuge carbonatite centres.	216
Table 8-8	Electron microprobe analyses of REEs in sample NR. 271 (calcite carbonatite).	218

## CHAPTER ONE

### INTRODUCTION TO THE INVESTIGATION OF SECONDARY PROCESSES IN VOLCANIC CARBONATITES

This thesis demonstrates the importance of secondary processes (meteoric-hydrothermal and supergene enrichment) during sub-solidus recrystallization and mineralization in carbonatites. It will be shown in this study that the geochemical characteristics of carbonatites, especially specific trace and major elements, stable isotopic ratios and rare earth element distribution-patterns, are greatly influenced during sub-solidus re-equilibration. Fingerprinting these secondary stages and their geochemical evolution is the key to understanding the meteoric-hydrothermal, and supergene processes involved in lanthanide re-distribution and re-concentration in volcanic carbonatites in the Nyanza Rift, western Kenya.

#### 1.1 KENYA - JAPANESE GEOLOGICAL COOPERATION.

A request was submitted in 1987 by the Government of Kenya to the Government of Japan to conduct a joint mineral exploration survey (Figure 1-1) in the Homa Bay area specifically concerning the carbonatite centres and their lanthanide potential in western Kenya (McCall, 1958, Le Bas, 1977). The Japanese Government entrusted the mineral survey to the Japanese International Cooperation Agency (JICA) and Metal Mining Agency of Japan (MMAJ) whereas selected staff from the Mines and Geological Department, Ministry of Environment and Natural Resources, Nairobi, represented the exploration survey team. The composition of the survey teams consisted of 8 geologists, a team Leader from JICA and a Co-Leader from the Department of Mines and Geology. The writer was the Co-

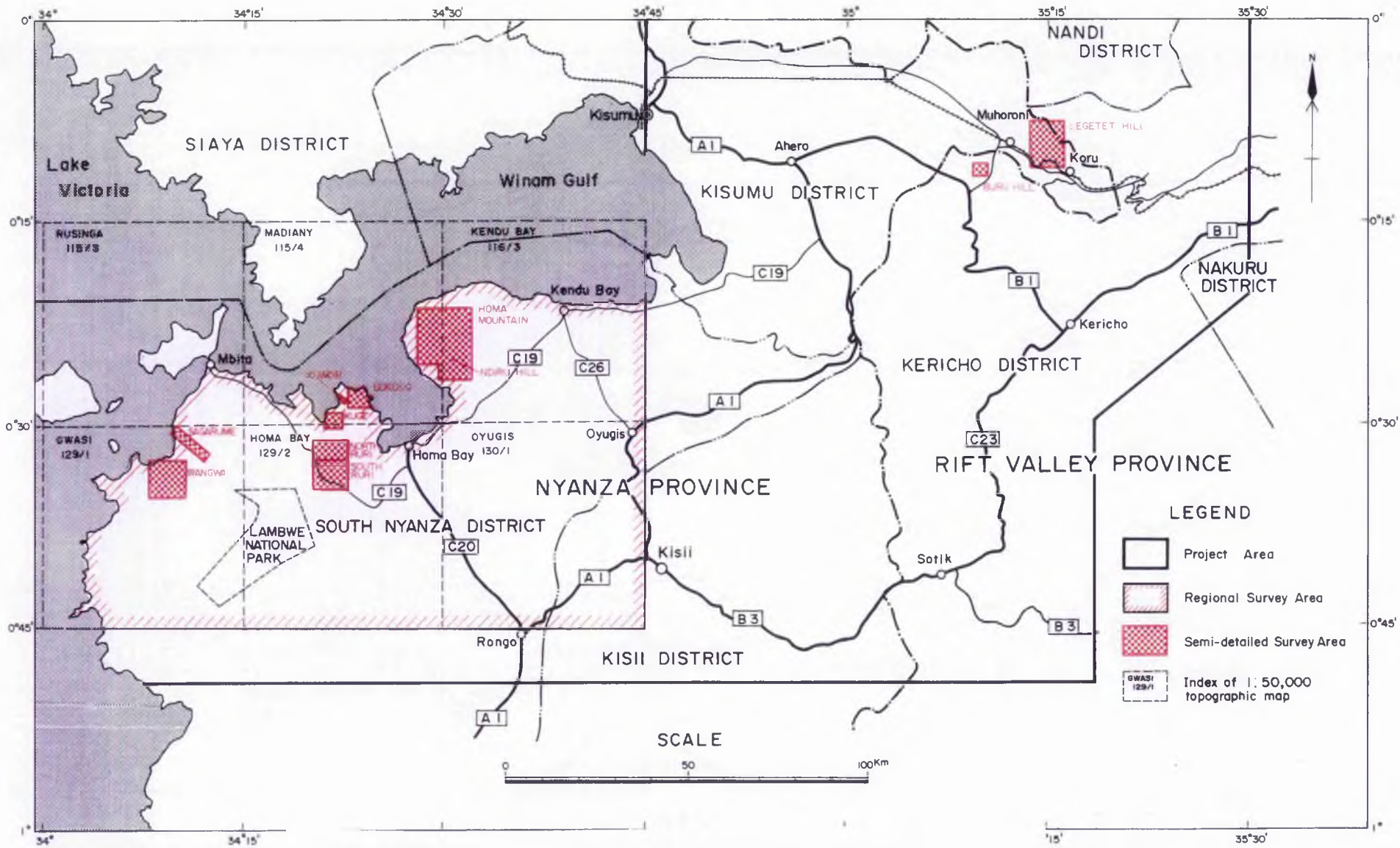


Figure 1-1 Location map of Homa Bay mineral exploration project (after JICA report phase 1, 1988).

Leader, seconded from his position of Provincial Geologist at the Mines and Geological Department, Kisumu.

## 1.2 AIMS OF THE JICA-MMAJ HOMA BAY EXPLORATION PROJECT.

The main objectives of the Homa Bay project (Figure 1-1) were to assess the lanthanide potential of the western Kenyan carbonatites and estimate the ore reserves in selected 'key' target areas. The Japanese-Kenya preliminary investigation which started towards the end of 1987 was carried out in three stages.

Stage 1 involved regional geological surveys of areas surrounding the carbonatite centres. 2,750 sq. km were covered during this reconnaissance survey. The data was compiled into 1: 50,000 geological maps. Also detailed geological mapping (1: 10,000) including geochemical sampling (soil and rock) were completed on all the Nyanza rift carbonatites. Preliminary interpretation of geochemical anomalies revealed potentially high concentrations of light rare earth elements (LREEs), yttrium and niobium especially at Buru, Kuge and Lwala, and the Ruri hills carbonatite centres (Figure 1-1). The findings of the stage 1 survey activities were compiled as a confidential document, "Report on the Mineral Exploration In The Homa Bay Area Phase I, March 1988". To aid this compilation the writer spent five months in Tokyo where he was actively involved in the preliminary interpretation of the geochemical data as well as drafting the geological maps for the Phase 1 report and making recommendations for the stage 2 survey.

The Stage 2 survey concentrated on geochemical targets selected from stage 1 (Buru and Kuge - Lwala and the Ruri hills carbonatite centres). Geological activities involved detailed geological and geochemical sampling including diamond drilling at Buru. Results of these investigations and the

recommendations for the third and final phase were published in " Report on the Mineral Exploration in the Homa Bay Area Phase II, March 1989". The results of the combined Japanese-Kenyan exploration programme revealed higher lanthanide potential within the ferrocarnatites at Kuge. Drilling at Buru revealed two key lanthanide concentration zones. The supergene zone, the most oxidized, had the highest REE values compared to the fresh carbonatite zone below the laterite cover. Because of higher abundances of rare earth elements at Buru and Kuge carbonatite centres, they were selected for further detailed investigation in stage 3.

The final 3rd stage involved drilling at Buru and at Kuge carbonatite centres. Detailed core-logging as well as geological mapping on the scale 1: 4,000 and 1: 5,000 for Buru and Kuge centres respectively were completed. Electron probe microanalysis (EPMA), Scanning electron microscopy (SEM) and X- ray diffraction studies, undertaken mainly in Tokyo suggested that fluorocarbonates could be the principal REE carrying minerals. Associated minerals identified in the drill cores included pyrochlore, huanghoite, rancieite and barite. Monazite was not identified.

Reserves for Buru hill were estimated to be 10, 700,000 tonnes of crude ore with total rare earth oxide (REO) averaging 2.63 %. Kuge had an average of 1.57% REO. Whereas the rare earth contents in Buru were low compared to those found in USA and China, it was recommended that open pit mining could be successful especially for local mining companies. The REE concentrations at Kuge hill were thought to be too low for exploitation.

The final document of the joint mineral exploration programme was published in 1990 (J.I.C.A Confidential Report 3) summarizing the activities and achievements of the Japan-Kenya International Cooperation Programme.

### 1.3 OBJECTIVES OF THE PRESENT INVESTIGATION.

The results of the Homa Bay project where the writer was actively involved in the administration of field programmes and production of the reports, forms the basic background information to the present study for the degree of PhD. The research programme undertaken at the Department of Geology, St Andrews University was sponsored by the Overseas Development Agency (ODA) and administered by the British Council.

The main objective of the present investigation is therefore to identify critical mineralogical and geochemical signatures associated with secondary processes (meteoric/hydrothermal and supergene) that were responsible for the re-distribution and concentration of rare earth minerals at Buru and Kuge carbonatite centres through detailed stable isotope systematics, mineralogical and geochemical studies.

#### 1.4 CARBONATITES: DEFINITION AND CLASSIFICATION.

Carbonatites are magmatic rocks containing more than 50% carbonate minerals (Heinrich, 1966 and Le Maitre et al., 1989). They are highly silica-undersaturated rocks and are characterized by a wide range of mineral compositions that are dominated by simple carbonates such as calcite, dolomite, ankerite, siderite and rarely magnesite. Carbonatites contain variable amounts of magnetite, biotite, apatite, phlogopite, K-feldspar, quartz, pyrochlore, nepheline, clinopyroxene and amphibole. Chemically, carbonatites are also enriched in incompatible elements such as Ba, Sr, Nb, Th, Ti, P and the rare earth elements. These elements are usually present in only minor or trace amounts in other igneous rocks (Woolley and Kempe, 1989).

Carbonatites have been widely reported from continental settings where they are commonly associated with nephelinitic igneous provinces and from oceanic settings such as Cape Verde and the Canary islands (Silva et al., 1981).

#### 1.5 HISTORICAL STUDIES OF CARBONATITES.

The term carbonatite was first introduced by A.G. Högbom in 1895 (Tuttle and Gittins, 1966) who applied the term carbonatite to describe dykes of igneous rocks containing considerable amounts of carbonate at Alnö. The term carbonatite was later expanded and defined by Brögger (1921) in his description of the geology and petrology of the alkaline rocks and associated carbonate rocks of the Fen area in Norway (Heinrich, 1966).

In 1924, Bowen strongly disputed Brögger's interpretation of the Fen rocks and through his detailed studies of textural relationships observed in thin-section, suggested that the mixed silicate-carbonate rocks were hydrothermal in origin (Tuttle and Gittins, 1966). According to Tuttle and

Gittins (1966), the criticism of Brögger's work by Bowen started the long history of controversy regarding the origin of carbonatites. The conception of an 'igneous limestone' was regarded as revolutionary by many geologists, and Daly (1933) advanced his theory of limestone syntexis in which he argued that most of the carbonate rocks associated with the alkaline rocks were sedimentary limestones. Daly accepted that carbonatite dykes cutting the Premier kimberlite in South Africa were truly magmatic but suggested that the magma was derived from an assumed "Great Dolomite" at depth. Daly believed in the existence of carbonatitic magma, but refused to consider the CO<sub>2</sub> as juvenile.

Shand (1943), a great advocate of limestone syntexis, considered carbonatites to be remobilized sedimentary rocks. Later, Pecora (1956) reviewed proposed modes of carbonatite formation, which included differentiation from alkaline magma and/or precipitation from hydrothermal solutions and gaseous phases.

The Chilwa Igneous Province in Malawi was recognized to contain carbonatite centres during the geological surveys undertaken by Dixey in 1934 (Garson and Smith, 1958). The main carbonatite complexes of Malawi (Chilwa island, Tundulu, Kangankunde and Songwe) were later re-investigated by Garson (1965). Interest and exploration for carbonatites continued in many parts of the world as demonstrated by the simultaneous release of two reviews, one by Pecora (1956) and the other by Smith (1956). Progress in carbonatite research continued, as witnessed by comprehensive accounts of intrusive carbonatite complexes by Tuttle and Gittins (1966) and Heinrich (1966).

The discovery of phosphate and rare earth minerals in some of these carbonatites, for example large residual apatite deposits in Uganda, monazite and bastnäesite at Kangakunde and niobium deposits in Canada, Brazil and the United States, encouraged more exploration which led to carbonatites being recognised in many parts of the world, especially Africa (Deans, 1966).

### 1.6 SEDIMENTARY LIMESTONE VS MAGMATIC CARBONATITE.

The concept of magmatic carbonate lavas at petrologically reasonable temperatures was at variance with the high decomposition temperatures and melting points of some of the carbonates as illustrated in Table 1-1 below (Data from Cooper et al., 1975).

Table 1-1 The thermal stability of carbonates.

	Decomposition temperature at atmospheric pressure (°C)	Melting point at 1 kb (°C)
CaCO <sub>3</sub>	900	1300
MgCO <sub>3</sub>	400	-
FeCO <sub>3</sub>	175	-
K <sub>2</sub> CO <sub>3</sub>	1950	912
Na <sub>2</sub> CO <sub>3</sub>	1750	872

Those geologists who opposed the magmatic nature of carbonatites often cited both high decomposition and melting points of the carbonates as evidence of the inability of carbonatite magmas to exist in nature and preferred to promote the concept of limestone syntexis instead.

Pioneering laboratory experiments by Wyllie and Tuttle (1960) and the description of effusive dolomitic carbonatites of Cretaceous age in Zambia

by Bailey (1960) demonstrated the possibility of the existence of carbonate lavas on the earth's surface. The extrusion of carbonatite lavas from Oldoinyo Lengai in northern Tanzania (Dawson, 1962) fully confirmed beyond doubt the existence of such lavas.

Whereas the discovery of Oldoinyo Lengai lavas confirmed the existence of carbonatite magmas, the experimental results showed that compositionally the lavas should be close to calcite-carbonatite and strongly hydrous, while the Oldoinyo Lengai lavas were anhydrous and very different in bulk composition from the commonly occurring fossil carbonatites, a difference which brought considerable controversy in relation to the problem of their origin, especially the nature of carbonatite magmas and their source regions. This problem remains unresolved even to the present day.

### 1.7 NOMENCLATURE.

A comprehensive classification of carbonatites was proposed by Brögger in 1921 (Heinrich, 1966), who introduced the term sövite and rauhaugite for calcitic and dolomitic carbonatites, while von Eckermann in 1948 (Heinrich, 1966) suggested alvikite and beforsite for the fine-grained equivalents of sövite and rauhaugite. Classification of carbonatites according to the IUGS Subcommittee on the Systematics of Igneous Rocks (Streckeisen, 1980) is as follows:

- i) (a) Calcite-carbonatite consisting of sövite (coarse-grained) and alvikite (fine-grained).
  - (b) Dolomite-carbonatite (beforsite).
  - (c) Ferrocarbonatite (essentially composed of iron-bearing carbonate minerals such as ankerite or siderite).
  - (d) Natrocarbonatite (composed essentially of sodium, calcium and potassium carbonate minerals of nyerereite and gregoryite). Oldoinyo

Lengai, an active volcano on the western flank of the East African Rift in northern Tanzania is the only known example in the world erupting carbonatite lava at the present time.

ii) Carbonatites containing a mixture of various carbonate minerals are indicated by prefixes according to the established rules for the quantitative composition of rocks at the 10, 50 and 90% boundaries as shown in Table 1-2 (after Streckeisen, 1980).

Calcite		Dolomite	
0%	10%	50%	90% 100%
Calcite	Dolomitic-Calcite	Calcitic-Dolomite	Dolomite

Table 1-2 Quantitative composition of rocks at the 10, 50 and 90% boundaries.

iii) Igneous rocks containing less than 10% carbonate minerals may be named calcite-bearing ijolite, dolomite-bearing peridotite etc.

iv) Igneous rocks containing between 10 and 50% carbonate minerals are classified as calcitic or carbonatitic ijolite.

v) The terms melanocratic and leucocratic are not recommended when describing carbonatites and should be discarded.

vi) Characteristic contents of other minerals are indicated by prefixes, for example apatite-pyroxhlore or aegirine-calcite carbonatite etc.

In addition to calcite and dolomite, some carbonatites contain either ankerite, siderite, or magnesite. It is surprising that these carbonate species are not well defined in the IUGS Subcommittee on the Systematics of Igneous Rocks outlined above. Ferrocarbonatites are the most poorly defined rock types among the carbonatite family. Many writers usually use

the term 'ferrocarbonatite' to name rocks that are enriched in iron-containing compounds such as magnetite, hematite or goethite. These rocks are usually dark-brown in colour. These 'ferrocarbonatites', however, do not contain any iron-bearing carbonates, such as siderite or ankerite. The contribution of Le Bas (1977) popularized the 'ferrocarbonatite' terminology, although the actual siderite mineralogy was not presented. Some workers, for example Reid et al. (1992), have found that rocks earlier recognized as 'ferrocarbonatites' from the Dicker Willen carbonatite complex in southern Namibia, turned out to be composed mainly of calcite grains with rims of complex iron oxide/hydroxides on closer mineralogical scrutiny.

Woolley (1982) and Woolley and Kempe (1989) have suggested further modifications to the IUGS System, in which they recommend the subdivision of carbonatites (except natrocarbonatites) into three groups on the basis of their bulk chemistry by utilising the wt% of the major oxides - CaO, MgO and FeO as  $\text{Fe}_2\text{O}_3 + \text{MnO}_2$ . They recommend that carbonatites be classified as:

- i) Calciocarbonatite, if  $\text{CaO (wt\%)}: \text{CaO} + \text{MgO} + \text{FeO} + \text{Fe}_2\text{O}_3 + \text{MnO} > 0.8 \text{ (wt\%)}$ .
- ii) Magnesiocarbonatite, if  $\text{MgO} > \text{FeO} + \text{Fe}_2\text{O}_3 + \text{MnO}$  and  $\text{MgO} < 0.8 \text{ (wt\%)}$  and
- iii) Ferrocarbonatite, if  $\text{MgO} < \text{FeO} + \text{Fe}_2\text{O}_3 + \text{MnO}$ .

The divisions of Woolley (1982) and Woolley and Kempe (1989) (Figure 1-1) involving the proportions of CaO, MgO and  $\text{FeO} + \text{Fe}_2\text{O}_3 + \text{MnO}$  seem to logically isolate the various carbonatite types into calciocarbonatites, magnesiocarbonatites and ferrocarbonatites.

Mineral names such as calcite, dolomite, ankerite or siderite in carbonatite classification may require the use of an electron microprobe to correctly identify them due to complex intergrowth among different carbonate species in some rocks, a condition that is not met by many researchers and therefore leads to the inadequate naming of most carbonatites. However, if mineral species are correctly identified, the writer recommends the use of such mineral names in classifying carbonatites to enable the carbonatite community to have a unified terminology.

The mineralogy of the carbonate phases as recommended by the IUGS Subcommittee and the Woolley and Kempe scheme (1989), will be used in naming the carbonatites in the study area. In this thesis, calcite-carbonatite will be used for calcite-bearing carbonatites and sövite and alvikite will only be used as textural qualifiers, for example a calcite carbonatite will be described as being sövitic if coarse-grained or alvikitic if fine-grained. The terms calciocarbonatite, magnesiocarbonatite and ferrocyanatite will be used when only bulk chemistry is available, otherwise siderite carbonatite or ankerite carbonatite will be retained for those carbonatite rocks containing the mineral siderite or ankerite, and ferrocyanatite, which is usually dark-brown or black in colour, will be used for those rocks that are enriched in iron in the form of either magnetite, hematite or goethite.

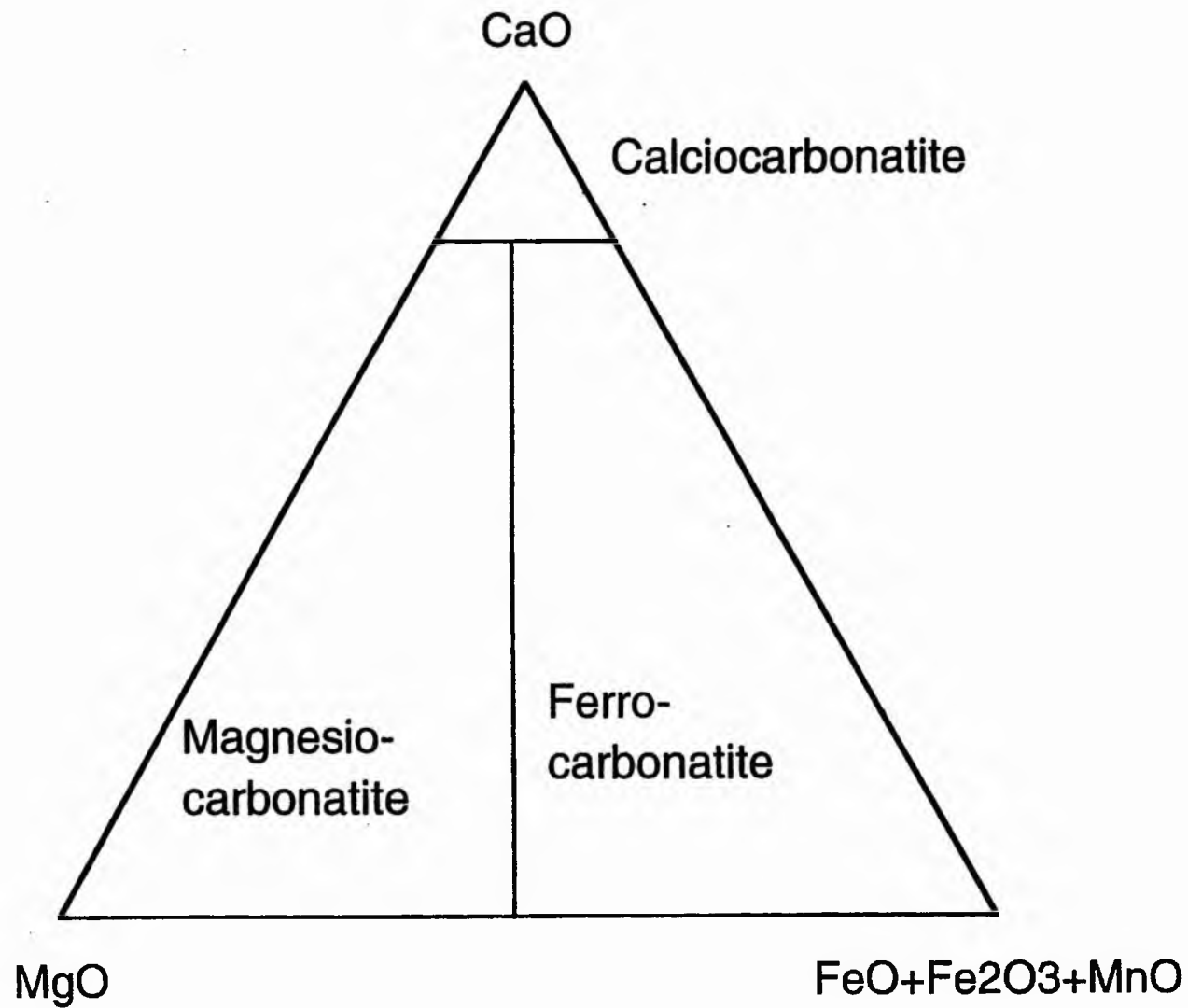


Figure 1-2 Carbonatite classification diagram (after Woolley, 1982).

## 1.8 PETROGENETIC CONCEPTS.

A number of petrogenetic models have been proposed for the genesis of carbonatites. The proposed models often have to account for those characteristics that render these rocks unique from other rocks, particularly the igneous rocks. These features include:

- i) The marked difference in mineral composition between natrocarbonatite with high alkali contents and all other carbonatites that are essentially Ca-Mg-Fe carbonates with very low alkali content.
- ii) Many carbonatites world-wide are closely associated with alkaline rocks.
- iii) Carbonatites range in age from Archean to Recent, and are found most in continental and rarely oceanic environments where they are generally associated with major rifting and faulting.
- iv) The carbonatite-kimberlite association.
- v) The enrichment of carbonatites in incompatible elements and lanthanides.

According to Gittins (1989), three main petrogenetic models have been proposed for the genesis of carbonatite magmas. These are:

- i) Separation of an immiscible carbonate liquid and a silicate liquid (nephelinitic or phonolitic) from a mantle-derived magma.
- ii) Direct partial melting of a carbonated, metasomatised mantle to produce separate carbonate and silicate lavas.
- ii) Fractional crystallization of a CO<sub>2</sub>-rich alkaline silicate magma at high or mid-crustal pressures.

The earliest experiments on silicate carbonate liquid immiscibility were those carried out by Koster van Groos and Wyllie (1966, 1968) where they demonstrated that at 1 kb a large miscibility gap existed between albite-rich and sodium-rich liquids. Watkinson and Wyllie (1969, 1971), working on the systems albite-calcite + 25% water and nepheline-calcite + 25% water

did not however observe liquid immiscibility. These early experiments used synthetic starting materials at high temperature and pressure and often large amounts of water to promote melting.

Freestone and Hamilton (1980) found liquid immiscibility in alkali-poor systems using natural lavas (phonolite and nephelinite) as starting materials. The results demonstrated that carbonatites can be generated by immiscible separation of either phonolitic or nephelinitic magma. The authors also investigated the effects of changing pressure and temperature on the miscibility gap and found that increasing  $P_{CO_2}$  and decreasing temperature promoted immiscibility. Kjarsgaard and Hamilton (1988), working with synthetic materials of different compositions at approximately 5 kb and 1100-1250°C, succeeded in showing that the miscibility gap extended into compositions containing no alkalis. These experiments showed that pure  $CaCO_3$  melt is immiscible with a silicate melt and hence pure  $CaCO_3$  magmas could also be produced by liquid immiscibility.

Most recent published schemes of carbonatite genesis have tended to favour an origin by immiscible separation from carbonated, silica-undersaturated silicate magma (Freestone and Hamilton, 1980; Le Bas, 1987, 1989; Kjarsgaard and Hamilton, 1988, 1989; Peterson, 1990 and Kjarsgaard and Peterson, 1991). The process of liquid immiscibility involves a mantle derived primary carbonated magma which separates immiscibly in the crust into silicate and carbonatitic magmas. Fractionation trends studied at Shombole, located at the southern end of the Kenya rift and Oldoinyo Lengai (Peterson, 1989a, 1989b), is suggested by Peterson to have a parental magma of an olivine nephelinite which fractionated to mildly peralkaline nephelinites and immiscible carbonate globules, which are sövitic in composition, whereas at Lengai, the parental magma is an olivine

melilite nephelinite, which fractionated to highly peralkaline wollastonite nephelinites and combeite nephelinites.

Recent experimental work on immiscibility at Oldoinyo Lengai (Kjarsgaard et al., 1995) using natural samples of wollastonite nephelinite with synthetic natrocarbonatite at low pressure (50-375 MPa) and temperature (700-850°C) has shown that the conjugate liquid to natrocarbonatite at Oldoinyo Lengai should be a wollastonite nephelinite. Church and Jones (1995) also proposed that the petrogenesis of natrocarbonatite involved extensive fractionation of a carbonated alkaline silicate magma (olivine melilite nephelinite) to a point where wollastonite is stable. According to Church and Jones (1995), the residual silicate melt becomes extremely peralkaline and contains large amounts of dissolved pyroxene, nepheline and melanite with continued fractionation. Eventually, the residual melt crystallizes wollastonite and nepheline, becomes progressively enriched in alkalis and volatiles, and subsequently exsolves natrocarbonatite when the critical point is reached.

These recent experiments tend to suggest that phonolite is not related at all to the genesis of natrocarbonatite at Oldoinyo Lengai, as previously proposed by Freestone and Hamilton (1980). In East Africa, and in particular the Nyanza rift carbonatites, phonolite plugs are observed to be closely associated with carbonatites and it is extremely unlikely that they are not connected at all with the genesis of these volcanoes.

Assigning natrocarbonatite to be parental to most types of carbonatites observed on the earth's surface gave birth to new controversy which has greatly hindered research in carbonatite genesis. This theory considers all the present calcite-rich carbonatites to have been initially alkali-rich and to

have contained nyerereite and gregoryite as the main minerals. Evidence of calcification of these original alkali carbonatites has been documented by Hay and O'Neil (1983), Deans and Roberts (1984), Clarke and Roberts (1986) and Dawson et al. (1987). Their models propose the loss of alkalis from natrocarbonatites to produce calcitic carbonatites. The loss of alkalis is suggested to have been due to leaching by rain water, followed by replacement with calcite.

Keller (1989), Barker (1989), and Kjarsgaard and Hamilton (1989) have, however, described primary tabular calcite which they do not ascribe to the calcification of natrocarbonatite. Gittins and Jago (1991) also suggest that most of the tabular calcites documented from extrusive carbonatites could be primary magmatic calcite and not necessarily pseudomorphs after nyerereite.

Twyman and Gittins (1987), Gittins (1989) and Harmer and Gittins (1995) have made numerous objections to the views of those who consider liquid immiscibility as the main process of generating carbonatites. Alternatively, they argue that carbonatites may be generated by small degrees of partial melting in the upper mantle. They propose an olivine calciocarbonatite parent which evolves through fractional crystallization to either Ca-Mg-Fe carbonatites or natrocarbonatite, depending on whether hydrous or anhydrous phases fractionate out first. Gittins' scheme of producing carbonatites by direct melting within the mantle is supported by experiments of Wallace and Green (1988), who document the formation of dolomitic liquids by partial melting of mantle materials to produce primary carbonatites with little or no evidence of immiscibility, the observation of mantle-derived chromite microphenocrysts in carbonatites from Uyayanah Area, United Arab Emirates (Woolley et al., 1991), the Sr and Nd isotope

differences between carbonatites and silicate rocks in some carbonatite complexes which could show that the associated silicate rocks may not be genetically related to carbonatites, and finally by the difficulty in explaining petrochemical evidence for the former existence of alkali carbonates, as detailed by Keller (1989).

Compared to Gittins' scheme, liquid immiscibility is supported by the existence in experimental runs of alkali carbonate globules in liquid of phonolitic composition (Freestone and Hamilton 1980), the presence of fenitized zones surrounding most carbonatites, the discovery of inclusions of alkali liquids in apatite (Le Bas and Aspden, 1981), the bimodal distribution of silicate and carbonatite rocks clearly seen in western Kenya, which suggests separation by liquid immiscibility followed by independent crystallization of the melts, and the description of natural examples of liquid immiscibility at Shombole (Peterson, 1989a, 1989b and Kjarsgaard and Peterson, 1991), Suswa (Macdonald et al. 1993) and Oldoinyo Lengai (Peterson, 1989a, 1989b and Church and Jones, 1995).

The process of producing carbonatites by fractional crystallization of a CO<sub>2</sub>-rich nephelinite was proposed by King and Sutherland (1966). The relationship between the nephelinitic volcanoes and their plutonic rocks was described by King and Sutherland (1966) in support of fractional crystallization in Napak, where the volcanic cone is composed of nephelinitic tuffs and agglomerates and the central vent by ijolite and carbonatite. The plutonic rocks were considered by King and Sutherland (1966) to have formed from the same magma which was parental to the nephelinites. Watkinson and Wyllie (1971) showed that CO<sub>2</sub>-bearing nepheline magmas could undergo fractional crystallization to produce nephelinite-bearing carbonatites, which are typical in the Oka carbonatite

complex. Le Bas (1987) and Gittins (1989) argued against the process of fractional crystallization of a CO<sub>2</sub>-rich nephelinite, pointing out that rocks intermediate between nephelinite and carbonatite required by such a scheme are unknown.

### 1.9 CONCLUSION.

It is clear from the above discussion that there is no single petrogenetic model that adequately explains the genesis of carbonatite magmas. The three models proposed above are all capable of producing carbonatite magmas given the proper conditions. Conclusions from experimental work for the generation of carbonatites, as reviewed by Wyllie et al. (1989, 1990), and isotopic investigations, for example Bell and Blenkinsop (1989), suggest that carbonatites are derived from the mantle.

However, progressive fractionation and differentiation, including multiple intrusions within the upper mantle and the crust, will modify the carbonatite magma. Hydrothermal alteration, sub-solidus recrystallization, supergene weathering and later metamorphism and erosion, which carbonatites are normally prone to, makes them very poor indicators of original magma compositions and consequently it is difficult to unravel their intimately guarded complex evolution.

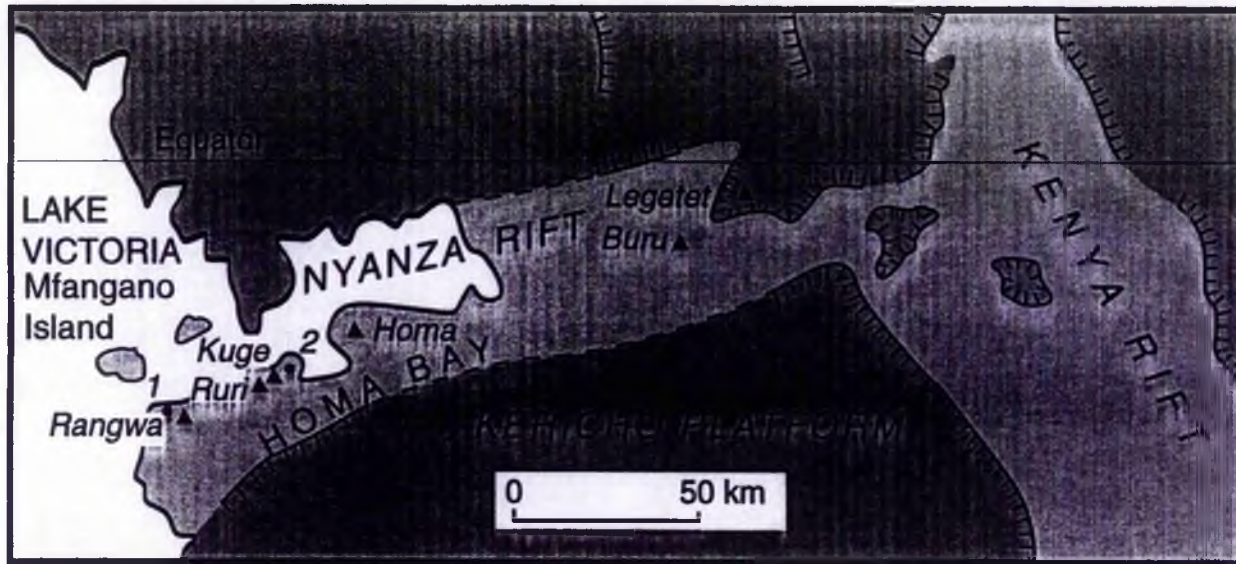
## CHAPTER TWO

### WESTERN KENYA VOLCANIC CARBONATITES

#### 2.1 INTRODUCTION.

Western Kenya hosts a number of Tertiary and Quaternary alkaline volcanic carbonatite centres such as Rangwa and its associated smaller volcanic cones at Sagarume-Nyamgurka and the North and South Ruri carbonatite centres, Kuge, Lwala, Ngou-Kuwor, Ugongo-Uyi-Kiyanya-Sokolo, Homa mountain, Buru and Legetet hill (Figure 2-1), where extrusive carbonatite lavas have erupted from magma chambers beneath and emplaced into both the Archaean and Proterozoic basement rocks within the Nyanza rift off the main Kenya (Gregory) rift.

It has long been recognized that the majority of carbonatites are found in alkaline igneous provinces. Typically, the alkaline rocks are phonolites and nephelinites commonly found in continental settings, where they are spatially related to areas of major rifting and crustal extension. Some carbonatites occur in cratonic areas linked to kimberlites, while others are found in an oceanic environment. In Africa, especially in East Africa, there are a number of central vent volcanoes of nephelinite-carbonatite composition that are associated with the rift systems. These volcanoes include Kisingiri (Shackleton, 1951; McCall, 1958 and Le Bas, 1977) Tinderet (Binge, 1962), Shombole (Peterson, 1989a), Kerimasi (Hay, 1983 and Church and Jones, 1995), Napak (King, 1949), Elgon (King and Sutherland, 1966) and Oldoinyo Lengai, the only volcano in the world known to have erupted carbonatite tephra and lava in historic time (Dawson, 1962 and Church and Jones, 1995).



1. Sagarume - Nyamgurka
2. Ugongo - Uyi - Kiyanga - Sokolo

**Figure 2-1.** Location map of Western Kenya Carbonatites in relation to Nyanza and Kenya Rifts.

Western Kenya and eastern Uganda carbonatites form part of a prominent Tertiary to Recent undersaturated alkaline petrographic province along with other classic occurrences found elsewhere in the world, such as Fen (Barth and Ramberg, 1966), Alno (Eckermann, 1966), Iron Hill, Colorado (Nash, 1972), and Chilwa Island, Malawi (Garson and Smith, 1958), where excellent examples of the carbonatite-nephelinite association is observed. A common feature of the nephelinite volcanoes, such as Tinderet and Kisingiri, is the occurrence of Miocene fossiliferous sediments near their bases, which has been used for age dating the Koru and Rusinga Island successions (Bishop et al., 1969).

## 2.2 CARBONATITE - NEPHELINITE ASSOCIATION.

The association of carbonatites with nephelinitic volcanism was first recognised by King (1949) at Napak in Uganda, where erosion has revealed an undersaturated nephelinite-ijolite-carbonatite structure with some of the erupted tuffs, agglomerates and lavas preserved on the flanks of the volcano. Although nephelinite-carbonatite complexes are rare, being only a fraction of 1% of all igneous rocks, their distribution is worldwide (Le Bas, 1987). Within the Gregory rift and the Tertiary volcanic centres of East Africa, two distinct groups of nephelinites (Group I and Group II) have been distinguished (Baker et al., 1971 and Le Bas, 1987).

Group I nephelinites are olivine-rich and are typically associated with alkali basalt and basanite. Group II nephelinites comprise olivine-poor nephelinites, which often occur with carbonatitic and ijolitic complexes. However, both olivine-rich and olivine-poor nephelinites have been observed to occur together in some areas, such as the Tanzanian sector of the Gregory rift valley, Tinderet volcano in Kenya (Le Bas, 1987), Moroto volcano in Uganda (Varne, 1968) and Shombole on the floor of the

Gregory rift, on the border between Kenya and Tanzania (Peterson, 1989a). These are often referred to as "mixed association" volcanoes and testify to the contemporaneous availability of mafic magmas over a wide range of alkalinity. Recently, Church and Jones (1995) have identified another type of strongly peralkaline nephelinite - wollastonite nephelinite which they consider to be a conjugate liquid to natrocarbonatite at Oldoinyo Lengai.

It is the opinion of the writer that the occurrence of nephelinites is not unique and essential for the formation of carbonatite magma, but the relationship between the two groups of nephelinites is only due to their origin being from a common source with spatial and compositional similarities. The association of "olivine-poor nephelinites" with carbonatites does not therefore have any genetic implications. The recent discovery of carbonatite globules at Suswa, a dominantly trachytic-phonolitic volcano in the floor of the Gregory rift in Kenya (Macdonald et al., 1993) suggests that carbonatites can also occur in very strongly differentiated rocks (low Mg, Ba and Sr).

### 2.3 GEOLOGICAL EVOLUTION OF THE WESTERN KENYA CARBONATITES.

The Tertiary and Quaternary alkaline igneous volcanic centres in western Kenya are underlain by Precambrian basement comprising two major rock suites, the Nyanzian-Kavirondian Group to the west of the Nandi fault and the Mozambique Belt to the east. The Precambrian basement of western Kenya is approximately 3000 my old (Dodson et al., 1973) and is composed of Archaean greenstone volcanic rocks and sediments intruded by granite and by small mafic to felsic intrusions. The Mozambique Belt, considerably younger than 3000 Ma, consists of highly metamorphosed sediments and

volcanics with quartz-feldspar and biotite-rich gneisses, ranging in age from 1100-600 Ma.

The Nyanzian Group, the oldest rocks in the region, consists of basaltic to rhyolitic volcanic rocks and a variety of sedimentary rock units within its succession. The Nyanzian rocks exhibit a low-grade, greenschist facies, regional metamorphism, characterized by the widespread occurrence of the assemblage quartz-chlorite-sericite-epidote (Onuong'a, 1983). The Nyanzian is overlain unconformably by the Kavirondian rocks, which are composed mainly of conglomerates with subordinate grits and mudstones. The date of the Kavirondian rocks has not been directly determined, but is later than 2900 my; post Nyanzian and earlier than about 2550 my (Le Bas, 1977). The whole rock geochemical data for the Archaean Nyanzian lavas from South Ruri and Homa mountain (Le Bas, 1977) indicates that the Nyanzian lavas are mainly calc-alkaline volcanics, similar to those found in mobile belts, and the least altered basalts show affinities with low-K oceanic tholeiitic lavas. Further south, towards the base of the Nyanzian rocks in the Migori Gold Belt, Onuong'a (1983) found that the felsic rocks (dacites, rhyolites and quartz porphyry) are mainly calc-alkaline, whereas the mafic rocks (basalts and dolerites) are tholeiitic in character.

From geological observations there appears to have been an extended period of erosion and relatively stable conditions in Neo-archean and Palaeoproterozoic times. There is however no evidence of sedimentation, volcanic activity or igneous intrusions until the eruption of the Kisii Group, consisting mainly of basalts, andesites, rhyolites and quartzites, shales and cherts. It is not clear how the Kisii Group fits in with the rest of the Precambrian history of western Kenya, but these relatively unmetamorphosed rocks could be correlated with the Bukoban of Tanzania

or represent the initial volcanism associated with the Mozambique orogeny, and escaped being deformed. It is possible that the differences in the metamorphic grade between the two groups is due to the fact that the Kisii rocks rested on a stable foreland of the Nyanzian/Kavirondian Shield, whereas the Mozambique Belt underwent severe deformation in its environment of deposition. Again stable continental conditions prevailed during the Palaeozoic and Mesozoic with only erosion and peneplanation taking place (Shackleton, 1951). There is therefore an enormous gap in the geological record of western Kenya before the onset of Tertiary volcanism with the extrusion of mostly alkali basalts, nephelinites and phonolites.

Erosion of these volcanoes has subsequently revealed complex magmatic features, including undersaturated intrusive complexes containing carbonatite in their cores (for example Kisingiri and Napak). The occurrence of Kisingiri and Tinderet volcanoes, to the west and east respectively, of the Nyanza rift is thought to be connected, to a large extent, to the distribution of carbonatitic-nephelinitic volcanoes in the area. Most of the fossil volcanoes in western Kenya are considered by the writer to be satellite cones related to the main strato-volcanoes of Kisingiri and Tinderet. The evolution and geological setting of Kisingiri and Tinderet and their closely related satellite carbonatite volcanoes are briefly discussed below.

#### 2.4 EVOLUTION AND GEOLOGICAL SETTING OF KISINGIRI VOLCANO.

The eroded remains of the large dissected central strato-volcano of Kisingiri at the western end of the Nyanza Rift was first mentioned by Kent (1944) and Shackleton (1951). Detailed geological mapping of Kisingiri and other western Kenya carbonatite-nephelinite volcanoes was carried out by

McCall (1958), while Le Bas (1977) compiled and presented an updated account of the geological and genetic setting of all the western Kenyan carbonatites.

Early alkaline silicate rocks, comprising a series of ultrabasic (alnöitic dykes) and alkaline igneous rocks (uncompahgrite, turjaite, micro-melteigite, pyroxenite, ijolite and urtite), were intruded into Precambrian granitic basement, which caused extensive fenitization and widespread brecciation and shattering of the basement rocks (McCall, 1958 and Le Bas, 1977). Although detailed and precise age dating of the carbonatite-nephelinite volcanoes has not been carried out, volcanism in Kisingiri is thought to have started in the early Miocene on the basis of fossil remains found in tuffs and agglomerates in the lowest member of the Rusinga Group, which resulted and accumulated just before and during the early eruptions of the Kisingiri volcano. This assumption is supported by K-Ar whole rock biotite and nephelinite dates of 19.6 Ma (Van Couvering and Miller, 1969). The dates of the volcanoes within the Nyanza rift, however, range from 20-1.0 Ma and it is thought that the spread in these dates may be due to either excess argon, or argon loss during emplacement of these volcanoes.

Hence, there is urgent need for precise age dating to be carried out on these carbonatite centres in order to evaluate the exact evolution of the carbonatite volcanoes. The Kisingiri complex covers a large area of high relief comprising five units, namely Rangwa, Gwasi and Gembe Hills, the islands in Lake Victoria (Rusinga, Mfangano, Kimaboni, Tavikere and Mbassa), the Kaniamwia escarpment and the Uyoma peninsula, which lies to the north of the Nyanza Gulf (Le Bas, 1977). The above units are all dominated by extensive accumulation of nephelinitic lavas, tuffs and

agglomerates. McCall (1958) divided the pile into three Groups; the Upper Kisingiri lavas, the Middle Kisingiri Pyroclastic Group and the Lower Kisingiri lavas comprising of melanephelinite, nephelinite and phonolitic melanephelinite. The division of the volcanic lavas into the three Groups is however oversimplified.

The early alkaline intrusions at depth possibly domed the Precambrian granitic basement and produced magmas and vents which were responsible for the accumulation of the three volcanic groups. Some of the dykes seen cutting the Precambrian granite could have been feeders to the Miocene volcanic lavas. The age and field relationships of these lavas, and the timing of the emplacement of the carbonatites, is not certain, but it is suggested that part of the lavas are earlier than the carbonatites, though some of the flows could have been contemporaneous with the carbonatites, as discussed by Le Bas (1977). The formation of the caldera at Rangwa (Figure 2-2) is interpreted to occur towards the end of the volcanic history, during which the pyroclastic rocks were deposited and some of the carbonatites emplaced. Continued erosion of Kisingiri has resulted in the formation of Pleistocene sediments, as witnessed in the Lambwe valley and various Recent alluvial deposits within the area.

## 2.5 THE RANGWA CARBONATITE CENTRE.

The Rangwa centre, which lies within the eroded central part of the large Kisingiri volcanic caldera, occupies a subsidiary caldera 4-5 km in diameter. Rangwa (Figure 2-2) consists mainly of a series of extrusive tuffs and agglomerates (divided into lower agglomerates, a tuff group and upper agglomerates (Le Bas, 1977) into which numerous carbonatite dykes and cone-sheets were intruded. The fragments, especially in the lower agglomerates, include granodiorite and fenite from basement rocks, ijolite

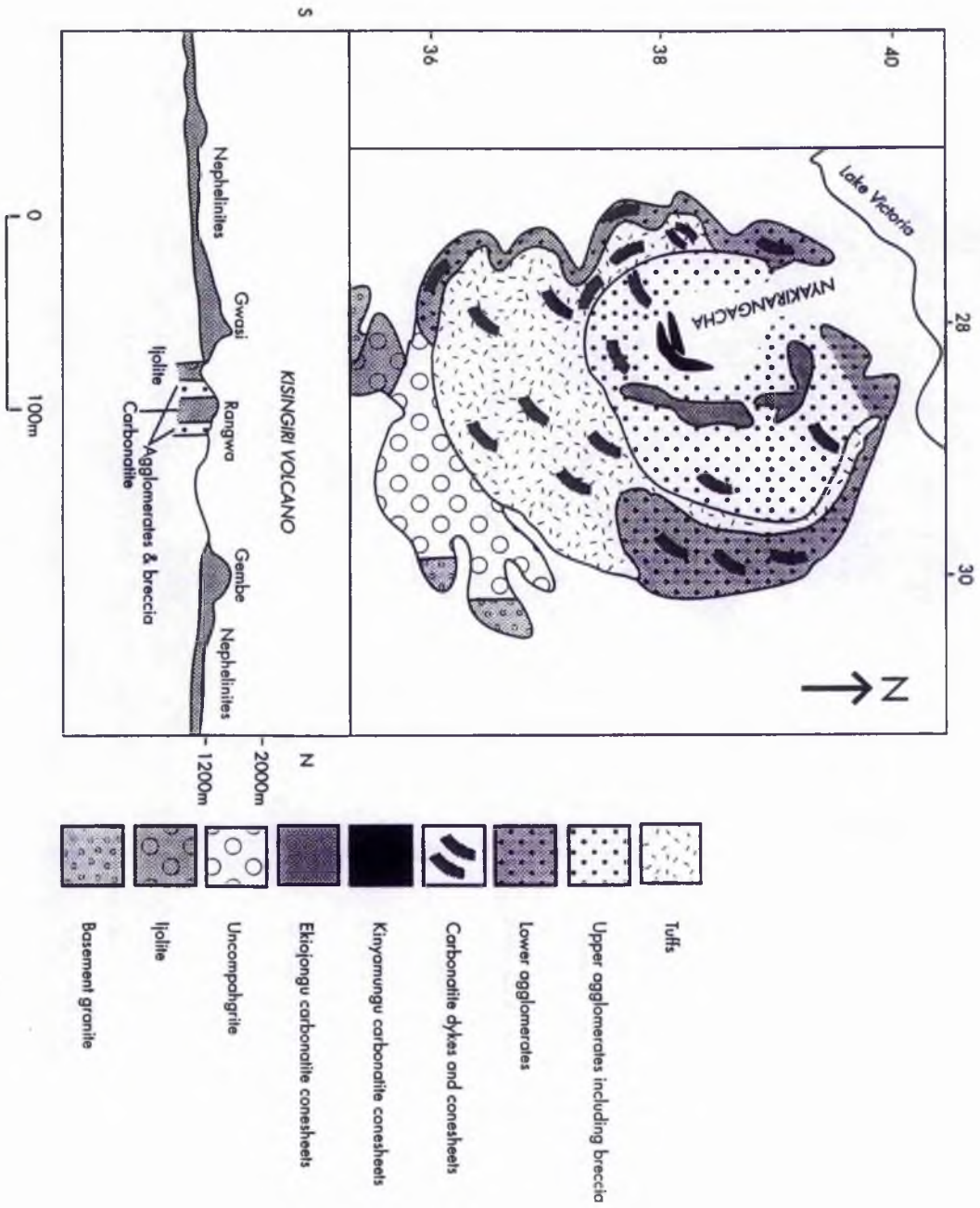


Figure 2-2

General Geology of Rangwa Carbonatite including generalised section of Kisingiri Volcano [after le Bos, 1977 and King et al, 1972]

and carbonatite and related volcanic rocks (melanephelinites and nephelinites). The agglomerates are mainly feldspathized, carbonated and limonitized. It is possible that some of the carbonate in the matrix is secondary, being introduced during the emplacement of the dykes and cone-sheets of carbonatite which invade these pyroclastic deposits. The carbonatites in the central area of the caldera and occupying the outer part of the volcanic centre include mainly small dykes and cone-sheets of fine-grained calcite-carbonatite that are clearly intrusive into the surrounding calcified tuffs and agglomerates. These are followed by the Ekiojango carbonatite, a coarse-grained calcite carbonatite containing biotite and apatite, and the innermost Kinyamungu carbonatite, a fine-grained calcite carbonatite consisting mainly of irregular streaks of magnetite (King et al., 1972 and Le Bas, 1977).

The sequence of emplacement of carbonatite types C<sub>1</sub> (sövite), C<sub>2</sub> (alvikite) C<sub>3</sub> (ferrocarbonatite) and late stage C<sub>4</sub> (alvikites), established and popularised by Le Bas (1977), appears to be well represented in Rangwa. The writer, however, suggests that the use of C<sub>1</sub>, C<sub>2</sub>, C<sub>3</sub> and C<sub>4</sub> to denote age relationships seems logical, but should be discouraged when used to imply genetic names such as sövite, alvikite, ferrocarbonatite and late alvikites, respectively. Excellent field relationships among these units are observed in Rangwa and in particular in the western sector of the caldera (Plate 2-1) where the carbonatite pyroclastics, including the breccias, tuffs and agglomerates, are clearly seen to be associated with, and cut by, high level fine-grained calcite carbonatite and ferrocarbonatite dykes and sheets.

The location of the western Kenyan carbonatites within the Nyanza rift cannot be entirely coincidental. The fact that the centres are all Miocene in age with their volcanic activity spanning between only 20 Ma and 1.0 Ma



Plate 2-1 Carbonatite pyroclastics (tuffs and agglomerates) cut by high level fine to medium-grained carbonatite dykes in the Rangwa carbonatite complex.

and that all are aligned at no great distance from each other along a crustal fracture zone, suggests and points to a very close genetic link involving derivation from a possible same magma chamber. The occurrence of Rangwa is hence thought to be connected with Kisingiri volcano and is considered by the writer to be a satellite vent or offshoot related to the once extensive magma chamber beneath Kisingiri. The former presence of large magma chambers beneath these volcanoes are suggested by the vast volume of volcanic lavas associated with Kisingiri. Other carbonatite centres considered as satellite subsidiary cones connected with Kisingiri are briefly discussed below.

## 2.6 THE RURI CARBONATITE CENTRES.

Both the North and South Ruri carbonatite centres (Figure 2-3) are part of the so-called twin-carbonatite agglomerate centres, which have similar rocks and equally a similar history (Le Bas, 1977). It is possible that the two centres, which are well exposed, are contemporaneous and probably have a connection at depth, but on initiation and growth of the volcanoes each developed separately. Nepheline-syenite and ijolite are the earliest igneous rocks in the North and South Ruri centres, where they are observed to be cut by carbonatite. The igneous activity is thought to have started around 7-4 Ma (Le Bas, 1977). The two centres reveal well developed and prominent, mainly inward dipping dykes and cone-sheets of fine-grained calcite carbonatite and ferrocarnatite (Plate 2-2). As observed in other carbonatite centres, Ruri has an extensive development of pyroclastic deposits, comprising principally tuffs, agglomerates and breccias with lapilli tuff outcropping on the lower slopes of the volcanoes. They are often cross-cut by later calcite carbonatite and ferrocarnatite sheets and dykes (Plate 2-3). The different types of angular to sub-angular fragments identified in the pyroclastic deposits include Archean metabasalt, ijolite,

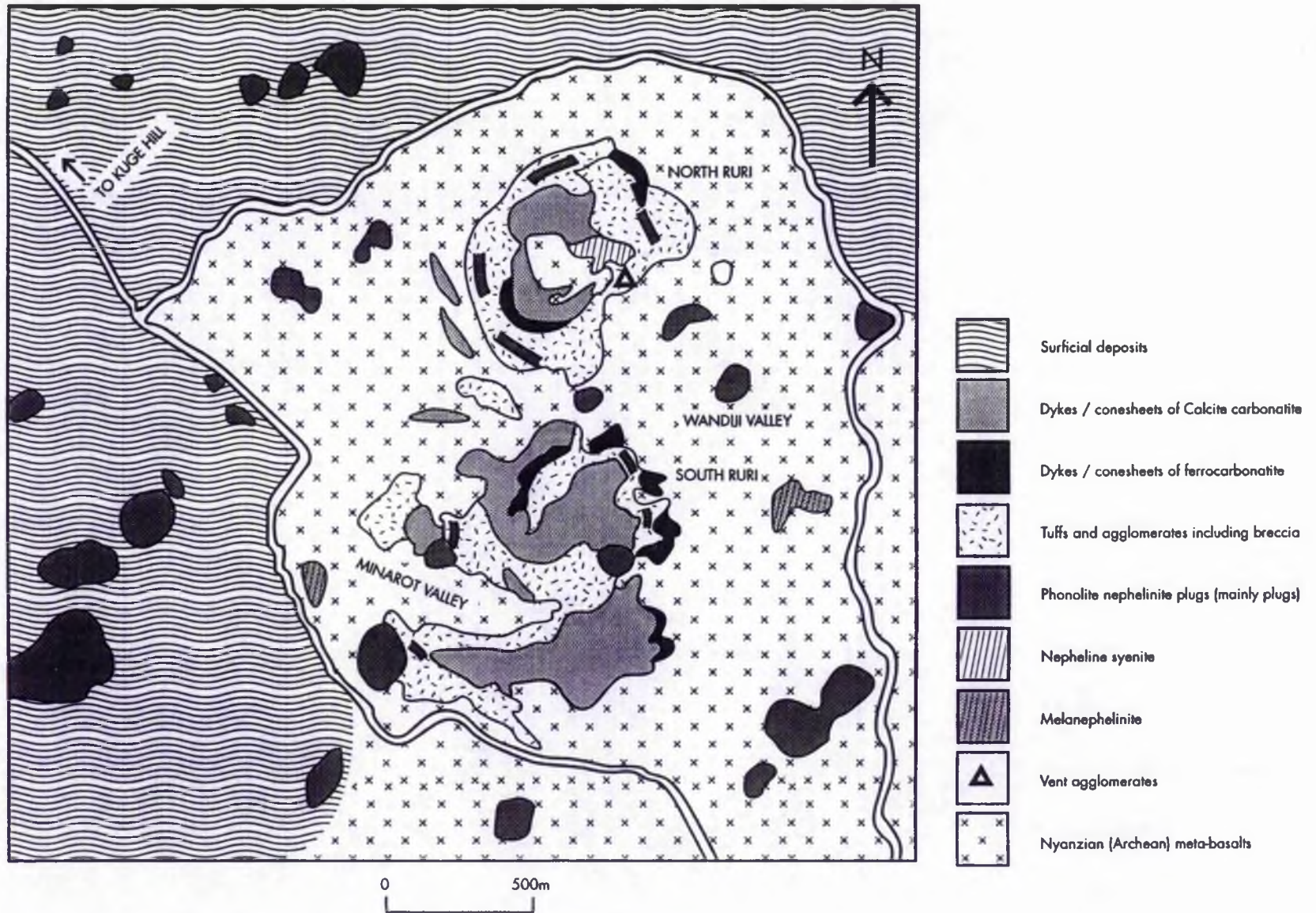


Figure 2-3 General Geological Map of Ruri Carbonatite Centres (simplified after Le Bas, 1972)



Plate 2-2 North Ruri carbonatite centre, viewed southwards from the top of the Kuge hill carbonatite. The photograph shows the prominent inward dipping cone-sheets and dykes of carbonatite.



Plate 2-3 South Ruri carbonatite. The lower slopes of the caldera is largely occupied by tuff sand agglomerates. To the north, a ferrocyanatite dyke cuts the pyroclastic deposits. The clear plug to the far north is a phonolitic plug.

nepheline-syenite and blocks of phonolite, nephelinite and carbonatite (Plate 2-4). The carbonatitic volcanoes were emplaced into fenitized Archaean basalts, whose remnants are found as shattered and brecciated pendants within the tuffs and agglomerates.

Three types of carbonatites are recognized: white, granular, coarse-grained and medium- to fine-grained calcite carbonatite and ferrocarnatite, which is composed of calcite impregnated with iron oxide as hematite. The carbonatite is dominantly composed of calcite and portrays a distinctive "vertical streaming" or "banding structure" produced either during emplacement or recrystallization of the carbonatite. The bands are composed mainly of magnetite and are often themselves invaded by different types of fragments (Plate 2-5). Other commonly observed minerals in thin-section in calcite-carbonatite include apatite, biotite and/or aegirine (Plates 2-6 and 2-7). There is evidence in South Ruri that the series of tuffs and agglomerates, calciocarnatite cone-sheets and dykes are repeated sequences in the early history of the volcanic complex, which are then invaded by ferrocarnatite sheets and dykes, often rich in magnetite octahedra.

The phonolite plugs associated with the carbonatites are very common in the Ruri hills, where they are observed to form numerous conical hills with rounded summits (Plate 2-8) with occasional minor dykes and flows. The majority of the phonolitic rocks are strongly porphyritic with phenocrysts of aegirine-augite, marginally zoned to aegirine, nepheline, sphene, iron ore and feldspar, all set in a fine-grained groundmass of fine alkali feldspar, nepheline and abundant aegirine (Plate 2-9). The age of the phonolite plugs, deduced by cross-cutting relationships with the carbonatites and pyroclastic rocks, is not clear. In some places, especially in the South Ruri caldera,



Plate 2-4 Bedded tuffs and agglomerates within the western side of the South Ruri caldera.



Plate 2-5 A finitized fragment of phonolite within the medium and coarse-grained calcite carbonatite at the South Ruri carbonatite centre.

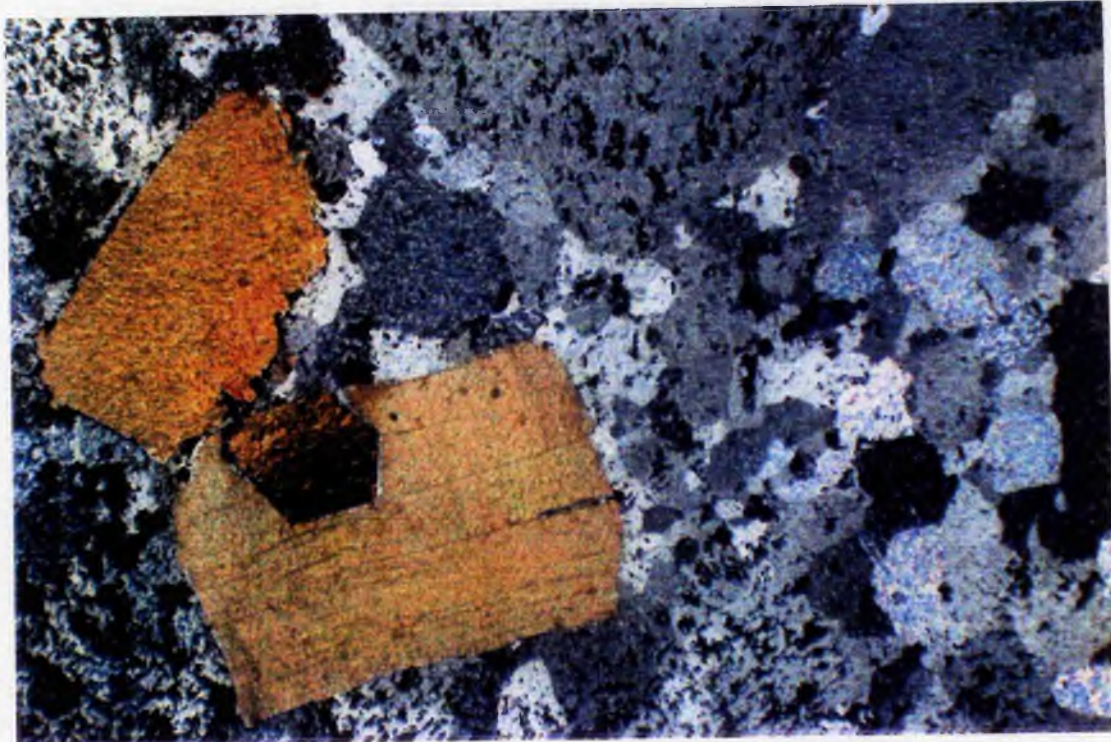


Plate 2-6 Large twinned rhombs of calcite carbonatite from North Ruri with disseminated magnetite. Note also the large euhedral crystal of biotite. Magnification x 20.

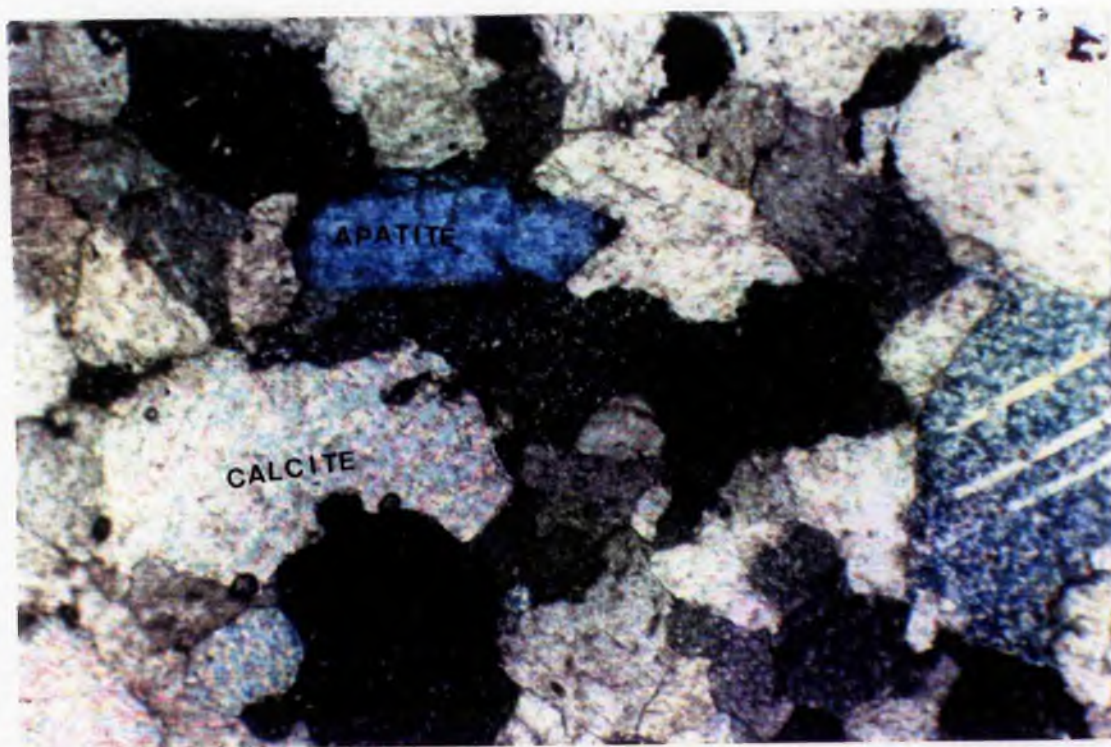


Plate 2-7 Euhedral crystal of hexagonal apatite and rhombohedral calcite in calcite carbonatite from North Ruri (NR-271) Magnification x 20.



Plate 2-8 Plugs of phonolite around the Ruri hills centre. Note the flourishing farming activities which utilize the rich phosphate soils derived from the weathering of carbonatite.

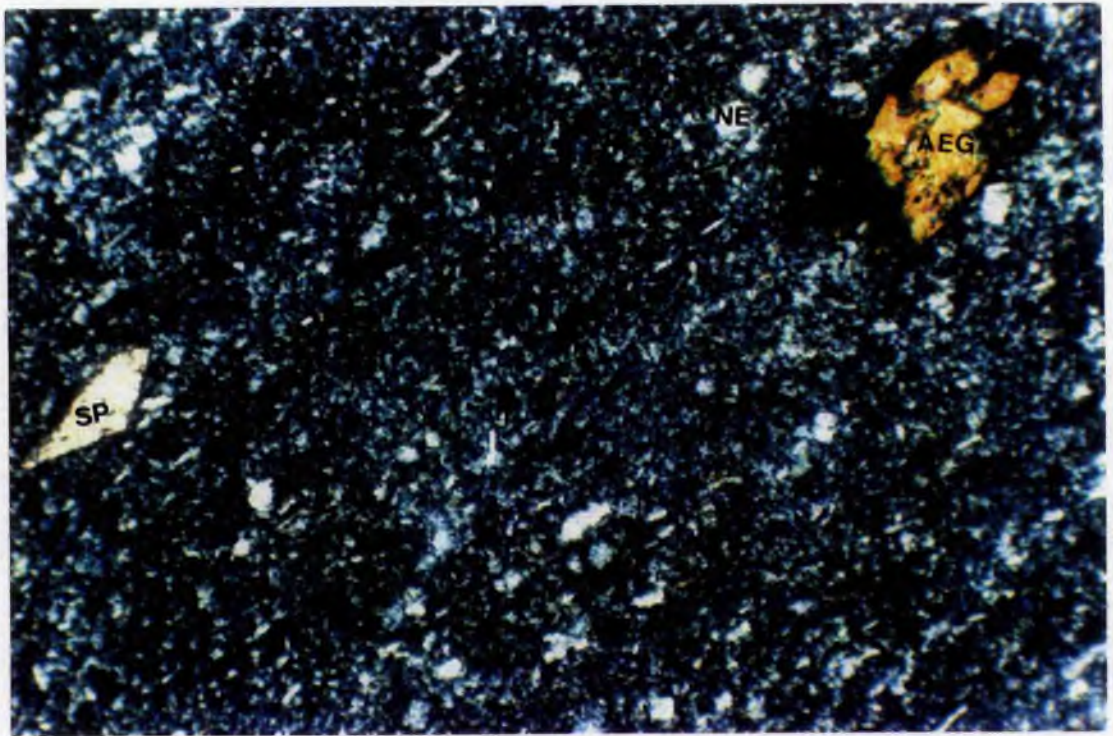


Plate 2-9 Phonolitic plug at South Ruri carbonatite. Nepheline (NE), aegirine-augite (AEG) and zoned sphene (SP) occur as phenocryst phases. Groundmass comprises of mainly nepheline and K-feldspar. Magnification x 10.

dykes of phonolite-nephelinite are seen cross-cutting the tuffs and agglomerates, while other intrusions show contrasting relationships in different parts of the complex. It is, however, possible that both the carbonate and silicate magmas, which produced the carbonatites and phonolite plugs, respectively, were available simultaneously, but not linked petrogenetically.

To the north of the Ruri hills, a number of small carbonatite centres are recognized (Figure 2-1 and Le Bas, 1977). These occurrences include Angalo, Sokolo, Kiyanga, Uyi, Ugongo and Ngou. The carbonatites are emplaced into Precambrian granodioritic rocks and contain both calcite carbonatite and ferrocarbonatite rock units, as well as the widespread occurrence of carbonatitic breccias and agglomerates. The Usaki ijolite complex, which is not intruded by the carbonatites, and the Nyamaji volcano dominate the scenery within the Wasaki peninsula.

## 2.7 THE HOMA MOUNTAIN CARBONATITE CENTRE.

Homa Mountain, the youngest centre of the Nyanza Rift carbonatite complexes, reveals an igneous history which is similar to that of the Ruri hills with the emplacement of silicate and carbonatite rocks during the Miocene and Early Pliocene (Le Bas, 1977). Homa Mountain, like the Ruri hills to the west, is not topped by a massive superstructure like that of the Kisingiri and Tinderet strato-volcanoes. According to King et al. (1972), Le Bas (1977) and Clarke and Roberts (1986), the main centre consists of complex multiple cone-sheets of mainly fine- to medium-grained calcite carbonatite and ferrocarbonatite with associated carbonatitic breccia invading shattered and fenitized Nyanzian metavolcanic country rocks (Figure 2-4). Fragments in the breccias are mainly Nyanzian and the matrix largely carbonatitic. Contemporaneous with the emplacement of the

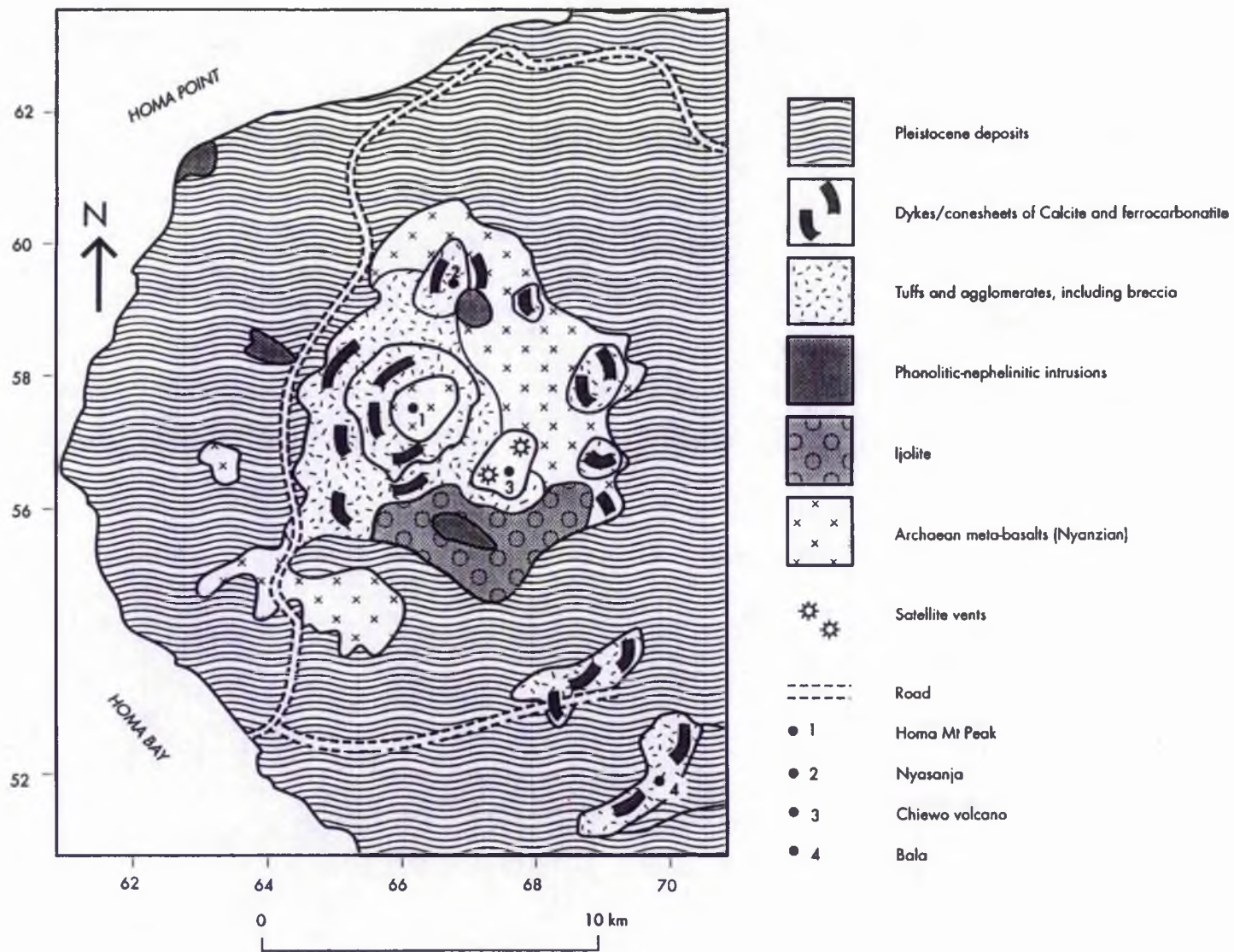


Figure 2-4

General Geological Map of Homa Mountain Carbonatite  
(simplified after Le Bas, 1977)

carbonatite cone-sheets was the intrusion of small satellite vents around the main Homa Mountain. The numerous vents, for example at Nyasanja and Bala among others (Le Bas, 1977), are also dominantly pyroclastic with two types of carbonate sheets and dykes intimately associated with alkaline-silicate rocks.

The late-stage igneous activity during the Pleistocene and Recent in and around the Homa Mountain centre is marked by the intrusion of small volcanic vents, for example at Chiewo which is also dominantly pyroclastic and contains two types (calcite and iron-rich) of carbonate sheets and dykes intimately associated with phonolites. The fine-grained, basalt-looking rock identified as melilitite by Le Bas (1977) at the Chiewo vents has been re-interpreted by Clarke and Roberts (1986), based on petrographic evidence as calcitized alkali carbonatite. It has, however, been noted earlier that without further chemical evidence on their transformation, these could possibly be interpreted as primary calcite carbonatite flows interbedded with the volcanic pyroclastic deposits. Present day activity is indicated by several hot springs found in most parts of Homa mountain.

## 2.8 TINDERET VOLCANO.

Towards the eastern end of the Nyanza rift and near the junction with the Kenya rift valley lies the Tinderet strato-volcano, which is spatially associated with the occurrence of satellite pyroclastic carbonatite vents of the Legetet, Songhor and Buru centres (Figure 2-5). Unlike Kisingiri, Tinderet does not reveal a central carbonatite complex. Only extrusive pyroclastic lavas are present; erosion has not been sufficiently extensive to expose any plutonic silicate-alkaline core and the same scenario applies at Mt. Elgon on the Kenyan-Ugandan border.

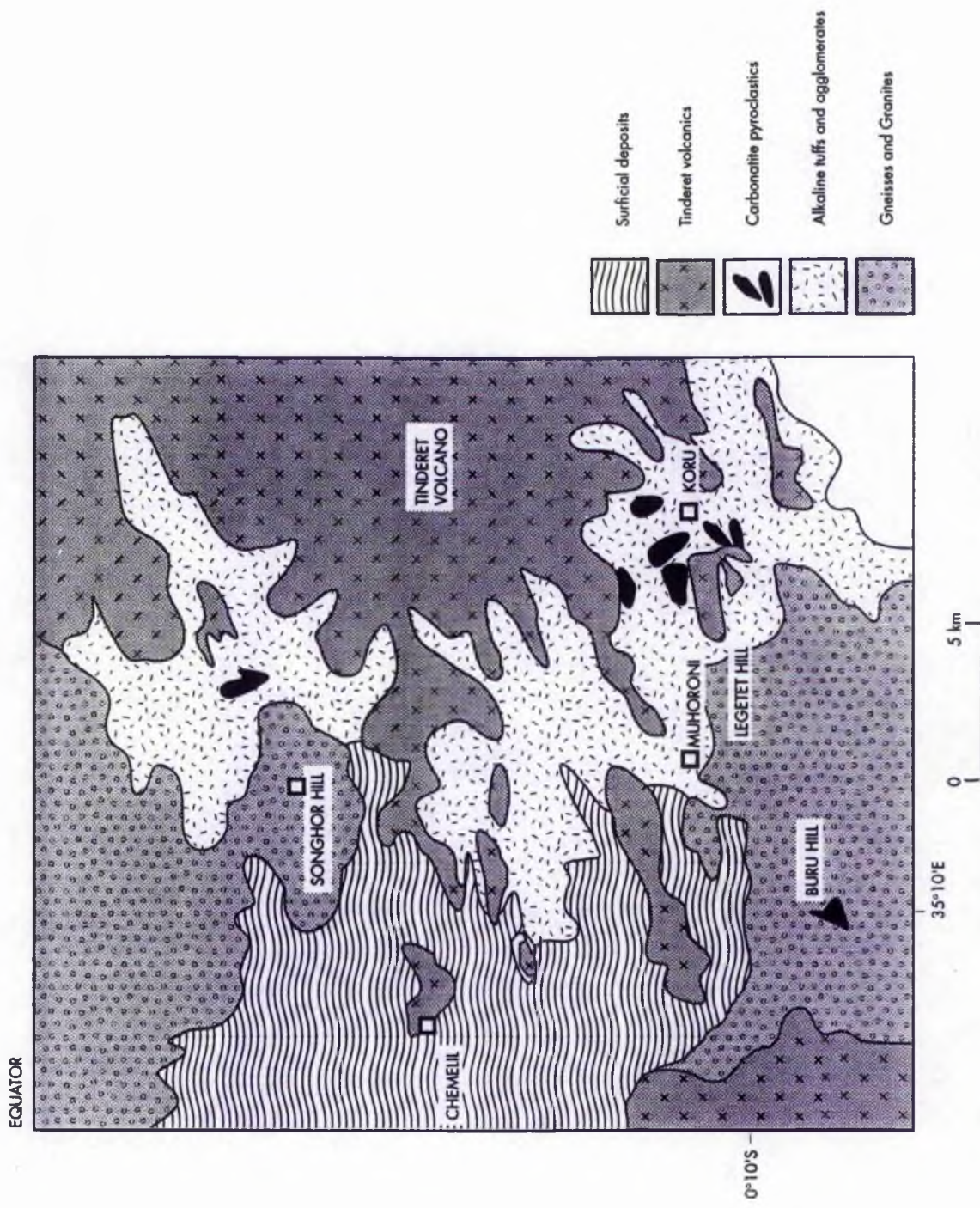


Figure 2-5 General Geology of Legelet Carbonatite Centre (simplified after Binge, 1962)

Tinderet volcanism (King et al., 1972 and Jones and Lippard, 1979), like that of Kisingiri, commenced in the Lower Miocene, as determined by Bishop et al. (1969), with extrusion of nephelinites and carbonatites during the early stages followed by extensive extrusion of basalt-nephelinite-phonolite-basanite lavas, presumably belonging to the basalt-nephelinite association of the Kenya rift (Le Bas, 1987).

Extrusive volcanic carbonatites that outcrop on Legetet hill are centred on "Limestone Hill", where a number of quarries are worked by the Homa Lime Co. and processed by wood-fired kilns into lime. Legetet is thought to be connected with the Tinderet volcano and is viewed as a satellite cone which developed on the lower flanks of the volcano. The stratigraphic succession at Legetet and Koru according to Binge (1962) is shown in Table 2-1.

Table 2-1 Stratigraphic succession at Legetet and Koru.

Age	Rock Unit	Rocks
Middle and Upper Miocene	Tinderet volcanics	Nephelinitic lavas and basanites
Lower Miocene	(ii) Walker "Limestone"	Water-lain bedded carbonatitic tuffs and volcaniclastics
	(i) Legetet Formation	Carbonatitic tuffs and agglomerates
19.5-19.6 Ma	Koru Formation	Fine-grained altered tuffs
23.5-23.6 Ma	Muhoroni Agglomerates	Coarse agglomerates
600-1000 Ma	Basement (Mozambique)	Gneisses and granites

The tuffs and agglomerates of the Legetet Formation are typically grey-brown in colour with crude horizontal bedding and numerous enclaves of basement rocks and carbonatite. The most common enclaves are of fenitized basement gneisses, which appear to be strongly hydrothermally altered and kaolinized (Plate 2-10). Some less altered basement enclaves still show the gneissic texture of the basement rocks.

The carbonatite fragments consist mainly of medium- to coarse-grained, fresh magnetite-bearing sövitic carbonatite. There are also blocks or bombs of carbonatite lavas, now consisting of calcite in which Deans and Roberts (1984), on the basis of petrographic evidence, considered the tabular calcite to be the product of secondary supergene calcification of natrocarbonatite. Minor small dykes and flows of fine-grained carbonatite lavas are frequently observed within the pyroclastic carbonatitic tuffs and agglomerates. The tuffs and agglomerates overlie, or merge laterally into, well-bedded fine- to medium-grained tuffs (Walker Formation) with small-scale graded bedding. These bedded volcanoclastic carbonate sediments are thought to be largely waterlain and probably represent lapilli tuffs and reworked material of the Legetet volcanics. Interbedded with the tuffs and agglomerates and the volcanoclastic sediments are beds of red marl which are exceptionally rich in fossils, including numerous vertebrate species and gastropods. Both units are also cut by alnöitic dykes. The presence of these ultrabasic dykes in a very shallow environment seems interesting, especially in regard to source, depth and the transport of the magma in relation to the origin of carbonatite melt.



Plate 2-10 Carbonatite tuffs and agglomerates with rounded and kaolinized basement enclaves from Legetet carbonatite centre.

## 2.9 DISCUSSION.

The existence of low-viscosity carbonatite melts under very low pressures and temperatures have been experimentally demonstrated to occur on the earth's surface (Cooper et al., 1975). Keller (1989) and Gittins and Jago (1991) have argued against considering most of the tabular calcite crystals observed in sub-volcanic carbonatite complexes to be pseudomorphs after nyerereite. It is also possible that the tabular calcite crystals in Koru and Homa mountain, which have been considered to be the product of calcification of former nyerereite (Deans and Roberts, 1984) and (Clarke and Roberts, 1986) respectively, could be interpreted as primary calcite carbonatite flows interbedded with tuffs and agglomerates. Pseudomorphs after nyerereite were not recognized by Armitage (1995) on a number of thin-sections studied from Legetet. Armitage (1995) regarded the Legetet carbonatite lavas as primary examples of calcite carbonatite flows.

Carbonatites have been considered to be high level, late differentiates, especially in nephelinitic-carbonatitic rock associations (Le Bas, 1977). In Koru, carbonatites seem to represent the earliest local volcanic activity based on a number of age determinations (Bishop et al., 1969 and Jones and Lippard, 1979) and observations on a number of holes drilled through the pyroclastic carbonatites within Legetet hill, where they were noted to comprise the first volcanic activity but later than the Tinderet volcanics (Alviola et al., 1985). In Rangwa, some carbonatites were equally noted to be associated with the early volcanic activity before the voluminous eruptions of the Middle Kisingiri Pyroclastic and Upper Kisingiri Lava Groups of McCall (1958). Table 2-2 compares the evolution of the the Kisingiri and Tinderet volcanoes.

Table 2-2 A comparison between the Kisingiri and Tinderet volcanoes.

<u>Kisingiri</u>	<u>Tinderet</u>
Located at the western end of the Nyanza rift.	Located at the eastern end of the Nyanza rift.
Evolution began with highly under-saturated volcanics with abundant pyroclastics, alkaline intrusives and carbonatite during the Lower Miocene.	The same evolutionary trends as Kisingiri.
Early Kisingiri volcanics contains a variety of pyroclastics and sediments where Lower Miocene fossil assemblages have been found.	Fossil assemblages intercalated near the base of the Koru beds gives a Lower Miocene age.
Volcanic activity accompanied by the continued build up of Kisingiri extended between 20-14 my.	Volcanic activity continued up to the Pliocene (5 my).
Erosion of the volcanics has revealed the Rangwa carbonatite complex.	Erosion has not been extensive enough to reveal carbonatite at depth.
Kisingiri belongs to Group II nephelinites.	Tinderet belongs to Group I nephelinites.

## 2.10 CONCLUSION.

The evolution of the Kisingiri and Tinderet volcanoes probably began with the production of undersaturated alkaline silicate rocks and possibly ended with extrusion of a series of carbonatite pyroclastic and intrusive events. The carbonatite volcanism can either be earlier, as shown in Tinderet, or

late, as exemplified by the Rangwa caldera which appears to occur at the end of the volcanic history of Kisingiri. The nephelinite dykes are not seen cutting the Rangwa caldera, as are other Kisingiri lavas. It is likely, however, that the production of silicate lavas and the carbonatite pyroclastic volcanism could be contemporaneous. The Ruri hills, Rangwa, Homa mountain and Legetet have extensively developed pyroclastic deposits, including tuffs, tuff-breccia, agglomerate and lapilli tuffs. The pyroclastic deposits are intimately associated with sheets and dykes of carbonatite, which frequently truncate the pyroclastic sequences.

Since the same sequence is repeated in all the carbonatite centres, it is assumed that the physical processes in the magma chambers feeding the centres were the same and therefore a similar volcanic evolution is proposed in order to explain the intimate relationships between the tuffs, breccias, agglomerates and the intrusive suite of carbonatite dykes and sheets that are characteristic within the Nyanza rift carbonatites. The proposed volcanic evolution is as follows:

- i) Early development of most products of carbonate magmas, such as carbonate tuffs, agglomerates, breccia and/or blocky lavas. The productions of these magmas is assumed to have been explosive as even the breccias themselves are further brecciated. It is possible that the eruptions were very explosive with CO<sub>2</sub> gas emissions due to decarbonation on approaching the earth's surface.
- ii) The introduction of carbonate magmas which intruded their own volcanic pile. Both carbonate magmas (iron-poor and iron-rich) were available simultaneously and at the same time as the silicate magmas which produced the phonolite-nephelinite plugs that are very common in these complexes.

iii) The extrusion of lava flows, mainly nephelinitic in composition, as seen in Kisingiri and Tinderet. Part of the early flows were, however, earlier or contemporaneous with the two stages above.

Erosion and repeated sequences, especially of tuffs and agglomerates and the carbonatite dykes and sheets, were common phenomena, as noted in these centres. Rangwa and the Ruri hills, unlike Kuge and Buru (see chapters 3 and 4) developed elaborate and numerous cone-sheets and dykes of carbonatite, which acted as a cover and prevented erosion removing part of their volcanic superstructure.

The association of carbonatites with the alkaline-silicate rocks is apparent. Field evidence has shown that the lithological units observed in western Kenyan carbonatite complexes may be related to either their erosional or emplacement level. Alkaline carbonatite centres range from deep-seated plutonic to sub-volcanic and volcanic complexes. Western Kenyan carbonatites may be described as shallow-seated volcanic centres. These centres will be seen in subsequent chapters to be affected by low-temperature hydrothermal alteration and supergene weathering processes, which contribute significantly to the distribution and variation in rare earth mineralization and stable isotope geochemistry. Figure 2-6 shows a schematic distribution of lithologic units encountered in western Kenyan volcanic carbonatites and their approximate levels of erosion.

The emplacement levels of the carbonatite complexes Ruri, Homa and Rangwa (shown in Figure 2-6) are relative and are only presented to serve as a working model for the understanding of ideas developed in this thesis. Field observations based on the distribution of lithological units discussed in this chapter support the proposed model. The estimated emplacement level

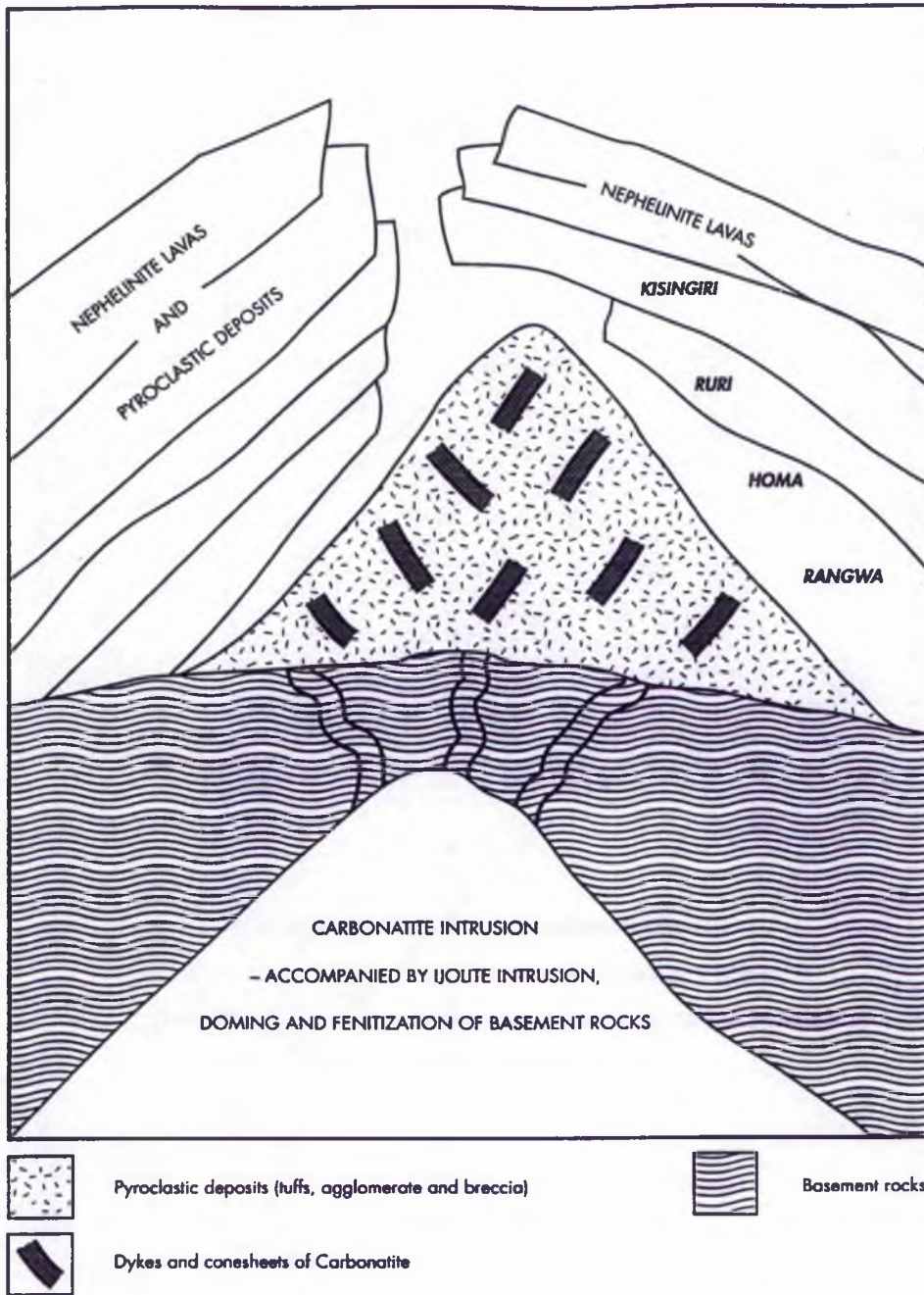


Figure 2-6

Schematic cross-section of an idealised carbonatite-ijolite-nephelinite volcanic complex and relative levels of erosion of Ruri, Homa and Rangwa (Modified from Le Bas, 1977)

for the Kuge carbonatite complex is thought to be higher than the Ruri, Homa and Rangwa complexes because the superstructure in Kuge is not preserved. The superstructure is thought to have been removed earlier because of its shallowness relative to other complexes. The early eruptions of the Kisingiri lavas is also thought to have covered the Ruri hills and Kuge. It is however unlikely that the Homa mountain carbonatite complex was covered by Kisingiri lavas. The relative emplacement levels for the Kuge and Buru volcanic centres obtained through their rock distributions is discussed in chapters 3 and 4.

## CHAPTER THREE

### GEOLOGY OF THE KUGE CARBONATITE CENTRE

#### 3.1 INTRODUCTION.

Kuge hill (Figure 3-1), situated to the north of the Ruri carbonatite centres, was emplaced into Archaean metabasalts. The general geological setting of the Kuge carbonatite centre has been summarized by McCall (1958), Dixon (1968), Le Bas (1977) and the reports compiled by JICA (JICA Reports, 1987-1990). McCall (1958) recognized the highly anomalous radioactivity connected with the Kuge carbonatite and suggested that it was similar to Mrima hill, a rare-earth enriched carbonatite located in Coast Province, Kenya. The Japanese-Kenyan geological team confirmed the occurrence of high REE contents within the the Kuge hill and high radioactivity was found to be related to the occurrence of thorium. Lanthanide mineralization at Kuge hill will be discussed in detail in chapter 8.

#### 3.2 GEOLOGICAL SETTING OF THE KUGE CARBONATITE.

The Kuge carbonatite centre, like the Ruri carbonatite centres, is composed mainly of small cone-sheets of calcite carbonatite and a ferrocarnatite dyke, which occurs on the eastern side of the hill (Figure 3-2). Calcrete formation, a normal supergene process associated with many carbonatites, is characteristic in Kuge. The fragments within the calcrete are cemented together by fine-grained carbonate ash. The calcite carbonatite and the ferrocarnatite breccia, which are characteristic rock types in Kuge hill, are briefly described below.



Figure 3-1 The Kuge hill carbonatite centre, viewed northwards from North Ruri. Clear central areas of the hill are composed of Nyanzian metabasalts.

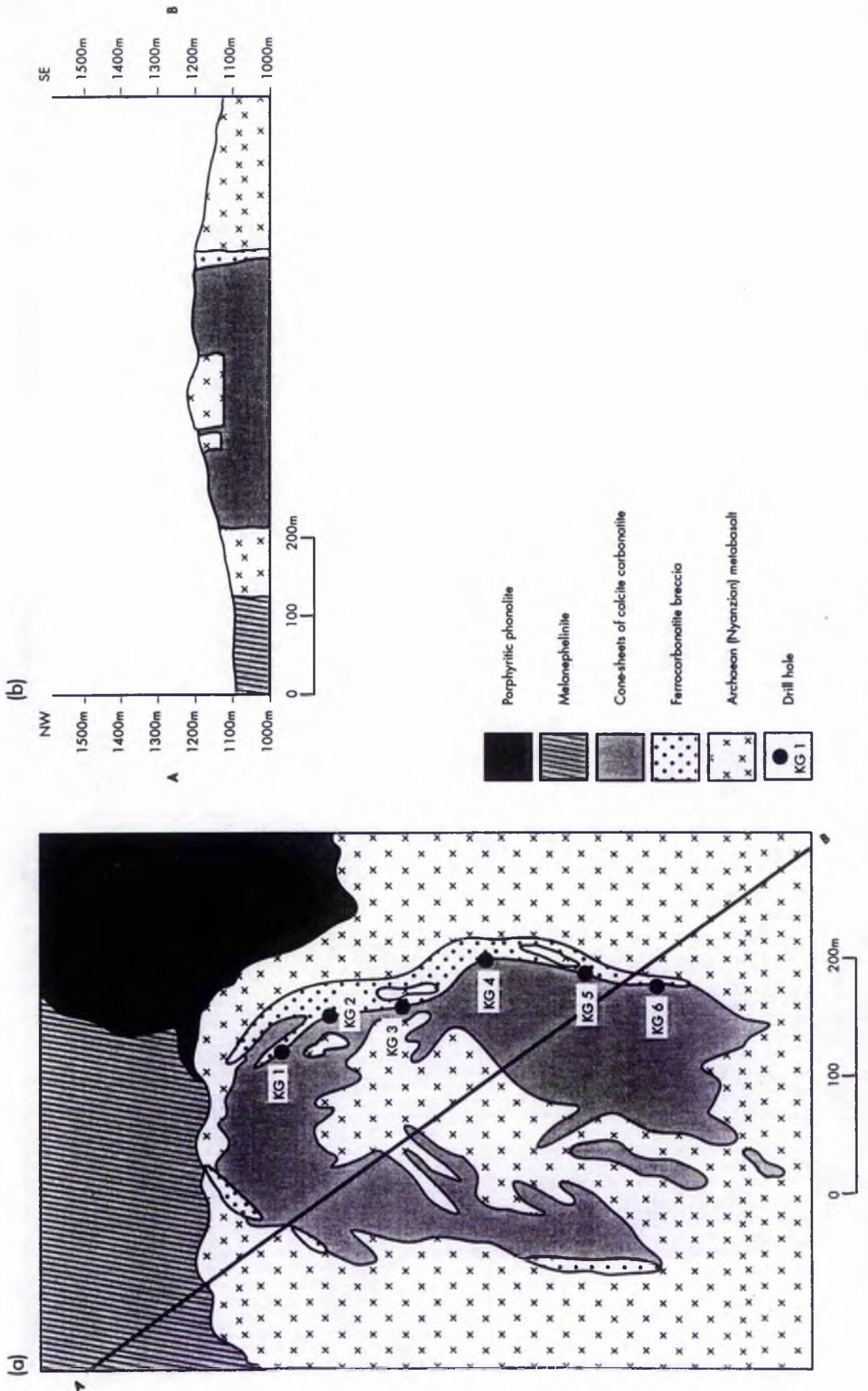


Figure 3-2 (a) Geological map of Kuge carbonatite (b) Cross-section along A — B

### 3.3 CALCITE CARBONATITE.

The calcite carbonatite (alvikite; Le Bas, 1977) is a fine- to medium-grained carbonatite with a distinctive cream-brown colour due to a weathering effect caused by the different degrees of oxidation of magnetite. It occurs as thin or multiple dykes or cone-sheets. The cone-sheets dip either inwards or outwards with dips varying from 30-80°. The calcite carbonatite usually contains magnetite, apatite and phlogopite. Apatite frequently occurs as folded sequences within the calcite carbonatite (Plate 3-1). The occurrence of phlogopite is also common (Plate 3-2) towards the contact of the flow-folded calcite carbonatite with the ferrocarbonatite breccia. The presence of phlogopite in calcite carbonatite at the margins of the ferrocarbonatite dyke is considered by the writer to be due to hydrothermal alteration by iron-rich fluids derived from the ferrocarbonatite during emplacement.

Magnetite octahedra commonly occur in "streams" (Plate 3-3) and sometimes are observed to occur as aggregates of magnetite within the calcite carbonatite cone-sheets (Plate 3-4). It is possible that these magnetite aggregates ('clots') could be magnetite cumulates.

According to Le Bas (1977), the Kuge calcite carbonatite is petrographically very similar to those of the Ruri hills. In thin-section, the calcite carbonatite shows equigranular and fine-grained texture (0.1-2 mm) and consists of over 90% calcite. The calcite commonly reveals a rhombohedral outline, even if there has been extensive crystallization (Plate 3-5). Accessory minerals that frequently accompany calcite in most of the thin-sections studied include magnetite, apatite, phlogopite and rarely fluorite, barite and aegirine-augite. It is difficult to confirm the nature of these minerals as either primary or secondary, though magnetite and apatite are thought to be primary, based on their mode of occurrence.



Plate 3-1 Flow-folded calcite carbonatite at the Kuge carbonatite centre.



Plate 3-2 Phlogopite flakes (small reflective mineral) in calcite carbonatite. Note the pitted and grooved texture of carbonatite due to weathering.



Plate 3-3 Magnetite octahedra trails in calcite-carbonatite, Kuge hill.



Plate 3-4 Magnetite aggregates in calcite carbonatite, Kuge hill.

### 3.4 THE FERROCARBONATITE BRECCIA.

The fine-grained, dark to brown ferrocarnatite breccia located mainly on the eastern side of the hill also forms multiple swarms of thin sheets and dykes cutting the calcite carbonatite (Figure 3-2). Segments of ferrocarnatite breccia are noted in the north-west and west of the hill (Figure 3-2). On the surface, the ferrocarnatite breccia is characterized by trails of magnetite octahedra and enclaves of Archaean metabasalt. Thin veinlets of hematite and phlogopite are also common (Plate 3-6). These hematite stringers are very similar to the iron-rich rodberg described by Andersen (1987) from the Fen complex, south-east Norway.

X-ray diffraction and the petrography shows that this ferrocarnatite breccia consists mainly of calcite with accessory barite, magnetite, fluorite, mica and iron hydroxides/oxides. The presence of iron-bearing carbonates as either siderite or ankerite was not confirmed. It is possible that this rock unit was initially either an iron-bearing carbonatite containing ankerite or siderite, or a calcite carbonatite but now altered by progressive introduction of  $Fe^{3+}$  into these earlier carbonate phases during post-hydrothermal oxidation processes, as Andersen (1984) has suggested for the rodberg from the Fen complex. As suggested earlier by the writer, the term ferrocarnatite will be retained and used only for carbonatites that are enriched in iron compounds. Different colours usually noted in these iron-rich carbonatites are due to the varying degrees of oxidation of iron compounds during weathering.

The major element geochemistry of the two rock units (ferrocarnatite breccia and calcite carbonatite from Kuge hill) is shown in Table 3-1 below. The data is compared with analyses given by Le Bas (1977) and by recent Japanese and Kenyan Government teams.

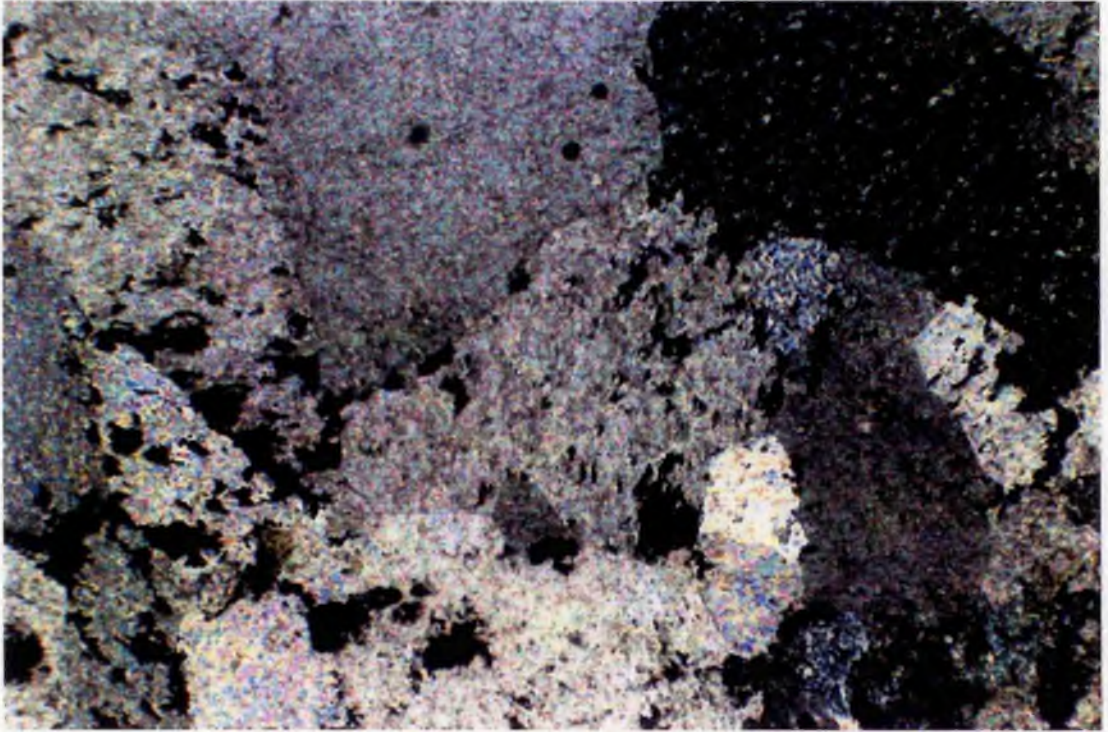


Plate 3-5 Calcite carbonatite (Kuge hill). Note large rhombs of calcite with magnetite and a few flakes of phlogopite.



Plate 3-6 Trails of hematite veins traversing a ferrocyanite breccia.

Table 3-1 Major element analyses of ferrocarnatite breccia and calcite-carbonatite from the Kuge hill.

Analysis	A	B	C	D	E
SiO <sub>2</sub>	1.55	4.17	0.66	2.52	1.57
Al <sub>2</sub> O <sub>3</sub>	0.61	1.02	3.12	1.10	0.57
Fe <sub>2</sub> O <sub>3</sub>	23.34	27.35	3.96	3.16	2.26
MgO	0.48	0.78	0.5	0.42	0.46
CaO	24.99	25.37	48.89	50.52	52.69
Na <sub>2</sub> O	0.10	0.09	0.41	0.21	0.25
K <sub>2</sub> O	0.06	0.59	0.00	0.10	0.13
TiO <sub>2</sub>	0.05	0.15	0.36	0.05	0.06
P <sub>2</sub> O <sub>5</sub>	1.66	0.91	1.70	0.54	0.33
MnO	5.18	5.46	0.31	1.00	0.56

Oxide values in wt %.

A (this study): Ferrocarnatite (average of 4 analyses) ICP- Royal Holloway and Bedford New College, University of London.

B (Japanese-Kenyan study): Ferrocarnatite (1 analysis) ICP-Tokyo, Japan.

C (Le Bas, 1977 page 318 ): Ferrocarnatite.

D (this study): Calcite carbonatite (average of 2 analyses) XRF-St Andrews University.

E (Japanese-Kenyan study): Calcite carbonatite (alvikite) ICP-Tokyo, Japan.

The analysis of ferrocarnatite obtained during this study is similar to that obtained by the Japanese-Kenyan investigation but is quite different from that presented by Le Bas (1977), especially in terms of FeO, MnO and CaO contents (Table 3-1). The FeO, MnO and CaO contents obtained during this study is comparable to averages and ranges of ferrocarnatites given in Woolley and Kempe (1989). The CaO and especially low FeO and MnO

contents given in Le Bas (1977) are unlikely to be representative ferrocarbonatite analyses. Chemically, the ferrocarbonatite breccia in Kuge hill can be distinguished from calcite carbonatite in terms of its FeO, MnO and CaO contents. Ferrocarbonatite is characterized by high contents in FeO and MnO and low values in CaO, whereas the calcite carbonatite has higher CaO contents and lower FeO and MnO contents. The ferrocarbonatite breccia at Kuge is also enriched in incompatible elements such as rare earths, Ba and Nb. A chemical classification of both the ferrocarbonatite breccia and calcite carbonatite is presented in chapter 6.

The ferrocarbonatite breccia at Kuge hill was the subject of detailed diamond drilling by the Japanese-Kenyan exploration team in which six drill holes were sunk along the exposed dyke breccia. Details of mineralogy, geochemistry and rare earth mineralization will be discussed in subsequent chapters. Observations of drill cores along the whole length reveal the pyroclastic nature of the carbonatite. The fragments within the unit are mainly Archean metabasalts that prominently show reaction rims, indicating that the carbonatite magma was out of equilibrium and had reacted strongly with the surrounding country rocks. Phlogopite was also noted in most of the drill-core sections studied. The ferrocarbonatite breccia is also cut by fenitized dykes of porphyritic phonolite.

A representative geological description of drill hole KG-2 (Figure 3-2) is given in Table 3-2.

Table 3-2 Summary of the geology in drill hole KG-2 from Kuge Hill.

Depth (m)	Geological description.
0 - 2	Calcrete which contains different fragments of carbonatite and meta-basalt.

Table 3-2 continued.

Depth (m)	Geological description.
2 - 36	An extensive brown, fine- to medium-grained and partly banded ferrocyanatite breccia. Some sections of the banded ferrocyanatite breccia are strongly magnetic. 90% of the fragments in the ferrocyanatite are dominated by metabasalt that is strongly feldspathized. Veinlets of <1 m of metabasalt are common within the cyanatite breccia.
36 - 60	Fine- to medium-grained weathered porphyritic phonolite.

In thin-section, the recrystallized ferrocyanatite breccia is dominated by calcite, which often shows a rhombohedral structure (Plate 3-7). Magnetite is common in most sections studied. Accessory minerals include apatite and phlogopite.

### 3.5 OTHER ROCK UNITS IN KUGE.

The central part of the Kuge cyanatite centre (Figure 3-2) is occupied by fine-grained Archaean (Nyanzian) metabasalts. The metabasalts occur as large pendants and enclaves within the sheeted dyke complex. The Nyanzian metabasalts are compact, bluish-green in colour and fine-grained in texture. In thin-section, the Nyanzian rocks consist mainly of plagioclase feldspar and augite with a few grains of iron ore and minor quartz within a fine-grained matrix, essentially composed of the same minerals. Carbonate traversing the metabasalts is common in most thin-sections studied (Plate 3-8). The Nyanzian metabasalts have also been fenitized by the fluids derived from the cyanatites.

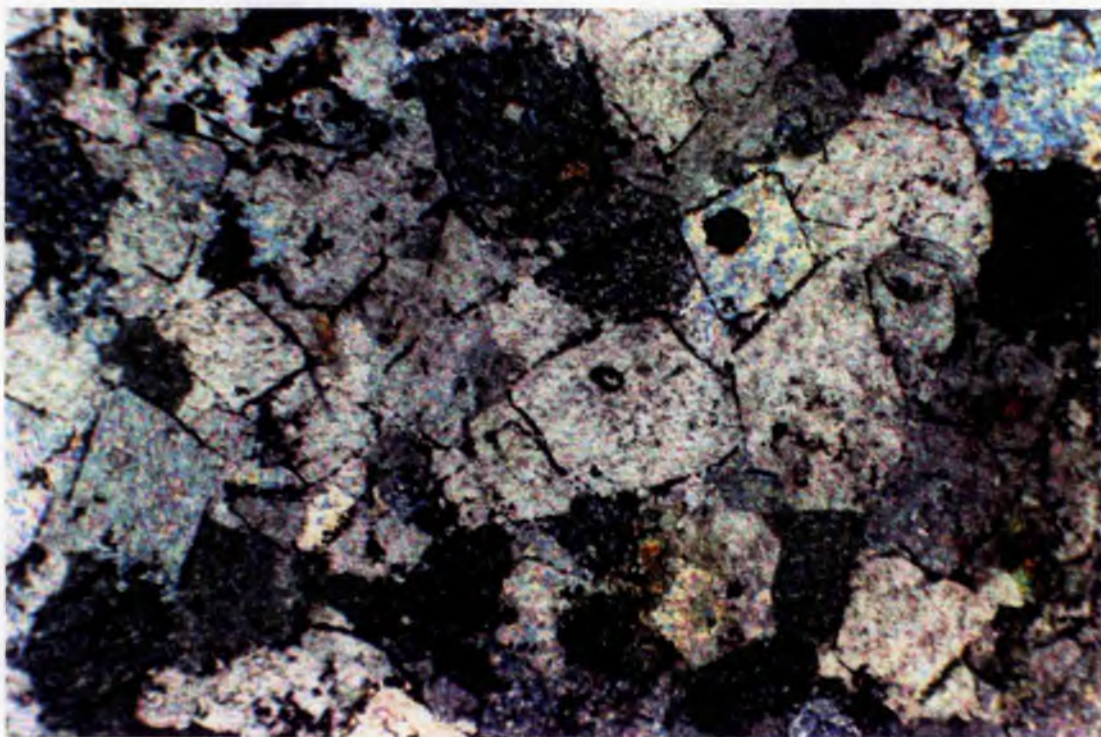


Plate 3-7    Recrystallized ferrocarbonatite breccia (Kuge hill).  
Euhedral calcite with magnetite concentrating at the edges of calcite.  
Flakes of phlogopite are also common.

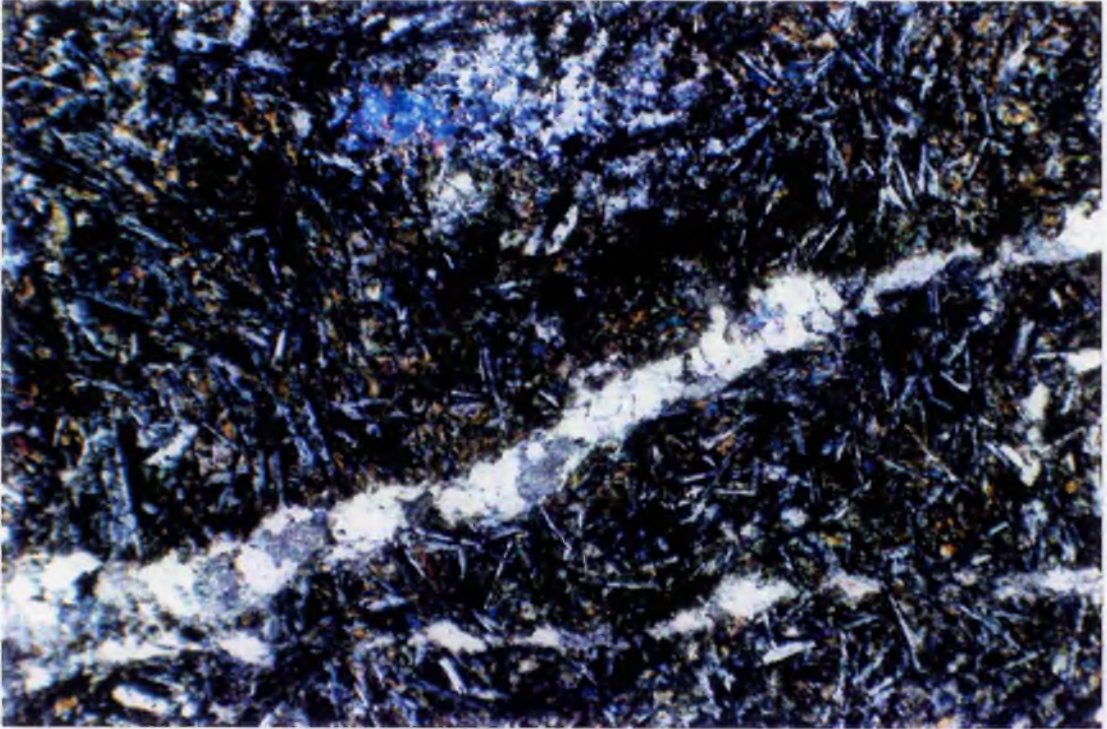


PLATE 3-8. Fenitized Archaean (Nyanzian) meta-basalt. The section is composed of clinopyroxenes and laths of plagioclase feldspar with minor iron-oxides. Note prominent cross-cutting veins of carbonate. Magnification x 10.

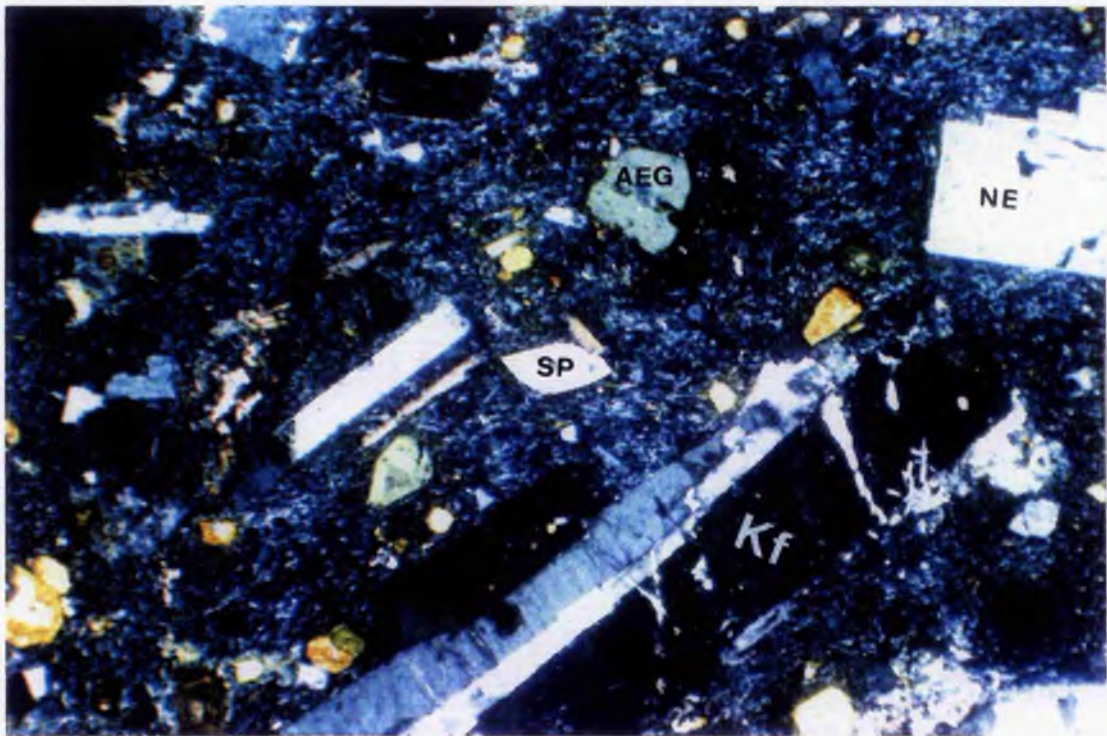


PLATE 3-9. Porphyritic phonolite showing phenocrysts of K-feldspar (Kf) with Carlsbad law twinning, nepheline (NE), aegirine-augite (AEG) and sphene (SP) in a matrix composed of the same minerals. Magnification x 10

Adjacent to the Kuge carbonatite centre lie two types of lava flows. Melanephelinite lava and agglomerates occupy the north-north-west section of the hill. The lavas are thought to be derived from the Kisingiri volcano and according to McCall (1958) the lavas are older than the Kuge carbonatite. Outcrops of phonolitic rocks, which can be correlated with similar lavas of the Nyamaji area, occur on the east and north-east side of Kuge. The lavas are typically light green and show phenocrysts of feldspar and nepheline. In thin-section the feldspar phenocrysts commonly show Carlsbad twinning. The feldspars are mainly fresh with minimal noticeable alteration. There are abundant phenocrysts of nepheline and pyroxene, zoned with cores of light green aegirine-diopside and outer rims of aegirine (Plate 3-9). Spene is also present.

### 3.6 SUMMARY.

The volcanic superstructure, comprising a network of carbonatite dykes and cone-sheets cutting the pyroclastic deposits (tuffs and agglomerates or breccia), is not preserved in Kuge. Only dykes and sheets of calcite carbonatite and ferrocarbonatite remain in Kuge. Most of the pyroclastic deposits could possibly have been removed by erosion. The relative emplacement level of Kuge and that of Buru is schematically shown at the end of chapter 4.

## CHAPTER FOUR

### GEOLOGY OF THE BURU HILL CARBONATITE

#### 4.1 INTRODUCTION.

The regional geology of the basement rocks adjacent to Buri hill was mapped in detail by Binge (1962). Shackleton (1951) noted the banded nature of Buru and interpreted the hill as being the gossanous cover of a pyritic sulphide body. Later investigation of the hill, including airborne scintillometer and diamond drilling, was carried out by New Consolidated Gold Fields Ltd (unpublished report by Cluver, 1958). Detailed diamond drilling intercepted carbonatite at depth and hence established Buru hill as being a carbonatite complex. Deans and Roberts (1984) noted Buru hill as being the only intrusive carbonatite occurring at the eastern end of the Nyanza rift. They considered the Buru carbonatite centre to be associated with similar eruptions in the Tinderet area, including the Legetet carbonatite where widespread deposits of carbonate pyroclastics have been identified.

Recently, the Metal Mining Agency of Japan (MMAJ), on behalf of JICA and the Mines and Geological Department, Ministry of Environment and Natural Resources, Government of Kenya, carried out joint geological mapping, geochemical and drilling surveys (JICA reports, 1988-1990) in the Buru carbonatite centre. Thirty vertical drill holes totalling 1,750 m (50 m x 27 holes, 100 m x 2 holes and 200 m x 1 hole) were implemented in Buru during the joint exploration programme. The hill was found to be enriched in lanthanide mineralization and dominated by the fluorocarbonates (bastnaësite, synchysite and parisite) and phosphates (monazite and apatite). The lanthanide mineralization is discussed in detail in chapter 8.

#### 4.2 STRUCTURAL SETTING AND BASEMENT GEOLOGY.

The Buru carbonatite centre was emplaced into a narrow zone of sheared Proterozoic gneisses whose margins have been extensively fenitized (Figure 4-1). The shear zones on the north-west side of Buru hill appear to pass both to the east and west of the hill and trend between  $330^{\circ}$  and  $340^{\circ}$ . Dips are apparently steeper to the west ( $>50^{\circ}$ ) and shallower to the east ( $<30^{\circ}$ ). On the south-east margin of the hill, the pale quartzofeldspathic gneisses observed have a strong linear fabric and a much more heterogeneous state of deformation. The trend here is at  $030^{\circ}$  with a crude spaced foliation dipping  $75^{\circ}$  to the south-east and a strong linear fabric plunging towards  $058^{\circ}$ . This trend is at right angles to the main shear zones that bound the Buru hill carbonatite and could possibly represent a late-stage cross-cutting transcurrent shear zone.

The  $030^{\circ}$  trend is also the orientation of the main Kendu-Kaniamiwa boundary fault on the southern side of the Nyanza rift. These two structures are possibly very widely different in age, but still may be related. The main shear zone where Buru is situated is almost certainly an extension of the Aswa shear zone (Nandi fault) and although not directly dated, the probable age of this ductile deformation, which took place at moderately deep crustal levels, would be between 600-630 Ma (Mosley, personal communication, 1992).

Between the ductile shear zones (15-30 m wide), the ortho-gneisses are less strongly deformed and in general have a relict igneous texture in spite of being metamorphosed and partially recrystallized. The two most common lithologies are quartz-feldspar gneisses, probably granitoids originally, and a more hornblende- and biotite-rich lithology, possibly originally granodioritic or dioritic in composition. Frequent occurrences of

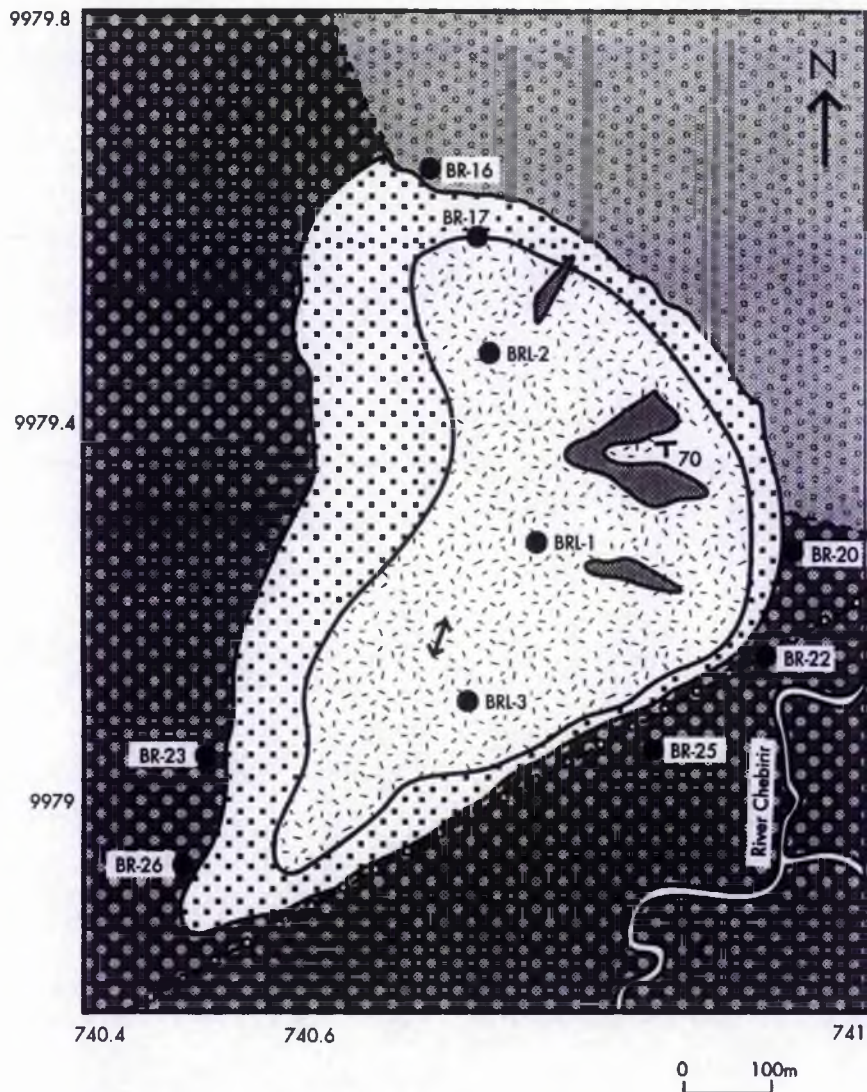


Figure 4-1 Geological Map of Buru Hill Carbonatite



Hematite veins



Lateritized carbonatite tuff



Fenite



Less deformed granitic gneisses



Sheared and strongly deformed granitic gneisses



Fault



Drill hole



Exploration adit

pegmatitic veins, quartz veins and narrow dolerite dykes are also notable within the basement rocks.

The ductile shear zones are strongly deformed. The shear zone observed along the river on the western side of the Buru carbonatite is at least 30 m thick and a dextral sense of shearing is most common. The flattened and ribbon-like quartzofeldspathic mylonites with quartz porphyblasts (Plate 4-1) appear to be particularly easy to penetrate either by the process of north-east - south-west trending faulting or by carbonatite intrusion, a factor which will be considered in detail later in this chapter. The characteristic mineral constituents of the gneisses are feldspar, quartz and mica, which is usually biotite or muscovite. The feldspars usually show cloudy cores bordered by clear rims. Quartz reveals a high degree of strain polarization in a number of thin-sections studied. The common accessory minerals present include epidote, sericite and chlorite.

### 4.3 GEOLOGY OF THE BURU CARBONATITE.

#### 4.3.1 Field observations.

Fresh rocks are not observed on the surface of Buru hill, which has an oval shape and measures about 500 m in length and 350 m in width (Figure 4-2). The surface is entirely composed of lateritized tuff with irregular veins of hematite and goethite (Figure 4-1). Some of the veins, now completely lateritized, are randomly distributed, but east-west and north-south trends appear to be the dominant directions. A number of hematite veins are observed along the north-west of the hill and a fluorite vein, purple in colour, is noted in the northern part of the hill trending in an east-west direction within the fenites. Fluorite is frequently associated with carbonatites and has been observed to form along fractures,

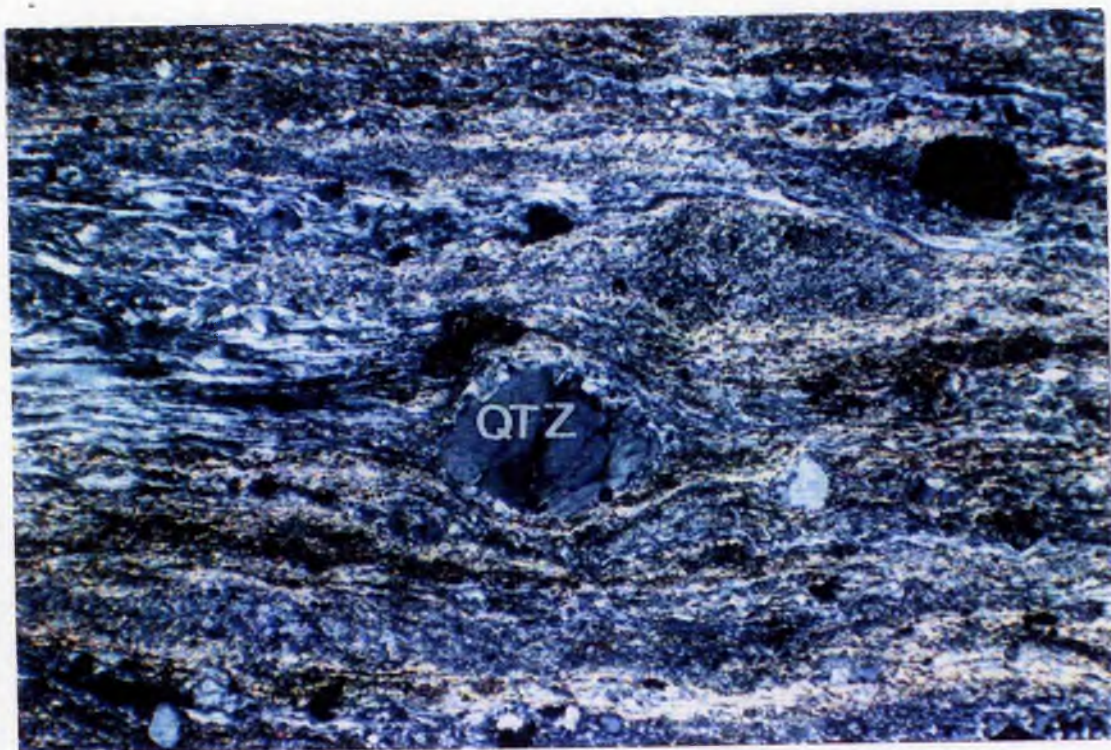


Plate 4-1 The Buru mylonite shear zone with quartz porphyroclasts in a matrix composed of quartz, feldspar and mica. Magnification x10.



Figure 4-2 The Buru hill carbonatite viewed westwards from Muhoroni town.

particularly in the roof zones of carbonatite complexes or in fractures along which fluids passed (Mariano, 1989b). Barite was not observed in the surface samples, although it occurs abundantly in thin-sections throughout the length of the drill cores.

The gneisses on which laterite has developed acted as a rim of resistant country rocks around the hill and consequently prevented most of the weathering solutions from escaping, although there is an opening at the southern end of the laterite through which there has been loss of mobile elements such as sodium, potassium and calcium. The soils towards the southern end of the hill are extremely magnetic.

Another significant feature on the surface of the Buru carbonatite centre is the existence of an exploration adit at the southern foot of the hill which surprisingly is not mentioned anywhere by early workers, although the local community are aware of active mining and excavation of ore from the adit in the late 1950's. The adit is mentioned by the local community to be quite long, almost reaching towards the middle of the hill. The writer has no idea about the nature of the ore that was being mined, but it could have possibly been iron-ore (hematite), which probably contained high concentrations of niobium derived from pyrochlore during weathering processes.

#### 4.3.2 Drill core observations.

Intensive supergene weathering processes witnessed in Buru hill have developed a thick lateritic cap overlying the Buru carbonatite with considerable economic enrichment in lanthanides. The Buru carbonatite, as revealed by drill cores at depth, is composed of a fine- to medium-grained calcite carbonatite, which is partly brecciated in some sections of the cores.

The carbonatites are cut by dykes of siderite carbonatite (confirmed by X-ray diffraction studies) and also by dykes of fine-grained ijolite.

Plate 4-2 gives a full pictorial summary of the different lithological units encountered in drill core BRL-1. The geological description of the rock units along drill core BRL-1 is summarized in Table 4-1. Details of the mineralogy and major and trace element geochemistry will be discussed in chapters 5 and 6.

Table 4-1. Summary of the geology along drill core BRL-1.

<u>Depth (m)</u>	<u>Geological description</u>
0 - 65	This section of the profile, which will be referred to as the 'Buru laterite', is composed mainly of iron hydroxides and oxides. The laterite exhibits different shades of colours; light grey to brown to reddish dark brown to brown to orange-brown towards the lower section of the laterite. Strongly weathered pseudomorphs of granitic gneiss fragments are recognized.
65 - 80	Transitional zone consisting of weathered pale brown medium-grained carbonatite and some iron compounds. This section, also called saprolite, is typically grey to brown in colour.
80 - 130	Fresh medium-grained, pale grey to white carbonatite. The carbonatite is sometimes banded and consists of disseminated magnetite and fluorite. Dykes of fine-grained light brown siderite carbonatite cross-cut the earlier carbonatite.

Table 4-1 continued.

Depth (m)	Geological description
130 - 142	Fine- to medium-grained brecciated carbonatite. The brecciated carbonatite contains minor disseminated fluorite and magnetite and also dark green fragments of pyroxene.
142 - 165	Fine- to medium-grained white to grey carbonatite with disseminated magnetite and fluorite. The carbonatite is cut by later dykes of siderite carbonatite.
165 - 196	Greenish-grey fine-grained dyke of ijolite cross-cutting the carbonatite. The ijolite is also cut by dykes of light brown siderite carbonatite.
196 - 200	Dark grey, medium-grained, magnetite-rich carbonatite.

Lithological observations along drill core BRL-1 (Table 4-1) reveal that three distinct zones (laterite, saprolite weathered carbonatite and fresh carbonatite) can be recognized. The other significant observation is the recognition of the brecciated nature of carbonatites and the cross-cutting relationships shown by both siderite carbonatite and ijolitic dykes.

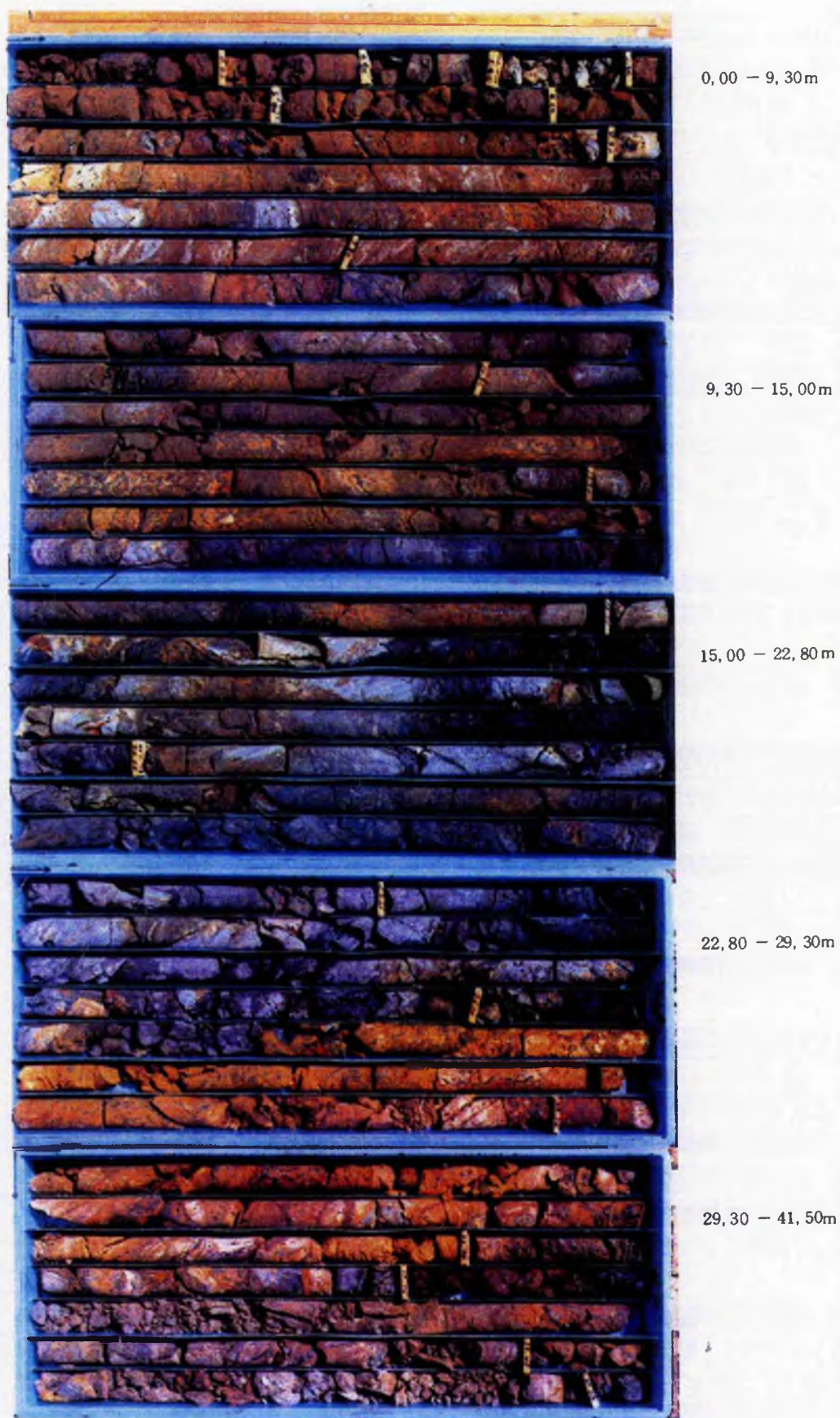


Plate 4-2 Summary (pictorial) of the different lithological units encountered in drill-core BRL-1, Buru carbonatite.



41,50 – 58,90 m

58,90 – 65,60 m

65,60 – 72,50 m

72,50 – 79,20 m

79,20 – 85,90 m

0 0,5 1 m



85, 90 — 92, 40m

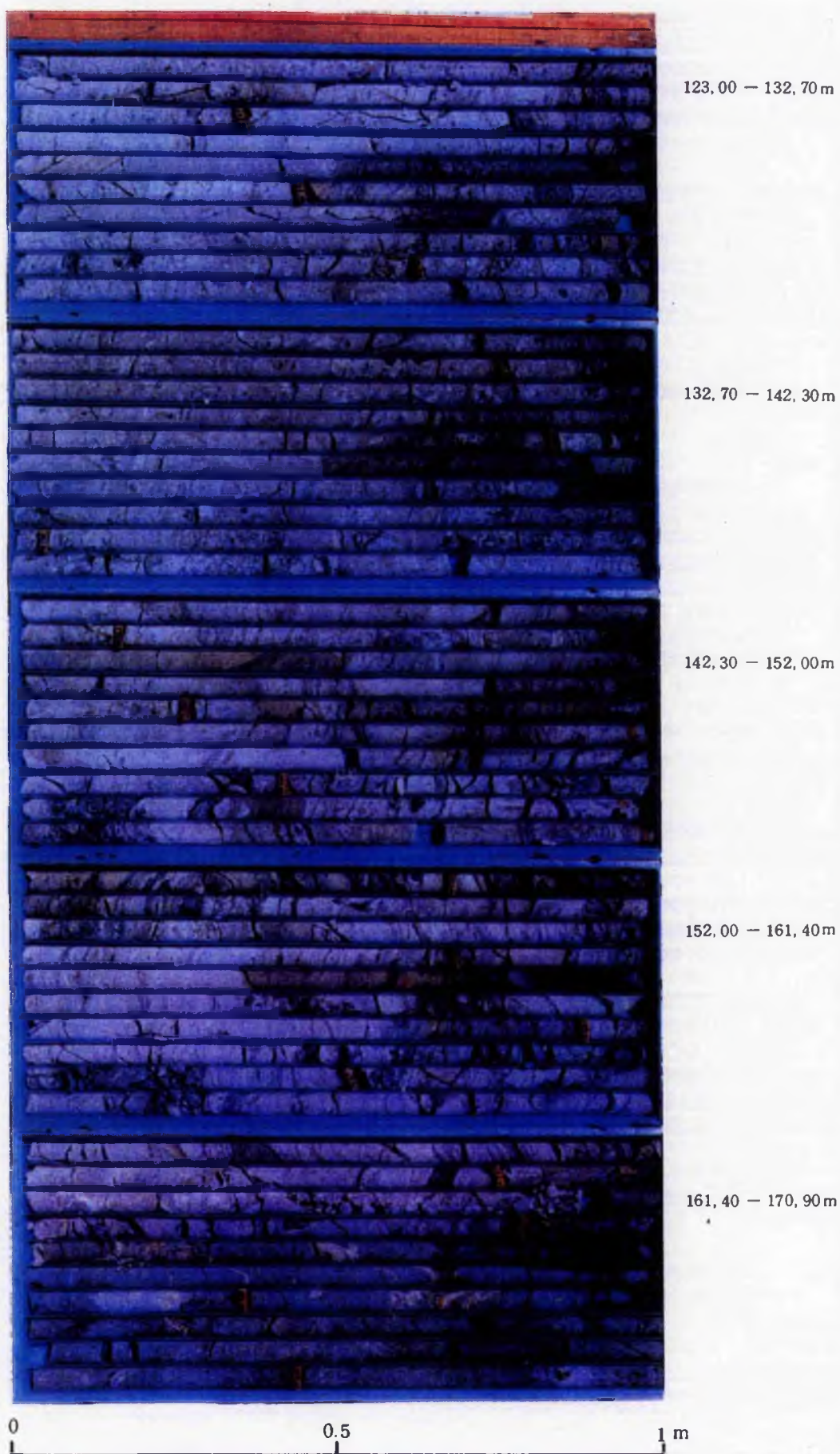
92, 40 — 102, 00m

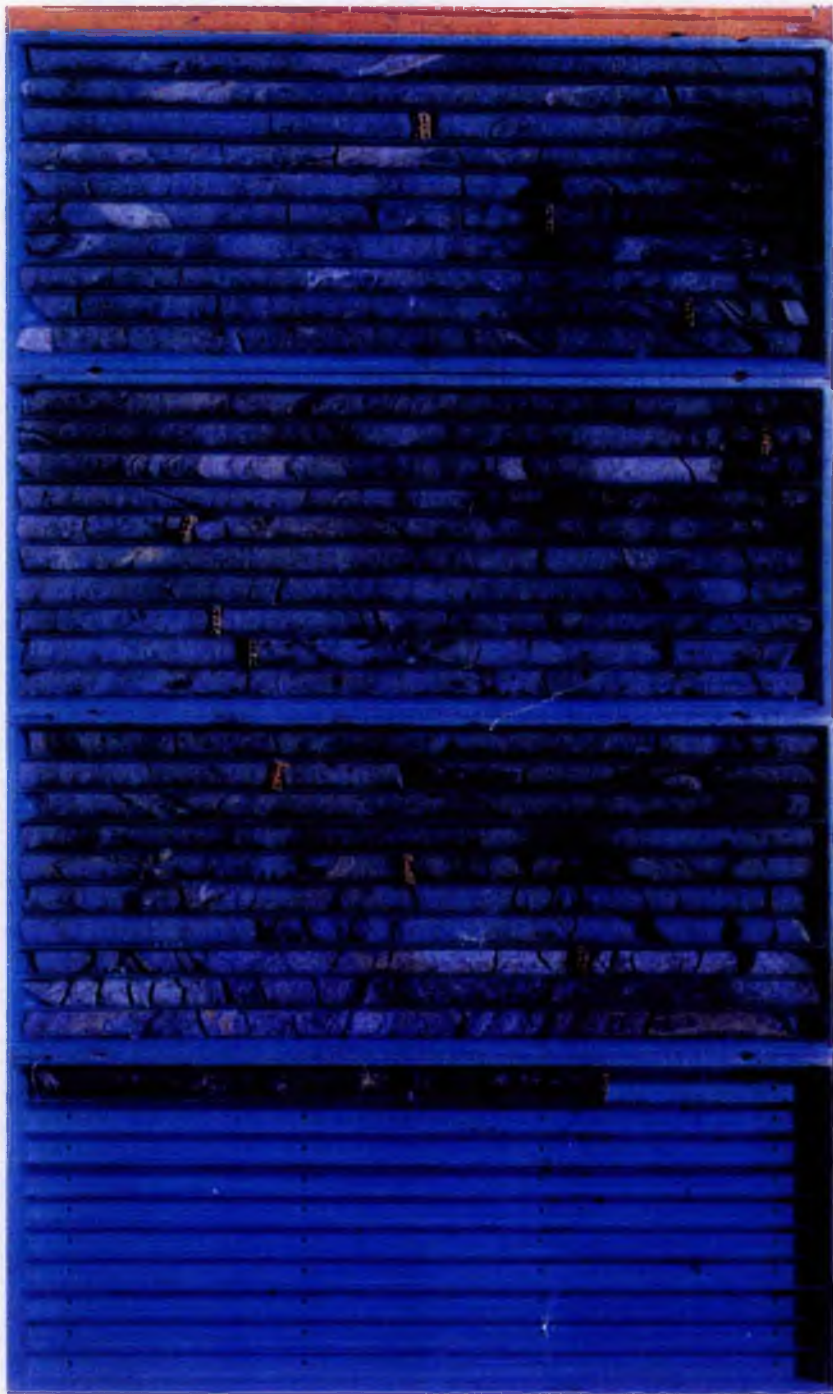
102, 00 — 109, 80m

109, 80 — 116, 40m

116, 40 — 123, 00m

0 0.5 1 m



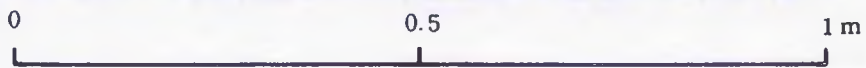


170, 90 — 180, 50m

180, 50 — 190, 10m

190, 10 — 199, 70 m

199, 70 — 200, 10m



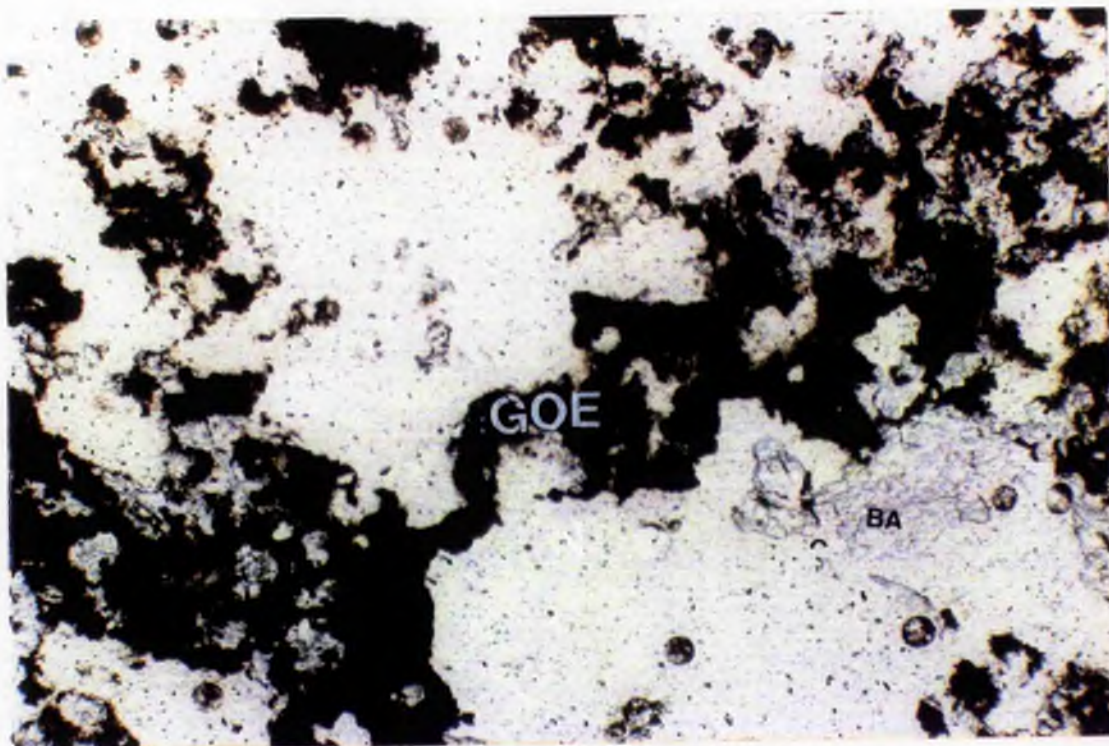


Plate 4-3 Laterite zone in the Buru carbonatite. Goethite (GOE) and barite (BA) are characteristic. Magnification x 20

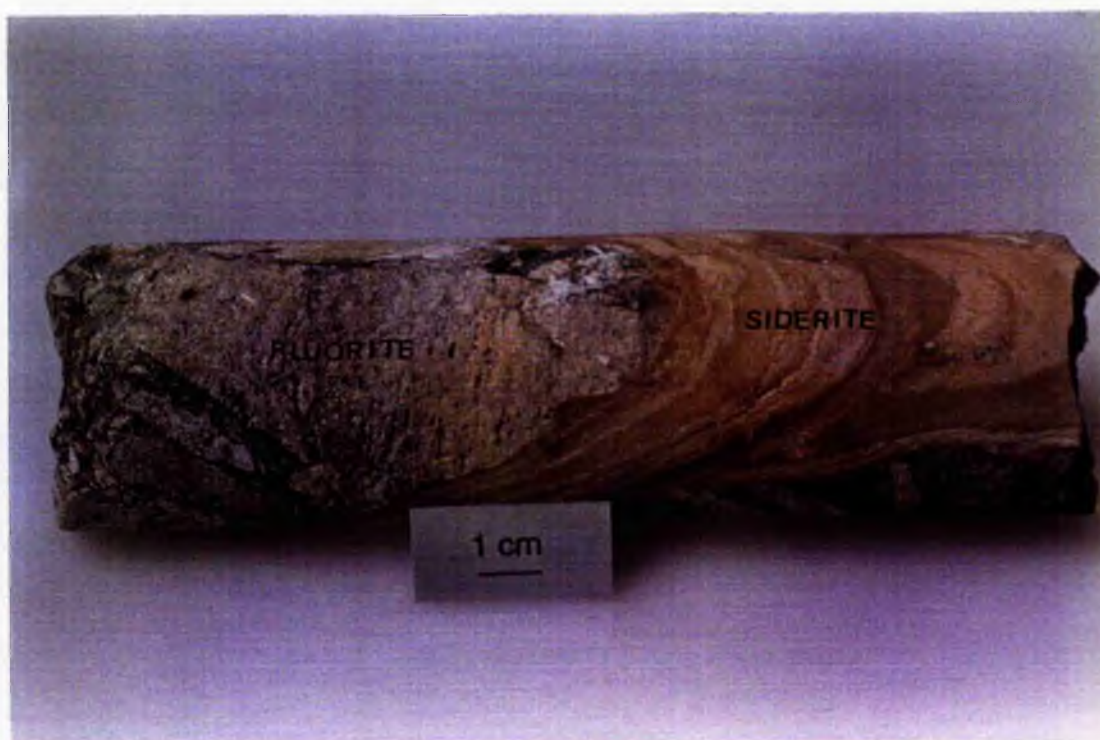


Plate 4-4 Drill core sample showing a brown and fine-grained siderite carbonatite dyke. Note the dominance of fluorite observed replacing calcite in the Buru cores. The dark vein to the left corner is aegirine (AEG).

#### 4.3.3 Thin-section studies.

Thin-section studies undertaken from samples selected from BRL-1 reveal a characteristic mineral zonation with depth. Thin-sections from the laterite are dominated by iron hydroxides/oxides (goethite and hematite), barite and fluorite (Plate 4-3). Fluorite (purple in colour; shown in Plate 4-4), appears to be reacting with and replacing calcite. The light brown fine-grained dyke of siderite carbonatite does not contain fluorite mineralization.

The carbonatites under the microscope show a typical fine- to medium-grained texture in which calcite, siderite, barite and fluorite are the most common minerals (Plate 4-5). Pseudomorphs of calcite rhombs are still recognized where they have not been completely destroyed by recrystallization. Barite occurs as anhedral crystals and is commonly colourless in colour, whereas fluorite is usually pale purple and typically isotropic under the microscope. The siderite carbonatite shows chilled margins and a cross-cutting relationship against the earlier Buru carbonatite and is therefore clearly magmatic. Some of the siderite carbonatite is also seen along the existing cavities of the earlier calcite carbonatite (Plate 4-6).

Accompanying the calcite and siderite in most of the thin-sections studied is the dominant occurrence of fluorite and barite and the accessory minerals magnetite, apatite, biotite and aegirine. Fluorite is pervasive and can be observed in several thin-sections and on outcrop, reacting with and replacing calcite (Plate 4-4). The biotite and aegirine are thought to be xenocrysts incorporated from fenites and the surrounding basement gneisses.

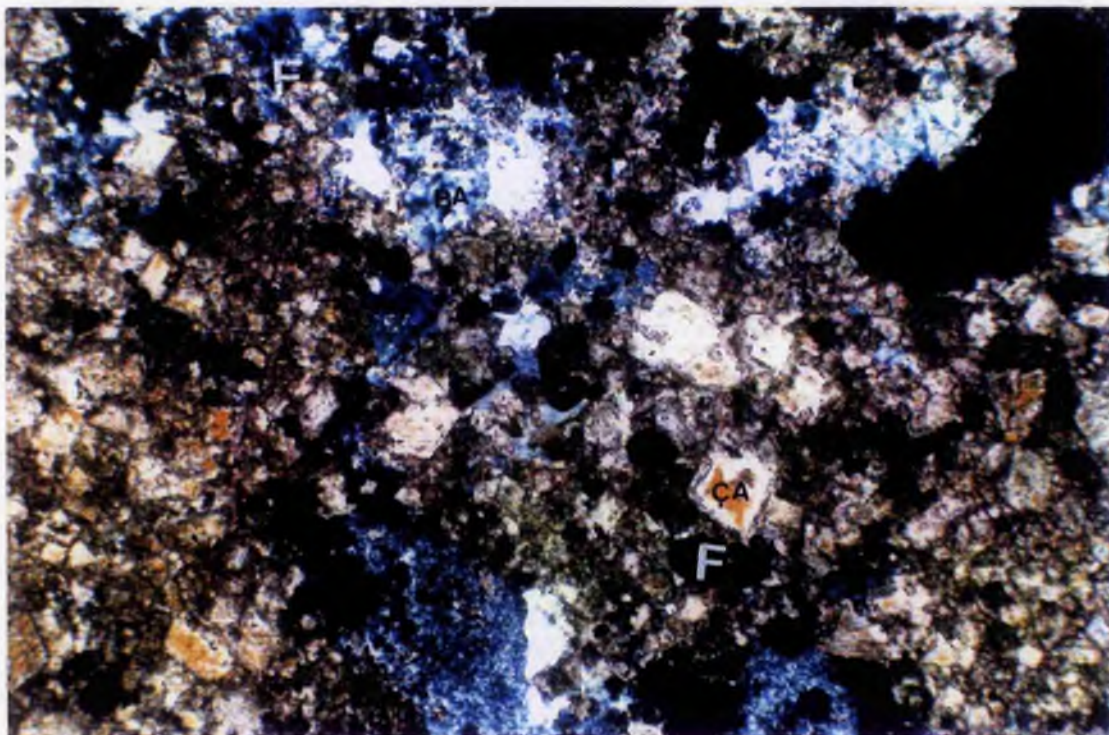


PLATE 4-5 Buru carbonatite. Rhombohedral pseudomorphs after calcite are recognized (CA) Fluorite ( F, dark rounded spheres) and barite (BA, white) are abundant within the section. Magnification x10

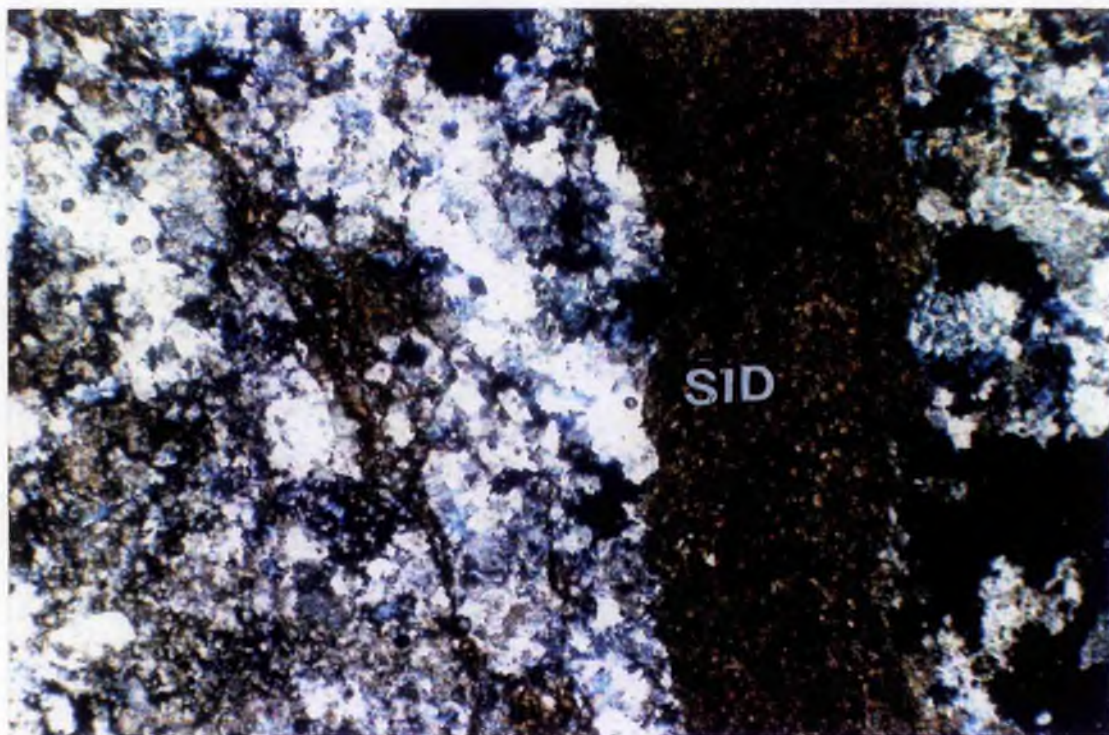


PLATE 4-6. Siderite carbonatite (SID) dyke revealing sharp contacts with Buru carbonatite. The sharp contacts confirm its intrusive nature. Magnification x10.

## 4.4 FENITIZATION AT BURU HILL

### 4.4.1 Introduction.

Brögger (McKie, 1966) coined the term "fenite" to represent a group of rocks, originally of approximately granitic composition and metasomatically altered towards an alkali-syenitic composition. He presumed the source to be an ijolite meltegeite magma (McKie, 1966). Fenitization therefore refers to the sum of physical and chemical changes that bring a country rock into equilibrium with an alkali silicate fluid. According to Le Bas (1981) and Woolley (1982), the hallmark of the ijolite carbonatite magmatic association is the alteration of the surrounding rocks to fenite.

Since the term "fenite" was introduced, numerous examples of fenitization have been reported, but the nature of fenitizing fluids either from carbonatite or ijolite, as well as the PTX conditions of equilibration are still debatable (Morogan, 1994). King and Sutherland (1960) suggested ijolite or nepheline syenite as the source of the fenitizing fluids whereas Dawson (1962) proposed a carbonatitic magma as the source of fenitization. Recently, Kresten and Morogan (1986), Morogan and Woolley (1988) and Morogan (1994) advocated both ijolitic and carbonatitic magmas as sources of fenitizing agents. There is now unanimous agreement that both ijolite and carbonatite magmas can produce fenitization, but the nature and evolution of the fenitizing fluids is still an enigma (Morogan, 1994).

The nomenclature of "fenites" as defined by many workers is rather confusing (compare Sutherland, 1969 and Woolley, 1982). Morogan (1994) has adopted a more general classification based on the increasing grade of

fenitization, as reflected in the formation of new mineral assemblages and texture. The categories identified include:

- i) Low grade fenites (LGF) - which contain abundant relict primary minerals and exhibit textures which can be attributed to deformation.
- ii) Medium grade fenites (MGF) - the relict primary materials are scarce and dominant textures are due to replacement and recrystallization.
- iii) High grade fenites (HGF) - primary minerals are entirely consumed and the textures are mainly of recrystallization type with the resulting fenites having the appearance of an igneous rock.
- iv) contact fenites (CF) - developed in the immediate vicinity of an igneous intrusion and considered as products of fenitization and contact metamorphism.

The categories proposed by Morogan (1994) appear to be the best approach to the study of fenites encountered in different environments. However, in the opinion of the writer, the classification suffers from possible overlap of the various categories suggested and the difficulties involved in distinguishing one category from the other. Another difficulty is the stability of minerals in different PTX conditions where a particular 'key' mineral is stable in one of the proposed categories, but will be unstable or transported away if formed in a different PTX environment.

#### 4.4.2 Fenitization at the Buru carbonatite centre.

The Proterozoic gneisses in contact with the Buru carbonatite centre have been fenitized. Fenitization in Buru is noted by the occurrence of thin blue veins of alkali amphibole, probably arfvedsonite or riebeckite on a number of fenite outcrops (Plate 4-7). Observation under the microscope of a number of Proterozoic gneisses obtained from various drill holes reveals that fenitization can be recognized by the development of a widespread



Plate 4-7 Fenite from the Buru carbonatite centre. Note the occurrence of thin blue veins of alkali amphibole.

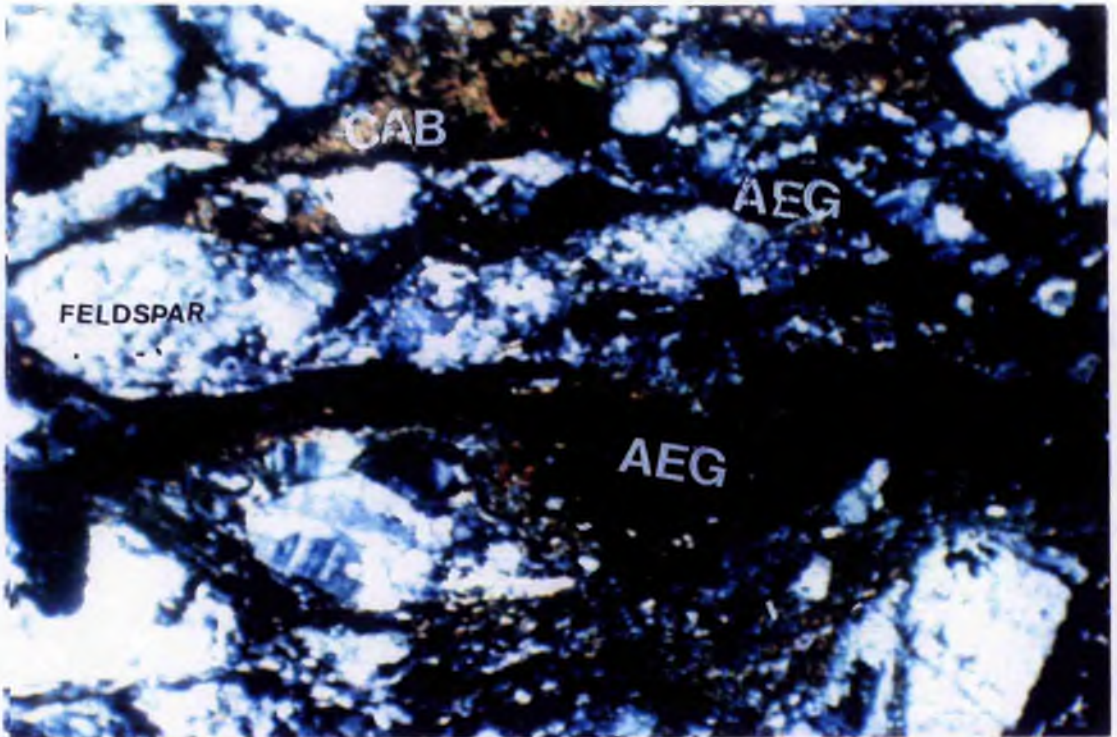


PLATE 4-8. Fenitized granitic gneisses, Buru hill. Note network granulation channels, now largely occupied by acicular aegirine (AEG). Carbonate (CAB) is also noted utilizing the existing channels within the feldspar. Magnification x 15.

network of thin dikelets and veinlets that are largely filled with aegirine or, rarely, blue green sodic amphibole (Plate 4-8). The dikelets or veins seem to occur along lines of weakness, such as fractures within the rock, and sometimes they appear to be penetrative. The primary minerals, plagioclase feldspar and quartz, appear altered with the feldspars being cloudy and the quartz strained. Other minerals observed in these fenites include iron oxide and hematite, which are probably oxidation products of an alkali amphibole.

The ijolitic dykes cross-cutting the carbonatites in the Buru carbonatite at depth are also fenitized. Plate 4-9 shows the sample obtained from BRL-1 to be dominated by tabular aegirine, sphene, apatite and carbonate, which is seen to replace highly altered nepheline, although the rectangular shape of earlier existing nepheline can be recognized. Plate 4-10, from BRL-2, also shows a network of veinlets that are filled with acicular aegirine and carbonate replacing nepheline. The ijolite sample shown in Plate 4-9 does not seem to have developed a network of veinlets characteristic of fenitized rocks, however, the turbidity of nepheline and the amount of carbonate introduced confirm that it is also fenitized.

A thin-section study of samples obtained from drill hole 16, which is located to the northern side of Buru hill (Fig. 4-1), does not show any evidence of fenitization. Plagioclase feldspars, however, show slightly cloudy cores of sericite alteration and the quartz is strained. The contacts between biotite and the plagioclase feldspars are straight and sharp with no evidence of replacement recognized (Plate 4-11). The observation of biotite at the edges of plagioclase feldspars might seem to suggest that the biotite formed later than the feldspars.

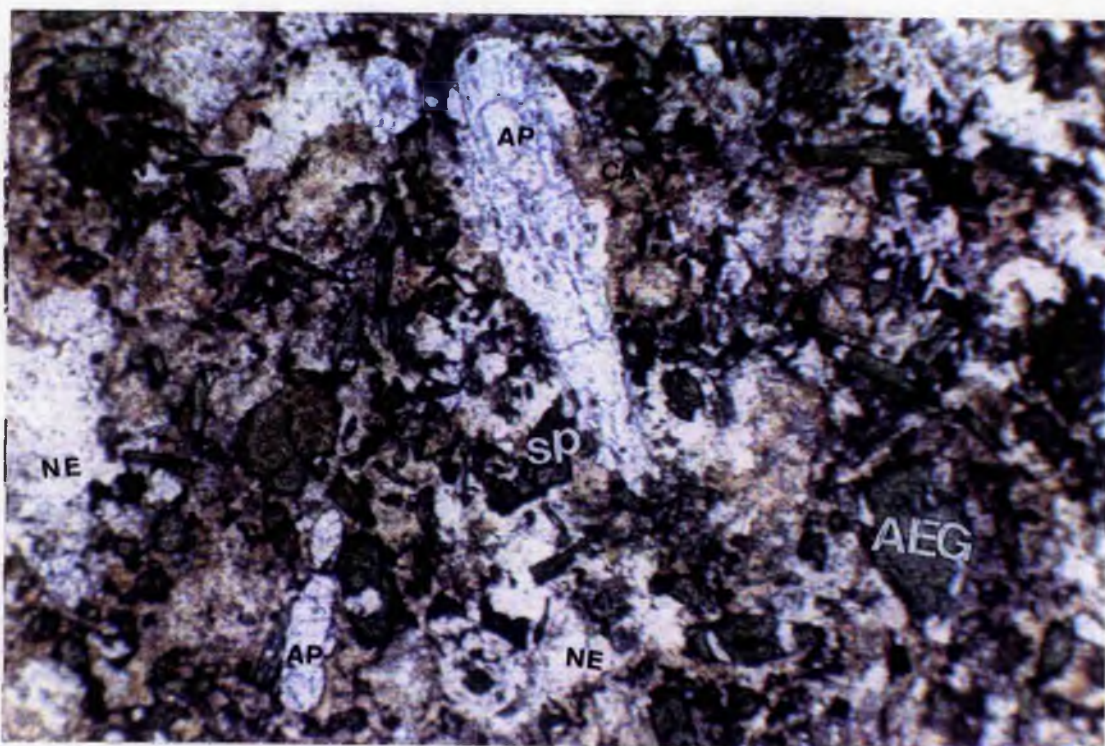


Plate 4-9 Fine-grained ijolite dyke cross-cutting BRL-1, Buru. The section shown contains tabular and zoned aegirine-augite, carbonate sphene and apatite. Nepheline (NE) appears cloudy and highly altered. Magnification x 20.

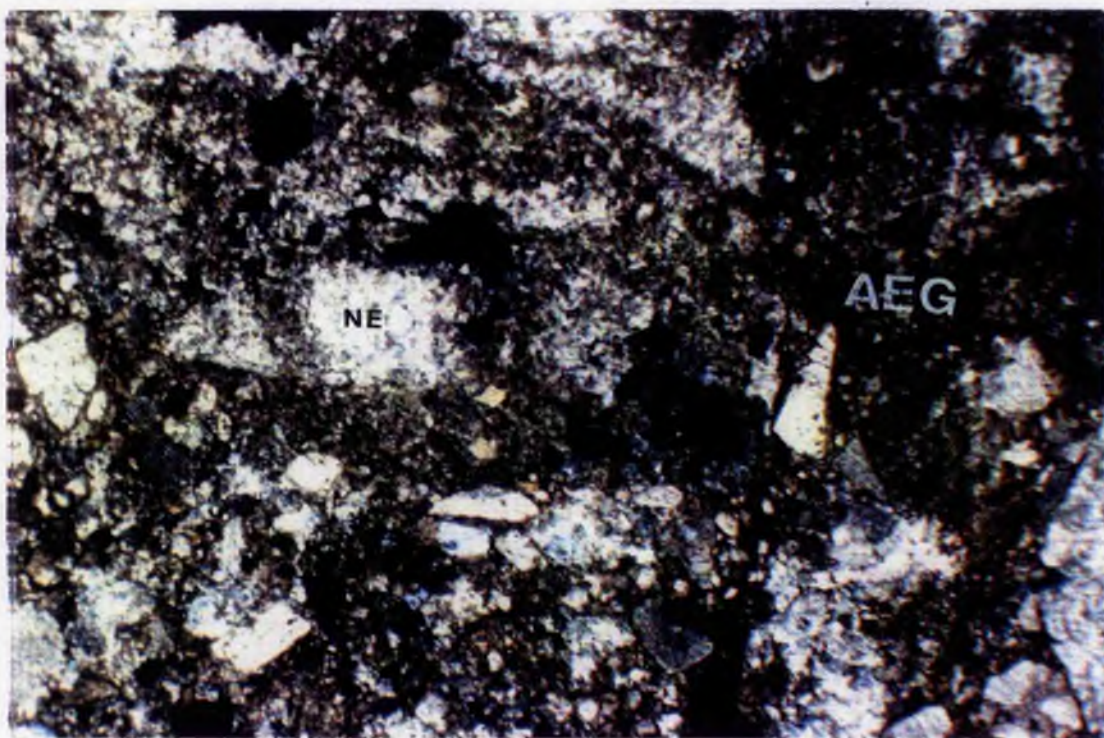


Plate 4-10 Fenitized ijolite dyke cross-cutting BRL-2, Buru. Nepheline is extensively altered with aegirine (AEG) veinlets and carbonate (CA) along the fractures. Magnification x 10.

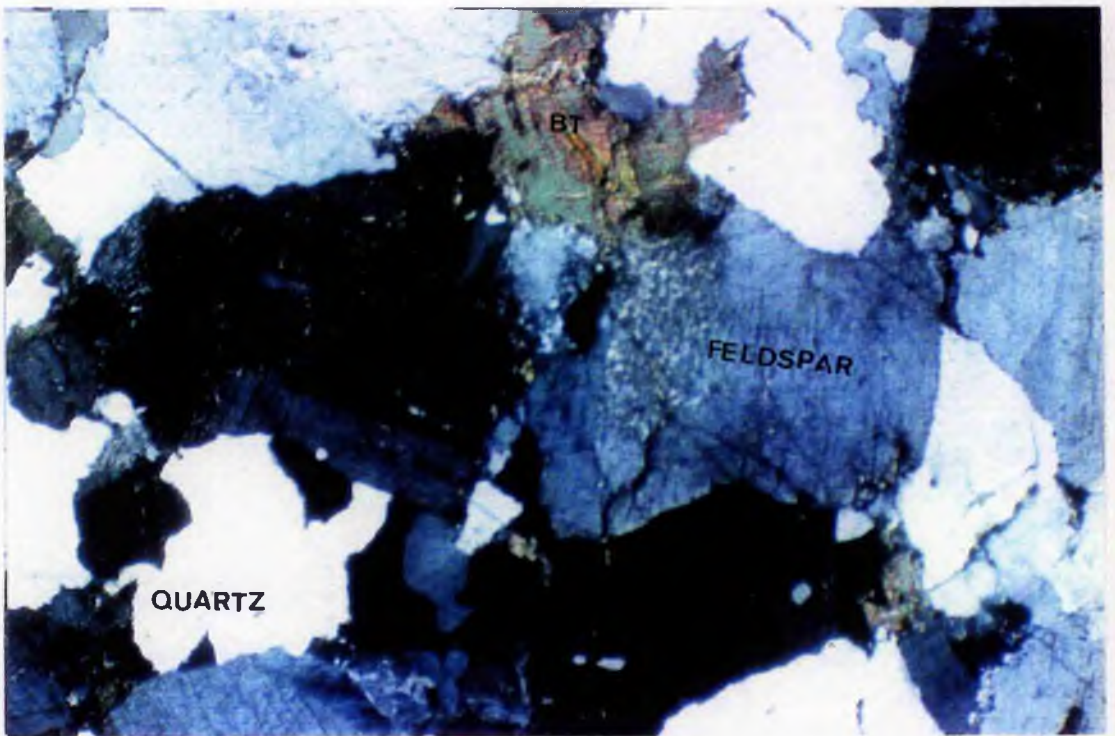


Plate 4-11 Less deformed granitic gneiss from Buru hill. The feldspars and biotite (BT) show sharp contacts. The feldspars show sericite alteration and the quartz appears slightly strained. Note the absence of any evidence of fenitization. Magnification x 10.

#### 4.4.3 Na:K ratios.

The ratio of Na/K of the interacting fluid can act as one of the main controls of fenitization, which eventually determines the type of fenite formed (Woolley, 1982). According to Morogan (1994), three types of fenite have been recognized on the basis of  $\text{Na}_2\text{O}/\text{K}_2\text{O}$ , namely sodic ( $\text{Na}_2\text{O} \geq 50\%$ ), intermediate ( $\text{Na}_2\text{O}$  between 40-50%) and potassic ( $\text{Na}_2\text{O} \leq 40\%$ ).

When the Na/K ratios involving BR-16, BR-17, BR-20 and BR-23 from the Buru carbonatite centre are plotted on a CaO -  $\text{K}_2\text{O}$  -  $\text{Na}_2\text{O}$  diagram (Figure 4-3), both the potassic and sodic type fenitization trends are identified. Samples selected which did not reveal fenitization in thin-section studies plot as a distinct unit with slightly higher CaO contents. The analyses of the major elements of selected gneisses and fenites from drill holes BR-16, BR-17, BR-20 and BR-23 (Figure 4-1) are shown in Appendix 6-2.

The east-west shear zone on which the Buru carbonatite centre is located, seems to control the fenitization processes. Samples that show evidence of fenitization, such as veinlets of amphibole and carbonate along the fractures of the gneisses, are all located within this shear zone. The samples that show no evidence of fenitization, such as those from drill hole 16 (Plate 4-1), lie within the less strongly deformed gneisses that are located at the far north-north-west of the map area (Figure 4-1). The writer proposes that the flattened, mylonitic shears were easier to brecciate during the process of carbonatite intrusion and were therefore easily penetrated by the fenitizing fluids emanating from the carbonatite during intrusion compared to the less strongly deformed gneisses.

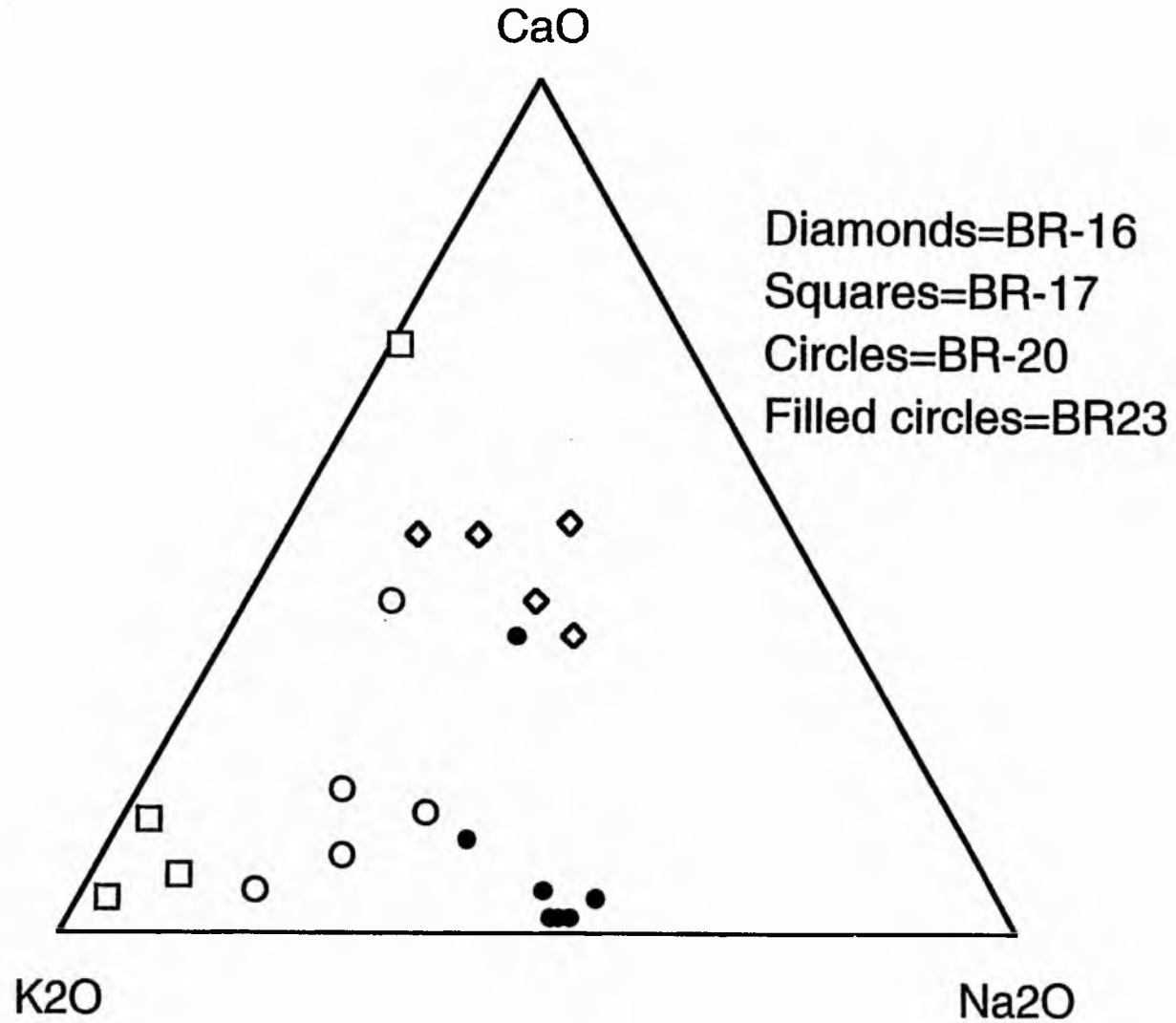


Fig.4-3 Fenite classification on the basis of Na<sub>2</sub>O/K<sub>2</sub>O variations.

#### 4.5 CONCLUSION.

The volcanic superstructure is not preserved in Buru compared to Rangwa, the Ruri's or Homa Mountain, where sheets and dykes of carbonatite truncating the pyroclastic deposits are a characteristic feature. It is possible that erosion removed most of the volcanic superstructure developed in Buru. The existence of tuff and breccia noted between 130 to 142 m from the surface of drill hole BRL-1 and at a depth of between 58 to 87 m in drill hole BRL-3 will, however, suggest that Buru is also dominated by tuff-agglomerate-breccia volcanic sequences that have been recognized in well exposed volcanoes within the Nyanza rift. The volcanic carbonatite pile in Buru hill is consequently cut by later dykes of siderite carbonatite, as revealed in core-samples. Ngwenya (1994) and Wall and Mariano (1996) both describe almost similar evolution paths from the Tundulu and Kangankunde carbonatites in Malawi, respectively.

The Buru carbonatite centre is suggested to have the same evolution trends as those proposed for other volcanoes within the Nyanza rift and is hence viewed as a satellite cone (vent) related to and connected with the evolution of the Tinderet basanite strato-volcano.

Both the Buru and Kuge carbonatite centres are unique among the Nyanza rift carbonatites. They both do not preserve their volcanic superstructures compared to Rangwa, the Ruri's, Homa mountain and, to some extent, Legetet. The Buru and Kuge centres are also small conical hills that are almost identical in comparison to other complexes. The relative emplacement levels of Buru and Kuge are difficult to determine. However, Kuge hill is frequently observed to have remnants of basement fragments within the sheets and dykes of carbonatites and, from stable isotope

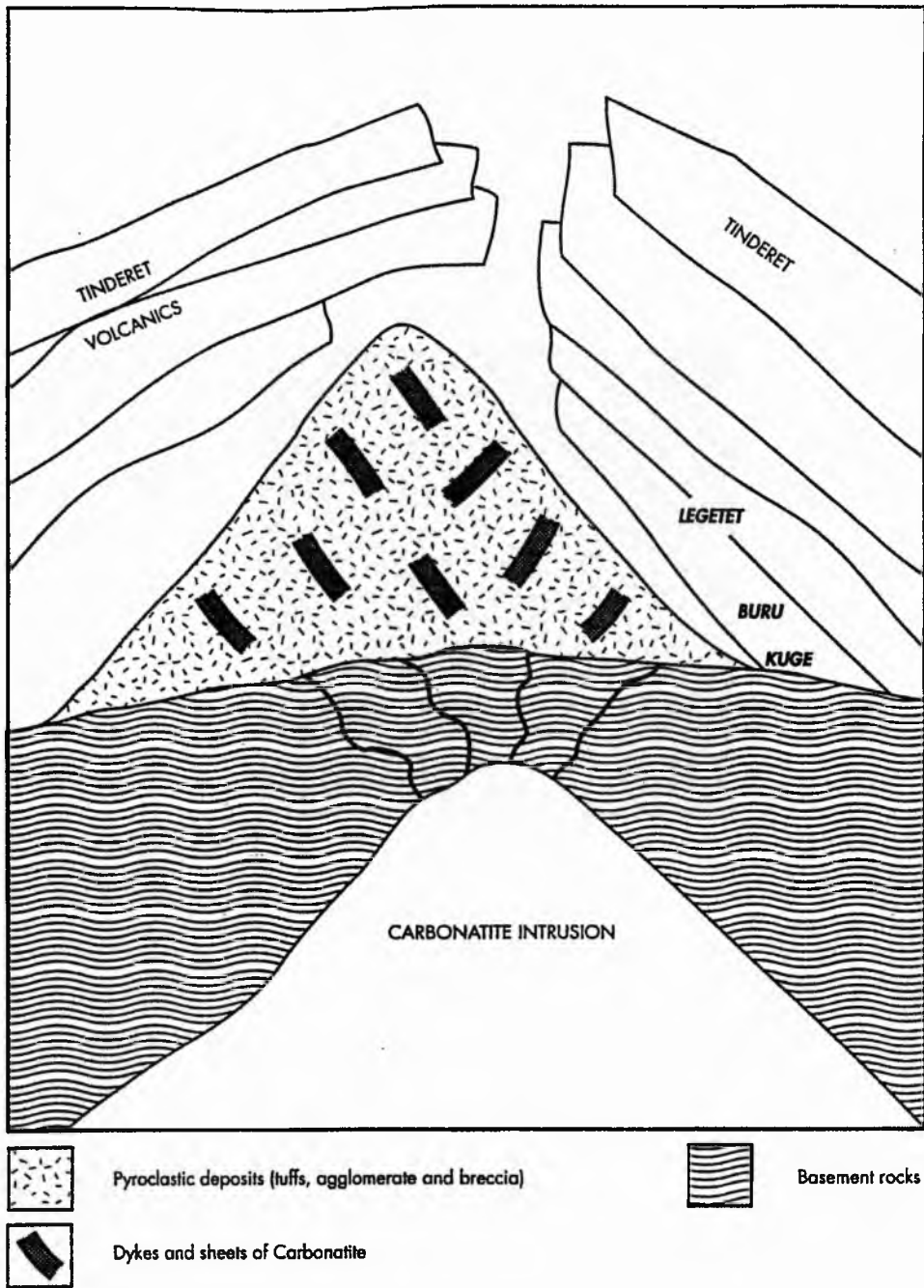


Figure 4-4 Schematic cross-section of an idealised carbonatite-nephelinite volcanic complex and relative emplacement levels of Kuge, Buru, Legetet and Tinderet

geochemistry discussed in chapter 7, Kuge is considered to be a slightly deeper facies than Buru (Figure 4-4).

Buru, from the relative emplacement levels shown in Figure 4-4, is lower than the Legetet carbonatite, which has part of its volcanic superstructure still intact. The Tinderet lavas, especially the extensive phonolites and basanites, were last in the proposed evolutionary history.

## CHAPTER FIVE

### GENERAL MINERALOGY OF THE BURU AND KUGE CARBONATITE CENTRES

#### 5.1 INTRODUCTION.

The mineralogy of carbonatites is extensive and diverse (Kapustin, 1980). The mineralogy of the carbonatites exposed on the earth's surface have also undergone modifications by various secondary processes (Andersen, 1984, 1987). In this chapter, the general mineralogical composition of both the Buru and Kuge carbonatite centres, including the carbonates, oxides, barite and fluorite and other non-carbonate minerals, will be presented and discussed.

#### 5.2 METHODS OF ANALYSIS.

Detailed X-ray diffractometer studies, supported by petrography and electron probe microanalysis (EPMA), were used to identify various minerals encountered in the two volcanic centres. Samples from drill holes BRL-1, BRL-2 and BRL-3 from the Buru carbonatite and KG-2 from the Kuge centre were selected for detailed examination using a Philips PW1050 Goniometer/Hiltonbrooks DG2 Generator at the Department of Geology, St Andrews University. The details for sample preparation, procedures and selected diffractograms are shown in Appendices 5-1 and 5-2, respectively. The diffractograms have been chosen to be representative of the lateritic zone from Buru (BR-1), the transitional zone marking the first appearance of the carbonate phase (BR-8), the carbonatite body below the weathering zone (BR-11), the siderite-carbonatite dyke (BR-183), the Kuge carbonatite breccia (BR-72) and a typical calcite carbonatite from the Ruri hills (NR-280).

### 5.3 SELECTED X-RAY DIFFRACTOMETER RESULTS.

5.3.1 The Buru centre - Minerals identified by XRD are shown in Table 5-1. The following observations from drill hole BRL-1 was noted.

- i) Fluorite, goethite, barite, hematite and fluorocarbonates dominate the upper parts of the core, which is composed of laterite to a depth up to 65 m
- ii) Carbonates are not observed between 0 to 65 m.
- iii) The first appearance of carbonate (calcite) was noted at 66 m.
- iv) The iron compounds, for example goethite and hematite, are not observed below 80 m.
- v) Calcite coexists with siderite below 79 m.
- vi) Fluorite and barite occur in all sections of the core, although they appear to be dominant in the upper sections of the lateritic profile.
- vii) Other rarely occurring carbonates observed along with calcite and siderite include ankerite, strontianite, alstonite and oligonite.
- viii) The non-carbonate minerals identified include micas, fluorapatite, aegirine, K-feldspar and magnetite. Magnetite and fluorapatite are not observed within the laterite but only occur in the carbonatite below the weathering zone.

#### 5.3.2 The Buru centre - BRL-2.

Examination of the X-ray diffractometer results illustrated in Table 5-2 for BRL-2 clearly reveals that the mineralogical characteristics observed for BRL-1 appear to be the same for BRL-2. These include the following:

- i) The upper sections of the laterite are dominated by fluorite, barite and the fluorocarbonates and also characterized by the absence of carbonates.
- ii) The appearance of carbonates (calcite), together with iron compounds (goethite), is first observed at 71 m. Goethite is not stable below 80 m where calcite and siderite coexist.

Sample No	Depth (m)	Major Minerals (XRD)													
		Calcite	Siderite	Ankerite	Strontianite	Oligonite	Alstonite	RE	Magnetite	Hematite	Goethite	Barite	Fluorapatite	Fluorite	Silicate
BR-1	5	-	-	-	-	-	-	RE	-	Hematite	Goethite	Barite	-	Fluorite	-
BR-201	11	-	-	-	-	-	-	RE	-	-	Goethite	Barite	-	Fluorite	-
BR-203	16	-	-	-	-	-	-	RE	-	Hematite	Goethite	Barite	-	Fluorite	-
BR-2	22	-	-	-	-	-	-	RE	-	Hematite	Goethite	Barite	-	Fluorite	-
BR-3	32	-	-	-	-	-	-	RE	-	-	Goethite	Barite	-	Fluorite	-
BR-4	58	-	-	-	-	-	-	RE	-	-	Goethite	Barite	-	Fluorite	-
BR-5	65	-	-	-	-	-	-	-	-	Hematite	Goethite	Barite	-	Fluorite	-
BR-6	66	Calcite	-	-	-	-	Alstonite	-	-	-	Goethite	Barite	-	Fluorite	-
BR-7	71	Calcite	-	-	-	-	-	RE	-	Hematite	-	Barite	-	Fluorite	-
BR-8	75	Calcite	-	-	-	-	Alstonite	-	-	Hematite	Goethite	Barite	-	Fluorite	-
BR-9	79	Calcite	Siderite	-	-	Oligonite	-	-	-	-	-	Barite	-	Fluorite	-
BR-10	85	Calcite	Siderite	-	-	Oligonite	-	RE	Magnetite	-	-	Barite	-	Fluorite	-
BR-11	92	Calcite	Siderite	-	-	-	-	RE	-	-	-	Barite	Fluorapatite	Fluorite	-
BR-12	101	Calcite	Siderite	Ankerite	-	-	-	-	-	-	-	Barite	Fluorapatite	Fluorite	-
BR-14	114	Calcite	Siderite	-	-	-	-	-	-	-	-	-	Fluorapatite	Fluorite	AEG -
BR-15	116	Calcite	Siderite	-	-	Oligonite	-	-	-	-	-	Barite	-	Fluorite	AEG
BR-16	130	Calcite	Siderite	-	-	-	-	-	-	-	-	Barite	-	Fluorite	-
BR-17	138	Calcite	Siderite	-	-	-	-	RE	-	-	-	Barite	-	Fluorite	-
BR-19	142	Calcite	Siderite	-	-	-	-	RE	-	-	-	Barite	-	Fluorite	-
BR-28	200	calcite	Siderite	-	Strontianite	-	-	-	Magnetite	-	-	Barite	Fluorapatite	Fluorite	-

Note, RE - Rare earth mineral, AEG - Aegirine

Table 5-1 Minerals identified by XRD from drill hole BRL-1 Buru carbonatite.

iii) Barite, fluorite and fluorocarbonates occur in both the laterite and the carbonatite.

### 5.3.3 The Kuge centre - KG-2.

Table 5-2, which also includes data for KG-2 from the Kuge carbonatite centre (ferrocarbonatite breccia) shows:

- i) The upper and lower sections of the sampling profile are characterized and dominated by calcite with accessory barite, fluorite, goethite and fluorapatite. Rare earth minerals are also observed.
- ii) The silicate minerals identified include orthoclase and biotite.
- iii) Distinct mineralogical zonation as observed in Buru are is apparent in Kuge. This could be due to the extent of minimal supergene oxidation experienced in Kuge and also partly due to the shallow depths of diamond drilling. The depth of the holes in Kuge are only 50 m compared to depths of 100 and 200 m for BRL-2 and BRL-1 from Buru.

### 5.3.4 Summary of XRD results.

The XRD work indicated that calcite and siderite are the major carbonate minerals encountered in Buru and Kuge with accessory ankerite, strontianite, fluorocarbonates and the extremely uncommon minerals alstonite and oligonite, which were only identified by X-ray diffractometer studies. Alstonite  $[\text{BaCa}(\text{CO}_3)_2]$  is chemically similar to barytocalcite, which has been reported by Platt and Woolley (1990) from carbonatites and fenites of Chipman Lake, Ontario. Kapustin (1980) lists alstonite as a rare carbonate phase occurring in late-stage calcite or ankeritic carbonatites. The other minerals observed and occurring in most of the drill core sections examined include fluorite, barite, fluorapatite, magnetite, mica, K-feldspar and aegirine.



The distinct mineralogical zones particularly from Buru hill as revealed in Tables 5-1 and 5-2, are clearly depth related. Dominant minerals in the laterite, such as fluorite, goethite etc., are followed at specific horizons from the surface by calcite, siderite and magnetite. Barite and fluorite are widespread along the sections, although both minerals are notably enriched and are the most prominent phases in the upper sections of the laterite towards the surface. Aegirine, mica and the K-feldspar appear to be concentrated mainly within the carbonatite, below the weathering profile. Some of the petrographic studies of these minerals were briefly discussed in chapters three and four. Electron microprobe analyses (EPMA) of some of the selected minerals from Buru and Kuge will be discussed below whereas others, particularly those prominent in the laterite (Mn-Ba-Fe compounds, mainly psilomelane), will be discussed in chapter 6.

## 5.4 DISCUSSION OF THE MINERALOGY OF THE BURU AND KUGE CARBONATITES

### 5.4.1 Introduction.

The great diversity in mineralogy encountered in the carbonatites has been documented in a review article by Le Bas (1989), which summarizes the salient parameters that contribute to the high chemical diversity observed in carbonatites compared to silicate igneous rocks. Some of the factors responsible for the diversification of carbonatites, according to Le Bas (1989), include the following:

- i) The nature of the upper mantle source where the carbonatites are thought to originate and the chemical composition of the parental magma.
- ii) The effects of fractional crystallization, liquid immiscibility, fenitization and contamination by crustal components.
- iii) The post-magmatic (hydrothermal and supergene) processes.

The above processes, either in isolation or in combination, drastically affected and changed both the mineralogical and chemical composition of the carbonatite volcanoes encountered on the earth's surface and, surprisingly, present research activities have not yet isolated the specific signatures of the above dominant processes in carbonatites.

The present carbonatite occurrences in Buru and Kuge have been equally affected by the above-mentioned processes. The mineralogical changes that were brought about mainly by processes of carbonatite fractionation through the upper mantle and crust have been superimposed upon by changes during post-magmatic processes because carbonatites as a group are easily susceptible to subsolidus re-equilibration. The processes of alteration during subsolidus re-equilibration probably result from late-magmatic, hydrothermal/meteoric and/or supergene processes, which are difficult to distinguish from each other easily.

In the Buru carbonatite centre and, to a lesser extent, the Kuge carbonatite centre, the distinct mineralogical zones, which are also depth related, could be easily explained as resulting from supergene processes during the weathering of the carbonatites. These processes resulted in the dissolution and leaching of the carbonatite carbonates, eventually leaving behind insoluble oxides. These oxides are now mainly represented by goethite, hematite and psilomelane. Below the weathering zone, relatively fresh carbonatites are encountered which are characterized by the presence of simple carbonates (calcite, siderite and strontianite). Chemical evidence will be presented in this chapter and subsequent chapters to show that hydrothermal and supergene processes are the dominant processes that control the mineralogical and chemical composition of the two carbonatite centres.

## 5.4.2 Carbonates.

Selected electron microprobe analyses of carbonate phases from the Buru and Kuge carbonatites are shown in Table 5-3.

Table 5-3 (i) Selected electron microprobe analyses of calcite from the Buru carbonatite.

Sample	BR-9	BR-12	BR-13	BR-16	BR-27
SiO <sub>2</sub>	0.04	0.05	0.01	0.29	0.13
FeO	0.66	0.72	0.66	0.59	1.51
MgO	0.32	0.20	0.21	0.24	1.14
MnO	1.27	0.45	0.77	1.24	0.94
CaO	53.40	55.46	55.29	52.93	50.48
SrO	0.29	0.16	0.47	0.14	1.24
BaO	0.02	0.11	0.03	0.05	0.05
TREO	0.10	0.06	0.45	0.15	0.43
Total	56.01	57.21	57.89	55.63	55.92
CO <sub>2</sub> *	43.99	42.79	42.11	44.37	44.08
Formula calculated on the basis of 6 O.					
Si	0.001	0.002	0.000	0.01	0.004
Fe	0.018	0.02	0.019	0.016	0.042
Mg	0.016	0.01	0.011	0.012	0.057
Mn	0.036	0.013	0.022	0.035	0.027
Ca	1.91	2.005	2.019	1.886	1.811
Sr	0.006	0.003	0.009	0.003	0.024
Ba	0.000	0.001	0.000	0.001	0.001
Total	1.987	2.054	2.080	1.963	1.966
C	2.005	1.972	1.959	2.014	2.015

Oxides in wt%.

Table 5-3 (ii) Selected electron microprobe analyses of siderite from the Buru carbonatite.

Sample	BR-9	BR-13	BR-14	BR-16
SiO <sub>2</sub>	0.50	0.36	3.57	0.18
FeO	47.36	45.49	37.57	54.81
MgO	3.22	4.60	0.25	0.17
MnO	0.96	1.16	1.96	2.23
CaO	3.53	5.21	2.27	0.36
SrO	0.07	0.23	0.21	0.19
BaO	0.10	0.12	0.23	0.03
TREO	0.08	0.07	0.21	0.11
Total	55.82	57.24	46.27	58.08
CO <sub>2</sub> *	44.08	42.76	53.73	41.92
Formula calculated to 6 (O).				
Si	0.018	0.013	0.113	0.007
Fe	1.392	1.350	0.992	1.684
Mg	0.169	0.243	0.012	0.009
Mn	0.029	0.035	0.052	0.069
Ca	0.133	0.198	0.077	0.014
Sr	0.001	0.005	0.004	0.004
Ba	0.001	0.002	0.003	0.000
Total	1.743	1.846	1.253	1.787
C	2.120	2.071	2.317	2.103

Oxides in wt. %.

Table 5-3 (iii) Selected electron microprobe analyses of calcite from the Kuge ferrocarbonatite breccia.

Sample	KG-72	KG-76	KG-80	KG-94
SiO <sub>2</sub>	0.07	0.75	0.07	0.07
FeO	0.1	0.1	0.12	0.13
MgO	0.85	0.89	0.23	0.35
MnO	0.02	0.01	0.1	0.12
CaO	55.23	53.19	55.53	54.43
SrO	0.06	0.07	0.16	0.05
BaO	0.01	0.02	0.01	0.02
TREO	0.01	0.03	0.05	0.03
Total	56.35	55.06	56.27	55.20
CO <sub>2</sub> *	43.65	44.94	43.73	44.80
Formula calculated to 6(O).				
Si	0.002	0.025	0.002	0.002
Fe	0.003	0.003	0.003	0.004
Mg	0.042	0.044	0.011	0.017
Mn	0.001	0.000	0.003	0.003
Ca	1.973	1.872	1.987	1.927
Sr	0.001	0.001	0.003	0.001
Ba	0.000	0.000	0.000	0.000
Total	2.022	1.945	2.009	1.953
C	1.987	2.015	1.994	2.021

Oxides in wt%.

Table 5-3 (iv) Selected electron microprobe analyses of accessory carbonate phases, ankerite (BR-28 and BR-59) and strontianite (BR-27) from the Buru carbonatite.

Sample No.	BR-28	BR-59	BR-27
SiO <sub>2</sub>	1.10	0.31	0.00
FeO	11.77	10.48	0.07
MgO	9.96	7.41	0.00
MnO	4.12	2.69	0.00
CaO	24.70	29.34	2.20
SrO	0.82	0.22	56.72
BaO	0.14	0.21	0.09
TREO	0.00	0.16	1.13
Total	52.61	50.82	60.21
CO <sub>2</sub> *	47.39	49.18	39.79

Formula calculated on the basis of 6 O.

Si	0.035	0.010	0.000
Fe	0.316	0.279	0.002
Mg	0.477	0.351	0.000
Mn	0.112	0.072	0.000
Ca	0.850	1.000	0.098
Sr	0.015	0.004	1.370
Ba	0.002	0.003	0.001
Total	1.807	1.719	1.471
C	2.079	2.136	2.264

Oxides in wt%.

\*: CO<sub>2</sub> was obtained by subtracting from electron microprobe totals from 100%.

Examination of Table 5-3 shows that the calcites from Buru generally have higher MnO values than FeO, which is characteristic for calcite in carbonatites. The total CaO values in the Buru and Kuge calcites are similar, though the Kuge calcites seem to be depleted in FeO and MnO. Siderite is slightly enriched in both Mg and Mn compared to both calcites from Buru and Kuge. Siderite appears to have more CaO compared to FeO in the calcites, suggesting that siderite shows a greater substitution for  $\text{Ca}^{2+}$  ions. Greater substitution for ions by siderite is also evident from the ion distribution in its structural formula. Ankerite contains more FeO than MgO and also substantial amounts of MnO.

Both SrO and BaO contents vary among the carbonate phases analyzed, although SrO is more enriched than BaO. Calcite from sample BR-27 and ankerite from sample BR-28 contains the highest SrO contents compared to other analyzed carbonate phases. The high SrO contents in these samples is due to the occurrence of the mineral strontianite.

Strontianite occurs as an accessory carbonate phase in the Buru carbonatite. On the basis of electron microprobe analyses, strontianite shows replacement of strontium by calcium and also very minor replacement by barium and iron. Strontianite was not observed in the Kuge carbonatite centre.

All the analyzed carbonate phases (calcite, siderite, ankerite and strontianite) in the Buru hill, as well as the Kuge hill carbonatites, have very low detectable REEs and since these volcanic centres are highly REE mineralized, this emphasizes the late-stage development of lanthanide mineralization associated with independent secondary rare earth minerals.

The carbonate assemblages of the carbonatites from Buru and Kuge may be considered to be close to the ternary system  $\text{CaCO}_3\text{-MgCO}_3\text{-FeCO}_3$  (Rosenberg, 1967), which includes the rhombohedral carbonate minerals calcite, dolomite and Fe-bearing dolomite magnesite and siderite. According to Rosenberg (1967), the sub-solidus relationship in this ternary system identifies three fields; a one phase field of magnesite-siderite-dolomite-ankerite solid solution and calcite, a two phase field and a three phase field with vertices calcite, iron-rich ankerite and siderite (Figure 5-1).

When the microprobe data of mole % carbonate compositions are plotted in the ternary system  $\text{CaCO}_3\text{-MgCO}_3\text{-FeCO}_3$  between 350-450°C (Figure 5-1), one dominant carbonatite trend enriched in calcite and iron is recognized. The inferred order of crystallization according to Figure 5-1 appears to be calcite-ankerite-siderite for the Buru carbonatite centre. Samples from Kuge all plot in the CaO apex portraying only a single phase (calcite) system.

The typical sequence of crystallization of carbonate minerals in most carbonatites is calcite-dolomite-ankerite-siderite, that order being indicative of decreasing temperature (Heinrich, 1966). The proposed sequence is also the order of crystallization as postulated by Wyllie (1965) on the basis of experimental evidence. Magnesite carbonatites are rare worldwide (Buckley and Woolley, 1990), though primary carbonatite melts are predicted to have high Mg and Ca (Eggler, 1989 and Dalton and Wood, 1993) with the implication that dolomite carbonatites occur commonly. Instead, most carbonatites are calcitic in composition and less commonly dolomitic, with the notable exception of Oldoinyo Lengai. Dalton and Wood (1993) suggested that the calcite carbonatites can be generated by the reaction between primary magnesian carbonatite melts and harzburgite in the upper

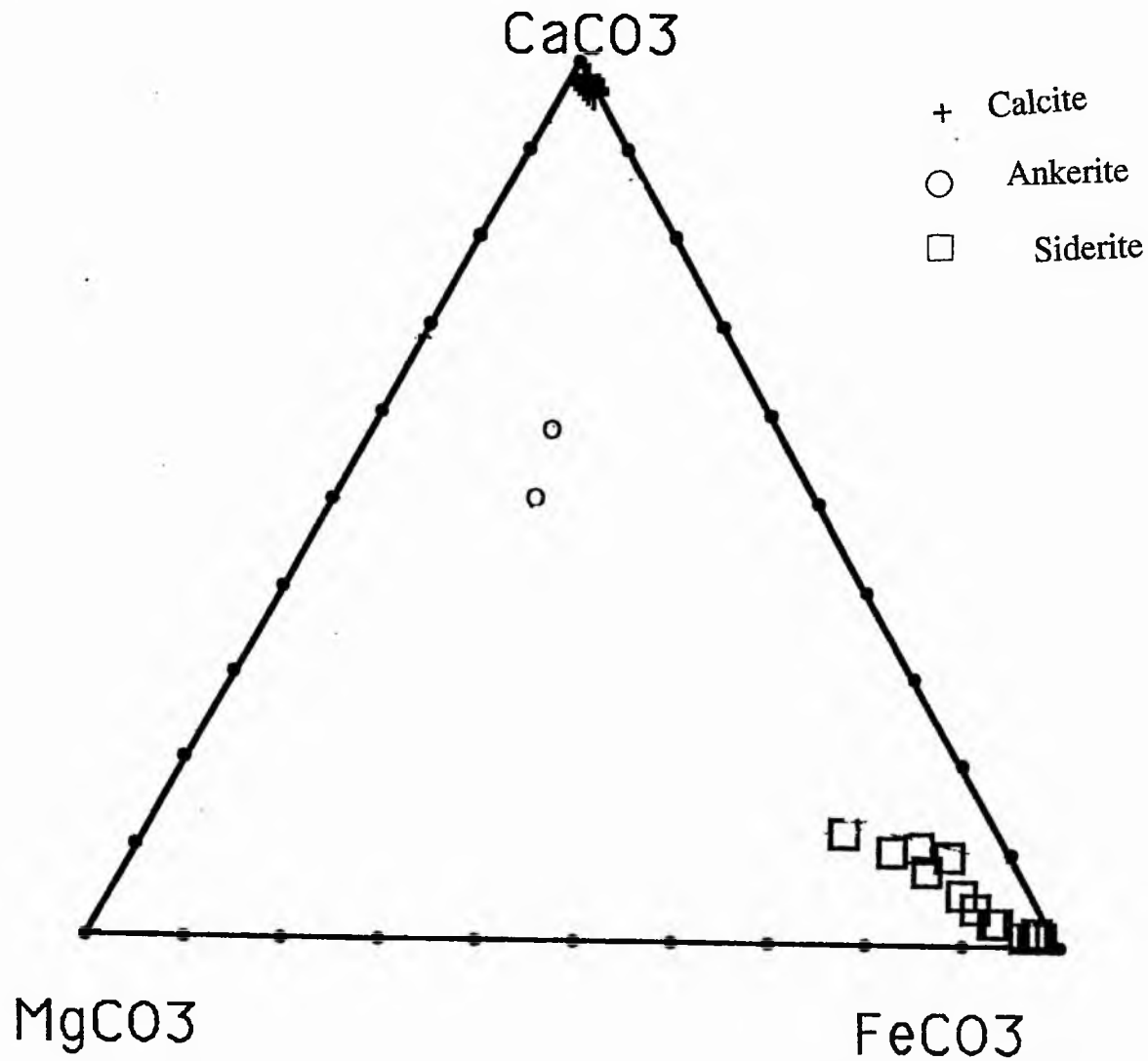


Fig. 5-1 Plots of carbonate compositions (molecular proportions) from Buru and Kuge centres in the system  $\text{CaCO}_3 - \text{MgCO}_3 - \text{FeCO}_3$ . The field boundaries are for the subsolidus system at  $450^\circ\text{C}$  (Rosenberg, 1967).

mantle. The authors have demonstrated that the interaction of a carbonatite with orthopyroxene to produce olivine and clinopyroxenes at lower pressures would result in the melt becoming more calcic than the ones observed in nature.

Sweeney (1994) suggested that the crystallization of olivine + phlogopite + clinopyroxene from a primary carbonatite at  $P < 25$  kbar would cause the melt to become more calcic and has formulated mechanisms to explain this by the interaction of  $\text{CO}_2$  migrating from the lower regions of the upper mantle with peridotite. Gittins and Harmer (1995) argue that at  $1000^\circ\text{C}$ , the temperature of carbonatite magmas, it is inevitable that magnesian carbonatite magmas will reach crustal levels where the pressure is too low to allow dolomite to crystallize. They propose that magnesian carbonatite magmas can survive to fairly high crustal levels, but eventually give rise to calcic magmas in the upper crust, as well as deeper levels if there is enough Si, Al and Fe to permit magnesian silicates to form. Surplus Mg left in the system can then form dolomite, which is consistent with the relatively common occurrence of the assemblage calcite - dolomite - silicate-oxide in deep-seated carbonatite complexes.

#### 5.4.3 Barite and fluorite.

Barite and fluorite are frequently found in association with carbonatites (Mariano, 1989b). Kueller et al. (1966) studied barite and fluorite in the system  $\text{CaCO}_3\text{-Ca(OH)}_2\text{-CaF}_2\text{-BaSO}_4$  and concluded that barite-calcite-fluorite assemblages, which are intimately related to and associated with carbonatites, owed their origin to magmatic processes. They noted, however, that the most common occurrence of these assemblages as low temperature fillings could be hydrothermal in origin. At Mountain Pass, barite has been found to be both primary and hydrothermal in origin

(Wyllie et al., 1996). Fluorite has also been documented from a number of localities confined essentially to late stage hydrothermal activities as indicated by the low crystallization temperatures of 100 to 150°C revealed by fluid inclusion studies (Roedder, 1973).

The occurrence of barite and fluorite is widespread in the Buru and Kuge carbonatite centres. The two minerals occur in both the weathered profile (laterite) and the carbonatites. Selected electron microprobe analyses of barite and fluorite from the Buru and Kuge carbonatites are shown in Table 5-4.

Table 5-4 Selected electron microprobe analyses of barite and fluorite from the Buru and Kuge carbonatite centres.

Mineral	Barite (Buru)	Barite (Kuge)	Fluorite (Buru)
No of analyses	4	4	2
SiO <sub>2</sub>	0.31	0.15	0.02
Al <sub>2</sub> O <sub>3</sub>	0.30	0.40	0.56
FeO	0.21	0.16	0.49
MnO	-	0.32	0.62
MgO	-	-	0.25
P <sub>2</sub> O <sub>5</sub>	0.03	0.15	0.15
CaO	0.07	0.10	67.86
BaO	65.89	66.52	0.27
SrO	0.36	0.33	1.82
SO <sub>3</sub>	33.75	33.42	0.05
F	0.73	1.65	24.14
F=O	0.31	0.70	10.17
Total	100.92	102.50	86.06

Oxides in wt%; -: below detection limit.

Barites from the Buru and Kuge carbonatite centres are chemically similar (Table 5-4). According to Kapustin (1980), barites of earlier generation carbonatites contain up to 5 wt% SrO, whereas later carbonatites usually contain low SrO contents. The average SrO from the Buru and Kuge hills is below 0.5 wt%, which indicates that these volcanic centres belong to 'late-stage carbonatites', according to the terminology of Kapustin (1980) and Sokolov (1985). The Buru and Kuge barites are therefore consistent with late-stage barites reported elsewhere (Walter et al., 1995b and Wall and Mariano, 1996). Microprobe analyses of a 'hydrothermal barite' reported by Walter et al. (1995b) has a similar BaO (64.83 wt%) content to barite from the two areas under study, but contains much lower SrO (0.03 wt%) compared to the Buru and Kuge hills.

Fluorite analyses (EPMA) from carbonatites are rarely available. Carbonatites where fluorite mineralization has been identified according to Mariano (1989b) include Amba Dongar; India, Okorusu; Namibia, Mato Preto; Parana; Brazil, Tchivira,; Quilengues; Angola and the Bayan Obo iron-REE deposit, China. Fluorite from the Buru carbonatite are mainly composed of CaO and F with a significant amount of SrO. Both fluorite and barite contains no REE elements.

The majority of barite and fluorite occurrences in carbonatites are confined to late stage hydrothermal activity, where they are deposited by low temperature hydrothermal fluids. Barite and fluorite are themselves derived from a carbonatite source. The presence of barite and fluorite in the laterite and supergene zones in the two centres suggests that these minerals are stable in the final stages of carbonatite alteration.

#### 5.4.4 Oxides (magnetite and goethite).

Magnetite is a common accessory mineral in carbonatites. It has been shown that portions of rock rich in magnetite, like those ones observed in Nyanza rift carbonatites, show characteristic 'flow trails' that are usually associated with apatite or mica (biotite or phlogopite). Electron microprobe data for the Buru and Kuge magnetites are shown in Table 5-5.

Table 5-5 Electron microprobe analyses of magnetite and goethite from the Buru and Kuge carbonatites.

Mineral	Magnetite (Buru)	Magnetite (Kuge)	Goethite(Buru)
No. of analyses	2	2	2
SiO <sub>2</sub>	0.3	0.41	2.09
Al <sub>2</sub> O <sub>3</sub>	0.01	0.05	0.82
FeO	86.28	91.05	58.00
MnO	0.89	0.12	11.19
MgO	-	-	-
CaO	0.05	-	0.14
F	1.81	3.01	2.68
F=O	0.76	1.27	1.13
TREO	0.08	0.35	1.69
Total	88.58	93.37	75.48

Oxides in wt %; total Fe as FeO; -: below detection limit.

Magnetite from Buru and Kuge are similar in composition. Small amounts of silicon, aluminium, manganese and fluorine substitute for iron. TiO<sub>2</sub> was not analyzed for, but on the basis of high FeO totals, which are close to the theoretical end-member composition, the TiO<sub>2</sub> content is considered to be minimal and therefore the magnetites are not titanomagnetites. Magnetites

from carbonatites are usually poor in titanium with usually only 1-2 wt% TiO<sub>2</sub> (Le Bas, 1987).

Goethite (iron hydroxide) is a common and typical iron mineral observed within the laterite in the Buru cores and also in the Kuge ferrocyanatite breccia, where it occurs as a weathering product of iron-bearing minerals such as magnetite and siderite. The representative electron microprobe analysis of goethite from Buru (shown in Table 5-5) shows high substitution by manganese and minor substitution of silicon, aluminium and fluorine for iron. Goethite is enriched in REEs compared to magnetites from the two centres.

The compositions of primary oxides (magnetite and pyrochlore) in the carbonatites, especially magnetite, will depend on the bulk chemistry of the magma, the depth of emplacement and the oxygen fugacity of the magma. These processes govern the distribution of magnetite and hematite in the Buru cores, where hematite is quite common towards the surface in areas of high redox potential whereas magnetite was commonly observed in deeper sections of the drill cores, where weathering is minimal.

#### 5.5.5 Biotite and phlogopite.

The micas (phlogopite and biotite) are also widely distributed in the carbonatites. According to Kapustin (1980), phlogopite constitutes over 90% of all the micas. This is not entirely true because a number of investigated carbonatite complexes do contain substantial amounts of biotite (Woolley et al., 1991 and Ngwenya, 1994). Phlogopite is frequent in the Buru and Kuge cores whereas biotite is very rare. The sample NR-271 from the North Ruri carbonatite complex does however contain significant amounts of biotite. Table 5-6 provides electron microprobe analyses of

biotite from the North Ruri carbonatite complex and a phlogopite analysis from the ferrocarbonatite breccia, Kuge carbonatite centre.

Table 5-6 Electron microprobe analyses (wt%) of biotite and phlogopite.

Mineral	Biotite	Phlogopite
No. of analyses	2	2
SiO <sub>2</sub>	38.51	43.01
TiO <sub>2</sub>	3.20	0.52
Al <sub>2</sub> O <sub>3</sub>	11.04	8.24
FeO	20.86	9.82
MnO	0.50	0.15
MgO	11.29	17.73
CaO	0.15	0.30
Na <sub>2</sub> O	0.16	0.23
K <sub>2</sub> O	8.50	9.21
Total	94.21	89.21
Formula calculated on the basis of 24 O.		
Si	6.507	7.241
Al	1.493	0.759
Z total	8.000	8.000
Al	0.704	0.875
Ti	0.407	0.066
Fe	2.948	1.383
Mn	0.072	0.021
Mg	2.843	4.449
Y total	6.974	6.794

Table 5-6 continued.

Mineral	Biotite	Phlogopite
Ca	0.023	0.054
Na	0.052	0.075
K	1.832	1.978
X total	1.907	2.107

The biotite from a calcite carbonatite (NR-271) is very similar to biotite analyzed by Ngwenya (1994) from a silicate-calcite carbonatite, Tundulu carbonatite complex, Malawi. The structural formula calculated compares well with the chemical composition of micas  $(X_2 - Y_6 - Z_8 O_{20})(OH)_4$  where:

X is mainly K, Na and minor Ca, Ba and Rb;

Y is mainly Al, Mg, or Fe and minor Mn and Ti;

Z consists mainly of Si and minor Al and Ti.

### 5.5 WEATHERING VS HYDROTHERMAL PROCESSES.

In most carbonatites that have been affected by weathering, a definite mineralogical sequence is recognized in relation to the degree and extent of chemical weathering. According to Mariano (1989b), typical mineralogical changes as weathering decreases with depth will show magnetite followed by decomposed pyrochlore and, with a continued increase in depth, fresh carbonatite is encountered where pyrochlore, apatite, calcite or dolomite are all observed. Because of great mineralogical heterogeneity exhibited by carbonatites worldwide, the mineralogical sequence outlined above is not necessarily portrayed by every carbonatite studied. The mineralogy, especially with regard to carbonatite laterites, is a function of age, depth of weathering, structure, geomorphology and the nature of the original carbonatite magma (Mariano, 1989b).

The significant parameters that seem to control the mineralogy of the carbonatites under investigation include the extent and depth of weathering where the mineral zonation with depth indicates the extent of dissolution, and reprecipitation during supergene processes. The oval structure in Buru and the rim of resistant gneisses prevented most of the weathering solutions from escaping and concentrated them within the site of lateritization.

The various iron phases identified by X-ray diffraction studies, for example in BRL-1 and BRL-2, appear to indicate a distinct geochemical environment of formation. Hematite and goethite are concentrated on the upper oxidized zones of the cores (laterite), whereas siderite is only observed towards the deeper sections of the drill cores where there is minimal weathering. These iron phases (goethite, hematite and siderite) indicate that the occurrence, composition and stability of the iron compounds are partly dependent on temperature and oxygen fugacity, among other factors, during their formation.

The oxidation of siderite to iron oxide (hematite) may occur either through increasing the temperature or through increasing the oxygen fugacity in the environment, particularly during exposure to the atmosphere or when oxygen-rich ground waters of shallow origin are in contact with iron compounds (Faure, 1992). The writer is of the opinion that the low temperature hydrothermal alteration and supergene weathering processes occurring in Buru can be distinguished simply by the occurrence of iron compounds. Low temperature hydrothermal processes are characterized by the presence of siderite or ankerite (iron-rich dolomite), and supergene processes by the occurrence of goethite or hematite mineralization. The other factors which could help distinguish between low temperature hydrothermal and supergene processes are discussed in chapters 7 and 8.

It is significant to firmly identify the chemical signatures that can help distinguish between hydrothermal and supergene processes. Late magmatic and hydrothermal stages of mineralization are usually characterized by the emplacement of veins and dykes, which contain large contents of niobium, thorium, zirconium and REEs. In order to understand the processes which control these REEs in carbonatites in various stages of alteration, the post-magmatic and supergene re-equilibration which they represent must also be well understood, an area that is discussed in detail in chapter 8.

## CHAPTER SIX

### GENERAL GEOCHEMISTRY OF THE BURU AND KUGE VOLCANIC CARBONATITES

#### 6.1 INTRODUCTION.

Carbonatites show a considerable diversity in terms of their major, minor and trace element composition, which is essentially a reflection of their heterogeneity, especially with regard to their mineralogy. The initial attempt to find the average chemical composition of carbonatites was proposed by Pecora (1956). Gold (1963) and Heinrich (1966) both published average composition values for carbonatites, although in each case they suffered from the incorporation of high silica values and the over-representation of one particular locality, for example the Oka carbonatite complex (Gold, 1963). Recently, however, the chemical classification of carbonatites has been reviewed by Woolley (1982) and Woolley and Kempe (1989), where the use of the modal mineralogy and bulk chemistry of the carbonatites, utilising the wt% of the major oxides CaO, MgO and FeO+Fe<sub>2</sub>O<sub>3</sub>+MnO, have complemented each other.

In this chapter, the bulk chemistry (major and trace element geochemistry) of both Buru and Kuge will be discussed. Major differences and similarities within the two deposits will be evaluated and compared with other carbonatites found elsewhere. Classification using both the bulk chemistry and modal mineralogy and its limitations will be discussed. Samples for major and trace element geochemistry for X-ray fluorescence (XRF) analyses were prepared and analyzed at the Department of Geology, St Andrews University. About 25 selected samples were analyzed at the Royal Holloway, University of London by ICP.

While it was not possible to completely eliminate the element of bias in choosing some analyzed results for discussion, great care was taken to have representative samples that helped address the main features of the thesis. Details of sample preparation, analytical methods used and results obtained are given in Appendices 6-1 and 6-2(1-4).

## 6.2 MAJOR ELEMENT GEOCHEMISTRY.

### 6.2.1 Buru.

Selected analyses of major elements from Buru are shown in Table 6-1. Samples BR-1, BR-5 and BR-8 are from the laterite while BR-13, -16, -28, -218 and -224 are selected from the carbonatite below the weathering profile. Samples BR-59, -150, -183 and -186 are representative of the siderite carbonatite dyke that cuts the Buru carbonatite. In terms of the major element geochemistry, Buru is characterized by high iron and manganese contents, especially within the lateritic profile. Iron and manganese are also enriched within the carbonatite compared to average values given in Woolley and Kempe (1989) for the calcite carbonatite. The general trend, however, is for iron and manganese to decrease down the drill hole where the effects of weathering are minimal. The average value of 5 wt % MnO of the siderite carbonatite dyke is within the range of ferrocarbonatite values quoted in Woolley and Kempe (1989), whereas the average of 46 wt % total iron for the siderite is slightly higher.

In the  $\text{SiO}_2\text{-Al}_2\text{O}_3\text{-Fe}_2\text{O}_3$  diagram (Figure 6-1) the samples from the laterite and carbonatite plot in a narrow field stretching along the  $\text{SiO}_2\text{-Fe}_2\text{O}_3$  side between 0 and 10%  $\text{SiO}_2$ . The samples show very strong enrichment in iron with most of them plotting at the  $\text{Fe}_2\text{O}_3$  corner. The

Sample No.	BR-1	BR-5	BR-8	BR-13	BR-16	BR-28	BR-218	BR-224	BR-59	BR-150	BR-183	BR-186
SiO <sub>2</sub>	1.75	3.39	1.43	12.86	2.23	2.39	2.74	10.86	1.28	2.46	0.10	0.64
Al <sub>2</sub> O <sub>3</sub>	0.39	0.42	0.24	2.55	0.36	0.14	0.44	0.64	0.41	0.35	0.08	0.21
Fe <sub>2</sub> O <sub>3</sub>	30.48	62.8	59.37	14.98	21.88	19.38	28.46	9.99	38.54	48.39	51.45	47.35
MgO	0.22	0.28	0.16	2.04	1.31	2.44	0.36	2.00	2.32	1.96	2.09	1.74
CaO	26.91	2.40	7.89	28.71	36.41	26.36	26.09	29.84	11.6	8.56	8.95	10.95
Na <sub>2</sub> O	0.12	0.06	0.06	0.85	0.27	0.38	0.07	0.21	0.16	0.26	0.21	0.33
K <sub>2</sub> O	0.12	0.20	0.09	1.55	0.29	0.35	0.19	1.06	0.29	0.23	0.06	0.12
TiO <sub>2</sub>	0.40	0.51	0.51	0.37	0.24	0.16	0.21	0.63	0.15	0.14	0.07	0.23
P <sub>2</sub> O <sub>5</sub>	1.23	0.64	0.50	0.94	0.29	2.80	0.24	0.25	0.21	0.44	0.25	0.36
MnO	7.22	9.48	8.9	2.37	2.67	4.17	5.56	2.37	5.65	5.68	5.00	5.83
TOTAL	68.72	80.18	79.15	67.22	65.95	58.57	64.33	57.64	60.61	68.47	68.26	67.76
Ba	13557	16386	12251	3220	4100	10528	9147	3989	3432	4876	3631	5165
Co	33	46	41	21	25	27	30	21	26	28	29	28
Cr	31	43	40	22	23	23	27	18	33	30	28	29
Cu	12	23	18	6	12	7	23	21	12	14	8	25
Li	28	183	25	360	130	321	82	1299	65	146	51	88
Nb	352	1349	769	80	706	200	263	462	268	248	133	327
Ni	4	10	6	11	8	5	3	7	2	1	0	2
Sc	48	41	17	24	14	20	42	69	32	15	14	16
Sr	3069	1205	1217	2379	2816	11654	1530	3704	1171	4598	1211	3051
V	155	179	109	162	135	57	96	113	131	118	132	200
Y	712	935	695	276	656	436	1371	1279	364	918	250	791
Zn	2893	2414	2261	1720	2035	1325	2709	5196	3791	2816	2345	1733
Zr	124	157	152	76	105	68	135	153	71	82	66	138

Oxides in wt %; trace elements in ppm

Table 6-1 Major and trace element analyses of Buru carbonatite (ICP analyses)

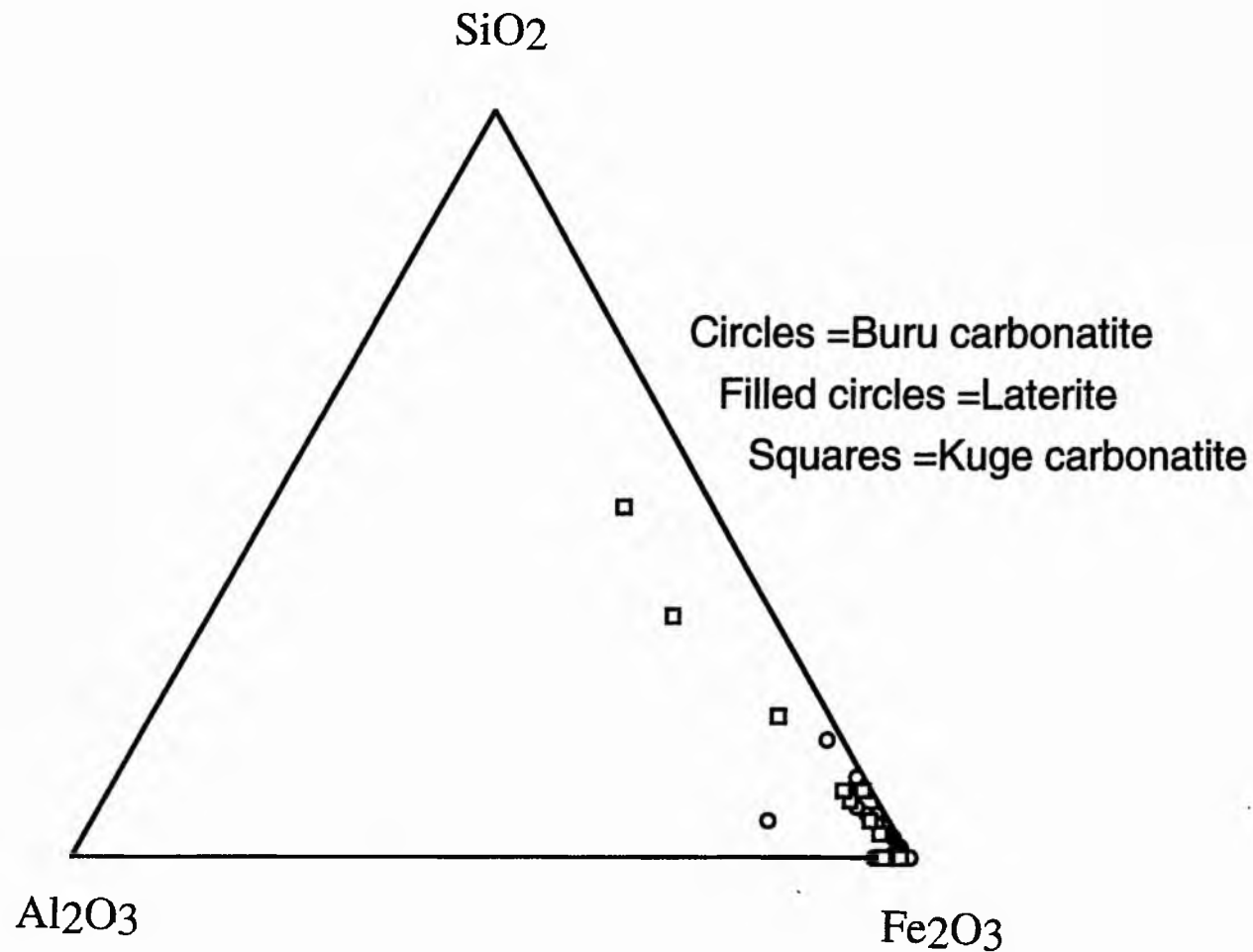


Figure 6-1 SiO<sub>2</sub>-Al<sub>2</sub>O<sub>3</sub>-Fe<sub>2</sub>O<sub>3</sub> (wt %) diagram showing fields for the laterite and the Buru and Kuge carbonatite centres (XRF analyses).

apparent depletion of Al and Si in the Buru samples is very noticeable from the diagram.

### 6.2.2 Kuge.

The Major and trace element analyses of the Kuge carbonatite are given in Table 6-2. The Kuge ferrocarbonatite breccia is also enriched in both iron and manganese with averages of 23 wt% FeO and 5 wt% MnO. These values are, however, within the expected range of values of ferrocarbonatites given in Woolley and Kempe (1989). It is interesting to note that the average FeO content of 23 wt% for the ferrocarbonatite from Kuge is much lower than the average of 46 wt % of the siderite carbonatite from Buru, though the two rock units have identical average values of MnO. The significance of this observation will be discussed later, in the section on geochemical classification. The trend of iron enrichment is also noted in the  $\text{SiO}_2\text{-Al}_2\text{O}_3\text{-Fe}_2\text{O}_3$  diagram (Figure 6-1), as well as a slight increase in silica in some Kuge samples compared to the Buru carbonatite.

### 6.2.3 Iron and manganese concentrations in Buru and Kuge.

Whereas iron and manganese are known to increase with fractionation of the carbonatites (Woolley and Kempe, 1989), the extremely high values noted in two areas under study, particularly in their supergene zones, can certainly be attributed to the late-stage formation of the secondary minerals goethite, hematite and manganese-rich oxides that characterize these oxidized sections. However, most of the iron in carbonatites is present as primary magnetite.

In both the Buru and Kuge carbonatite centres, the presence of a manganese bearing mineral is not obvious from outcrop or petrography. Barber (1974) also found high concentrations of manganese in his melacarbonatites

Table 6-2 Major and trace elements from Kuge carbonatite (ICP analyses).

Sample No	KG-69	KG-71	KG-72	KG-76	NR-271
SiO <sub>2</sub>	0.78	1.18	1.17	3.12	0.05
Al <sub>2</sub> O <sub>3</sub>	0.15	0.28	0.58	1.42	0.03
Fe <sub>2</sub> O <sub>3</sub>	15.34	15.98	23.16	38.89	0.32
MgO	0.45	0.36	0.71	0.41	0.11
CaO	27.03	23.59	27.92	21.43	54.71
Na <sub>2</sub> O	0.06	0.09	0.12	0.14	0.11
K <sub>2</sub> O	0.05	0.06	0	0.06	0.06
TiO <sub>2</sub>	0.1	0.02	0.05	0.05	0.01
P <sub>2</sub> O <sub>5</sub>	0.34	1.73	2.28	2.29	0.42
MnO	3.82	6.75	4.25	5.9	0.21
Total	48.12	50.04	60.24	73.71	56.53
Ba	7939	12847	10737	13937	666
Co	24	28	35	41	8
Cr	19	30	38	53	7
Cu	10	13	18	27	6
Li	9	6	7	5	2
Nb	51	17	139	658	9
Ni	6	0	3	6	0
Sc	45	32	49	30	3
Sr	1676	1649	2349	2400	7620
V	98	80	168	179	11
Y	133	330	831	993	78
Zn	2005	1852	1530	1166	12
Zr	27	29	59	65	4

Oxides in wt %; trace elements in ppm

(ferrocarbonatites), but he was unable to trace it to any particular manganese mineral. Rhodochrosite ( $\text{MnCO}_3$ ), the main manganese carbonate mineral, easily decomposes when exposed close to the earth's surface to produce a superficial brown or black layer of complex manganese oxides (Deer et al., 1992).

In this study, the unusually high values of manganese, which is mainly concentrated in the supergene zones of the two carbonatite centres, has been found, through electron probe microanalysis (EPMA), to be associated with the mineral psilomelane. Psilomelane [ $\text{Ba}(\text{H}_2\text{O})_2\text{Mn}_2\text{O}_{10}$ ] is mainly found as a secondary mineral in association with manganese deposits and in residual deposits due to weathering. In most of the polished thin-sections studied, the geochemistry of the mineral psilomelane is dominated mainly by manganese and barium oxides with lower values of Fe and fluorine (Table 6-3). It resembles some members of the isostructural hollandite-cryptomelane-romanechite group of high manganese and barium minerals typically found in near-surface environments (Fleischer, 1960).

The mineral identified here closely resembles the mineral romanechite from the type locality Romaneche-France (Perseil and Pinet, 1976). One of the first reported examples of the mineral psilomelane from a weathered carbonatite is from the Mrima hill carbonatite complex, Kenya (Deans, 1966). There are also several occurrences in Russia (Lapin, 1992) where psilomelane is listed as one of the minerals, occurring together with goethite and hematite in lateritic weathered crusts. Psilomelane has also been reported from the Lueshe carbonatite complex, where it was observed to be in association with cryptomelane (Von Maravic et al., 1989). Unfortunately, neither of these references contain any analytical data on the psilomelane. Dawson (1993) also found a similar mineral within the calcite

carbonatite from Oldoinyo Lengai. He interpreted this mineral as being romanechite because it was similar to the romanechite of the type locality, from Romaneche in France.

Table 6-3 Electron microprobe analyses of psilomelane.

Sample	BR-207	BR-210	KG-80	J.D.	P.P.
SiO <sub>2</sub>	0.25	0.73	0.5	1.27	na
Al <sub>2</sub> O <sub>3</sub>	0.25	0.47	0.08	0.19	1.80
FeO	0.45	1.66	0.18	-	na
MnO	55.83	51.33	55.68	70.60*	75.30*
MgO	0.04	0.03	0.05	0.03	0.07
ZnO	0.69	0.09	0.27	na	na
F	2.81	-	0.91	na	na
P <sub>2</sub> O <sub>5</sub>	-	0.15	0.18	na	na
CaO	0.82	0.45	0.36	1.64	0.45
BaO	12.9	12.49	15.49	12.70	11.87
SrO	-	0.31	0.32	0.16	na
SO <sub>3</sub>	0.2	0.09	0.07	na	na
La <sub>2</sub> O <sub>3</sub>	-	0.19	-	na	na
Ce <sub>2</sub> O <sub>3</sub>	-	0.09	0.14	na	na
Total	73.14	68.08	74.23	98.71	90.53

J.D.: Total in J.D. includes 2.14% Na<sub>2</sub>O and 0.87 % K<sub>2</sub>O (from Dawson, 1993).

P.P.: Total in P.P. includes 0.52% Na<sub>2</sub>O, 2.12% K<sub>2</sub>O and 5.42% H<sub>2</sub>O (from Perseil and Pinet, 1976).

-: Below detection limit; na: not analysed; \*: Mn as MnO<sub>2</sub>

Chemically, the mineral psilomelane from both Buru and Kuge is broadly similar in terms of their MnO, BaO, MgO contents and other major oxides,

though there appears to be a slight increase in FeO in the Buru samples. Compared with the mineral romanechite from France and Tanzania, the Buru and Kuge carbonatite centres have similar contents in BaO and MgO, but the two volcanic centres have very low totals in MnO. The sample from Tanzania seems to have relatively high CaO (1.64 wt %) compared to an average of 0.5 wt.% from the Buru and Kuge carbonatite complexes and 0.45 wt % from Romaneche, France.

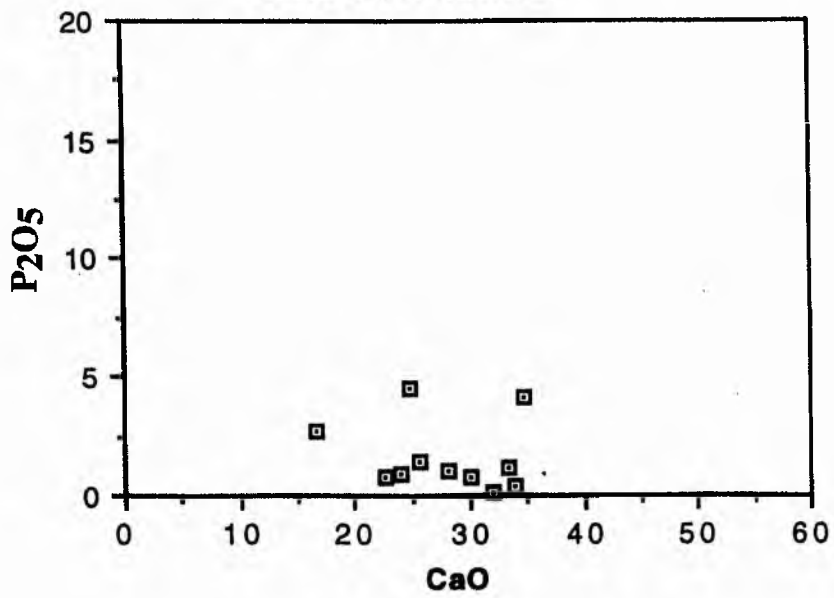
The low values of MnO from Buru and Kuge could be due water, which was not analyzed for, and the uncertainty as to the oxidation state of the Mn sought in the analysis. All of the psilomelane examined from Buru and Kuge appear to be void of REE mineralization.

#### 6.2.4 CaO and P<sub>2</sub>O<sub>5</sub> content.

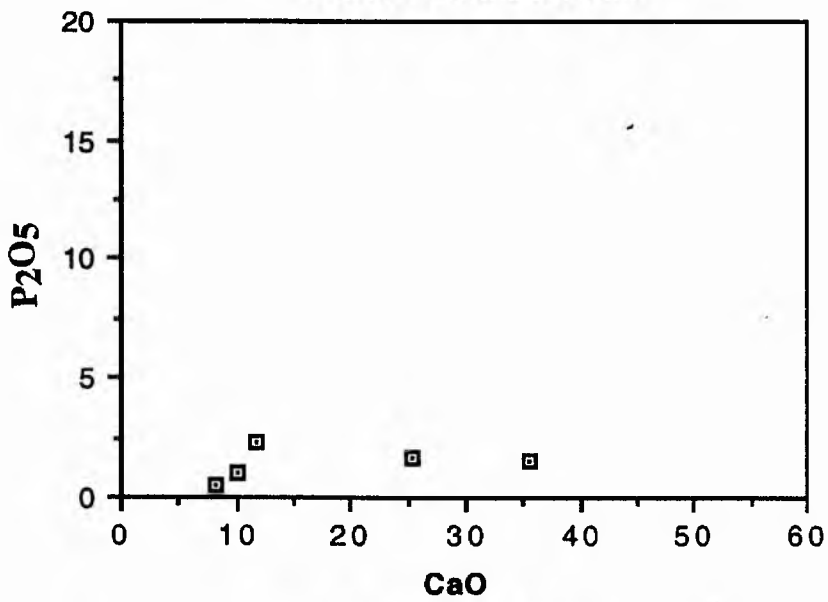
In the CaO vs P<sub>2</sub>O<sub>5</sub> diagram (Figure 6-2), it can be observed that carbonatite rocks from both Buru and Kuge, including the laterite have no correlation between CaO and P<sub>2</sub>O<sub>5</sub> values which indicate that Ca is present mainly as carbonate. The Buru and Kuge carbonatites are seen to be enriched in CaO compared to the laterite, which is attributed to leaching of the carbonates during weathering processes. P<sub>2</sub>O<sub>5</sub> values are slightly higher in some of the lower samples of the cores, which could also indicate a possible chemical destruction of apatite in the supergene zone.

#### 6.2.5 TiO<sub>2</sub> and total alkalis.

Titanium and the alkalis have low values which is characteristic of carbonatites worldwide, except the unusual Oldoinyo Lengai lavas which are enriched in alkalis. Western Kenya carbonatites are also characterized by low contents of magnesium compared to other carbonatites in Africa, especially Central and Southern African carbonatites which are characterized by the common occurrence of dolomite.



BURU - Lateritized zone



KUGE CARBONATITE

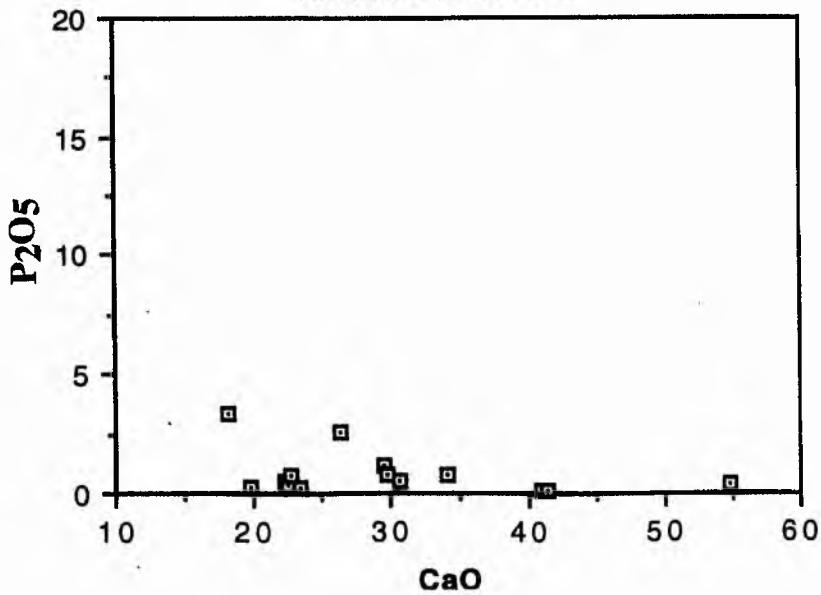


Figure 6-2 CaO vs P<sub>2</sub>O<sub>5</sub> for the Buru laterite and the Buru and Kuge carbonatites (analysis by XRF).

### 6.3 TRACE ELEMENTS.

Barium and strontium, which are characteristic trace elements of carbonatite, are extremely enriched in the two centres studied. Again, the samples from the laterite have the highest contents, especially for Ba with values of between 12,000 to 16,000 ppm encountered. The high Ba contents means that this element should be classified as a 'major element' rather than a trace mineral. Kuge also has elevated values of Ba. These high 'trace element' contents account for some of the deficiency in major element totals. Compared with the Buru and Kuge carbonatites, the siderite carbonatite has slightly lower values of Ba and Sr. The calcite carbonatite (NR-271) from the Ruri hills contains the highest Sr contents (7620 ppm) rather than samples from the Buru and Kuge carbonatites. The depletion of Sr in late-stage carbonatites that have evolved fluids has been noted by Platt and Woolley (1990). The high value of Sr (11,654 ppm) observed in sample BR-28 is due to the presence of strontianite.

Niobium concentrations are low (compare Woolle and kempe, 1989) and this explains why the mineral pyrochlore was not easily identified by the writer. It is noted, however, that niobium contents seem to increase down the drill hole as the effect of supergene processes diminishes, suggesting the breakdown of the mineral pyrochlore in the weathering zone. Yttrium and particularly zinc are also enriched and are seen to exceed the normal average values quoted in Woolley and Kemp (1989).

Lithium is rarely reported or analyzed for in carbonatites. In Buru, both the calcite carbonatite and the siderite carbonatite contain high values of lithium compared to values given in Woolley and Kempe (1989). Sample BR-224 from BRL-2 contains very high lithium contents (1299 ppm). Lithium, however, is depleted in the Kuge samples, where it has an average

of only 5 ppm lithium. Sample NR-271, the calcite carbonatite from North Ruri, is also depleted in lithium (2 ppm).

Recently, Cooper and Paterson (1995) have described a rare Li-mica [taeniolite,  $\text{KLiMg}_2\text{Si}_4\text{O}_{10}(\text{F},\text{OH})_2$ ] from the Dicker Willem carbonatite complex, Namibia, and from the Haast River, New Zealand. The authors argue that the presence of lithium in these two complexes reflects the geochemical character of the magmatic source rather than being due to crustal assimilation or interaction. Lithium concentrations in Buru and Kuge are clearly different and distinct. Both Buru and Kuge have intruded different rock units and it is therefore possible that lithium concentrations in the intruded rocks were different. The occurrence of lithium in the two centres might reflect contamination with the country rocks, though small localized mantle heterogeneity with respect to lithium cannot be ruled out.

#### 6.4 CHEMICAL COMPOSITIONS OF THE BURU AND KUGE CENTRES.

##### 6.4.1 Woolley (1982) and Woolley and Kempe (1989) classification.

On the basis of the major elements, the Buru carbonatite and the Kuge ferrocarbonatite breccia plot entirely as ferrocarbonatites on the carbonatite classification diagram proposed by Woolley (1982) and Woolley and Kempe (1989). However the fine- to medium-grained calcite carbonatite from Kuge (chapter three) plots as calciocarbonatite as expected. The apparent absence of dolomite in these carbonatites is clearly visible (Figure 6-3). In a classic carbonatite sequence, an evolutionary trend of calciocarbonatite, magnesiocarbonatite and ferrocarbonatites, which is also the sequential order of intrusion from early to late, is recognized in very few carbonatites. Chemical and microprobe studies suggest the presence of

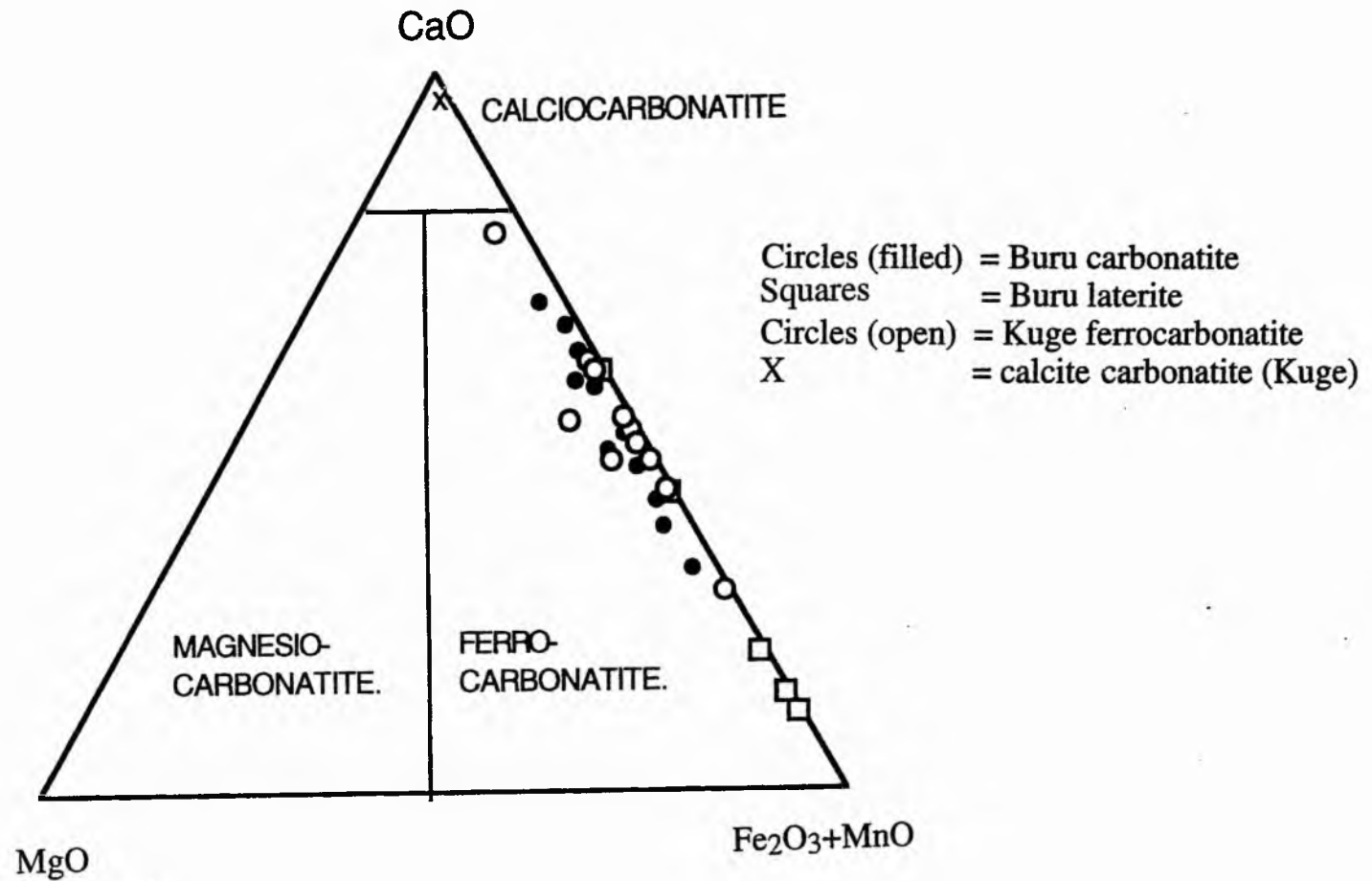


Figure 6-3 Buru and Kuge carbonatite and laterite from Buru (whole rocks) plotted in terms CaO-MgO-Fe<sub>2</sub>O<sub>3</sub>+MnO (wt %). Boundaries and suggested nomenclature from Woolley and Kempe (1989).

calcite in the Kuge ferrocarbonatite breccia and calcite and siderite with minor ankerite in Buru, yet all samples plot as "ferrocarbonatites" in the carbonatite classification diagram, despite the absence of iron-bearing minerals in some of the samples studied.

Figure 6-4 also indicates that the ferrocarbonatite breccia from Kuge and the siderite carbonatite from Buru plot as distinct units within the field of ferrocarbonatites and are clearly different. The trend for siderite carbonatite is towards the iron-rich corner, whereas the trend for Kuge is towards the CaO corner. As mentioned earlier, there is confusion as to the use of the term 'ferrocarbonatite' in the classification of carbonatites using major element chemistry.

Another difficulty in applying the Woolley (1982) and Woolley and Kempe (1989) scheme is the fact that most carbonatites do contain relatively high amounts of magnetite or hematite in their modal chemistry, which the scheme does not take into account, and hence they will consequently plot as 'ferrocarbonatites'. The trend towards the iron corner is also potentially difficult to explain unless the chemistry of the samples are known. The lateritic samples from Buru and the siderite carbonatite all plot towards the iron corner (Figures 6-3 and 6-4). It can be argued that the increase in iron shown by samples from the supergene zone could be attributed to the presence of secondary iron, whereas the trend shown by siderite is largely due to a primary magmatic trend where there is increase in iron and manganese with carbonatite fractionation.

#### 6.4.2 Multi-element variation diagrams (spider diagrams).

In the multi-element variation condensed spider diagram (Figure 6-5), normalized to a hypothetical primordial mantle composition (Wood et al.,

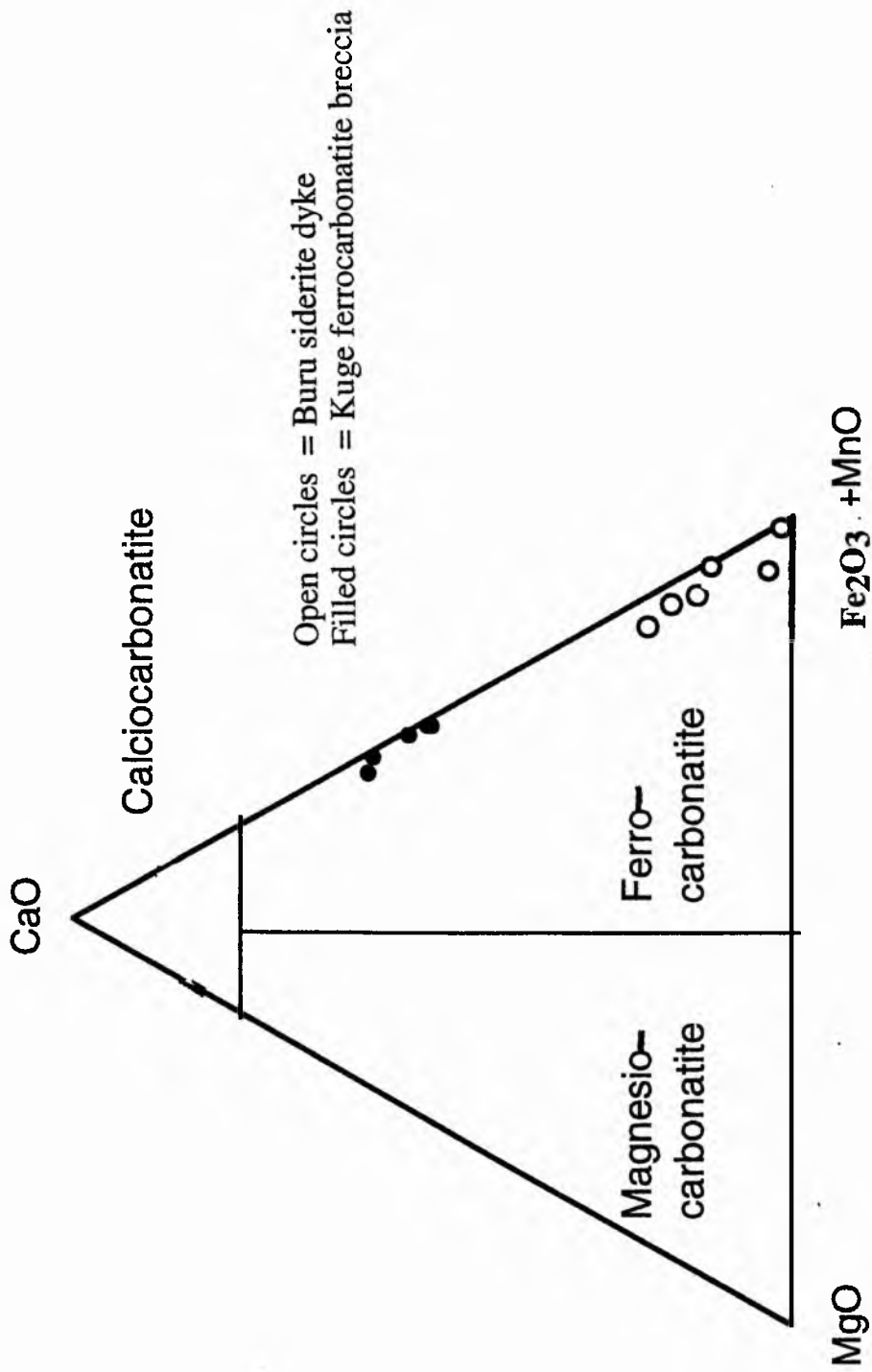


Figure 6-4 Carbonatite classification for the Buru siderite and the ferrocarbonatite breccia from Kuge (after Woolley, 1982 and Woolley and Kempe, 1989).

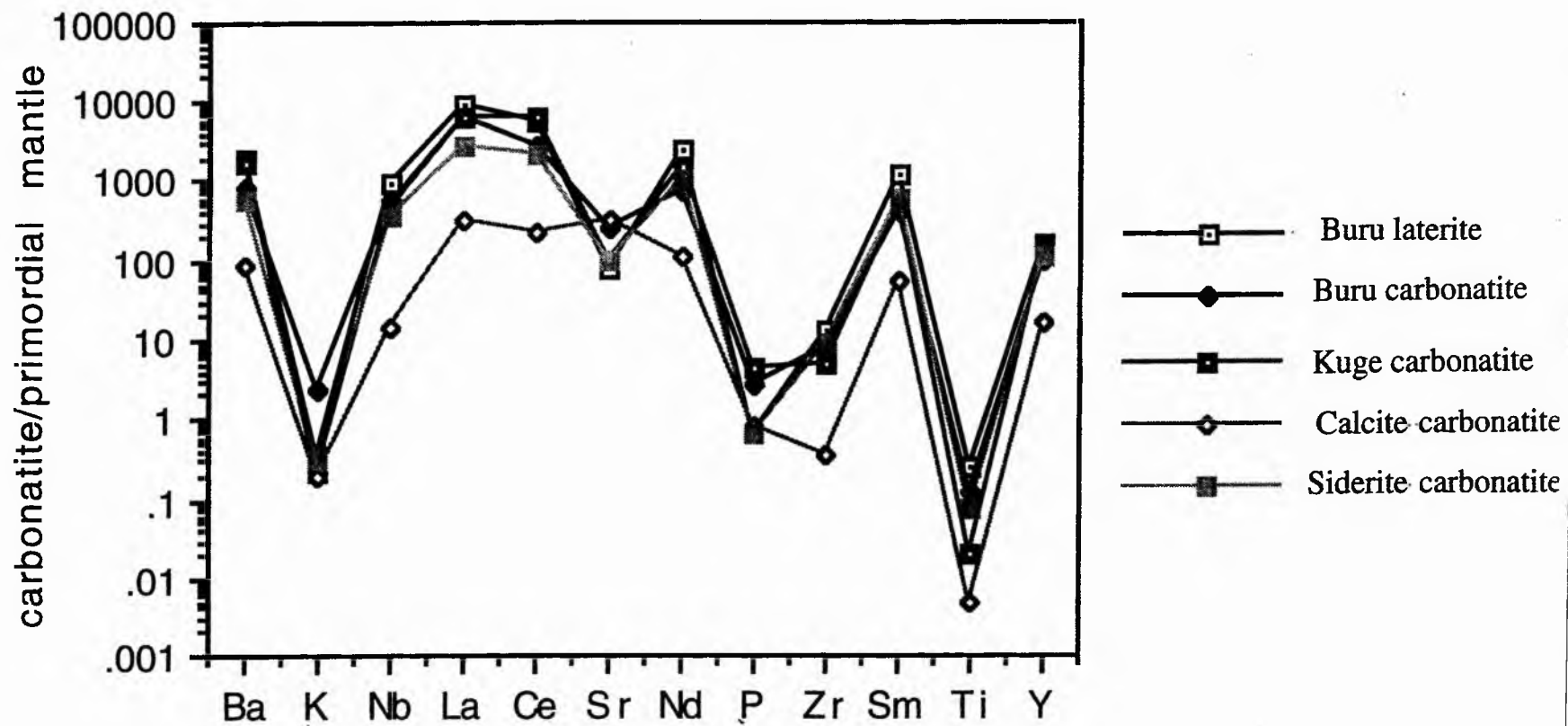


Figure 6-5 Condensed mantle-normalized spider diagram for Buru and Kuge carbonatite centres. Mantle values from Wood et al. (1979).

1979), the Buru and Kuge carbonatites show a general enrichment in Ba, Nb, La, Ce, Sr, Nd, Sm and Y and are depleted in K, P and Ti relative to the primitive mantle. The averaged samples from the laterite, the Buru carbonatite, the siderite dyke, the Kuge carbonatite breccia and the sample from the Ruri carbonatite have all comparable patterns, except that the laterite is slightly enriched in most of the analyzed elements. The calcite carbonatite from Ruri is depleted in all elements except Sr as expected. The enrichment of Sr over Ba is a typical characteristic feature of calcite carbonatites (the first stage carbonatites of Sokolov, 1985).

### 6.5 Summary

The enrichment and depletion of the western Kenyan carbonatites noted in this chapter is consistent with the chemical character of carbonatites that have been observed in several areas such as the Uyaynah Area, United Arab Emirates (Woolley et al., 1991), Rajasthan, India (Wall et al., 1993), Chilwa island, Malawi (Simonetti and Bell, 1994), and Huang et al., (1995). When compared with the average calciocarbonatites and ferrocarnatites of Woolley and Kempe (1989), the average Buru and Kuge carbonatites are seen to have comparable patterns.

## CHAPTER SEVEN

### STABLE ISOTOPE GEOCHEMISTRY

#### 7.1 TERMINOLOGY AND STANDARDS IN USE IN STABLE ISOTOPE GEOCHEMISTRY.

Carbon, oxygen and sulphur isotopes have various stable isotopes that are subject to isotope fractionation in nature. The relative abundances of these stable isotopes, according to Hoefs (1987), are shown below:

	Isotopic abundances
Carbon	$^{12}\text{C} = 98.892\%$
	$^{13}\text{C} = 1.108\%$
Oxygen	$^{16}\text{O} = 99.759\%$
	$^{17}\text{O} = 0.037\%$
	$^{18}\text{O} = 0.204\%$
Sulphur	$^{32}\text{S} = 95.02\%$
	$^{33}\text{S} = 0.76\%$
	$^{34}\text{S} = 4.22\%$
	$^{36}\text{S} = 0.014\%$

The isotopic ratios of  $^{18}\text{O}/^{16}\text{O}$ ,  $^{13}\text{C}/^{12}\text{C}$  and  $^{34}\text{S}/^{32}\text{S}$  are normally measured because of their high abundances relative to other isotopes.

The isotope analyses are expressed as per mil deviations (‰) from a reference sample:

$$\delta = \frac{R_{\text{sample}} - R_{\text{standard}}}{R_{\text{standard}}} \times 1000,$$

where R stands for the ratio of the heavy to the light isotope. The standards commonly used are:

Standard Mean Ocean Water (SMOW) for  $^{18}\text{O}/^{16}\text{O}$ ;

Pee Dee Belemnite (PDB) for  $^{13}\text{C}/^{12}\text{C}$ ; and

Canyon Diablo Troilite (CDT) for  $^{34}\text{S}/^{32}\text{S}$ .

The relationship between  $\delta^{18}\text{O}$  (SMOW) and  $\delta^{18}\text{O}$  (PDB) is given by the following equation:

$$\delta^{18}\text{O} (\text{SMOW}) = 1.03086 \delta^{18}\text{O} (\text{PDB}) + 30.86 \text{ (Faure, 1992)}.$$

Standards have a fixed value of 0 by definition, with the sample ratio being expressed as a delta ( $\delta$ ) value in per mil ( $\text{‰}$  - parts per thousand) units as a deviation away from the standard. Both positive or negative values are possible, which signify enrichment or depletion of the heavy isotope in the sample relative to the standard.

Isotope fractionation, the partitioning of isotopes between two substances (A and B) with different isotope ratios, is defined by the fractionation factor  $\alpha$ :

$$\alpha_{\text{A-B}} = \frac{\text{Ratio in A}}{\text{Ratio in B}}.$$

The difference between the  $\delta$  values for the two minerals is expressed as  $\Delta$ . The relationship of the  $\Delta$  value to the associated fractionation factor is provided by the approximation:

$$\Delta_{A-B} = \delta A\text{‰} - \delta B\text{‰} \approx 10^3 \ln a_{A-B}$$

The temperature variation of isotope fractionation factors for specific exchange reactions is usually determined experimentally and is expressed by the general equation:

$$10^3 \ln a = \frac{A \times 10^6}{T^2} + B$$

where T is in degrees kelvin and A and B are constants normally determined by experiment.

## 7.2 INTRODUCTION TO THE STUDY OF CARBON AND OXYGEN STABLE ISOTOPES IN CARBONATITES.

Although carbonatites are volumetrically rare, their distribution is worldwide. The widespread occurrence of carbonatites makes them suitable for monitoring the chemical evolution of the sub-continental upper mantle by use of various isotopes. The use of stable and radiogenic isotopes in carbonatites help to evaluate the behaviour of REEs during magma generation and evaluation, the relationship between carbonatites and associated silicate rocks and the cause of the isotopic variation in the carbonatites. It should, however, be emphasized that isotopic fractionation in nature, due to isotopic exchange reactions and kinetic and physico-chemical processes, complicate the fingerprinting of the above processes.

The use of isotopes in carbonatites dates back to the early 1960's when strontium isotopes in particular were used to demonstrate that carbonatites were indeed magmatic and not sedimentary in origin (Powell et al., 1962 and Hamilton and Deans, 1963). Progress in the use of both radiogenic and

stable isotopes in carbonatites has increased tremendously due to improved modern equipment and techniques, as observed by the number of papers dealing with isotope geochemistry in the carbonatite book edited by Bell (1989).

Based on earlier work by Taylor et al. (1967), carbonatites with a restricted isotopic composition range between -4 to -8‰ (PDB) for  $\delta^{13}\text{C}$  and +6.0 to +10.0‰ (SMOW) for  $\delta^{18}\text{O}$  were considered to be homogeneous and hence the birth of the term "carbonatite box" in the  $\delta^{13}\text{C}$  -  $\delta^{18}\text{O}$  diagram. Samples plotting inside the box were considered to represent the limits established for primary, unaltered carbonatites, which were also thought to originate from the mantle. The word "primary" was used to imply those carbonatites not affected by surficial secondary processes and representing unmodified partial mantle melt. Subsequent studies by Pineau et al. (1973), Deines and Gold (1973), Sheppard and Dawson (1975) and Nelson et al. (1988) have since confirmed that many carbonatites have isotopic compositions within the above ranges, but they have also demonstrated that a large number of samples have high  $\delta^{13}\text{C}$  and, in particular, high  $\delta^{18}\text{O}$  values.

Large variations in isotopic compositions have also been observed by many workers, for example Suwa et al. (1975), Hubberton et al. (1988), Deines (1989) and Knudsen and Buchardt (1991), who have noted carbon and oxygen isotopic compositions in the range of -10 to +3‰ (PDB) for  $\delta^{13}\text{C}$  and +6 to +30‰ (SMOW) for  $\delta^{18}\text{O}$ . A number of processes have been proposed to explain the trend toward isotopically heavier carbon and oxygen in carbonatites. These include protracted Rayleigh fractionation, crustal contamination during magma emplacement and/or derivation from different mantle sources (Deines, 1989). Higher values observed in most carbonatite complexes, especially high in  $\delta^{18}\text{O}$ , have been interpreted as

secondary in origin resulting from alteration and isotopic exchange. A large number of carbon and oxygen isotope investigations are based on the assumption that those carbonatites that plot inside the Taylor box (carbonatites with a restricted range between -4 to -8‰ for  $\delta^{13}\text{C}$  and +6 to +10‰ for  $\delta^{18}\text{O}$ ) represent the primary isotopic compositions of typical carbonatites, while those that are displaced away from the box, especially those with elevated  $\delta^{18}\text{O}$  values, are interpreted to be due to mainly post-magmatic alteration processes.

The primary carbonatite box, as proposed by Taylor et al. (1967), seems to logically divide carbonatite samples into two simple categories: those that have been affected by mainly high temperature magmatic processes, including liquid immiscibility and fractional crystallization, and those that have been affected by post-magmatic alteration reactions, including contamination by country rocks and hydrothermal/meteoric and supergene weathering processes, that plot mainly outside the box. Deines and Gold (1973) and Santos and Clayton (1995) argue that the two groups can also be related in respect to their emplacement level, where those that plot inside the box are mainly thought to be deep-seated and those that plot outside the box have shallow emplacement levels and hence are frequently observed to have a wider range in isotopic composition attributed to near-surface processes. This is rather simplistic because the exposure and weathering of intrusive deep-seated carbonatites could reproduce the near-surface signatures observed in shallow carbonatite complexes.

Keller and Hoefs (1995) consider the constant and low carbon and oxygen  $\delta$  values (+6.6‰ for  $\delta^{13}\text{C}$  and +6.4‰ for  $\delta^{18}\text{O}$ ) in the volcanic carbonatite of Oldoinyo Lengai to be at variance with the observation that shallow level volcanic complexes usually have elevated carbon and oxygen isotopic

values. The writer suggests that the low values observed in the Oldoinyo Lengai natrocarbonatite are because the samples have not been exposed to the atmosphere for a long time and, due to its young age compared to other carbonatites, secondary processes are minimal. Overlapping of the isotopic values of the two groups (deep and shallow seated complexes), particularly in  $\delta^{18}\text{O}$  values, makes it very difficult to identify those values that are due to primary or secondary processes.

Isotopic composition values plotting outside the primary carbonatite box have been attributed mainly to post-magmatic alteration processes. Primary factors which have been used to explain variations in carbon and oxygen isotopic compositions, as depicted in  $\delta^{13}\text{C}$  and  $\delta^{18}\text{O}$  diagrams, include degassing of isotopically light C/O volatiles (Rayleigh fractionation) and the isotopic heterogeneity of the mantle (Deines and Gold, 1973 and Nelson et al., 1988). Deines (1989) suggested a model in which  $\delta^{18}\text{O}$  values of up to +25‰ (SMOW) can be produced by exchange between a primary magmatic carbonate and a magmatic fluid. However, large oxygen and carbon fractionation factors are only possible when the temperatures are much lower than those encountered in magmatic environments. Again, carbonatite magmas are easily prone to various alteration processes during their ascent through the crust and may therefore not preserve their mantle isotopic compositions. The writer suggests that  $\delta^{18}\text{O}$  values of up to +25‰ observed in some carbonatite samples are secondary and are unlikely to be produced by primary processes.

In the present investigation, detailed carbon, oxygen and sulphur studies were carried out on both Buru and Kuge rocks, primarily to investigate the following:

- i) To compare the carbon, oxygen, sulphur isotopic compositions of the two volcanic centres and those of carbonatites elsewhere.
- ii) To study and identify possible signatures for magmatic, hydrothermal (meteoric/hotspring) and supergene processes affecting the carbonates of the carbonatites after emplacement.
- iii) To determine the relationship or correlation of the different isotopic compositions with the timing and mineralization of the REEs.
- iv) To propose models to explain the variations of stable isotopes in the carbonatite centres investigated.

Very few detailed isotope studies of carbonatites that combine  $\delta D$ ,  $\delta^{13}C$ ,  $\delta^{18}O$  and  $\delta^{34}S$  have been undertaken (Deines, 1989). It is also true that most of the isotopic measurements reported in the literature have been obtained from specimens from surface outcrops where interaction with both magmatic, hydrothermal fluids and supergene weathering processes may have significantly modified their isotopic composition. The combined detailed measurements of  $\delta^{13}C$ ,  $\delta^{18}O$  and  $\delta^{34}S$  isotopic compositions of these single carbonatite centres using mainly drill core samples is intended to evaluate firmly the variations in carbon, oxygen and sulphur isotopic compositions of the carbonatites during and after emplacement. The details of sample preparation and experimental procedures are given in Appendix 7-1.

### 7.3 CARBON AND OXYGEN ISOTOPIC COMPOSITION FROM BURU.

#### 7.3.1 Introduction.

The variation in carbon and oxygen isotopic compositions from carbonatite carbonate samples from Buru will be discussed. The reasons for the observed variations will be discussed in terms of those due to primary and

secondary processes. Evidence for the primary and/or secondary alteration processes will be evaluated and results compared with the already published data from some of the Nyanza rift carbonatites and elsewhere. From available field evidence, for example the dominance of high level cone-sheets and dykes of calcite carbonatite and ferrocarnatite within Nyanza rift carbonatites and the non-occurrence of deeper level ultrabasic rocks or dykes in both Buru and Kuge, it is assumed by the author that these centres are not deep-seated and hence have been influenced mainly by a lower temperature overprint. However, high temperature magmatic processes do not lead to high isotopic variations in carbonatites. Matsuhisa (1979) and Matthey et al. (1990) suggest that fractional crystallization and liquid immiscibility, two dominant processes during the evolution of carbonatites, do not lead to significantly large variations in the  $\delta^{13}\text{C}$  and  $\delta^{18}\text{O}$  of carbonatites.

### 7.3.2 Results.

The  $\delta^{13}\text{C}$  and  $\delta^{18}\text{O}$  values for calcite and siderite from Buru are shown in Table 7-1 and Figure 7-1. According to Figure 7-1, the following significant features are noted:

- i) The Buru carbonatite carbonates are seen to be displaced away from the primary igneous carbonatites (PIC) values to higher  $\delta^{13}\text{C}$  and  $\delta^{18}\text{O}$ .
- ii) Three groups are distinguished in the Buru calcites according to their isotopic composition values. Group 1 calcites are characterized by  $\delta^{18}\text{O}$  values ranging between +11.25 and +16.28‰ (SMOW) with an average of +14.53‰ (SMOW) and by  $\delta^{13}\text{C}$  values of -3.23 to -2.15‰ (PDB) with an average of -2.47‰ (PDB). Group 2 calcites have  $\delta^{18}\text{O}$  values in the range of +17.02 to +19.86‰ (SMOW) and an average of +18.39‰ (SMOW), whereas  $\delta^{13}\text{C}$  values range from -2.88 to -1.37‰ (PDB) with an average of -2.05‰ (PDB). Group 3 calcites are quite distinct from the other two

Table 7-1 Distribution of oxygen and carbon isotopes from the Buru carbonatite centre.

i) Calcite from drill hole BRL-1.

Sample No.	Depth(m)	$\delta^{13}\text{C}$	$\delta^{18}\text{O}$
BR.7	70	-1.45	25.29
BR.167	71	+0.55	26.21
BR.8	75	+1.00	24.90
BR.165	79	-1.68	19.23
BR.163	82	-2.62	18.85
BR.161	86	-2.06	13.31
BR.159	92	-1.37	18.47
BR.178	98	-2.15	17.02
BR.12	101	-2.18	17.09
BR.13	108	-1.91	17.04
BR.14	114	-2.15	15.02
BR.15	116	-2.94	14.92
BR.184	118	-2.43	11.25
BR.16	130	-2.63	15.13
BR.17	138	-2.69	14.91
BR.187	142	-2.68	18.89
BR.19	144	-2.98	16.28
BR.28	200	-3.23	15.32

ii) Calcite from drill hole BRL-3.

BR.46	6	-1.41	21.98
BR.118	8	-0.58	23.14
BR.126	10	-0.77	25.96
BR.131	23	-2.26	22.82
BR.133	25	-1.39	18.56
BR.141	38	-1.95	18.11
BR.143	46	-2.38	18.49
BR.147	57	-2.87	13.70
BR.57	59	-2.33	15.28
BR.149	60	-2.51	15.97
BR.151	61	-2.85	15.46

iii) Calcite from drill hole BRL-2.

BR.218	71	+1.27	23.27
BR.219	74	+0.07	21.87
BR.222	82	-2.02	19.17
BR.223	86	-1.69	18.77

BR.224	89	-2.30	17.39
--------	----	-------	-------

## iv) Calcite from drill hole BR-4.

BR.235	41	-2.88	18.95
BR.236	44	-0.62	22.81
BR.237	46	-0.47	22.20

## v) Calcite from drill hole BR-9.

BR.245	29	-1.56	19.86
BR.247A	47	-2.59	12.39

## vi) Calcite from drill hole BR-10.

BR.262	26	-0.66	25.24
--------	----	-------	-------

## vii) Siderite from drill hole BRL-1

BR.162	82	-3.91	15.28
BR.158	89	-4.09	14.49
BR.175	92	-4.39	14.53
BR.177	98	-3.31	16.10
BR.14	114	-3.94	16.00
BR.183	118	-4.38	15.51
BR.186	142	-4.13	13.57
BR.192	172	-4.23	12.61
BR.194	187	-4.25	13.61

## viii) Siderite from drill hole BRL-3.

BR.144	54	-4.00	15.07
BR.146	57	-3.07	14.32
BR.148	60	-3.91	13.75
BR.150	61	-4.08	13.49
BR.152	68	-4.11	13.65
BR.59	78	-3.35	14.58

## ix) Siderite from drill hole BR-9.

BR.247B	47	-3.91	15.06
---------	----	-------	-------

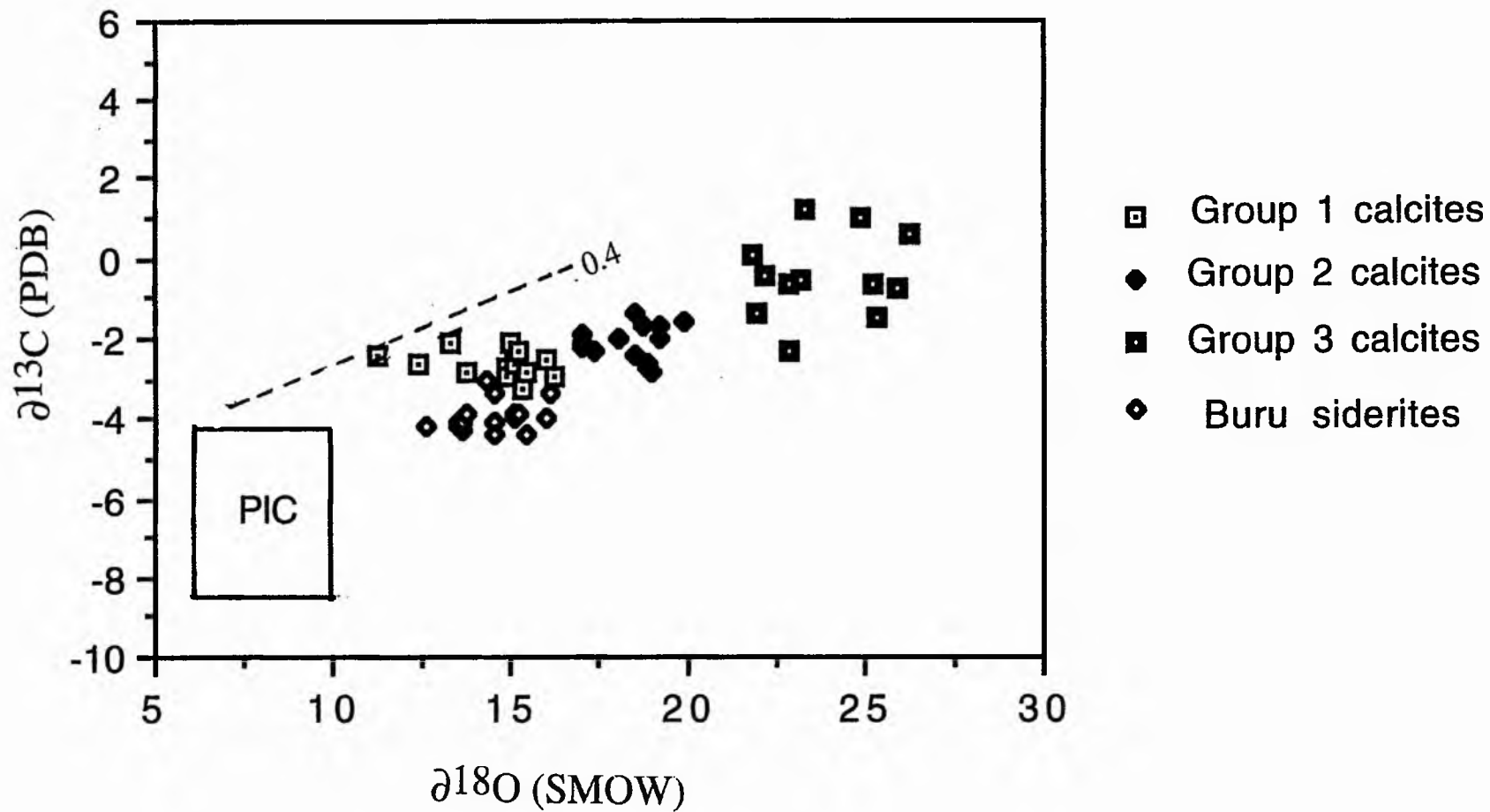


Figure 7-1  $\delta^{13}\text{C}$  (PDB) vs  $\delta^{18}\text{O}$  (SMOW) of calcite and siderite from the Buru carbonatite centre. The dashed line is a Rayleigh fractionation line from Pineau et al. (1973) superimposed on the Buru data. PIC- Primary Igneous Carbonatite.

groups in having both higher  $\delta^{18}\text{O}$  and  $\delta^{13}\text{C}$  values in the range of +21.98 to +26.21‰ (SMOW) with an average of +23.81‰ (SMOW) and -1.48 to +1.27‰ (PDB) and an average of -0.45‰ (PDB), respectively.

iii) The three groups taken in isolation do not show any correlation.

iv) The Buru siderites plot in a narrow and restricted range (Figure 7-1) at lower values of  $\delta^{18}\text{O}$  values in the range of +12.61 to +16.10‰ (SMOW) with an average of +14.48‰ (SMOW) and distinctly lower  $\delta^{13}\text{C}$  than the three calcite groups identified in Buru. The  $\delta^{13}\text{C}$  for the Buru siderites range between -4.39 to -3.07‰ (PDB) with an average of -3.94‰ (PDB).

The distribution of  $\delta^{13}\text{C}$  and  $\delta^{18}\text{O}$  values for calcite and siderite from the Buru carbonatite centre noted above (Figure 7-1) are clearly observed in the histograms shown in Figures 7-2 and 7-3, respectively. The  $\delta^{13}\text{C}$  histogram displays a continuous distribution, without a break for the Buru calcite, from a value of -4‰ to a maximum of +2‰ with the mode between -3 to -2‰ (PDB). The Buru siderites portray narrow values which are distinctly lower in  $\delta^{13}\text{C}$  than the calcites. The  $\delta^{18}\text{O}$  histogram for the Buru calcites also shows a continuous distribution (+10 to +28‰) with a mode between +18 and +20‰ (PDB), whereas the Buru siderites reveal a lower  $\delta^{18}\text{O}$  distribution with a mode between +14 and +16‰ (PDB).

#### 7.4 VARIATION OF $\delta^{13}\text{C}$ AND $\delta^{18}\text{O}$ FROM THE BURU CARBONATITE CENTRE.

##### 7.4.1 Primary factors.

The Buru calcites in the present investigation do not retain their primary isotopic signature, as suggested by Keller and Hoefs (1995). Isotopic compositions for calcites range from +1.27 to -3.23‰ for  $\delta^{13}\text{C}$  and +11.25

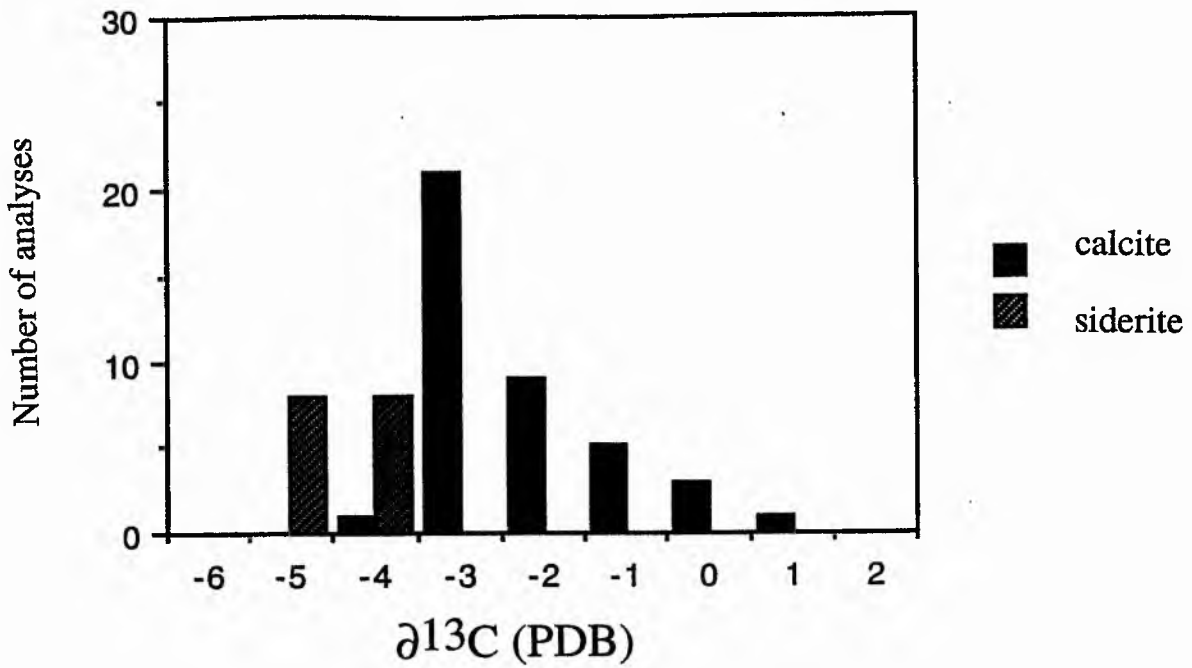


Figure 7-2 Histogram plot of  $\delta^{13}\text{C}$  for calcite and siderite from Buru carbonatite centre.

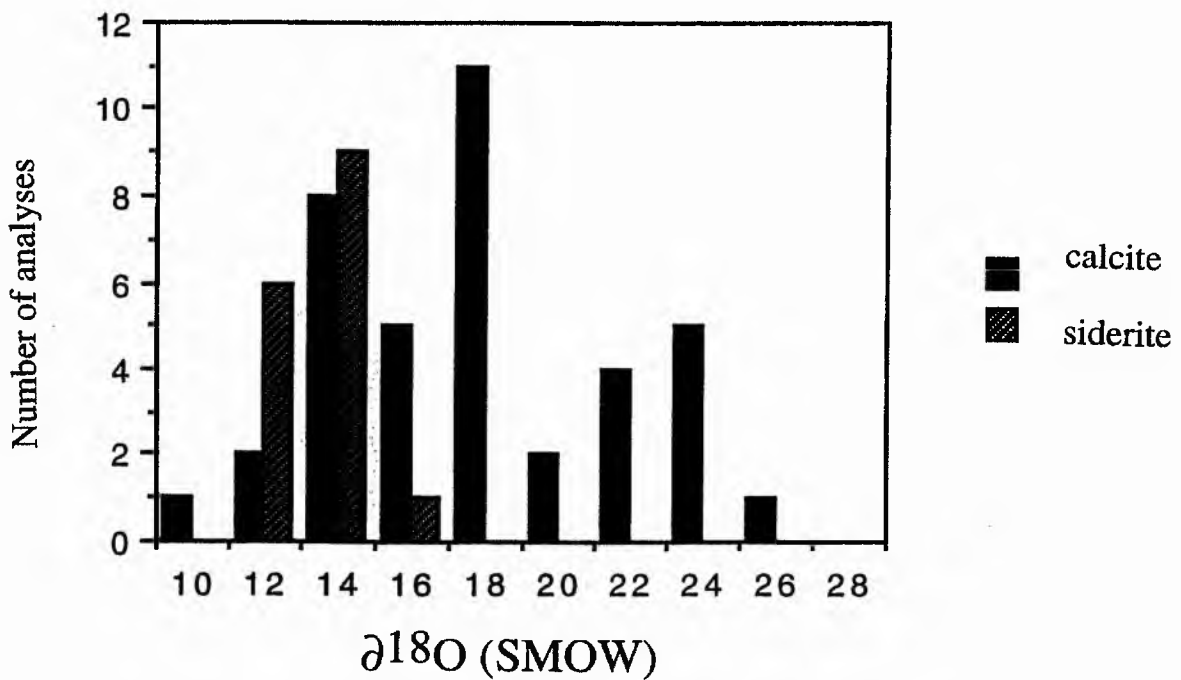


Figure 7-3 Histogram plot of  $\delta^{18}\text{O}$  for calcite and siderite from Buru carbonatite centre.

to +26.21‰ for  $\delta^{18}\text{O}$ . Three distinct groups, based on their different isotopic compositions, have been identified (Figure 7-1).

Deines (1970, 1989), Pineau et al. (1973) and Reid and Cooper (1992) have recognized in carbonatites a positive correlation between  $\delta^{13}\text{C}$  and  $\delta^{18}\text{O}$  and in particular in the  $\delta^{18}\text{O}$  range from +5 to +15‰. These authors argue that carbonate minerals easily re-equilibrate when subjected to various secondary alteration processes and yet this positive correlation between  $\delta^{13}\text{C}$  and  $\delta^{18}\text{O}$ , within the restricted  $\delta^{18}\text{O}$  range, can be recognized in many carbonatites in different parts of the world. The observation could indicate a primary process which is unique to carbonatite formation. Deines (1970, 1989) and Pineau et al. (1973) have attributed this process to protracted Rayleigh fractionation, i.e. the preferential loss of lighter isotopes in volatile phases.

The carbonate phases (calcite and siderite) in Buru do not show any apparent correlation between  $\delta^{13}\text{C}$  and  $\delta^{18}\text{O}$  isotopic values. When Figure 7-1 is superimposed onto Pineau's Figure 2, the Buru carbonates define a linear array with a slope value outside that expected from Rayleigh fractionation (Pineau et al. 1973). The linear slope of about 0.4 expected from Rayleigh fractionation processes is much steeper than the Buru isotopic data shown in Figure 7-1. However, Rayleigh fractionation is unlikely to have occurred in the Group 2 and 3 calcites since it cannot produce  $\delta^{18}\text{O}$ -values greater than +17‰, as suggested by Deines (1989), and certainly not as high as the average of +18.39 and +23.81‰ (SMOW) for Groups 2 and 3.

Evaluation of other primary factors, such as contamination by crustal rocks, is not possible in the case of the Buru hill carbonatite centre because

additional analyses such as Sm-Nd, Pb-Pb and Rb-Sr isotopic data of the carbonatite carbonates and associated fenites are not available. However, if the carbonatite intrudes country rock containing limestone, contamination of the carbonatite by limestone will readily be recognized. The Buru carbonatite intruded the Proterozoic gneisses, so it will be difficult to distinguish whether the high  $\delta^{18}\text{O}$  values shown by the Buru calcites had some contribution from contamination by country rock, without the aid of radiogenic stable isotopes.

Regional differences pointing to isotopically heterogeneous sources of carbonatites have been noted by Deines and Gold (1973) and Nelson et al. (1988) and have been used to account for the variations in  $\delta^{13}\text{C}$  and  $\delta^{18}\text{O}$  noted in the carbonatites. Deines (1989), in an update of the original compilation of carbon and oxygen isotopes discussed earlier (Deines and Gold, 1973), suggested a north-south trending zone of carbonatites characterized by average  $\delta^{13}\text{C}$  values between -2.8 and +3.9‰ within the eastern Ugandan - western Kenyan Miocene carbonatite complexes and the Chilwa Island carbonatite complex in Malawi. In contrast, carbonatites lying in the eastern and western rift areas were characterized by significantly lower  $\delta^{13}\text{C}$  values of between -6 and -7‰. The average  $\delta^{13}\text{C}$  for the Buru calcites, Buru siderites and Kuge calcites in the present investigation is -1.76, -3.94 and -5.02‰, respectively (only drill core samples were averaged). The Buru siderite has similar values to those noted by Deines and Gold (1973), but calcites from Buru are higher in  $\delta^{13}\text{C}$ , whereas  $\delta^{13}\text{C}$  values for Kuge are lower, similar to the values shown by the eastern and western carbonatites.

The present data do not confirm the findings of Deines and Gold (1973) and the differences in carbon isotopic composition among the carbonatites in

particular may be related to the processes involved in the extraction of carbon during the evolution and emplacement of the carbonatite magma and also due to the influence of various post- emplacement alteration processes.

#### 7.4.2 Secondary factors.

Deines (1989), in a compilation of carbon and oxygen isotopic composition in carbonatite carbonate minerals from several carbonatite complexes, noted a large range in  $\delta^{18}\text{O}$  which was accompanied by only minor changes in  $\delta^{13}\text{C}$ . Deines attributed the more extreme  $\delta^{18}\text{O}$  values (+15 to +28‰) to a number of secondary processes such as an influx of meteoric water and isotope exchange at lower temperatures. Recently, Keller and Hoefs (1995) have clearly demonstrated the effects of secondary alteration and recrystallization on the isotopic composition of natrocarbonatite.

The three groups identified within the Buru calcites with  $\delta^{18}\text{O}$  averages of +14.53, +18.39 and +23.81‰ (SMOW) and  $\delta^{13}\text{C}$  averages of -2.47, -2.05 and -0.45‰ (PDB) have isotopic composition that are unlikely to have been generated by primary processes. Group 3 is quite distinct from Groups 1 and 2, though they are obtained from the same drill hole; the data suggest that another process different from that affecting Groups 1 and 2 is unique to the Group 3 calcites. Field and chemical data presented in Table 7-2 can be used to account for the isotopic differences encountered in the Buru calcites of Groups 1, 2 and 3.

Examination of Table 7-2, which represents the Buru calcites of Groups 1, 2 and 3, respectively, reveal the following notable mineralogical and isotopic features:

i) Group 3 calcites are from the uppermost sections of the drill cores immediately below the laterite. They are dominated by various compounds

GROUP 1 CALCITES		GROUP 2 CALCITES		GROUP 3 CALCITES		
Sample No	Drill Hole	Depth(m)	Major minerals (XRD)	$\delta^{13}C$	$\delta^{18}O$	Sr
BR 14	BRL-1	114	calcite, siderite, feldspar, aegirine, fluorite, REE	-2.15	15.02	664
BR 15	BRL-1	116	calcite, siderite, barite, fluorite, aegirine	-2.94	14.92	2550
BR 16	BRL-1	130	calcite, siderite, barite, fluorite, REE	-2.63	15.13	2621
BR 17	BRL-1	138	calcite, siderite, fluorite, REE	-2.69	14.91	7967
BR 19	BRL-1	144	siderite, calcite, barite, fluorite, REE	-2.98	16.28	10120
BR 28	BRL-1	200	siderite, calcite, barite, fluorite, REE	-3.23	15.32	33000
BR 165	BRL-1	79	calcite, barite, magnetite, fluorapatite, oligonite	-1.68	19.23	
BR 178	BRL-1	98	calcite, fluorite, fluorapatite	-2.15	17.02	
BR 12	BRL-1	101	calcite, siderite, barite, fluorite, fluorapatite	-2.18	17.09	2830
BR 13	BRL-1	108	calcite, siderite, fluorite, Barite	1.91	18.89	
BR 222	BRL-2	82	calcite, siderite, fluorite, barite, allstonite	-2.02	19.17	
BR 223	BRL-2	86	calcite, siderite, fluorite, barite, REE	-1.69	18.77	
BR 224	BRL-2	89	calcite, siderite, fluorite, barite, REE	-2.30	17.39	
BR 7	BRL-1	70	calcite, barite, goethite, hematite, REE	-1.45	25.29	787
BR 8	BRL-1	75	calcite, goethite, barite, hematite	1.00	24.90	9999
BR 46	BRL-3	6	calcite, goethite, barite, hematite, REE,	-1.41	21.98	
BR 118	BRL-3	8	calcite, barite, hematite, goethite, fluorite	-1.58	23.14	
BR 126	BRL-3	10	calcite, barite, goethite, hematite, fluorite	-0.77	25.96	
BR 131	BRL-3	23	calcite, barite, goethite, fluorite, hematite	-2.26	22.82	
BR 218	BRL-2	71	calcite, barite, goethite, fluorite,	1.27	23.27	1530
BR 219	BRL-2	74	calcite, barite, goethite	0.07	22.81	3704

TABLE.7.2 The effect of weathering on mineralogical composition of the Buru calcites.

of iron (notably goethite and hematite) and calcite and are characterized by the absence of siderite.

ii) Group 1 and 2 calcites obtained from relatively fresh carbonatite below the transitional zone (chapter 5) are dominated by simple carbonates of calcite and siderite. Accessory phases of ankerite and strontianite occur rarely.

iii) Barium and fluorite, as well the REEs represented by mainly fluorocarbonates, tend to appear in both the upper and lower sections of the drill cores.

iv) Higher values of both  $\delta^{13}\text{C}$  and  $\delta^{18}\text{O}$  are observed in the Group 3 calcites, whereas the Group 1 and 2 calcites progressively indicate lower  $\delta^{13}\text{C}$  and  $\delta^{18}\text{O}$  values towards the lower sections of the drill-cores where the effects of weathering are minimal. The lower isotopic values are in the most weathered sections of the cores. Minimal weathering is indicated by the absence of iron-compounds in both Groups 1 and 2.

iv) Low temperature carbonates, especially the Group 3 calcites which are close to the surface, are expected to have low values of strontium compared to Groups 1 and 2. However, the distribution of strontium is uneven among the three calcite groups. Extremely high values of strontium observed in BR-28 is due to the presence of strontianite (chapter 5).

From the above depth-related mineralogical composition noted in Table 7-2, the writer suggests that variations in isotopic composition between the Group 1 and 2 calcites may be attributed to secondary processes involving hydrothermal alteration and isotopic exchange, whereas supergene weathering processes are involved in the Group 3 calcites.

### 7.5 HYDROTHERMAL ALTERATION AND ISOTOPIC EXCHANGE.

Barite and fluorite are dominant phases observed especially in the Buru drill cores. They are the typical products of the late stage crystallization of carbonatites where they are deposited by late stage hydrothermal fluids. According to Mariano (1989b), hydrothermal mineralization is usually accompanied by barite and fluorite. The significant occurrence of these minerals in the Buru cores is therefore evidence of a circulating hydrothermal system within the Nyanza rift carbonatites. The two huge, central strato-volcanoes of Kisingiri and Tinderet (chapter 2) were responsible for the initiation of hydrothermal circulation. Present day hydrothermal activity is witnessed in a number of hot-springs in Homa Mountain and the large geothermal areas in Olkaria and Eburru within the floor of the Kenya (Gregory) rift.

Indirect evidence for the presence of a hydrothermal system in the volcanic centres under investigation, which consequently indicate the effect of hydrothermal alteration in the carbonatites, is the occurrence of REE-carrying minerals such as fluorocarbonates and monazite. These minerals, particularly the fluorocarbonates, are typical of hydrothermal mineralization (Gieré, 1996), whereas in magmatic systems which are not encountered in Buru or Kuge, REEs are commonly associated with calcite, apatite or pyrochlore. Meteoric/groundwater is suggested by the writer to have been the major significant source of the fluids. Variations in isotopic values are also related to the nature of the fluids.

Significant enrichment of  $\delta^{18}\text{O}$  in the Group 1 and 2 calcites relative to mantle oxygen can be ascribed to interaction with meteoric water. Meteoric/groundwaters have typically negative  $\delta^{18}\text{O}$  (Hoefs, 1987) and if such waters were involved in secondary alteration of the carbonatites as

proposed, and in order for the isotope exchange model to work, the process would have to occur below 250°C to be able to raise the  $\delta^{18}\text{O}$  content of the carbonates. At higher temperatures an exchange with meteoric water would lead to an  $\delta^{18}\text{O}$  depletion in the carbonates (Deines, 1989). The proposed oxygen isotopic exchange between the fluid phase and the carbonatite carbonates can be written as:

$$F\delta^{18}\text{O}_{\text{fluid}(i)} + R\delta^{18}\text{O}_{\text{rock}(i)} = F\delta^{18}\text{O}_{\text{fluid}(f)} + R\delta^{18}\text{O}_{\text{rock}(f)},$$

where (i) and (f) stand for the initial and final isotopic composition of the fluid and rock (carbonate). The final isotopic composition of the rock is represented by:

$$\delta^{18}\text{O}_{\text{rock}(f)} = [(F/R) (\delta^{18}\text{O}_{\text{fluid}(i)} + \Delta_{\text{R-F(O)}}) + \delta^{18}\text{O}_{\text{rock}(i)}] / [1 + F/R],$$

where  $\Delta_{\text{R-F(O)}}$  represents the isotopic fractionation between rock and fluid.

Since Groups 1 and 2 are also accompanied by variations in carbon isotopes (from -3.23 to -1.37‰) compared to  $\delta^{13}\text{C}$  mantle values of around -6‰, this suggests that carbon ions and molecular  $\text{CO}_2$  related to the carbonatites may play an important role in the isotopic evolution of the carbonatites. Crustal rocks contain low abundances of carbon unless the rock is carbon-rich, such as limestone, and therefore, in the case of Buru, the variations in carbon isotopes are attributed to hydrothermal alteration due to isotopic exchange involving  $\text{H}_2\text{O}-\text{CO}_2$  fluids rather than contamination by country rocks. Carbon dioxide gas reservoirs are a characteristic feature within the rift system in Kenya indicating that, apart from  $\text{CO}_2$  exsolved from the carbonatite magma during crystallization, the meteoric fluids that interact

with the carbonatite carbonates do also contain a substantial amount of mantle-derived CO<sub>2</sub>.

Chacko et al. (1991) studied the oxygen and carbon isotopic fractionation between CO<sub>2</sub> and calcite and showed that the carbon isotope fractionation varies from -3.8 to +3.8‰ between temperatures of 500 to 100°C. Javoy et al. (1989) also noted a large isotopic fractionation between CaCO<sub>3</sub> and the CO<sub>2</sub> gas phase. Carbon isotopic compositions of CO<sub>2</sub> from a number of fumarolic vents reported by Taylor (1986) normally range between -8.0 to -3.0‰. Keller and Hoefs (1995) argue that CO<sub>2</sub> should have a minor effect in changing the primary carbon isotope composition of carbonatites on the assumption that fractionation between CaCO<sub>3</sub> and CO<sub>2</sub> is rather small, based on earlier work by Bottinga (1968), but this has now been updated by Chacko et al. (1991). On the basis of large carbon isotopic fractionation reported by Chacko et al. (1991) and the heavier δ<sup>13</sup>C isotopic values shown by the Group 1 and 2 calcites than those expected of PICs, the writer suggests that the CO<sub>2</sub> phase could play an important role during the isotopic evolution of carbonatites, especially in low temperature environments.

## 7.6 ESTIMATING THE EQUILIBRATION TEMPERATURE INVOLVING CARBONATITE CARBONATES AND FLUIDS.

Oxygen isotope fractionations between co-existing minerals can give useful information on their crystallization temperature. The oxygen isotope exchange equation in a mineral, for example the calcite and water system, can be expressed in the form:

$$10^3 \ln a = A/T^2 + B \approx \delta^{18}_{\text{calcite}} - \delta^{18}_{\text{water}}.$$

In estimating the equilibration temperature of calcites from Buru, an estimate of the  $\delta^{18}\text{O}$  values for the meteoric water is required. An average of -3.5‰ on the present day water within the Kenya rift geothermal system obtained by Clarke et al. (1990) appears reasonable since the two centres lie on the Equator, which is a region characterized by such  $\delta^{18}\text{O}$  values (Sheppard, 1986). Values for constants A and B determined by O'Neil et al. (1969) are  $2.78 \times 10^6$  and -2.89, respectively. Therefore,  $\delta^{18}\text{O}_{\text{calcite}}(\text{measured}) - \delta^{18}\text{O}_{\text{water}} = (2.78 \times 10^6/T^2) + -2.89$  (the equation assumes that calcite precipitation is in isotopic equilibrium with the fluid). The average values for  $\delta^{18}\text{O}$  obtained for the Group 1, 2 and 3 calcites from Buru as shown above is +14.53, +18.39 and +23.81‰ (SMOW), respectively. If the values are substituted in the above equation, a temperature of 100°C is obtained for the Group 1 calcites and 62°C for the Group 2 calcites, whereas the Group 3 calcites are characterized by the lowest temperature (30°C).

The low temperatures calculated above, i.e. 100°C for Group 1 and 62°C for Group 2, are values expected in low temperature hydrothermal systems. Values of 97 and 42.9°C obtained by Michard (1989) on measuring the continental active hydrothermal fluids from New Mexico and Dominica, respectively, compares well with the temperature values estimated for the hydrothermal fluids in Buru. The spread of  $\delta^{18}\text{O}$  to higher values, for example the average +14.53‰ for the Group 1 and +18.39‰ for the Group 2 calcites, corresponds to a temperature drop of 38°C (from 100 to 62°C).

## 7.7 WEATHERING AND ISOTOPIC COMPOSITION OF CARBONATITES.

The process of supergene weathering on carbonatite carbonates has rarely been considered as one of the processes capable of significantly changing the

isotopic composition of most carbonatites, particularly in hot and humid tropical environments. The isotopic composition may be altered during weathering through partial removal of the carbonate in solution, precipitation of secondary carbonate or equilibration with surface or ground water fluids. In a detailed study of the carbon and oxygen isotopic composition of carbonates from the Oka carbonatite complex, Deines (1970) found no effect of weathering on either  $\delta^{13}\text{C}$  or  $\delta^{18}\text{O}$  between highly weathered rocks and fresh samples from drill cores. He concluded that most of the  $\delta^{13}\text{C}$  and  $\delta^{18}\text{O}$  variations observed were not related to weathering, a conclusion he still held after much further work (Deines, 1989) where he emphasized that during the weathering of carbonatites, no significant changes in the oxygen isotopic composition was recognized.

Some workers, however, have noted weathering effects on carbonatite carbonates. For example Hubberten et al. (1988) were able to distinguish the isotope composition of non-magmatic carbonates, which they considered to have been precipitated from meteoric water, in the Kaiserstuhl area. Recently, Keller and Hoefs (1995) have clearly demonstrated the dramatic compositional and isotopic changes that occur during the weathering of carbonatites when fresh natrocarbonatite with isotopic values of  $-6.87\text{‰}$  (PDB) and  $+6.32\text{‰}$  (SMOW) was exposed to the atmosphere for several weeks and then re-analyzed. Weathering and hydration effects on the exposed natrocarbonatite produced distinctly higher  $\delta^{13}\text{C}$  ( $-3.29\text{‰}$ ) and  $\delta^{18}\text{O}$  ( $+17.38\text{‰}$ ) values.

Although natrocarbonatite is a very special case and unlikely to be a suitable analogue for carbonatites in general, the results of Keller and Hoefs (1995) provide the only available carbonatite known in the world for which the effects of secondary alteration can be excluded. The chemical composition

of the altered carbonatite clearly demonstrates the effect of weathering of natrocarbonatites when exposed at the earth's surface. The results obtained by Keller and Hoefs (1995) could assist in evaluating and interpreting some isotopic variations observed in shallow-seated volcanic carbonatites. As noted in chapter 5, carbonatites are prone to weathering, where they are accompanied by an almost total loss of soluble carbonates and an enrichment of iron and manganese oxides. Similar compositional changes are observed in altered carbonatites (Keller and Hoefs, 1995), where they are characterized by a loss of sodium and potassium and a small but significant increase in iron and manganese.

Group 3 calcites are characterized by high average values of  $\delta^{13}\text{C}$  (-0.45‰) and  $\delta^{18}\text{O}$  (+23.81‰) compared to Groups 1 and 2. If it is assumed that one fluid is involved in the alteration at Buru (there is no evidence of mixing of fluids from two or more sources), then it is probable that a different process is responsible for the variations in isotopic composition shown by the Group 3 Buru calcites. On the basis of experimentally determined calcite-H<sub>2</sub>O fractionation factors (O'Neil et al., 1969), the extreme enrichment in  $\delta^{18}\text{O}$  values of over 21.87‰ (SMOW) shown by Group 3 calcites will require much lower temperatures (below 50°C). From mineralogical and variations in isotopic values presented in Table 7-2, the writer proposes that the Group 3 calcites have possibly been reprecipitated by weathering processes rather than hydrothermal fluids.

Plots of  $\delta^{13}\text{C}$  and  $\delta^{18}\text{O}$  from drill hole BRL-1 for calcite and siderites from the Buru carbonates versus depth (Figure 7-4) show that calcite samples from the top of the drill core (transitional zone) have more elevated  $\delta^{13}\text{C}$  than samples in the deeper sections of the drill core, where isotopic values nearer to magmatic values occur. The siderites, however, do

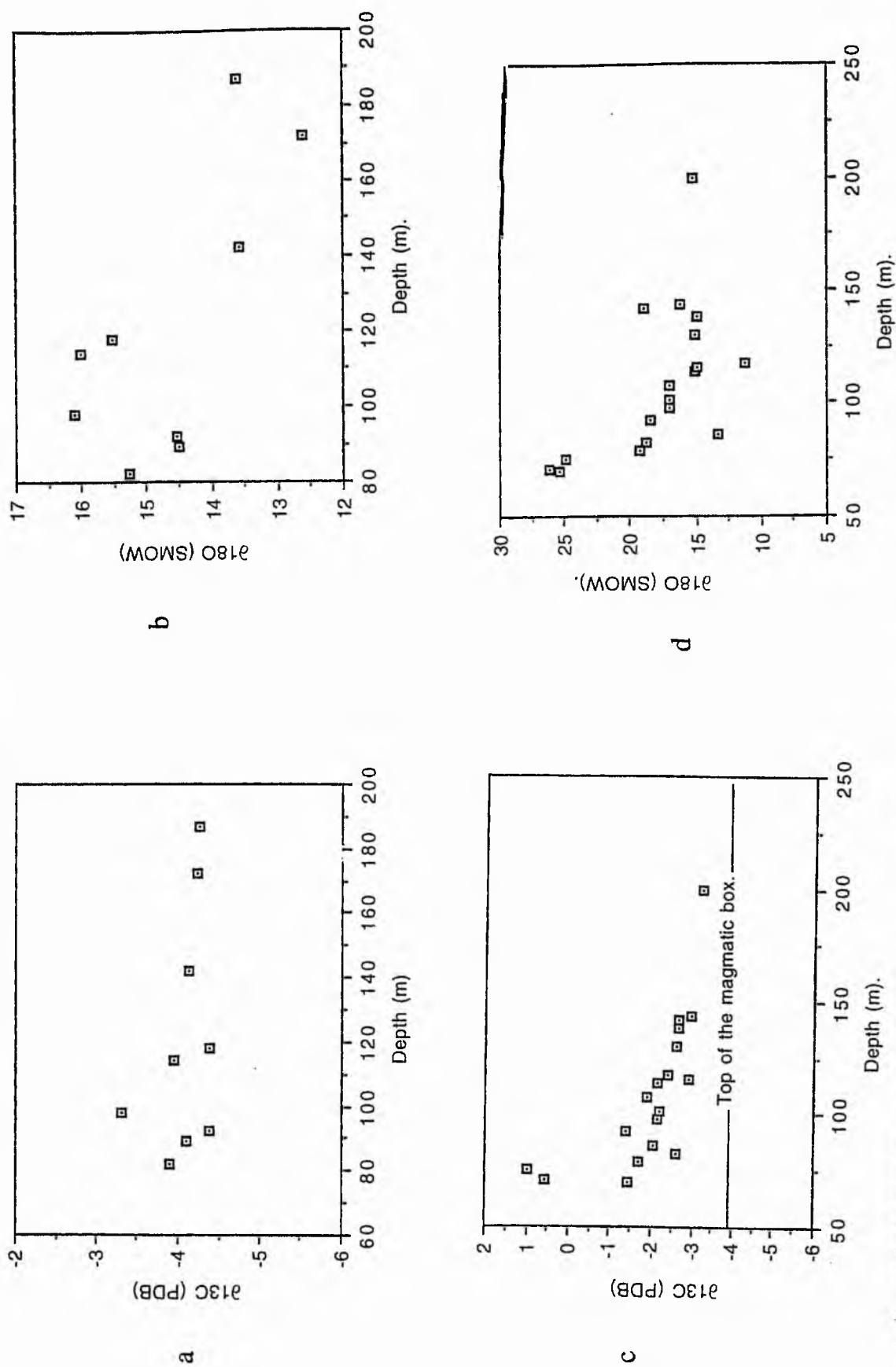
not show any any noticeable  $\delta^{13}\text{C}$  changes with depth. The  $\delta^{18}\text{O}$  for calcite seem to decrease with depth, whereas  $\delta^{18}\text{O}$  for siderite is erratic, though samples towards the bottom of the drill hole have lower  $\delta^{18}\text{O}$  values (Figure 7-4). It can be argued that samples showing elevated  $\delta^{13}\text{C}$  and  $\delta^{18}\text{O}$  (Group 3 calcites obtained from the transitional zone) have been affected by supergene processes and a definite influence of atmospheric carbon dioxide ( $\text{CO}_2$ ) compared to those that occur towards the bottom of the drill cores (Group 1 and 2 calcites), where they have been mainly affected by hot to warm hydrothermal processes.

#### 7.8 CARBON AND OXYGEN ISOTOPIC COMPOSITION OF SIDERITE FROM BURU.

The occurrence of siderite in carbonatites is not very common and is therefore rarely reported in carbonatite investigations. In classic carbonatites, the typical crystallization of carbonate minerals is calcite-dolomite-ankerite-siderite, that order being also indicative of decreasing temperature (Heinrich, 1966). Although carbon and oxygen isotope equilibrium fractionation factors between dolomite and calcite in carbonatites is not well understood (Deines, 1989), the available data on fractionation factors presented by Deines (1989) do indicate a small enrichment of (+1 to +2‰), particularly in the  $\delta^{18}\text{O}$  of dolomite over  $\delta^{18}\text{O}$  of calcite. Recently, Santos and Clayton (1995) have also shown a positive carbon isotope fractionation of dolomite over calcite in their study of Brazilian alkaline complexes.

Enrichment of calcite in  $\delta^{13}\text{C}$  and  $\delta^{18}\text{O}$  relative to dolomite has been documented from the Fen complex, Norway (Andersen, 1987), Chilwa Island, Malawi (Simonetti and Bell, 1994), and from the Amba Dongar carbonatite complex, west-central India (Simonetti et al., 1995). The

Figure 7-4 Plot of (a)  $\delta^{13}\text{C}$  and (b)  $\delta^{18}\text{O}$  vs depth for Buru siderite. Plot of (c)  $\delta^{13}\text{C}$  and (d)  $\delta^{18}\text{O}$  vs depth for Buru calcite. Samples from BRL-1.



negative fractionation shown by the calcite-dolomite pairs from these complexes have been attributed to secondary alteration processes by the above authors. Deines (1989) also invoked the formation of the carbonates in two or more magmatic and or hydrothermal phases and the formation of carbonatites at different temperatures to account for the highly variable oxygen isotope fractionations observed between calcite and dolomite.

Although siderite is very rare it is well represented, particularly in the lower sections of the Buru drill cores. The presence of siderite in Buru is confirmed by both X-ray diffraction (XRD) and electron probe microanalysis (EPMA). Siderite mainly occurs as dykes cross-cutting the earlier volcanic carbonatites that are brecciated in parts and predominantly calcitic in composition (Chapter four). The  $\delta^{13}\text{C}$  and  $\delta^{18}\text{O}$  values of the Buru siderites are shown in Table 7-1 and Figure 7-1. The following characteristic features were noted earlier.

- i) The Buru siderites plot in a narrow and restricted isotopic range. The  $\delta^{18}\text{O}$  values range from +12.61 to +16.10‰ (SMOW) with an average of 14.48‰ (SMOW) and the  $\delta^{13}\text{C}$  values range between -4.39 to -3.07‰ (PDB) with an average of -3.94‰ (PDB).
- ii) The  $\delta^{18}\text{O}$  shows a higher variation in isotopic composition than the  $\delta^{13}\text{C}$ .

In Buru, where the two carbonate phases have been analyzed from the same sample (Plate 7-1), the calcite is observed to be enriched both in  $\delta^{13}\text{C}$  and  $\delta^{18}\text{O}$  relative to siderite (Table 7-3, Figure 7-5). Only three samples (BR-158 & 159, BR-183 & 184 and BR-148 & 149) show a higher  $\delta^{18}\text{O}$  in siderite relative to calcite.

Table 7-3 Stable isotopic data for the calcite and siderite phases.

Sample No.	Mineral	$\delta^{13}\text{C}$	$\delta^{18}\text{O}$
BR-162 & 163	calcite	-2.62	+18.85
	siderite	-3.91	+15.28
BR-158 & 159	calcite	-2.06	+13.31
	siderite	-4.09	+14.49
BR-176 & 175	calcite	-1.37	+18.47
	siderite	-4.39	+14.53
BR-177 & 178	calcite	-2.15	+17.02
	siderite	-3.31	+16.00
BR-183 & 184	calcite	-2.43	+11.25
	siderite	-4.38	+15.51
BR-186 & 187	calcite	-2.68	+18.89
	siderite	-4.13	+13.57
BR-146 & 147	calcite	-2.87	+13.70
	siderite	-3.07	+14.32
BR-148 & 149	calcite	-2.51	+15.97
	siderite	-3.91	+13.75
BR-150 & 151	calcite	-2.85	+15.46
	siderite	-4.09	+13.49

Only limited experimental studies of oxygen isotope fractionation between siderite and water exist. Rosenbaum and Sheppard (1986) studied siderites, dolomites and ankerites at high temperatures and obtained oxygen fractionation factors ( $\alpha$ ) between the  $\delta^{18}\text{O}$  of the siderite and that of the acid-liberated  $\text{CO}_2$  to be 1.00881 and 1.00771 at 100 and 150°C,

respectively. Carothers et al. (1988) also experimentally determined the oxygen isotope fractionation between siderite and water at temperatures ranging from 33 to 197°C and obtained fractionation factors ranging from 1.01067 to 1.03033. The latter authors calculated the fractionation between siderite and water over the temperature range (33-197°C) to be approximated by the equation:

$$10^3 \ln a = 3.13 \cdot 10^6 T^{-2} - 3.50.$$

From limited oxygen isotope fractionation factors among the carbonatite minerals and water given in Deines (1989) and Zheng and Hoefs (1993), siderite often shows slight enrichment in  $\delta^{13}\text{C}$  and  $\delta^{18}\text{O}$  over calcite.

The Buru siderite clearly shows a negative isotopic fractionation between calcite and siderite. The siderite dyke in Buru is clearly intrusive into the carbonatite breccia, which therefore indicates that it is later than the main carbonatite. The negative isotopic fractionation between calcite and siderite in Buru could be attributed to the formation of siderite from a late magmatic phase which is probably different from the one which precipitated calcite. It is also possible the two carbonate phases (calcite and siderite) were formed at different temperatures. The equilibration temperature for siderite based on the Carothers et al. (1988) equation given above is 144°C, taking an average  $\delta^{18}\text{O}$  of 14.48‰ and -3.5‰ as the average  $\delta^{13}\text{C}$  of the present day water within the Kenya rift geothermal system (Clarke et al., 1990). The estimated temperature of 144°C is much higher than the temperatures obtained for the Group 1, 2 and 3 Buru calcites, which gave 100, 62 and 30°C, respectively. The difference in temperature re-emphasizes the reasons given above for the isotopic fractionation shown by calcite and siderite.

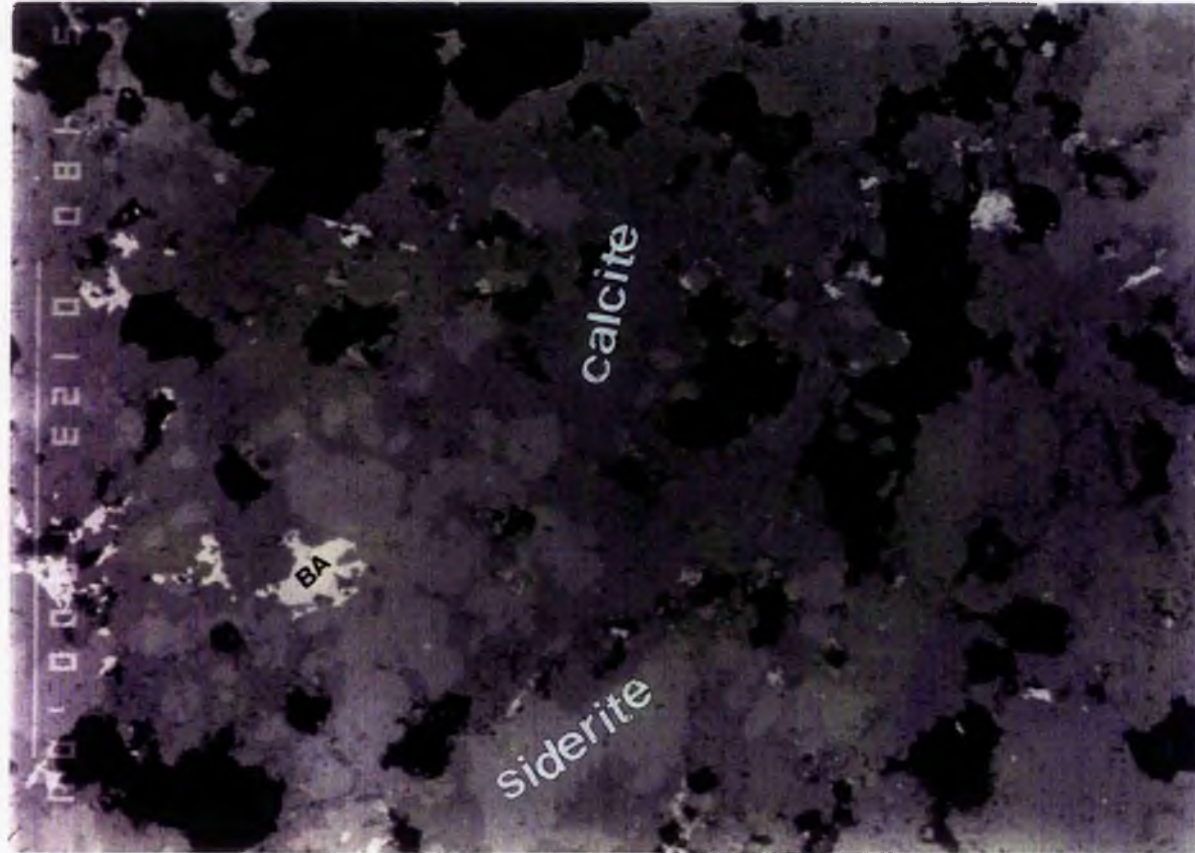


Plate 7-1 Backscattered electron image showing coexisting calcite and siderite phases with some barite from Buru carbonatite.  
Scale bar = 1000 $\mu$ .

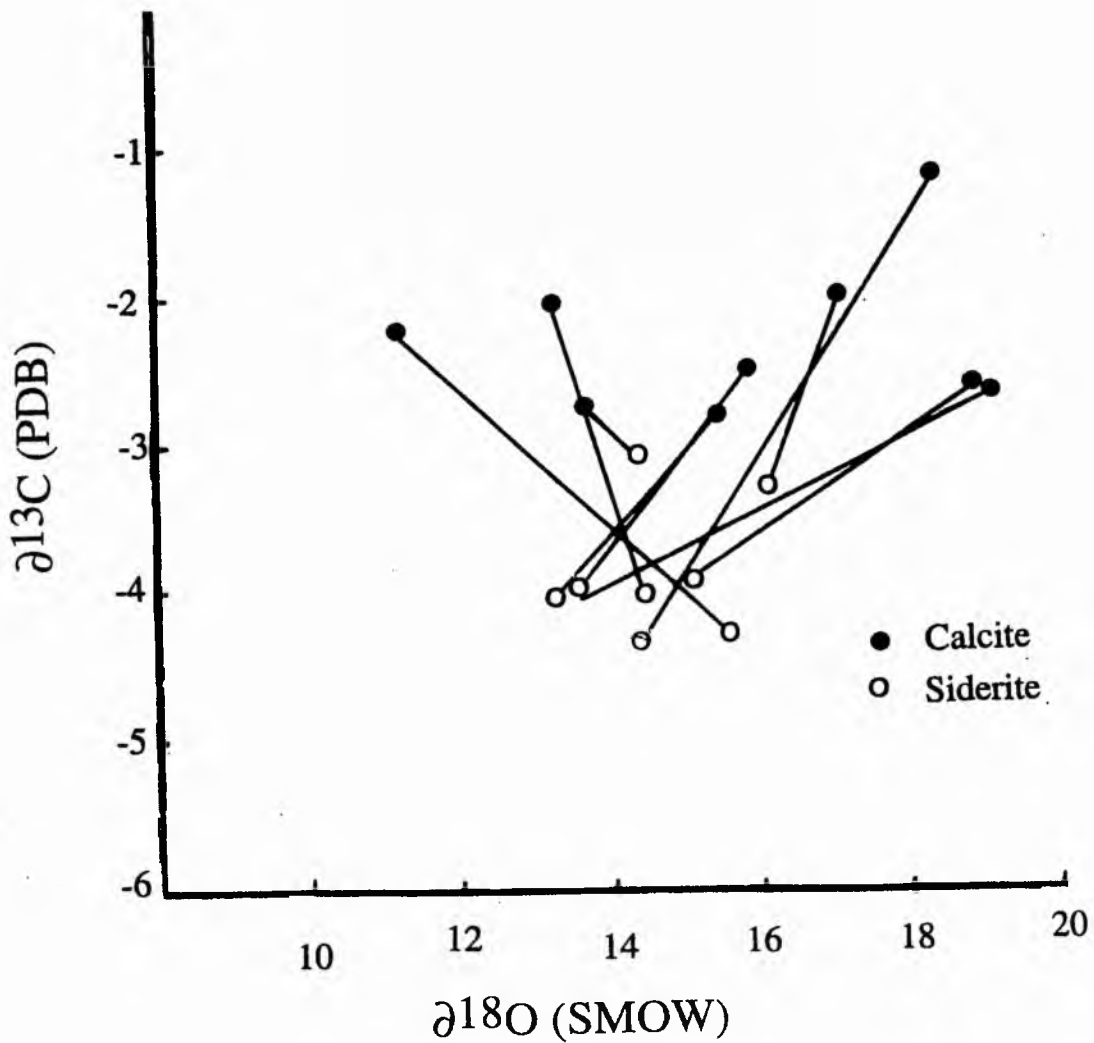


Figure 7-5 Plot of  $\delta^{13}\text{C}$  (PDB) vs  $\delta^{18}\text{O}$  (SMOW) for the Buru carbonatite centre. The tie lines connect calcite-siderite pairs from the same sample.

The Buru siderites, as shown above, have a more restricted range in carbon and oxygen isotopic values compared to the Buru calcites. The process of Rayleigh fractionation is considered by the writer to have not been active within the Buru siderites. The average  $\delta^{13}\text{C}$  of approximately  $-4\%$  for the Buru siderite is within the upper limit of the carbonatite box (Deines and Gold, 1973), although they are slightly enriched in  $\delta^{18}\text{O}$  with an average of  $+14.48\%$ . The writer suggests that the Buru siderites, which portray a slightly larger variation in  $\delta^{18}\text{O}$  but a smaller variation in  $\delta^{13}\text{C}$ , are compatible with a late-magmatic to hydrothermal alteration during solidification rather than through alteration by low temperature hydrothermal (meteoric) solutions. For the process proposed for siderite to work, a separate evolution and crystallization is advocated for the siderite in Buru since it cuts and post-dates the calcite.

#### 7.9 CARBON AND OXYGEN ISOTOPIC COMPOSITION FROM THE KUGE CARBONATITE.

The distribution of  $\delta^{13}\text{C}$  and  $\delta^{18}\text{O}$  from the Kuge carbonatite centre, including those from the ferrocarbonatite breccia and the calcite carbonatite are shown in Table 7-4 and Figure 7-6.

From Figure 7-6, the following features are recognized:

- i) Both the ferrocarbonatite breccia and the calcite carbonatite have high values of both  $\delta^{13}\text{C}$  and  $\delta^{18}\text{O}$  ranging between  $-8.44$  to  $-3.06\%$  and  $+21.99$  to  $+25.73\%$  for the carbonatite breccia, respectively, and  $-3.84$  to  $-3.11\%$  and  $+18.09$  to  $+24.05\%$  for the calcite carbonatite.
- ii) The Kuge calcites, particularly those of the ferrocarbonatite breccia, seem to retain the "magmatic" signature for carbon.
- iii) Calcrete shows the most elevated  $\delta^{18}\text{O}$  value at  $27.83\%$ , as expected.

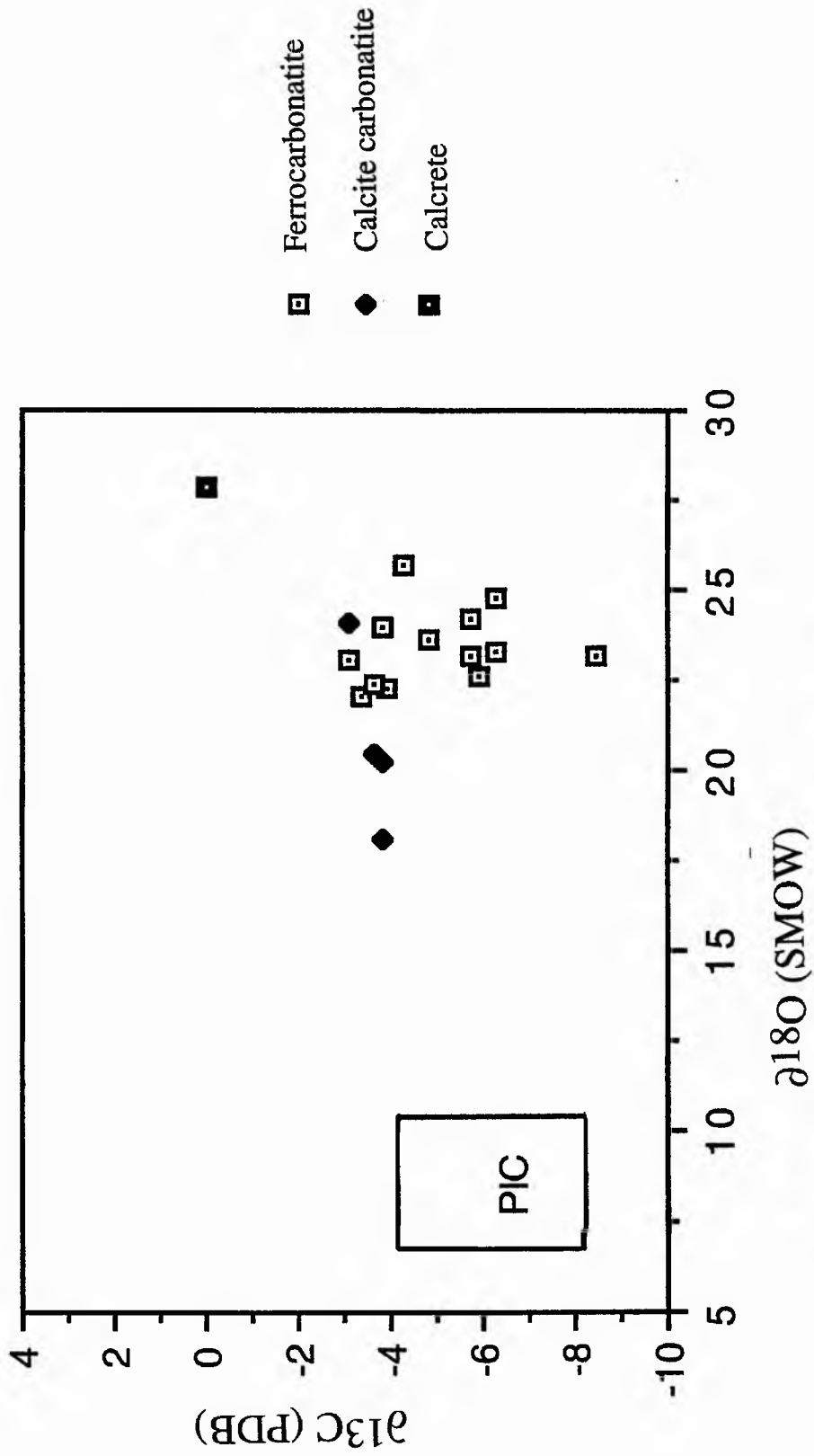


Figure 7-6 Plot of  $\delta^{13}\text{C}$  (PDB) vs  $\delta^{18}\text{O}$  (SMOW) from Kuge carbonatite.  
 PIC - Primary Igneous Carbonatites.

Table 7-4 Carbon and oxygen isotopic data from the Kuge centre.

Sample No.	Drill Hole	Depth (m)	$\delta^{13}\text{C}$	$\delta^{18}\text{O}$
KG-64	KG-2	5	-5.89	+22.60
KG-69	KG-2	22	-6.31	+23.30
KG-71	KG-2	33	-5.76	+24.15
KG-72	KG-2	36	-5.73	+23.23
KG-76	KG-2	43	-8.44	+23.18
KG-94	KG-3	14	-4.84	+23.66
KG-99	KG-3	35	-6.31	+24.72
KG-249	KG-5	4	-3.82	+23.99
KG-252	KG-5	35	-3.94	+22.32
KG-253	KG-6	5	-3.60	+22.42
KG-254	KG-6	8	-3.06	+23.04
KG-255	KG-6	10	-3.33	+21.99
KG-256	KG-6	12	-4.24	+25.73
KG-119	surface sample		-3.11	+24.05
KG-120	surface sample		-3.63	+21.99
KG-122	surface sample		-3.80	+20.21
KG-124	surface sample		-3.84	+18.09
KG-269	calcrete		+0.04	+27.83

#### 7.10 VARIATION IN $\delta^{13}\text{C}$ AND $\delta^{18}\text{O}$ OF THE KUGE CARBONATITE - DISCUSSION.

Compared to the Buru calcites, the Kuge carbonatite carbonates appear to be quite different. The apparent lack of correlation of  $\delta^{13}\text{C}$  vs  $\delta^{18}\text{O}$  is very clear in this deposit. Higher  $\delta^{18}\text{O}$ , indicating complete or nearly complete oxygen exchange, and  $\delta^{13}\text{C}$  values in the range of magmatic carbon is suggestive of equilibration with a large volume of fluid. Any mineral which

equilibrates in a fluid-dominated environment will obviously have its oxygen isotopic composition determined solely by temperature and the isotopic composition of the fluid, whereas the carbon isotopic composition need not be significantly changed. A water-dominated environment is suggested at Kuge on the basis of carbon and oxygen isotopic composition. It can be concluded that the variations in carbon and in particular oxygen shown by Kuge carbonatite are secondary in nature and are possibly attributed to the equilibration of the recrystallized carbonates with low temperature meteoric/groundwater fluids. It is also significant to note that the Kuge carbonatite carbonates were not affected by the introduction of atmospheric CO<sub>2</sub>.

The sample KG-269, which is a calcrete, has both the highest  $\delta^{18}\text{O}$  (+27.83‰) and  $\delta^{13}\text{C}$  (+0.04‰) isotopic values indicating extensive to complete exchange with meteoric water and atmospheric carbon dioxide to account for the observed shift towards the isotopic composition range of secondary carbonates. Temperatures of equilibration calculated for the Kuge carbonatite carbonates using the average  $\delta^{18}\text{O}$  of +23.41 and +20.70‰ for the ferrocarbonatite breccia and calcite carbonatite, respectively, is 52°C for the ferrocarbonatite breccia and 70°C for the calcite carbonatite. The temperatures obtained for the two rock units are consistent with field and isotopic evidence where calcite carbonatite is earlier than the ferrocarbonatite breccia and shows less equilibration with the hydrothermal fluids. The estimated temperatures are, however, below 250°C, which is in line with the temperature required in order to raise the  $\delta^{18}\text{O}$  contents of the carbonates (Deines, 1989). The temperature obtained from the calcrete sample (KG-269) is about 24°C, which is the lowest temperature so far obtained from both the Buru and Kuge carbonates, confirming the extensive to complete exchange with meteoric water.

The combined  $\delta^{13}\text{C}$  and  $\delta^{18}\text{O}$  isotopic composition for the Buru and Kuge carbonatite carbonates shown in Figure 7-7 reveals two distinct trends. The first trend, involving mainly the Buru calcite carbonates, is dominated by hydrothermal alteration and reprecipitation at lower temperatures and is also accompanied by the introduction of atmospheric  $\text{CO}_2$ . The second trend for the Kuge carbonates involves low temperature recrystallization in a water-dominated environment without the influence of surface carbon. From the distribution of the  $\delta^{13}\text{C}$  isotopic values, Kuge is considered to be a deeper facies than Buru. Lithological considerations discussed in chapters 3 and 4 also postulated Kuge as a deeper facies compared to Buru.

## 7.11 SULPHUR ISOTOPIC COMPOSITION IN CARBONATITES.

### 7.11.1 Introduction.

Sulphur isotopes have been used extensively in ore deposits to reveal the sources of the sulphur and fluids involved in ore genesis, as discussed in Ohmoto and Rye (1979) and the references quoted therein. Surprisingly, very few published data on the isotopic composition of sulphur in carbonatites exist (Deines, 1989). Barite is very common in drill cores from both Kuge and in particular Buru, which has been more extensively weathered and lateritized than Kuge. Sulphide minerals are very rare in the two centres, only a few grains of disseminated pyrite have been observed in some sections of the drill cores from Buru while galena was only identified by electron microprobe analysis. Barite mineral concentrates from both Buru and Kuge were prepared from drill core samples for sulphur isotope determinations. The sample preparation and experimental procedures are presented in Appendix 7-1.

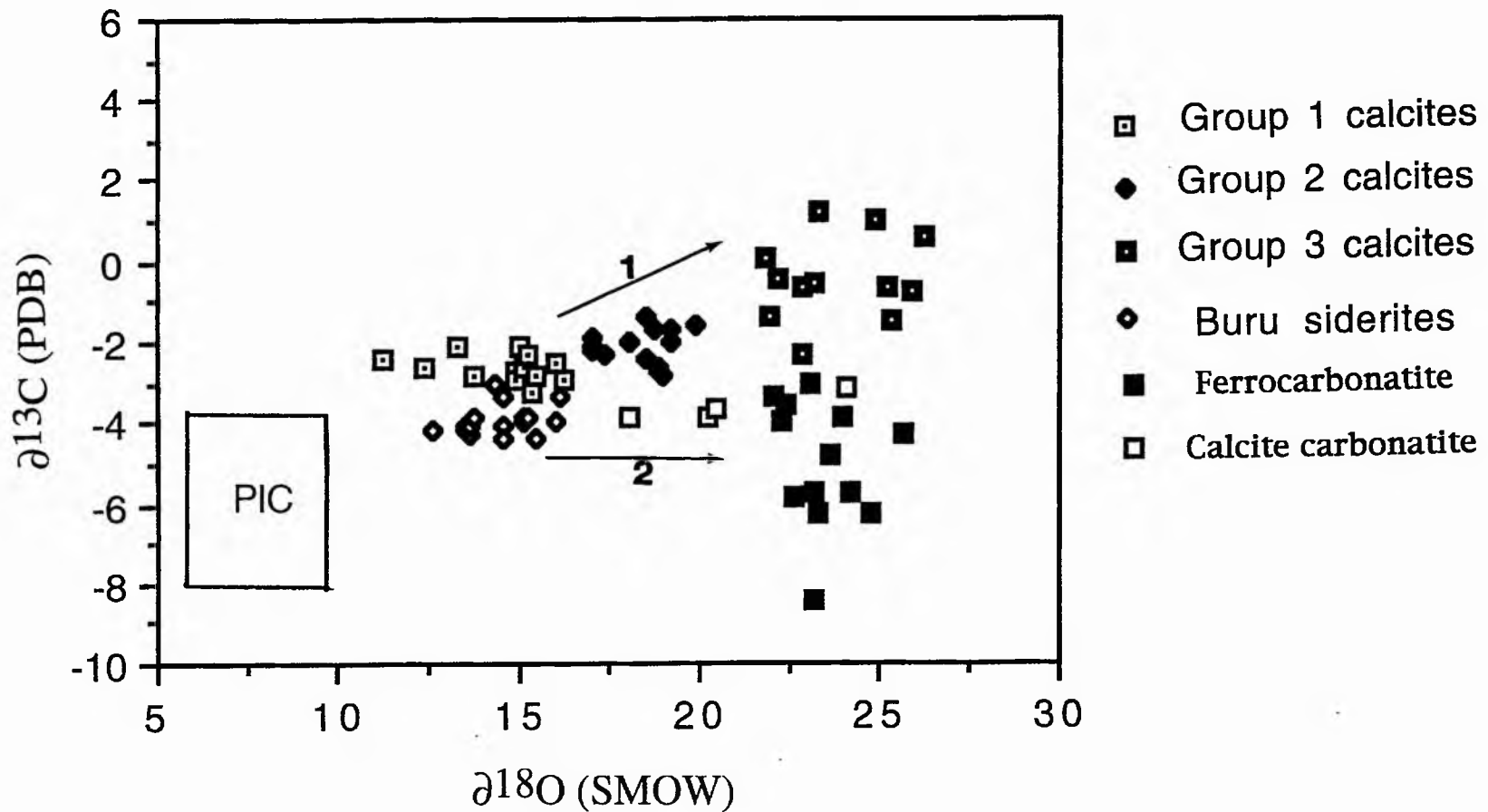


Figure 7-7 Combined plot of  $\delta^{13}\text{C}$  (PDB) vs  $\delta^{18}\text{O}$  (SMOW) showing the two alteration trends (1 & 2) in the Buru and Kuge carbonatite centres.

### 7.11.2 Summary of sulphur isotope determinations in the carbonatites.

Relatively few  $\delta^{34}\text{S}$  determinations in carbonatites are found in the literature. However, some of the earlier work on sulphur isotope composition in carbonatites was carried out by Von Gehlen (1967), who showed that the sulphides at the Phalaborwa carbonatite complex exhibited little variation in sulphur isotope composition, ranging from +2 to -2‰ (CDT). He concluded that the very narrow spread was consistent with a derivation of both carbonatite and sulphides from the earth's mantle. Grinenko et al. (1970), in their extensive study of isotopic composition of sulphide sulphur in carbonatites from a number of Russian carbonatite occurrences, obtained  $\delta^{34}\text{S}$  values ranging from -6.4 to +3.0‰ (CDT). They noted that individual carbonatite complexes possessed their own distinct isotopic composition and, more importantly, they observed that during the closing stages of carbonatite formation, sulphides became noticeably enriched in  $^{32}\text{S}$ . The authors concluded that the enrichment of the sulphides in  $^{32}\text{S}$  indicated a gradual increase of the oxidation potential of the solutions and gases from which the sulphides of the later carbonatites were deposited. Under favourable conditions, the oxidized sulphur formed sulphates. They also noted that the barites, like those from ankerite carbonatites, had heavier sulphur isotopic values ( $\delta^{34}\text{S} = +7.6$  to  $+8.0$ ‰).

Galena from the Mountain Pass carbonatite complex was reported by Mitchell and Krouse (1971) to be highly enriched in  $^{32}\text{S}$  with values ranging from -16.1 to -22.8‰ whereas barite from the same deposit gave  $\delta^{34}\text{S}$  values of +1.3 to +7.2‰ (CDT). Mitchell and Krouse (1975) also studied sulphur isotopic data for sulphides and barite from Mountain Pass, Oka, Magnet Cove, the Bearpaw Mountains and Phalaborwa and came to the same conclusion as Grinenko et al. (1970). Barite from Mountain Pass was shown by the authors to increase progressively to higher  $\delta^{34}\text{S}$  with sequence

of intrusion. Equally, Mäkelä and Vartiainen (1978) also found that isotope data for sulphide sulphur from the Sokli carbonatite, showed a variation of  $\delta^{34}\text{S}$  from -0.6 to -5.6‰ (CDT).

Deines (1989), in a review of sulphur isotopic data in carbonatites, observed that sulphates were characterized by enrichment in  $\delta^{34}\text{S}$  compared to sulphides and also concluded from the isotopic data available that carbonatite complexes were unique in their mean sulphur isotopic composition, which suggested sulphur heterogeneity within the mantle. Recently, Dawson et al. (1995) reported  $\delta^{34}\text{S}$  data for both sulphide (+2.8‰) and sulphate (+9.8‰) from Oldoinyo Lengai and concluded that the high values were due to the preferential vapour loss of light  $^{32}\text{S}$ .

#### 7.12 SULPHUR ISOTOPIC COMPOSITION FROM THE BURU AND KUGE CENTRES.

Sulphur isotope values of the analyzed barite samples from the Buru and Kuge carbonatite complexes are shown in Table 7-5 and Figure 7-8.

Table 7-5 Sulphur isotope composition of barite from Buru and Kuge.

Sample No.	Drill Hole	Depth (m)	$\delta^{34}\text{S}$ in ‰ (CDT)
<b>BURU</b>			
BR-1	BRL-1	5	+11.1
BR-3	BRL-1	31	+12.4
BR-5	BRL-1	65	+6.6
BR-8	BRL-1	75	+7.2
BR-1	BRL-1	92	+4.5
BR-1	BRL-1	116	+6.5
BR-17	BRL-1	138	+6.9
BR-18	BRL-1	141	+4.5

Table 7-5 continued.

Sample No.	Drill hole	Depth (m)	$\delta^{34}\text{S}$ ‰ (CDT)
BR-213	BRL-2	29	+12.2
BR-215	BRL-2	46	+6.1
BR-219	BRL-2	74	+6.3
BR-223	BRL-2	86	+8.9
BR-57	BRL-3	59	+7.8
<b>KUGE</b>			
KG-69	KG-2	22	+2.9
KG-71	KG-2	33	+5.1
KG-72	KG-2	36	+1.1
KG-80	KG-4	4	+1.2
KG-249	KG-5	4	+4.8
KG-252	KG-5	42	+2.9
KG-254	KG-6	8	+1.3
KG-256	KG-2	12	+4.2
KG-119	-	-	+5.3
KG-120	-	-	+2.7

Note: KG-119 and KG-120 are surface samples.

The following features are noted:

- i) Data on the sulphur isotope composition of the barite samples from Buru show a fairly widespread variation ranging from +4.5 to +12.4‰ (CDT) with an average of +7.8‰ (CDT).
- ii) Kuge compared to Buru shows a more homogeneous isotopic composition with  $\delta^{34}\text{S}$  values ranging between +1.1 to +5.3‰ (CDT) and an average of +3.2‰ (CDT).

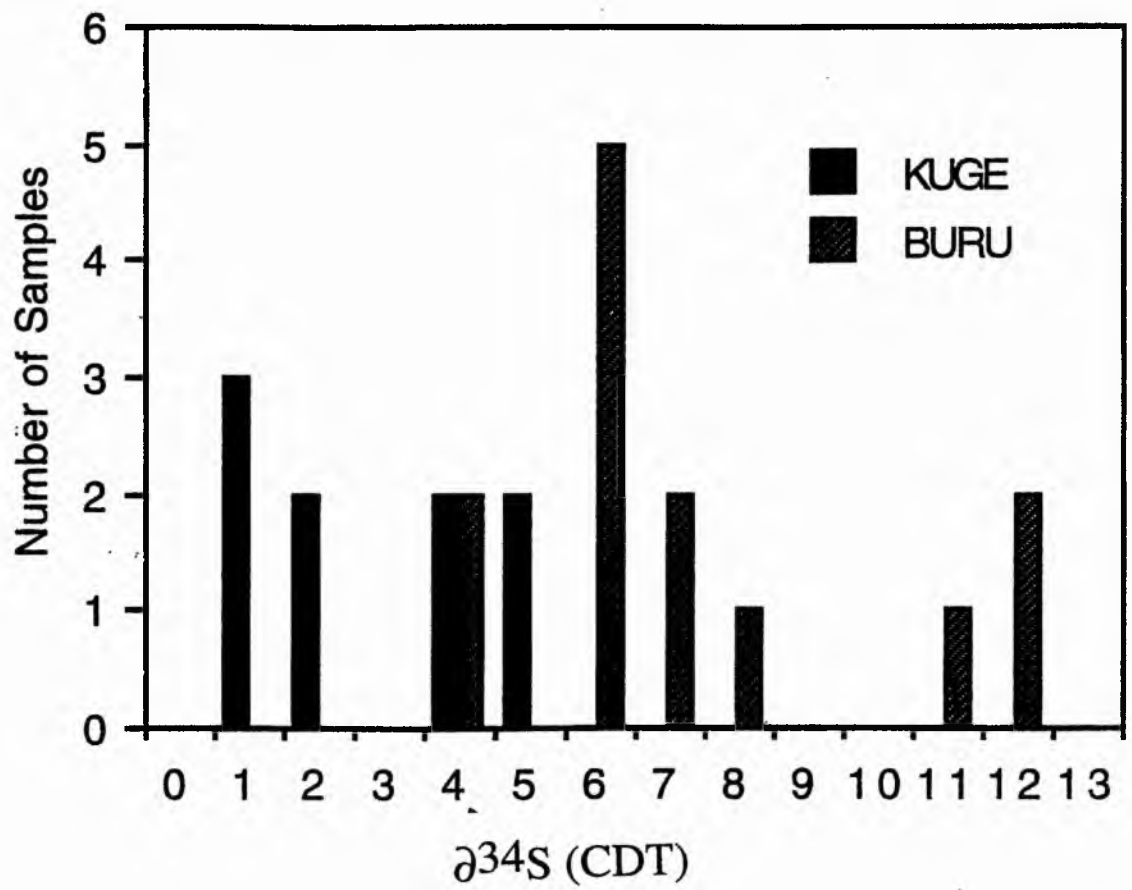


Figure 7-8 Isotopic composition of sulphur in barite from the Buru and Kuge carbonatite centres.

iii) Three samples containing the highest positive values of  $\delta^{34}\text{S}$  from Buru (+11.1, +12.2 and +12.4‰) were obtained from the laterite, which is the most oxidized section of the drill core.

### 7.13 VARIATION OF SULPHUR ISOTOPIC DATA FROM THE BURU AND KUGE CARBONATITE CENTRES.

Ohmoto (1972) demonstrated that the isotopic composition of, for instance sulphur, in hydrothermal minerals, is strongly controlled by the temperature of deposition, the fluid from which the mineral was deposited, the chemical composition of the fluid (pH and oxygen fugacity) at the time of deposition and the dissolved species. It could also be expected that the isotopic composition of sulphur in carbonatites could be influenced by the same conditions. On the basis of sulphur isotopic fractionation factors, Deines (1989) suggested that  $\delta^{34}\text{S}$  values as high as +5‰ are possible only if fractionation is governed by oxidized species in the melt when substantial amounts of S would have to be lost during the magma emplacement to produce large deviations from a magma value of mantle sulphur.

The oxidation state of sulphur in carbonatites is not well understood. Available evidence (Grinenko et al., 1970 and Deines, 1989) shows that sulphur is mainly present as sulphide in carbonatite magmas at temperatures of over 700°C, therefore the sulphides have mantle isotopic signatures. Isotope fractionation between primary sulphide minerals and magma has been estimated to be only about 1-3‰ (Chaussidon et al., 1989). With falling temperatures, the oxidized species ( $\text{SO}_2$ ,  $\text{SO}_4^{2-}$ ) are expected to become important, leading to large variations in  $\delta^{34}\text{S}$  due to isotope fractionations between the oxidized and reduced species. The occurrence of barite in some carbonatites is indicative of oxidizing conditions at lower temperatures. The presence of barite in both Buru and Kuge and the

scarcity of sulphides suggests high oxidation conditions and, together with the occurrence of goethite and hematite, high  $fO_2$ .

Buru is characterized by high  $\delta^{34}S$  with values in the range of +4.5 to +12.4‰ (CDT). The average of +7.8‰  $\delta^{34}S$  from Buru is similar or close to values obtained from the last stages of barite-bearing carbonatites from the Kola-Karelia province, Russia (Grinenko et al., 1970), Mountain Pass (Mitchell and Krouse, 1975) and Oldoinyo Lengai, Tanzania (Dawson et al., 1995). Kuge is quite different from Buru in its  $\delta^{34}S$  (Figure 7-9). The  $\delta^{34}S$  values for Kuge are between +1.1 and +5.3‰ (CDT) with an average of +3.2‰, which is close to values assumed to represent average mantle sulphur ( $\pm 3\%$ ; Zheng, 1990). When carbon and sulphur isotopic data for Buru and Kuge is plotted on a  $\delta^{13}C$  vs  $\delta^{34}S$  diagram, both the two centres are clearly distinct (Figure 7-9). Different carbonatite complexes are characterized by distinct  $\delta^{34}S$  and  $\delta^{13}C$ , as demonstrated in Figure 7-9 for Phalaborwa, Sokli and Oka (Deines, 1989), Oldoinyo Lengai (Dawson et al., 1995) and the Buru and Kuge volcanic centres.

The trend in carbonatite sulphides towards more negative  $\delta^{34}S$  values in the later stages can be interpreted as resulting from an increase in oxidizing conditions in consecutive carbonatite stages (Deines, 1989). If the sulphur is being shared by reduced (sulphide) and oxidized (sulphate) species and yet the total sulphur  $\delta^{34}S$  stays constant, as  $\delta^{34}S$  of sulphide decreases,  $\delta^{34}S$  sulphate must increase to maintain the mass balance. Both Buru and Kuge are equally characterized by high oxidizing conditions and yet their barites show positive  $\delta^{34}S$ . This is thought by the writer to be either due to a preferential loss of light  $^{32}S$  while progressively concentrating  $^{34}S$  based on Rayleigh degassing of  $SO_2$ , or due to redox processes involving reduced and

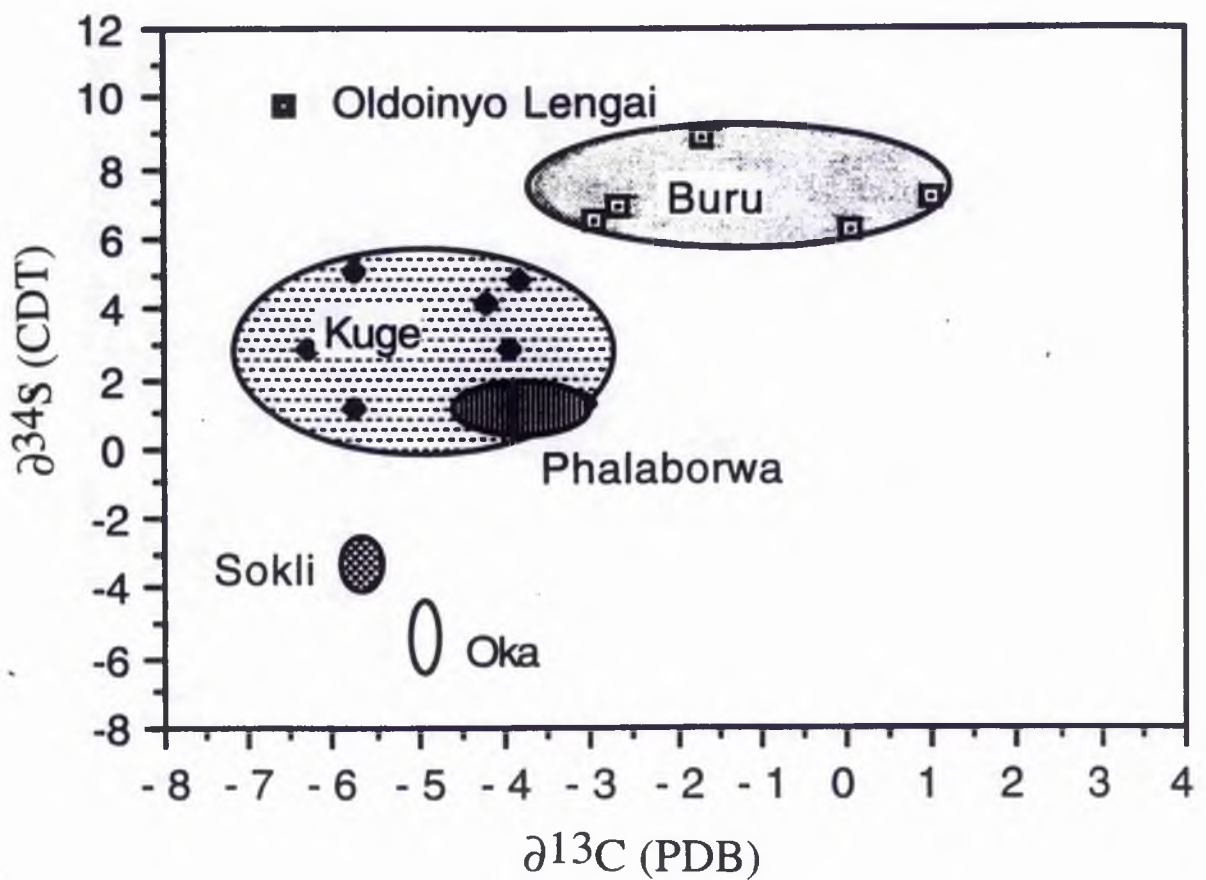


Figure 7-9 plot of  $\delta^{34}\text{S}$  (CDT) vs  $\delta^{13}\text{C}$  (PDB) for the Buru and Kuge carbonatite centres and other carbonatite complexes.

oxidized sulphur species. The specific process accounting for the positive  $\delta^{34}\text{S}$  in both the Buru and Kuge centres is unclear.

Large  $\delta^{34}\text{S}$  variation caused by changes in  $f\text{O}_2$ , as in Buru, will require a significant proportion of sulphide and sulphate, but the sulphides only occur as traces in the deposit. To explain the lack of correlation between the  $\delta^{34}\text{S}$  values and the sulphur concentrations, Zheng (1990) proposed a "selective flux" sulphur mechanism, in which the isotopic composition of sulphur in the magma is very small when one species (either sulphide or sulphate) is dominant at the time of crystallization. However, this mechanism is difficult to evaluate.

#### 7.14 CONCLUSION.

Figure 7-1 shows that carbonatite carbonates from Buru do not plot close to the carbonatite box. The range in isotopic compositions shown by the Buru carbonates suggest that Rayleigh processes were not responsible for the variability in carbon and oxygen isotopic values. Large differences in isotopic composition depicted by the Buru carbonates suggest that isotopic heterogeneity within the mantle cannot account for these large differences. The variation in carbon and oxygen isotopic composition in Buru is secondary in origin and hence attributed to secondary alteration processes.

Most of the carbon and oxygen isotopic variations shown by the Group 1 and 2 calcites from the Buru carbonatite centre may be explained by hydrothermal alteration processes involving fluids where isotopic exchange takes place between the carbonatite carbonates and the  $\text{H}_2\text{O}-\text{CO}_2$  fluids at low temperatures. Primary factors involving Rayleigh fractionation, magmatic processes related to liquid immiscibility and fractional crystallization and contamination by country rocks are suggested by the

writer not to have contributed significantly to the isotopic variations shown by the Group 1 and 2 calcites from Buru.

The  $\delta^{34}\text{S}$  isotopic composition for Buru and Kuge are quite different and distinct. The values for the Kuge centre are close to values expected for mantle sulphur whereas the Buru carbonatite is characterized by high values of  $\delta^{34}\text{S}$ . The variations in  $\delta^{34}\text{S}$  shown by the two centres compared to mantle sulphur could be due to either redox processes or isotopic fractionation from volatile loss.

## CHAPTER EIGHT

### APPLIED MINERALOGY AND GEOCHEMISTRY OF RARE EARTH ELEMENTS

#### 8.1 CLASSIFICATION OF RARE EARTH ELEMENTS (REE).

The rare earth elements (REE) compose part of the Group IIIA elements in the Periodic Table, consisting of yttrium, lanthanum and the lanthanides from cerium (58) to lutetium (71) (Henderson, 1996). Group IIIA also includes scandium (atomic number 21), which, because of its size, has a geochemical behaviour that differs from the other REEs and is therefore not included in the rare earth element classification. Similarly, the actinides uranium and thorium, although they commonly substitute for REEs in nature, are not treated as lanthanides (Burt, 1989). The REEs as a group are perhaps a misnomer in that several of the elements are more abundant than, for example, lead, bismuth or iodine, which are not normally considered as rare. The name 'earth' is however appropriate since the elements have properties more akin to those of the alkaline earth elements such as the formation of basic oxides and hydroxides (Richens, in press). The term rare earth elements (REE) in this thesis will be restricted to lanthanides including lanthanum and yttrium. The lanthanides are conveniently divided into two main sub-groups, those with low atomic numbers (La-Sm), which are termed the light rare earths (LREE), and those with higher atomic numbers (Gd-Lu), the heavy rare earths (HREE). Less commonly, the middle members of the group (Pm-Ho) are known as the middle rare earths (MREE).

The light rare earth elements (LREE) can also be named for crystal chemical purposes as the "Ce-group" lanthanides (from lanthanum to

europium) and the heavy rare earths elements (HREE), except yttrium, as the "Y -group", which are the lanthanides from gadolinium to lutetium. The REEs exist in the trivalent state (3+) under most conditions and have similar chemical properties, except cerium and europium which can behave anomalously under certain redox conditions due to the formation of  $Ce^{4+}$  and  $Eu^{2+}$  species respectively. The 3+ state is, however, still the most stable thermodynamically.

The REEs behave as a coherent group and appear together in most geological environments and processes. The arrangement of the electrons (Table 8-1) around the nuclei of the different REEs is a determining factor of the properties of these elements (Henderson, 1996). There is a progressive decrease in the ionic size of REE trivalent ions with increasing atomic number, often referred as to the "lanthanide contraction". The progressive decrease in atomic number is in turn reflected in the gradual and systematic variations in the fundamental chemical properties of the REEs, which allow the REEs as a group to be used as a tool for interpreting many petrogenetic processes, especially in igneous systems involving crystal fractionation, partial melting or magma mixing. The presence of more than one valency exhibited by cerium and europium in relation to other REEs can also be used to gain information concerning the redox and pH conditions of supergene processes (Sverjensky, 1984).

The lanthanide contraction may also influence the complexing properties of the REE group and hence the way the elements are transported in solution. If the mechanism of REE transport properties in solution are properly understood, complex problems of ore formation, rock alteration and the genesis of crustal fluids will be better resolved, in conjunction with the use of rare earth isotopes (Henderson, 1996).

Owing to the highly radioactive properties of the actinides, which render them unsuitable and dangerous in experimental investigations, REEs have recently been used as proxies to the actinides in evaluating actinide transport from high-level waste repositories to the surface or ground-water accessible environments (Haas et al., 1995).

Table 8-1 Names, symbols, atomic number and electron configuration of the rare earth elements (after Henderson, 1996).

Name	Symbol	Atomic Number	Electron Configuration
Yttrium	Y	39	[Kr]4d <sup>1</sup> 5s <sup>2</sup>
Lanthanum	La	57	[Xe]5d <sup>1</sup> 6s <sup>2</sup>
Cerium	Ce	58	[Xe]4f <sup>2</sup> 6s <sup>2</sup>
Praseodymium	Pr	59	[Xe]4f <sup>3</sup> 6s <sup>2</sup>
Neodymium	Nd	60	[Xe]4f <sup>4</sup> 6s <sup>2</sup>
Promethium*	Pm	61	[Xe]4f <sup>5</sup> 6s <sup>2</sup>
Samarium	Sm	62	[Xe]4f <sup>6</sup> 6s <sup>2</sup>
Europium	Eu	63	[Xe]4f <sup>7</sup> 6s <sup>2</sup>
Gadolinium	Gd	64	[Xe]4f <sup>7</sup> 5d <sup>1</sup> 6s <sup>2</sup>
Terbium	Tb	65	[Xe]4f <sup>9</sup> 6s <sup>2</sup>
Dysprosium	Dy	66	[Xe]4f <sup>10</sup> 6s <sup>2</sup>
Holmium	Ho	67	[Xe]4f <sup>11</sup> 6s <sup>2</sup>
Erbium	Er	68	[Xe]4f <sup>12</sup> 6s <sup>2</sup>
Thulium	Tm	69	[Xe]4f <sup>13</sup> 6s <sup>2</sup>
Ytterbium	Yb	70	[Xe]4f <sup>14</sup> 6s <sup>2</sup>
Lutetium	Lu	71	[Xe]4f <sup>14</sup> 5d <sup>1</sup> 6s <sup>2</sup>

\* Promethium has no long lived nuclei and therefore has no natural abundance in rocks or minerals.

## 8.2 DISTRIBUTION OF RARE EARTH ELEMENTS.

The REEs occur as trace elements in mantle rocks, where they may be stored in titanates in mantle peridotite (Haggerty, 1989 and Jones, 1989), mantle-derived magmas and in the majority of crustal rocks. This includes sedimentary, igneous or metamorphic rocks, where they are usually found concentrated in a number of rock forming minerals, for example apatite. The structure of apatite  $[\text{Ca}_5(\text{PO}_4)_3(\text{OH},\text{F},\text{Cl})]$  is capable of concentrating a number of trace elements, in particular REEs, and therefore has an important role in controlling the distribution of REEs in many rocks of different environments. Other similar accessory phases that concentrate REEs include sphene, garnet, perovskites, monazite, zircon etc.

The majority of REEs are produced from monazite-bearing marine placers, especially from western Australia (Nearly and Highley, 1984) and from carbonatite-hosted deposits. Most of the worlds rare earth production is from Mountain Pass, California (USA), and Bayan Obo, Inner Mongolia (China), and together these two localities are the leading REE producers in the world. In recent years there has been an increasing interest in REEs found at the laterites overlying carbonatite complexes, such as those found in the Mt Weld alkaline complex in western Australia (Lottermoser, 1991), Araxá and Catalão, Brazil (Morteani and Preinfalk, 1996), and Mrima Hill, Kenya (Notholt et al., 1990). It is very likely that in future REE production based on the traditional sources from beach sands and primary carbonatite hard rocks, may have to compete with production from lateritic/regolith REEs from Australia, Brazil and Africa.

### 8.3 RARE EARTH ELEMENTS IN CARBONATITES.

The mineralogy of REEs in carbonatites is diverse (Heinrich, 1966). Over 300 minerals were described by Kapustin (1980). Hogarth (1989) also compiled a number of rare earth minerals, including 27 from carbonatites. Wall and Mariano (1996) have recently compiled a list of rare earth minerals found in carbonatites and related rocks. Rare earths are concentrated in carbonatites mainly as three chemical compounds (Wyllie et al., 1996):

- i) Oxides such as pyrochlore and perovskite,
- ii) Phosphates such as apatite and monazite and
- iii) Fluorocarbonates including bastnaësite, synchysite and parisite.

Mariano (1989b) suggested a genetic classification of REEs associated with carbonatites in which he proposed three main categories:

- i) Primary magmatic crystallization, such as those observed in Mountain Pass, USA,
- ii) Hydrothermal mineralization (the most common occurrence) and
- iii) Supergene mineralization, produced by the weathering of carbonatite complexes.

As discussed later, distinguishing the three categories is not easy because rare earth minerals can be precipitated under a variety of different conditions.

## 8.4 RARE EARTH ELEMENTS FROM THE BURU AND KUGE CARBONATITE CENTRES.

### 8.4.1 Introduction.

The initial detailed studies on REE mineralization in the Nyanza rift carbonatites was carried out by the joint exploration programme undertaken by the Metal Mining Agency of Japan (MMAJ) on behalf of the Government of Japan and the Mines and Geological Department, Ministry of Environment and Natural Resources, Government of Kenya (JICA Reports, 1988-1990). Enhanced REE mineralization was confirmed to occur mainly in the Buru and Kuge carbonatite centres. The main aims of this chapter are therefore as follows:

- i) To discuss the occurrence and distribution patterns of the REEs in both the Buru and Kuge carbonatite complexes,
- ii) To identify rare earth minerals in the two centres,
- iii) To evaluate the relative importance of the magmatic, hydrothermal and supergene signatures in order to classify the occurrence of REEs in the Buru and Kuge centres,
- iv) To propose a mode of concentration and transport of the rare earth elements in their identified environments and
- v) To evaluate whether there are any observed systematic changes or correlation in the distribution of REE patterns and the stable isotopes discussed in chapter 6.

### 8.4.2 Methods of study.

Samples were collected from selected drill cores from both the Buru and Kuge carbonatite centres. The samples were systematically taken from the weathered top to the fresh bottom sections of each drill core. In Buru, where a thick lateritic cap overlying the carbonatite is developed, core

samples were systematically selected to represent the different weathering profiles encountered. The mineralogy of the samples was determined by X-ray diffraction (chapter 5). The total REE contents were determined by X-ray fluorescence (XRF) at the University of St Andrews and inductively coupled plasma (ICP) methods at Royal Holloway, University of London.

Electron wavelength-dispersive microprobe analyses for the identification of the rare earth minerals were carried out on polished and carbon-coated thin-sections at the Department of Geology, University of St Andrews, using a JEOL JCSA 733 Superprobe operating at 15kV with a beam current of 20nA. Quantitative analysis was performed using a combination of pure metal REEs and synthetic rare earth phosphates, oxides and fluorides as standards. Matrix corrections were done by using ZAF correction factors. Additional compositional information was also obtained by using a JEOL JSM-35CF scanning electron microscope (SEM) located at Gatty Marine Laboratories, University of St Andrews. Samples were coated for SEM analysis by using an Emscope 500 Sputter Coater, Gold Target. Approximately 2 minutes was required at 15mA for a 10 nm coating.

## 8.5 RARE EARTH ELEMENTS AT THE BURU HILL CARBONATITE.

### 8.5.1 Introduction.

The Buru carbonatite centre is characterized by the occurrence of a lateritic cap overlying the carbonatite. Fresh carbonatite is not encountered on the present erosional surface and is only revealed at depth by drilling. Detailed mineralogical studies (chapter 5) distinguish three distinct mineralogical zones, which appear to be depth related. The upper and most oxidized zone (the laterite) consists of iron oxides/hydroxides and various Ba-Mn-Fe complexes. This zone is also characterized by the absence of carbonates.

The middle zone (saprolite or transitional zone) revealed a partial breakdown of carbonatite carbonates and is mainly represented by calcite and iron hydroxides. The lower zone is characterized by relatively fresh carbonatite comprising calcite, siderite and magnetite. Barite and fluorite occur in all three zones, whereas apatite and some silicate xenocrysts, probably from the country rocks, are observed towards the lower sections of the drill cores.

Samples in Table 8-2 (BR-1, BR-5, BR-13, BR-16 and BR-28), from the 200 m deep drill hole BRL-1 from Buru (Figure 4-1), are representative of the mineralogical zones mentioned above and were selected to show the distribution of REEs within the laterite and below the weathering profile. Sample BR-183 is from a siderite dyke cross-cutting the Buru carbonatite. In order to evaluate and compare the nature of the REE abundance in carbonatites it is usually necessary to be able to sample unaltered rocks that are exactly the same in mineralogy and chemistry as those that are altered, a condition that is rarely fulfilled in most investigations. The calcite carbonatite from the North Ruri carbonatite complex (NR-271) has been chosen on the basis of its mineralogical and chemical composition as it seems to be relatively fresh and will therefore be used for comparison with carbonatite rock samples from the Buru and Kuge carbonatite centres.

For ease of discussion in this chapter, the chemistry of the lateritic zone noted in BRL-1 is considered by the writer to be dominated by processes related to supergene reactions, whereas in the fresh zone below the weathering profile, where the protolith is clearly the parent rock carbonatite, hydrothermal processes are considered to dominate and influence the chemistries observed. It is, however, very difficult to separate the two processes, especially in the transitional (saprolite) zone where the

two processes might be both involved at the same time. Plate 4-2 illustrates the different zones mentioned and particularly the differences in colour within and below the weathering profile, which is a function of the mineralogical compositions encountered.

#### 8.5.2 Distribution of REEs in the Buru carbonatite.

The REEs data for whole rock samples from Buru is given in Table 8-2.

The following features are noted:

- i) The Buru carbonatite is enriched in LREEs (La, Ce and Nd). When compared to averages of carbonatites given in Woolley and Kempe (1989), Buru lies within the range of values for the ferrocarnatites.
- ii) The siderite carbonatite dyke is also enriched in LREEs, although its contents are lower than the carbonatite it cross-cuts at Buru hill.
- iii) The upper and the most oxidized sections of the cores (carbonatite laterite represented by samples BR-1 and BR-5) are characterized by higher LREE contents and higher total rare earth oxide contents compared to the lower, fresh sections of the drill cores.
- iv) Higher  $(La/Yb)_N$  values are observed in the carbonatite laterite and seem to progressively decrease with depth, except for samples BR-13 and BR-28.
- v) The North Ruri calcite carbonatite (NR-271) has a lower total REE content and  $(La/Yb)_N$  value than those observed in the Buru centre, but has a comparable REE abundance to the calciocarnatite given in Woolley and Kempe (1989).
- vi) The distribution and abundance of major elements, particularly  $Fe_2O_{3T}$ , MnO and CaO, mirrors that of the REEs. Higher contents of FeO and MnO are associated with the supergene zone, whereas higher CaO and possibly slightly higher values of  $P_2O_5$  are connected with samples below the weathering profile.

Table 8-2 Major elements and rare earth elements from the Buru carbonatite.

Sample	BR-1	BR-5	BR-13	BR-16	BR-28
Depth (m)	5	65	108	130	200
SiO <sub>2</sub>	1.75	3.39	12.86	2.23	2.39
Al <sub>2</sub> O <sub>3</sub>	0.39	0.42	2.55	0.36	0.14
Fe <sub>2</sub> O <sub>3</sub>	30.48	62.80	14.98	21.88	19.38
MgO	0.22	0.28	2.04	1.31	2.44
CaO	26.91	2.40	28.71	36.41	26.36
Na <sub>2</sub> O	0.12	0.06	0.85	0.27	0.38
K <sub>2</sub> O	0.12	0.20	1.55	0.29	0.35
TiO <sub>2</sub>	0.40	0.51	0.37	0.24	0.16
P <sub>2</sub> O <sub>5</sub>	1.23	0.64	0.94	0.29	2.80
MnO	7.22	9.48	2.37	2.67	4.17
Total	68.72	80.18	67.22	65.95	58.57

## Rare earth elements

La	11176	6740	6736	1594	5564
Ce	17059	10734	6705	3182	6215
Pr	1324	1085	417	308	447
Nd	3118	3400	910	1058	1038
Sm	245	550	88	254	109
Eu	55	145	24	76	31
Gd	137	392	63	192	89
Dy	104	201	46	102	77
Ho	23	33	9	19	15
Er	56	53	18	41	34
Yb	52	38	18	32	34
Lu	7	4	2	3	4
(La/Yb) <sub>N</sub>	143.5	118.05	252	32.63	108.77
Sum	33356	23345	15036	6862	13657

Table 8-2 continued.

Sample	BR-183	NR-271(North Ruri)
Depth (m)	118	-
SiO <sub>2</sub>	0.10	0.05
Al <sub>2</sub> O <sub>3</sub>	0.08	0.03
Fe <sub>2</sub> O <sub>3</sub>	51.45	0.32
MgO	2.09	0.11
CaO	8.95	54.71
Na <sub>2</sub> O	0.21	0.11
K <sub>2</sub> O	0.06	0.06
TiO <sub>2</sub>	0.07	0.01
P <sub>2</sub> O <sub>5</sub>	0.25	0.42
MnO	5.00	0.21
Total	68.26	56.53

#### Rare earth elements

La	2568	216
Ce	4167	408
Pr	365	38
Nd	1036	136
Sm	124	21
Eu	32	6
Gd	79	16
Dy	48	12
Ho	9	2
Er	17	5
Yb	17	4
Lu	2	0.4
(La/Yb) <sub>N</sub>	98	30
Sum	8464	864.44

Major oxides in wt %. rare earth elements in ppm.

Analysis by ICP.

vii) The sums of the major element analyses are quite low. The low contents are attributed to higher abundances of REEs in the rocks, and to CO<sub>2</sub> which was not analyzed for.

viii) The aluminium contents are very low within the laterite, as well as in the carbonatite.

### 8.5.3 REE normalized patterns - the Buru carbonatite.

Normalized REE distribution patterns (chondrite values from Nakamura, 1974) from the Buru carbonatite are shown in Figure 8-1. The Buru carbonatite samples are characterized by relatively steep LREE and slightly flat HREE distribution patterns. They are enriched in LREEs by a factor of slightly over 10<sup>4</sup> and in HREEs by a factor of between 10<sup>2</sup> and 10<sup>3</sup> relative to chondrite. Sample BR-1 from the carbonatite laterite has the highest La+Ce+Nd contents. This is supported by a large increase in the (La/Yb)<sub>N</sub> ratio of 143.5 (see Figure 8-2). It is also significant to note that BR-1 is slightly depleted in MREE compared to most samples below the sampling profile. BR-1, however, appears to be enriched in ytterbium and lutetium. The siderite-carbonatite dyke (BR-183) from Buru hill is also characterized by steep LREE distribution patterns although its REE contents are slightly lower than the other Buru carbonatite samples.

The calcite carbonatite from North Ruri (NR-271) shows a similar REE distribution pattern to those from the Buru samples and also has a similar pattern to the calciocarbonatite presented in Woolley and Kempe (1989). The general similarity in distribution patterns noted from western Kenya carbonatites confirms the general observation that all carbonatites worldwide are characterized by steep LREE distribution patterns.

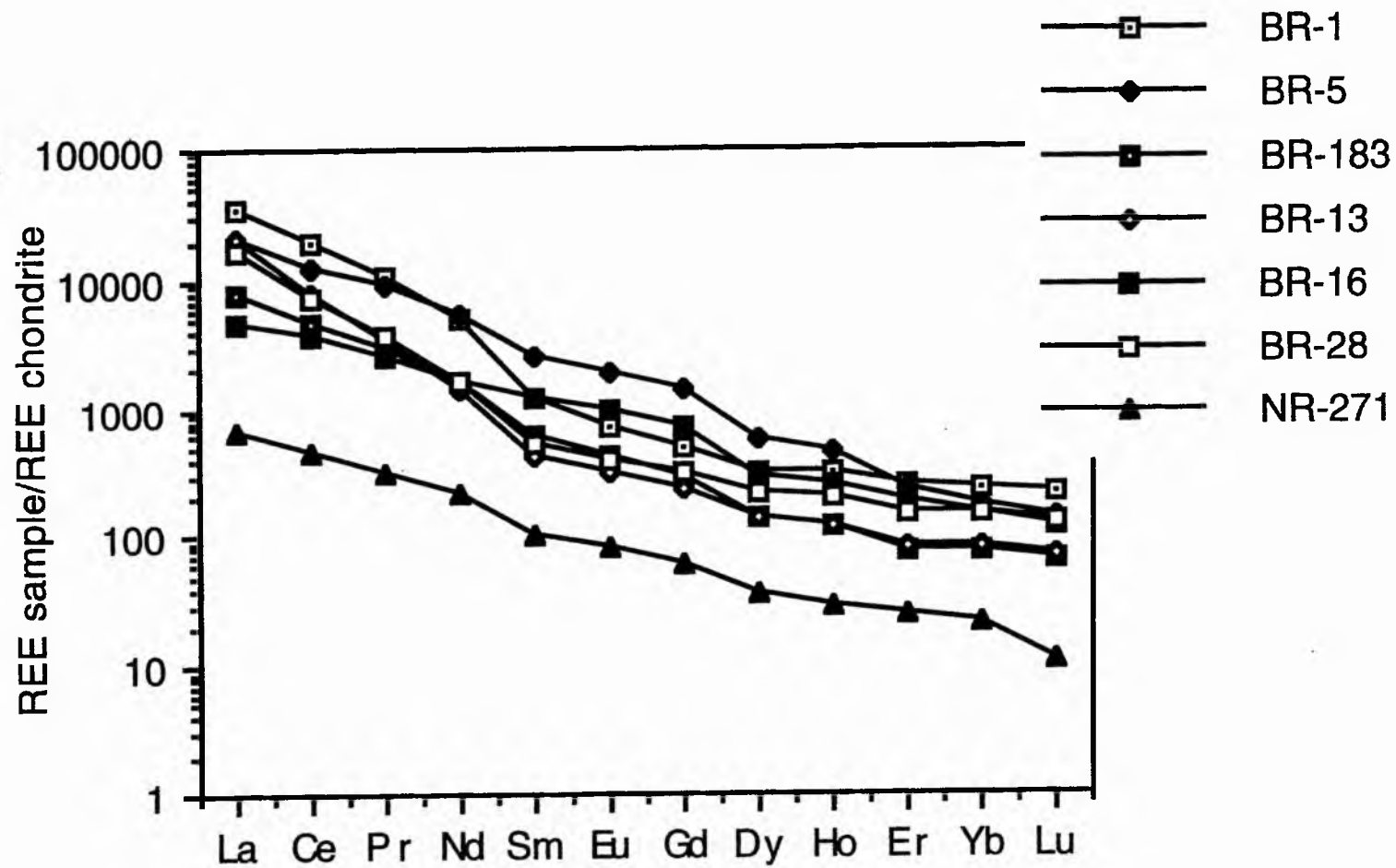


Figure 8-1 Chondrite-normalized REE distribution patterns for the Buru carbonatite.

The enrichment in La+Ce+Nd shown by REE chondrite-normalized distribution patterns from the Buru centre (Figure 8-1) is clearly supplemented and supported by Figure 8-2. Slight enrichment in the La+Ce+Nd content is evident in the oxidized (supergene) zone. Like BR-1 above, the most oxidized zone shows a decrease in MREEs compared to the zone immediately below it, and eventually an increase in HREEs, Yb+Lu and yttrium. The lower fresh carbonatite zone consistently reveals lower REE contents than the other two zones. The three zones from BRL-1 are also characterized by a moderate increase in the  $(La/Yb)_N$  ratio from 189.54 to 176.13 and 100 for the oxidized upper zone, oxidized middle zone and fresh lower zone, respectively.

## 8.6 RARE EARTH ELEMENTS AT THE KUGE CARBONATITE CENTRE.

### 8.6.1 Introduction.

The REE mineralization observed in Kuge during the Japanese-Kenyan mineral exploration programme (JICA Reports, 1988-1990) was found to be closely connected with a brecciated iron-rich carbonatite dyke (ferrocarbonatite breccia) composed mainly of calcite and iron hydroxides. Detailed drilling was carried out on the ferrocarbonatite dyke in order to confirm the REE mineralization at depth. The mineralogical zones recognized in Buru are not apparent in the Kuge carbonatite centre, where both the upper and lower sections of the drill core samples are characterized by calcite. The development of laterite is not noticeable in Kuge as in Buru, but, the distinctive red/brown colour of both the ferrocarbonatite dyke within the drill core samples and on the surface outcrops, and also that of the calcite carbonatite, is an indication of iron enrichment due to supergene reactions.

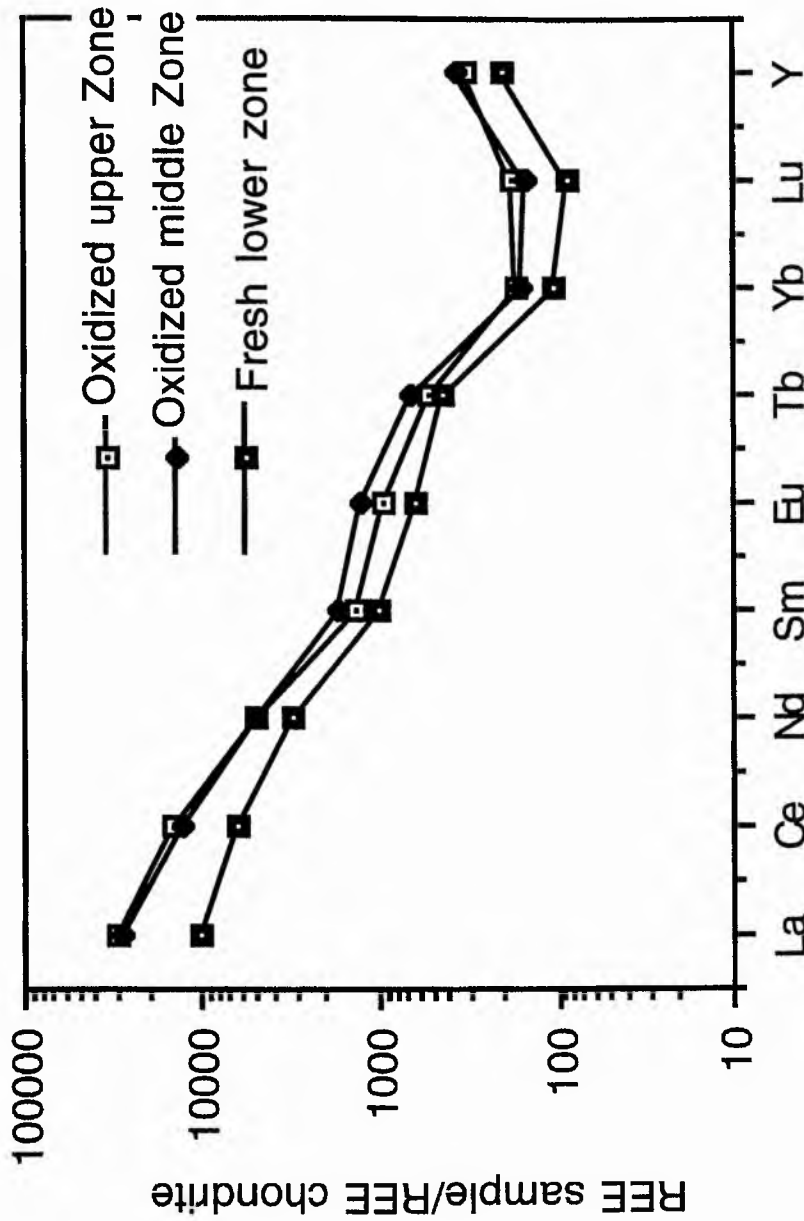


Figure 8-2 Chondrite-normalized REE distribution patterns for the Buru carbonatite, Data based on averages of the zones sampled (JICA reports, 1988 - 1990).

It is probable that most of the iron oxides and hydroxides noted in Kuge are due to the oxidation of iron-bearing minerals such as magnetite or siderite. Andersen (1984, 1987) described a similar process for the transformation of ferrocarnatite at Rodberg, although a slight contribution of iron through the normal carbonatite crystallization sequence, where late carbonatites are enriched in iron, cannot be ignored.

As in Buru, samples were selected along the drill cores to show the abundance and distribution of REEs within the sampling profile. Samples KG-69, KG-71, KG-72 and KG-76 were selected from drill hole KG-2. The diamond drill holes at the Kuge carbonatite centre are only 60 m deep and it is most likely that the samples selected are representative of only the supergene zone. The sample from North Ruri (NR-271) is included among the Kuge samples for comparison, as was done for the Buru samples.

#### 8.6.2 Distribution of REEs in the Kuge carbonatite.

The distribution and abundance of REEs for the ferrocarnatite breccia at Kuge is shown in Table 8-3. The following are noted:

- i) The Kuge ferrocarnatite dyke is enriched in LREEs (La, Ce and Nd) and is comparable to the average ferrocarnatite given in Woolley and Kempe (1989), except KG-76 which is extremely low in lanthanum.
- ii) The upper sections of drill hole KG-2 are characterized by higher rare earth contents, the sum of which decreases with depth.
- iii) The upper sections of the drill core samples have a higher  $(La/Yb)_N$  ratio, which progressively decreases with depth. Sample KG-76 has a very low La/Yb ratio because of the extremely low lanthanum content compared to the other samples.
- iv) As expected, NR-271 has the lowest REEs.

Table 8-3 Major and rare earth elements from Kuge carbonatite centre

Sample	KG-69	KG-71	KG-72	KG-76	NR-271
Depth (m)	22	33	36	44	-
SiO <sub>2</sub>	0.78	1.18	1.17	3.12	0.05
Al <sub>2</sub> O <sub>3</sub>	0.15	0.28	0.58	1.42	0.03
Fe <sub>2</sub> O <sub>3</sub>	15.34	15.98	23.16	38.89	0.32
MgO	0.45	0.36	0.71	0.41	0.11
CaO	27.03	23.59	27.92	21.43	54.71
Na <sub>2</sub> O	0.06	0.09	0.12	0.14	0.11
K <sub>2</sub> O	0.05	0.06	0.00	0.06	0.06
TiO <sub>2</sub>	0.10	0.02	0.05	0.05	0.01
P <sub>2</sub> O <sub>5</sub>	0.34	1.73	2.28	2.29	0.42
MnO	3.82	6.75	4.25	5.90	0.21
Total	48.12	50.04	60.24	73.71	56.53

## Rare earth elements

La	9536	4444	8436	334	216
Ce	11129.98	8908.18	13342.97	2575.12	408
Pr	744.01	732.69	1016.32	459.39	28
Nd	1588	1758	2326	1760	136
Sm	118.4	151.8	200	213.2	21
Eu	26	37	53.80	53.40	6
Gd	60.71	92.48	153.36	147.6	16
Dy	34.4	62.4	139.2	133.6	12
Ho	6.6	11.8	28.4	29.4	2
Er	1.69	17.1	54.53	71.31	5
Yb	12.40	18	39.4	37.6	4
Lu	2	2	4	4	0.4
(La/Yb) <sub>N</sub>	512	164	142	5.9	30
Sum	23260.19	16235.45	14579.98	5818.62	864.4

Major oxides in wt %, rare earth elements in ppm.

Analysis by ICP.

v) The major element totals are low. This suggests the presence of elements that were not analyzed for. These will include  $\text{CO}_2$ , trace elements such as barium and strontium and some REEs, for example lanthanum and cerium. Sample KG-69 has the lowest major element total, but the sample contains the highest barium and strontium contents and also the highest REE content compared to the other samples.

vi) The distribution of  $\text{P}_2\text{O}_5$  seems to increase with depth, whereas  $\text{Fe}_2\text{O}_3\text{T}$ ,  $\text{CaO}$  and  $\text{MnO}$  do not significantly change along the sampling profile. Their contents are within the ferrocarnatite ranges quoted by Woolley and Kempe (1989).

### 8.6.3 Normalized REE distribution patterns.

Normalized REE distribution patterns from the Kuge carbonatite centre are illustrated in Figure 8-3 (chondrite values taken from Nakamura, 1974). Kuge is also characterized by relatively steep patterns and high LREEs, typical of carbonatites. Sample KG-76 is unusual in its LREE distribution pattern, which shows positive anomalies in cerium, praseodymium and neodymium. The negative erbium anomaly shown by sample KG-69 is most likely due to analytical error. Both the petrography and X-ray diffractometer studies on KG-76 reveal the same mineralogical compositions as other samples within the same sampling profile. Sample KG-69, which was taken towards the top of the drill hole (KG-2), has the highest LREE ( $\text{La}+\text{Ce}+\text{Nd}$ ) content and also a large increase in the  $(\text{La}/\text{Yb})_{\text{N}}$  ratio (512) compared to samples selected from the lower sections of the same drill hole (compare KG-76). It is also important to note that KG-69 is slightly depleted in MREEs compared to KG-71, KG-72 and KG-76, which are directly below sample KG-69.

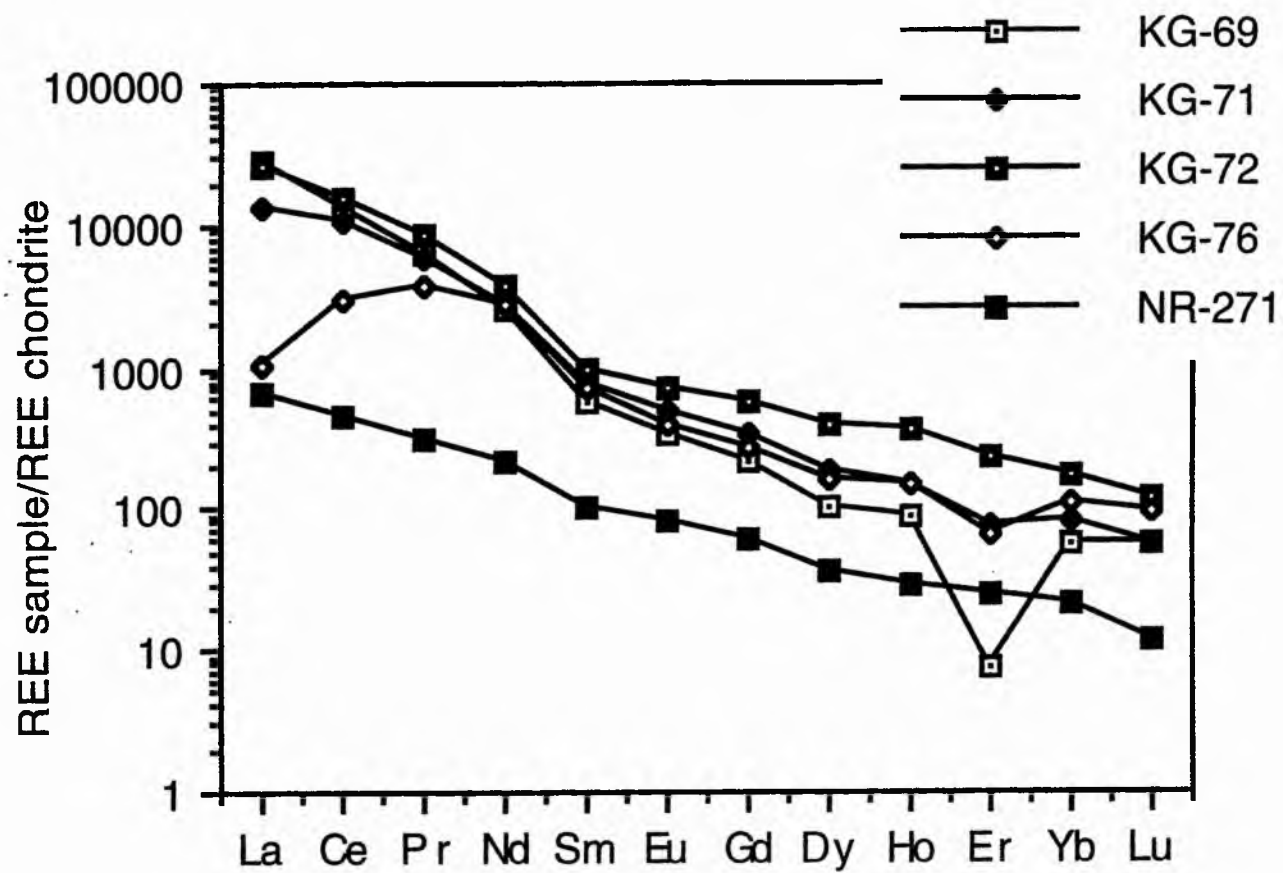


Figure 8-3 Chondrite-normalized REE distribution patterns for the Kuge carbonatite.

## 8.7 DISCUSSION OF RARE EARTH ELEMENT ABUNDANCES AND DISTRIBUTION PATTERNS AT THE BURU AND KUGE CENTRES.

### 8.7.1 Introduction.

The enrichment in REEs, especially the LREEs, is characteristic of carbonatites (Heinrich, 1966, Loubet et al., 1972, Möller et al., 1980 and Woolley and Kempe, 1989). They contain the highest LREE:HREE (La:Lu) ratios of any igneous rocks. High and steep LREE distribution patterns observed in the Buru and Kuge volcanic carbonatites are also typical of carbonatites worldwide (Nelson et al., 1988, Woolley and Kempe, 1989). High REEs, especially the LREEs in carbonatites, have been reported by many workers (for example Möller et al., 1980, Andersen, 1986, 1987, Lottermoser, 1990, Woolley et al., 1991, Ngwenya, 1994 and Wall and Mariano, 1996).

In some areas anomalous concentrations of REE are often sufficiently high to produce rare earth minerals of potential commercial interest, such as those currently found in Mountain Pass, California, and Bayan Obo, Inner Mongolia, China. Another characteristic aspect of REEs in carbonatites is the transformation of a carbonatite protolith to a lateritic regolith during tropical weathering, with significant ore concentrations such as those currently being worked in Brazil, Africa and Australia.

The REEs in carbonatites have been observed to show a progressive increase from early to late carbonatites (Barber, 1974, Le Bas 1977, 1989). In most cases this trend is accompanied by a well defined rock compositional sequence, where the early stage carbonatites are represented by calcite carbonatite followed by dolomite carbonatite and finally by ferrocarbonatite.

The compositional sequence as proposed by Barber and Le Bas and other authors elsewhere is clearly an over-simplification because the sequence is rarely observed in many of the carbonatites studied (Wall and Mariano, 1996).

The brecciated carbonatite in Buru, dominated by calcite, is entirely REE mineralized and could certainly be classified as a "late REE-rich carbonatite" (compare Wyllie et al., 1996 and Wall and Mariano, 1996). The REE mineralized carbonatite in Buru does not appear to represent an earlier carbonatite stage, whereas the siderite dyke is clearly a later phase based on its intrusive nature. It is interesting to note that the siderite dyke has slightly less REEs than the brecciated carbonatite, which is contrary to the observed progressive increase of REE from early-stage carbonatites to late-stage carbonatites, an observation which reinforces the idea that late calcite carbonatites can also be host to rare earth minerals.

#### 8.7.2 Factors governing the behaviour and distribution of REEs.

Researchers in the past have speculated on the factors that govern the behaviour and the distribution of REEs in carbonatites by invoking a combination of petrological and geochemical factors. Balashov and Pozharitskaya (1968) suggested that temperature and alkalinity were the main factors that controlled the behaviour and hence the distribution of REEs. They showed that a decrease in temperature and alkalinity towards late carbonatites could explain the enrichment of late carbonatites with REEs and a predominance of fluorocarbonates over other rare earth minerals. Eby (1975) explained the distribution of REEs in the Oka carbonatite complex in terms of relative proportions of calcite and apatite. He showed that samples with high apatite contents had higher REE contents.

The mineralogy of REEs also depends on the chemistry of the parent magma. Mariano (1989b) showed that the presence of phosphates in the parent magma could lead to early precipitation of monazite, even in the presence of large amounts of carbonates. The observation of Mariano (1989b) might not be applicable to a number of carbonatite occurrences where both monazite and fluorocarbonates coexist, such as Kangankunde in Chilwa Island, Malawi (Wall and Mariano, 1996), and Buru and Kuge, the present study areas. It appears that speciation of REEs depends on the relative proportions of carbonate, fluoride or phosphate, the three dominant ligands associated with carbonatites and, in the case of the Buru and Kuge carbonatite centres or Kangankunde where both fluorocarbonates and phosphates occur together, the writer suggests that after crystallization of monazite there was still enough REEs left in the fluids to precipitate fluorocarbonates at progressively lower temperatures.

### 8.7.3 Transport of REEs.

Numerous studies have provided petrological and compositional evidence for and against the mobility of REEs in various environments (magmatic, hydrothermal and supergene), as detailed in Grauch (1989). The REEs are clearly soluble and mobile in aqueous solution under some conditions. Experimental measurements on the complexing constants of REEs (e.g. Cantrell and Byrne, 1987 and Lee and Byrne, 1992, 1993) reveal the strong tendency of the REEs to form aqueous complexes at room temperature. Wood (1990a) and Millero (1992) provide detailed reviews on the complexing of REEs in the presence of various ligands at 25°C and 1 bar.

Experimental studies on the complexation of REEs in the presence of various ligands in high temperatures are lacking. In the absence of sufficient experimental data at higher temperatures, several theoretical attempts have

been made to predict the behaviour of REEs, especially in hydrothermal solutions, by Wood (1990b) and Haas et al. (1995). These authors have shown that  $\text{Cl}^-$ ,  $\text{F}^-$ ,  $\text{OH}^-$ ,  $\text{CO}_3^{2-}$ ,  $\text{SO}_4^{2-}$  or  $\text{PO}_4^{2-}$  are potential ligands with which REEs form soluble complexes that facilitate their transport in solution. Haas et al. (1995) suggested that at higher temperatures REE chlorides are dominant under acidic conditions, REE fluorides under neutral conditions and REE hydroxides under basic conditions. At lower temperatures and pressures, sulphate and carbonate complexes account for a larger fraction of the REEs in solution. In high temperature fluids, REE carbonate complexes have been found to be generally of little importance, as shown by the calculations of Haas et al. (1995). Wood (1990b) has also shown that carbonate complexes of REEs only form in near-neutral to basic conditions. Gieré (1996) has also suggested that speciation of the REE cations in hydrothermal fluids are strongly dependent on the relative concentrations of the possible ligands and on the pH of the solution.

The abundance and occurrence of REEs in the Buru and Kuge carbonatite centres attest to the major transport of REEs. It has been assumed in this study that the occurrence of barite and fluorite is believed to be indicative of hydrothermal processes. Goethite and associated manganese and iron hydroxides that dominate the upper sections, especially in the Buru carbonatite centre, are products of supergene alteration. The stable isotope studies (chapter 7) suggest a low temperature environment. The occurrence of REEs in the Buru and Kuge hills is therefore considered by the writer to be mainly of low temperature hydrothermal in origin, except for those found in the upper zones in the Buru and Kuge centres, which are thought to be concentrated by supergene processes. These REEs are either fluorocarbonates, phosphates or carbonates and their presence, particularly

below the weathering zone, is in accord with the REEs being transported as either carbonate, fluoride, phosphate or sulphate species.

The occurrence of these complexing species (carbonate, phosphate, fluoride and sulphate) together in the Buru and Kuge centres suggests that mixed carbonate-fluoride-phosphates complexes may be stable in this environment of low temperature and near-neutral conditions and could easily be candidates in transporting large amounts of REEs. Experiments on these mixed ligands, particularly in addressing their thermodynamic stability at various temperatures and pressures, are lacking and hence desired.

#### 8.8 FACTORS GOVERNING THE BEHAVIOUR OF RARE EARTH ELEMENTS DURING WEATHERING.

Although the REE behaviour during weathering processes has been extensively studied in a variety of weathering environments (Nesbitt, 1979, Alderton et al., 1980, Duddy, 1980, Tazaki et al., 1987, Braun et al., 1990 and Mongeli, 1993), there has been no unanimous agreement as to what extent elements are mobilized and fractionated during weathering processes. REE studies on weathering profiles, in particular those overlying carbonatite complexes, have been investigated by many workers, including Kamitani and Hirano (1987), Mariano (1989a, b) Lapin (1992, 1994), Lottermoser (1990, 1991), Walter et al. (1995b) and Morteani and Preinfalk (1996). The factors responsible for REE patterns in weathering profiles are complex and not well understood. According to Nesbitt (1979), the mobilization of REEs during weathering processes results from different factors related to the parent rock mineralogy and specifically to the distribution of the REEs in the primary bearing minerals, the stability of the minerals that develop and their ability to retain REEs in the weathering products.

Another factor which has an effect on REE separation in lateritic weathering is the capacity of HREEs to form more soluble complexes than the LREEs. The solubility of HREEs is enhanced by the formation of more stable complexes such as carbonate or fluoride (Cantrell and Byrne, 1987) and the result of this is that HREEs can stay longer in solution, which is characterized by elevated pH and alkaline conditions, and transported further away from where the LREEs precipitate. It is observed that LREEs are generally less mobile than HREEs, which consequently induces enrichment of LREE relative to HREE in the weathering profile and hence the high  $(La/Yb)_N$  ratio that is normally used to quantify this fractionation. This type of fractionation trend has been observed in both the Buru and Kuge carbonatite complexes.

The tendency for cerium ( $Ce^{3+}$ ) in an oxidizing environment to form  $Ce^{4+}$  helps the element to segregate from the other REE elements and form its own highly selective mineral, cerianite ( $CeO_2$ ). Cerianite is insoluble whereas other REEs which maintain the +3 ionic state are more soluble and can be transported by circulating fluids and hence contribute to the distribution of REEs. A few of the cerium anomalies on weathered profiles have been reported by Braun et al., (1990), Marsh (1991), Mongelli (1993) and Lapin (1994).

The significant observation obtained from the REE abundances, and in particular the REE distribution patterns from the two centres studied, is that samples from the most oxidized zones, especially in Buru and the supergene zone in Kuge, have consistently higher  $La+Ce+Nd$  contents and  $(La/Yb)_N$  ratios and are slightly depleted in MREEs than the carbonatite samples from the lower sections of the cores. Mariano (1989b) has also suggested that there is evidence of natural separation of REEs during hydrothermal and

weathering processes, which ultimately produces an enrichment in mid-atomic number REEs and yttrium in carbonatites.

Carbonatites from the Buru and Kuge centres are therefore noted to exhibit a pronounced fractionation of REEs with depth. Fractionation of REEs within the Buru and Kuge hills is also supported by the mineralogy and geochemical studies presented in chapters 5 and 6. It is suggested that the REEs are fractionated and distributed within the weathering profile between the different secondary minerals as a result of weathering processes, whereas below the weathering profile fractionation occurs through the complexing agents, such as carbonates, fluorides and sulphate, that are available for REE mobilization. The formation of cerianite in the weathering environment can also influence the fractionation of some REEs and hence control their distribution.

Amorphous and poorly crystalline compounds comprising of various contents of iron, manganese, barium and silicon are very common in weathering profiles and some of them can act as scavengers, which may also have an effect on the REE complexation and fractionation, as observed by Lottermoser (1995) and Walter et al. (1995b). These poorly crystalline compounds are very common, especially in Buru, but they do not contain any detectable REEs as discussed later in this chapter.

## 8.9 RARE EARTH MINERALS IN BURU CARBONATITE CENTRE.

### 8.9.1 Introduction.

Electron microprobe and scanning electron microscope (SEM) studies were carried out on selected samples from Buru hill to identify the rare earth minerals which are host to the REEs. Samples BR-206, BR-3 and BR-208 are representative of the laterite, whereas samples BR-12, BR-16 and BR-27 are representative of the lower sections of the carbonatite core, where supergene processes are minimal. The samples selected are all obtained from drill hole BRL-1.

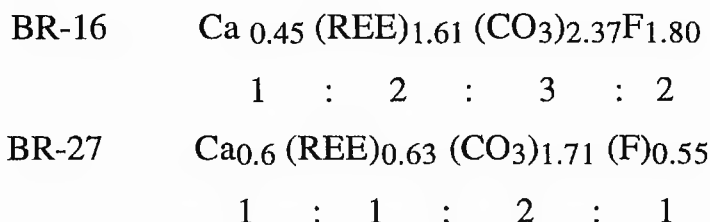
### 8.9.2 Rare earth bearing minerals in the Buru carbonatite.

Selected electron microprobe analyses of rare earth minerals (fluorocarbonates) are shown in Table 8.4a. The most common fluorocarbonate encountered include bastnäesite and the chemically analogous minerals of parisite and synchysite, represented by the formulae  $(\text{REE})(\text{CO}_3)\text{F}$  for bastnäesite,  $\text{Ca}(\text{REE})_2(\text{CO}_3)_3\text{F}_2$  for parisite and  $\text{Ca}(\text{REE})(\text{CO}_3)_2\text{F}$  for synchysite. The fluorocarbonate in samples BR-206, 208 and 12 conforms well to the generally accepted formula for bastnäesite -  $(\text{REE})(\text{CO}_3)\text{F}$ :

BR-206	$\text{Ca}_{0.1}(\text{REE})_{0.51}(\text{CO}_3)_{0.9}(\text{F})_{0.62}$ .
	1 : 1 : 1
BR-208	$\text{Ca}_{0.11}(\text{REE})_{0.70}(\text{CO}_3)_{0.80}(\text{F})_{0.73}$
	1 : 1 : 1
BR-12	$\text{Ca}_{0.15}(\text{REE})_{0.68}(\text{CO}_3)_{0.90}(\text{F})_{0.58}$ .
	1 : 1 : 1

The fluorocarbonate mineral in samples BR-16 is close to the accepted formula for parisite [ $\text{Ca}(\text{REE})_2(\text{CO}_3)_3\text{F}_2$ ], whereas the mineral in BR-27

corresponds well to the formula of synchysite  $[\text{Ca}(\text{REE})(\text{CO}_3)_2\text{F}]$ , as illustrated below.



The following features are revealed by examining Table 8-4a:

- i) The major rare earth fluorocarbonate minerals in the Buru carbonatite centre are dominantly bastnäesite, synchysite and parisite.
- ii) The rare earth fluorocarbonates in Buru are LREE selective and, according to the terminology proposed by Bayliss and Levinson (1988), the species names bastnäesite (Ce), parisite (Ce), and synchysite (Ce) are applicable to the identified rare earth minerals.
- iii) Samples BR-206 and BR-208, which are characterized by the absence of carbonate minerals (calcite and siderite), are dominated by bastnäesite whereas BR-27, dominated by calcite, siderite and strontianite, is dominated by synchysite over bastnäesite.

Another rare earth-carrying mineral in the Buru carbonatite centre is monazite (Table 8-4b).

- i) The monazite from the Buru hill carbonatite is also (Ce) selective.
- ii) Monazite has a slightly higher CaO content compared to monazites reported elsewhere (Wall and Mariano, 1996).
- iii)  $\text{ThO}_2$  content of around 1% in the Buru samples is slightly lower than an average of 1.8% of monazite from 14 carbonatites (Overstreet, 1967).
- iv) Low totals in the monazite might suggest the substitution of REEs within its crystallographic structures by both calcium and thorium.

Table 8-4a Selected electron microprobe analyses of fluorocarbonates from Buru.

Sample	BR-206	BR-208	BR-12	BR-16	BR-27
Depth(m)	23	35	101	130	197
CaO	3.88	2.63	4.7	5.95	13.62
FeO	3.25	0.39	0.1	0.81	1.24
La <sub>2</sub> O <sub>3</sub>	17.27	11.16	28.87	12.66	14.32
Ce <sub>2</sub> O <sub>3</sub>	24.94	50.94	27.41	25.49	20.66
Pr <sub>2</sub> O <sub>3</sub>	1.64	1.63	1.55	2.47	1.20
Nd <sub>2</sub> O <sub>3</sub>	4.60	4.08	3.03	8.92	4.44
Sm <sub>2</sub> O <sub>3</sub>	0.34	0.13	0.11	1.26	0.25
Yb <sub>2</sub> O <sub>3</sub>	0.03	0.03	0.07	0.12	0.04
ThO <sub>2</sub>	4.94	0.37	0.43	6.42	0.19
F	7.27	7.23	6.30	7.34	4.18
O=F	3.06	3.05	2.65	3.09	1.76
Total	66.36	75.92	70.40	69.45	58.52
CO <sub>3</sub>	33.64	24.08	29.60	30.55	41.48
Formula calculated on the basis of 4O (BR-206, 208, 12), 11O (BR-16) and 7O (BR-27).					
Ca	0.07	0.10	0.15	0.49	0.60
Fe	0.03	0.01	0.00	0.05	0.04
Total	0.10	0.11	0.15	0.54	0.70
La	0.17	0.01	0.31	0.36	0.23
Ce	0.24	0.60	0.29	0.72	0.31
Pr	0.01	0.01	0.01	0.07	0.02
Nd	0.04	0.04	0.03	0.25	0.07
Sm	0.00	0.00	0.00	0.03	0.00
Yb	0.00	0.00	0.00	0.02	0.00
Y	0.02	0.01	0.01	0.05	0.00
Th	0.03	0.03	0.03	0.11	0.00
Total	0.51	0.70	0.68	1.61	0.63
CO <sub>3</sub>	0.90	0.80	0.90	2.37	1.71
F	0.62	0.73	0.58	1.80	0.55

Table 8-4b A representative electron microprobe analysis of monazite from Buru hill carbonatite.

Sample	BR-3
Depth (m)	31
CaO	2.64
FeO	1.55
La <sub>2</sub> O <sub>3</sub>	15.51
Ce <sub>2</sub> O <sub>3</sub>	23.76
Pr <sub>2</sub> O <sub>3</sub>	3.37
Nd <sub>2</sub> O <sub>3</sub>	10.73
Sm <sub>2</sub> O <sub>3</sub>	0.96
Yb <sub>2</sub> O <sub>3</sub>	0.17
Y <sub>2</sub> O <sub>3</sub>	0.85
ThO <sub>2</sub>	1.15
UO <sub>2</sub>	0.80
P <sub>2</sub> O <sub>5</sub>	26.19
Total	87.68

Formula calculated on the basis of 16O

Ca	0.49
Fe	0.23
La	1.00
Ce	1.53
Pr	0.22
Nd	0.67
Sm	0.06
Yb	0.01
Y	0.08
Th	0.05
U	0.03
Total	4.37
P	3.90

Oxides in wt %.

The chondrite-normalized patterns of rare earth minerals are illustrated in Figure 8-4 (chondrite values obtained from Wakita et al., 1971 and Taylor and MacLennan, 1985).

- i) Both the fluorocarbonates and the monazite are LREE selective.
- ii) Sample BR-208 from the supergene zone shows a positive Ce anomaly where  $Ce^{3+}$  has been oxidized to  $Ce^{4+}$ . Variations in the La+Ce contents (Table 8-3), especially in the oxidized zone, could suggest complex chemical reactions in this environment.
- iii) Monazite has a slightly higher rare earth content, particularly in the MREEs compared to the fluorocarbonates.

### 8.9.3 Rare earth-bearing minerals from the Kuge carbonatite.

Selected electron microprobe analyses of rare earth minerals from Kuge are shown in Tables 8-5 and 8-6, which show the following features:

- i) Rare earth carrying minerals in Kuge are characterized by the occurrence of phosphates (monazite) and fluorocarbonates. The fluorocarbonate is synchysite which is close to the general formula  $Ca(CeLa)(CO_3)_2(F)$  (Table 8-6).
- ii) Both types of rare earth mineral (the phosphates and the fluorocarbonates) are LREE selective and, like those from Buru, are also cerium dominated.
- iii) The Kuge monazites are enriched in  $ThO_2$  with values ranging from 0.85 to 2.12 wt% and an average of over 1.9%, which is more than twice the average of below 0.5% for the Kangankunde monazites (Wall and Mariano, 1996) and slightly more than the average of 1.8% for monazites reported by Overstreet (1967) from 14 different carbonatites. The fluorocarbonates from Kuge have lower thorium contents compared to monazite.

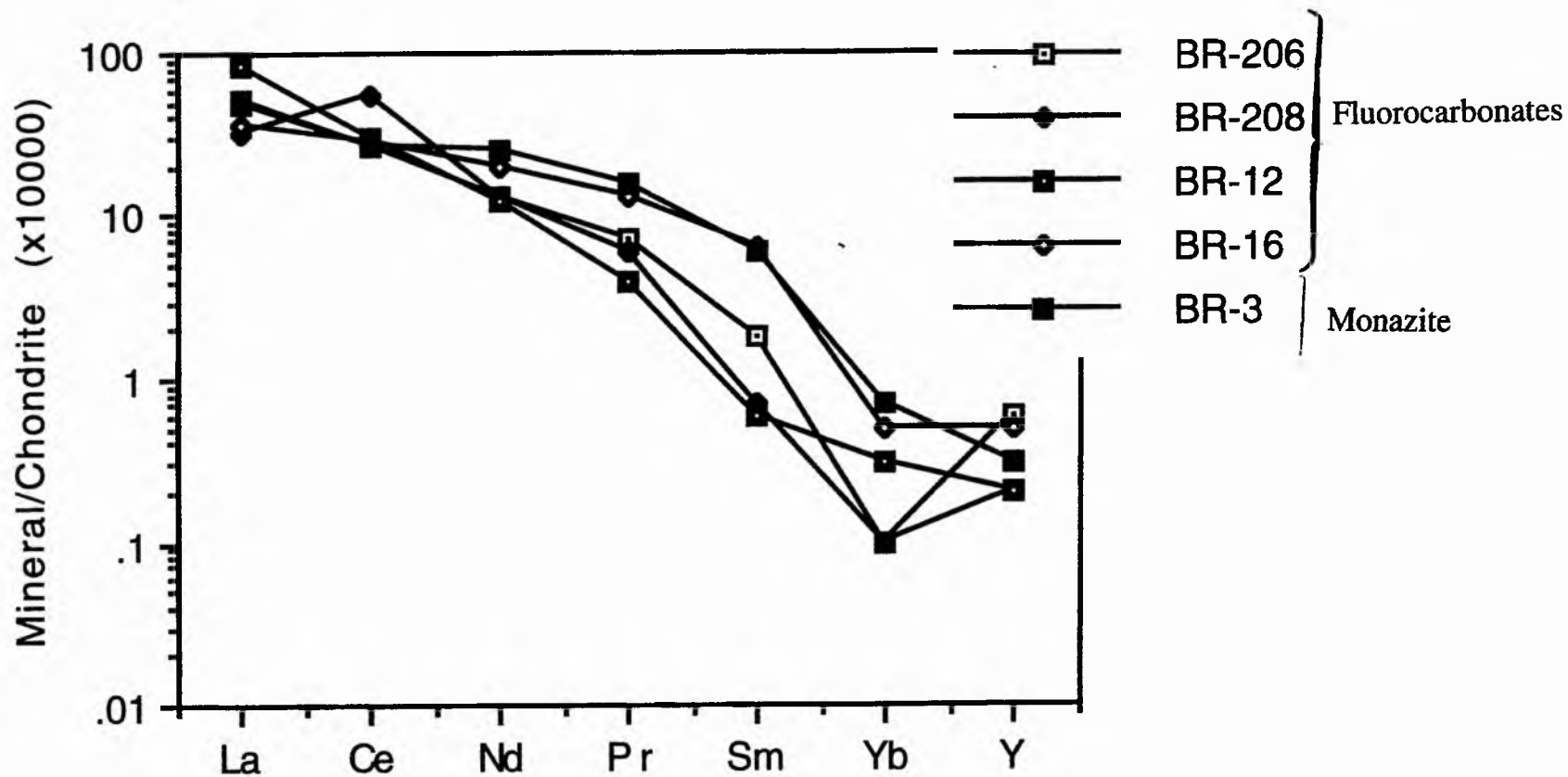


Figure 8-4 Chondrite-normalized plot of rare earth (RE) minerals from Buru.

Table 8-5 Selected microprobe analyses of monazite (Ce) from Kuge hill

Sample	KG-72	KG-76	KG-80	KG-94	KG-275
CaO	4.19	10.30	9.28	4.56	5.43
FeO	0.44	0.50	0.20	0.46	0.13
La <sub>2</sub> O <sub>3</sub>	16.37	14.73	14.44	13.99	14.02
Ce <sub>2</sub> O <sub>3</sub>	29.45	24.00	20.98	21.72	23.46
Pr <sub>2</sub> O <sub>3</sub>	2.16	1.56	1.83	1.88	2.39
Nd <sub>2</sub> O <sub>3</sub>	7.12	5.57	6.15	5.36	8.90
Sm <sub>2</sub> O <sub>3</sub>	0.19	0.44	0.70	0.44	1.26
Yb <sub>2</sub> O <sub>3</sub>	0.15	0.22	0.21	0.18	-
Y <sub>2</sub> O <sub>3</sub>	0.81	0.09	0.63	0.80	-
ThO <sub>2</sub>	1.67	2.85	1.88	2.12	1.07
UO <sub>2</sub>	0.09	-	0.14	0.23	0.09
P <sub>2</sub> O <sub>5</sub>	25.18	18.35	16.53	20.14	24.41
Total	87.46	78.25	72.97	71.88	81.16

Formula calculated on the basis of 16O

Ca	0.789	2.249	2.248	1.064	1.088
Fe	0.064	0.085	0.037	0.083	0.020
U	0.003	-	0.007	0.011	0.003
La	1.06	1.104	1.202	1.122	0.967
Ce	1.893	1.789	1.734	1.730	1.606
Pr	0.138	0.115	0.150	0.149	0.162
Nd	0.446	0.450	0.496	0.416	0.594
Sm	0.011	0.030	0.054	0.032	0.081
Yb	0.008	0.013	0.014	0.001	-
Y	0.075	0.009	0.075	0.092	-
Th	0.066	0.132	0.096	0.105	0.045
Total	4.553	5.931	6.113	4.815	4.701
P	3.747	3.166	3.163	3.713	3.868

Oxides in wt %, (-) below detection limit.

Table 8-6 Electron microprobe analyses of fluorocarbonates from Kuge hill.

Sample No.	KG-69	KG-256
CaO	10.85	11.90
FeO	0.51	0.32
La <sub>2</sub> O <sub>3</sub>	17.92	17.21
Ce <sub>2</sub> O <sub>3</sub>	21.02	25.75
Pr <sub>2</sub> O <sub>3</sub>	1.19	1.56
Nd <sub>2</sub> O <sub>3</sub>	3.73	4.62
Sm <sub>2</sub> O <sub>3</sub>	0.36	0.19
Yb <sub>2</sub> O <sub>3</sub>	0.09	0.02
Y <sub>2</sub> O <sub>3</sub>	0.05	0.05
ThO <sub>2</sub>	0.41	1.33
UO <sub>2</sub>	0.06	0.04
F	5.67	6.85
O=F	2.39	2.88
Total	59.47	66.96
CO <sub>3</sub> *	40.53	33.04
Formula calculated on the basis of 7O		
Ca	0.47	0.59
Fe	0.01	0.01
Total	0.48	0.60
La	0.28	0.29
Ce	0.32	0.43
Pr	0.02	0.02
Nd	0.06	0.07
Sm	0.01	0.00
Yb	0.00	0.00
Y	0.00	0.00
Th	0.00	0.01
U	0.00	0.00
Total	0.69	0.82
F	0.75	1.00
CO <sub>3</sub>	1.70	1.50

\* CO<sub>3</sub> inferred by difference.

iv)  $P_2O_5$  values ranging from 18.35 to 25.18% with an average of about 20 wt% for the monazites from Kuge hill is low compared to monazites reported elsewhere (Andersen, 1986, Lottermoser, 1990 and Wall and Mariano, 1996).

v) The Kuge monazites are also enriched in CaO contents, which range from 4.19 to 10.03 wt%.

vi) Substitution for REEs in their crystal structure by calcium and thorium will possibly account for the low total rare earth contents of monazite.

The chondrite-normalized plots of rare earth minerals from Kuge are shown in Figure 8-5. Both the Kuge monazites (represented by samples KG-72, KG-80 and KG-275) and synchysite (samples KG-69 and KG-256) are strongly enriched in LREEs, but the monazite appears to have slightly higher ratios in the middle rare earths.

#### 8.9.4 Apatite

Apatite is characteristic of carbonatites, commonly making 2-5% by volume (Hogarth, 1989). According to Mariano (1989b), apatite is the most widespread accessory mineral in early and intermediate stage carbonatites. An unknown mineral identified from Buru and Kuge volcanic centres (Table 8-7) has CaO and  $P_2O_5$  close to that expected for apatite except for extremely high values of fluorine.

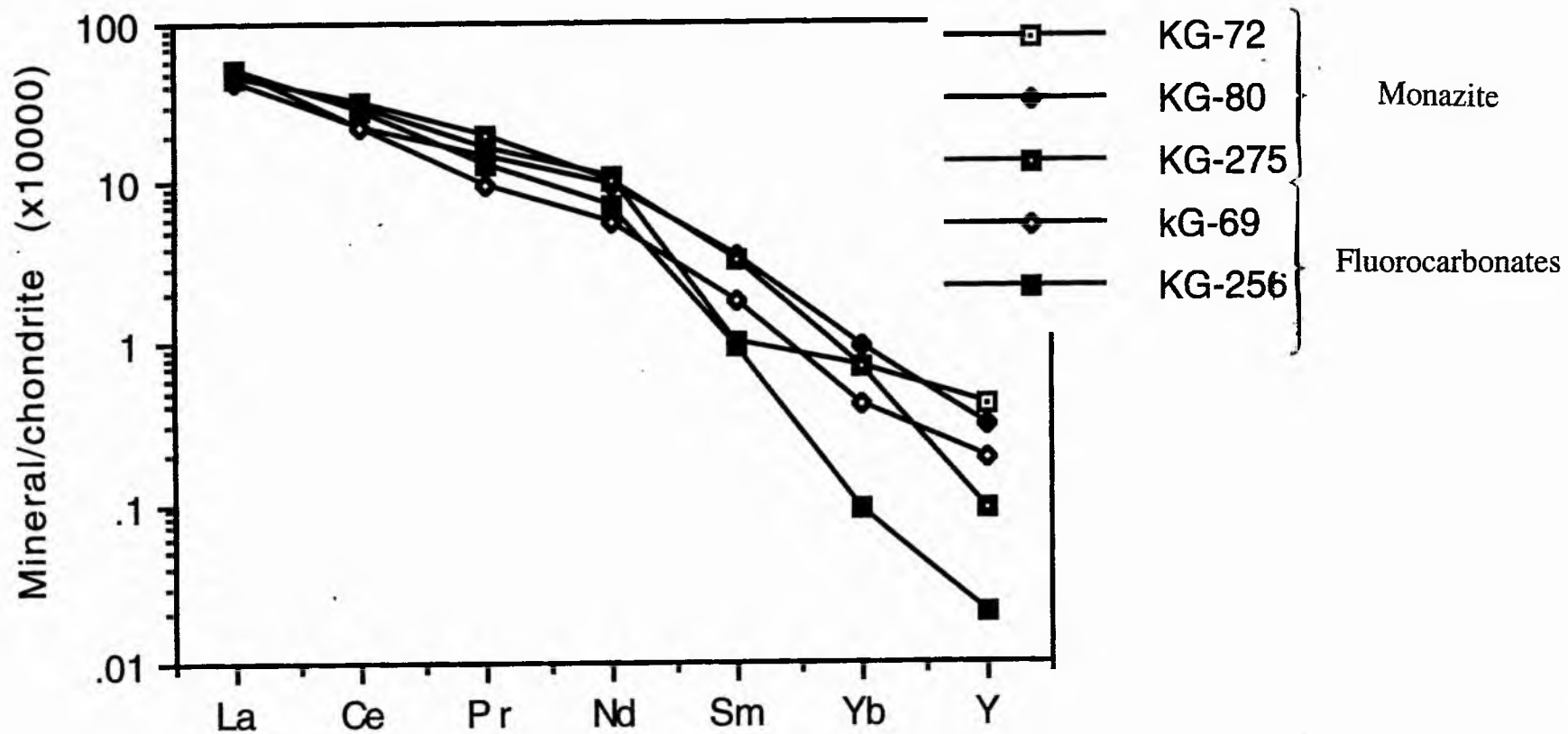


Figure 8-5 Chondrite-normalized plot of rare earth (RE) minerals from Kuge.

Table 8-7 Electron microprobe analyses of an unknown mineral.

Sample	Buru hill	Kuge hill
SiO <sub>2</sub>	0.10	0.12
Al <sub>2</sub> O <sub>3</sub>	0.05	1.63
FeO	1.22	0.38
MnO	0.70	0.03
MgO	0.03	0.23
P <sub>2</sub> O <sub>5</sub>	32.04	30.00
CaO	42.87	43.87
BaO	0.15	0.65
SrO	2.54	0.69
F	21.06	21.09
O=F	8.86	8.88
TREO	0.01	1.38
Total	91.91	91.19
Formula calculated to 26 O		
Si	0.018	0.021
Al	0.011	0.337
P	4.685	4.452
Z total	4.714	4.810
Fe	0.176	0.056
Mg	0.008	0.060
Mn	0.102	0.004
Sr	0.254	0.070
Ba	0.010	0.045
Ca	7.934	8.241
A total	8.685	8.476
F	11.504	11.693

However, in the ideal formula for apatite  $[\text{Ca}_5(\text{PO}_4)_3(\text{OH}, \text{F}, \text{Cl})]$ , fluorine, chlorine and hydroxyl ions replace each other to form almost pure end-members (Deer et al., 1992). The rare earths can also replace and be accommodated in the sites occupied by the  $\text{Ca}^{2+}$  ions. High values of fluorine in the unknown mineral observed in both Buru and Kuge is, however, not easy to explain. The writer suggests that the unknown mineral could have been apatite and during low temperature hydrothermal and processes, it decomposed and lost most of the rare earths. This process may involve an increase in fluorine in the apatite structure. The apatite presented in Table 8-8 from the calcite carbonatite from North Ruri, which has not suffered much from weathering processes, has less than 1% fluorine. The high Sr:Mn ratio noted in the sample from Buru is characteristic of carbonatites (Hogarth, 1989).

The mineral shown in Table 8-7 from Buru and Kuge is, however, seen to contain minimal rare earth elements compared to the apatite from the North Ruri carbonatite complex shown in Table 8-8. The mineral (fluorapatite?) from the supergene zones at the Buru and Kuge carbonatite centres may have lost most of the rare earths it contained during low temperature processes. The apatite shown in Table 8-8 from the Ruri hills contains the bulk of the rare earth minerals because weathering has not been intense enough compared to the Buru and Kuge centres to release the REEs from the apatite sites. It is also possible that small grains of the mineral fluorite ( $\text{CaF}_2$ ) could have been analyzed by the electron microprobe but the similarities in the analyzed contents from the two centres do not suggest analytical error.

Table 8-8 Electron microprobe analyses of REE-rich apatite and fluorocarbonate from sample NR-271 (calcite carbonatite).

	A	B
CaO	26.63	7.60
FeO	0.07	0.00
P <sub>2</sub> O <sub>5</sub>	25.12	0.21
La <sub>2</sub> O <sub>3</sub>	17.09	20.48
Ce <sub>2</sub> O <sub>3</sub>	10.74	24.81
Pr <sub>2</sub> O <sub>3</sub>	2.06	3.80
Nd <sub>2</sub> O <sub>3</sub>	4.04	12.22
Sm <sub>2</sub> O <sub>3</sub>	0.03	0.99
Yb <sub>2</sub> O <sub>3</sub>	0.00	0.00
Y <sub>2</sub> O <sub>3</sub>	0.76	0.00
ThO <sub>2</sub>	0.05	0.00
UO <sub>2</sub>	0.00	0.24
F	0.62	3.17
F=O	0.26	1.34
Total	86.95	72.18

Analysis A = apatite which is enriched in lanthanum rather than cerium.

Analysis B = fluorocarbonate (cerium selective).

## 8.10 THE OCCURRENCE OF RARE EARTH MINERALS IN THE BURU AND KUGE CARBONATITES.

### 8.10.1 Introduction.

According to Mariano (1989b) and Wall and Mariano (1996), REEs in the early carbonatites are usually hosted by the rock-forming minerals apatite and calcite and by accessory phases such as pyrochlore, perovskite and sometimes monazite, which often forms at the end of apatite crystallization.

The bastnäesite-parisite mineralization at Mountain Pass is a unique and rare occurrence in which the rare earth minerals are primary phases in a late stage carbonatite. Wyllie et al. (1996) have experimentally demonstrated that the rare earth fluorocarbonates and calcite could precipitate together from a primary melt. Mountain Pass is therefore the only example known in the world where rare earth minerals are produced by primary crystallization from a carbonatite magma.

The majority of the REEs are, however, hosted in late carbonatites, where the greatest abundance of rare earth minerals are also found and where they appear to have been introduced by late stage magmatic or hydrothermal processes (Mariano, 1989b). The rare earth minerals are observed to occur in a wide variety of geological environments ranging from veinlets, interstitial fillings, fine-grained polycrystalline aggregates or large-scale metasomatic bodies (Le Bas, 1989, Mariano, 1989b and Gieré, 1996). A large number of hydrothermal rare earth minerals have been reported: the most common ones are monazite, bastnäesite, parisite, synchysite, britholite, florencite and allanite (Mariano, 1989a, b and Gieré, 1996). These hydrothermal rare earth minerals are usually accompanied by barite, fluorite, strontianite, hematite and quartz (Le Bas, 1989 and Mariano, 1989b).

Rare earth minerals are also formed during the weathering of carbonatites where the chemical breakdown of primary minerals, for example apatite, calcite or dolomite, releases REEs and, together with any rare earth minerals from the fresh rock, may become concentrated in the weathering products (laterite). According to Mariano (1989b), large quantities of supergene rare earth minerals can be produced in tropical climates with

moderate to high rainfall and in those complexes where interior drainage and basin-type topography traps residuum from decalcified carbonatite.

The above description of both REEs and rare earth minerals being hosted by apatite or calcite in primary carbonatites and consequently released during weathering processes, is clearly seen in sample NR-271 from the North Ruri carbonatite complex. The sample has the typical mineralogy of calcite carbonatites in which rhombohedral calcite, magnetite and apatite minerals predominate (Plate 7-11). Strontium, as expected, is higher than barium (7620 ppm and 666 ppm, respectively). The sample and has  $\delta^{13}\text{C}$  and  $\delta^{18}\text{O}$  values of -4.2 and +11.0, respectively. The carbon and oxygen isotope values plot close to the primary high temperature carbonatites within the 'carbonatite box', although the values do indicate a slight overprint by low temperature hydrothermal fluids. The electron microprobe analyses of the REEs (Table 8-8) clearly indicate that they are hosted by apatite and also that the calcite carbonatite contains rare earth minerals (fluorocarbonates). The apatite crystals and fluorocarbonate analysed are shown in Plates 8-1 and 8-2.

### 8.11 DISCUSSION.

In the Buru carbonatite centre, rare earth bearing minerals identified include the fluorocarbonate group of minerals (bastnäesite, parisite and synchysite), and monazite. The most abundant rare earth mineral was found to be the bastnäesite with monazite and apatite occurring as accessory rare earth mineral phases. Apatite was also found to contain extremely low rare earth minerals within the supergene zones. From the above introduction, rare earth minerals can concentrate in a wide variety of geological settings and under variable physico-chemical conditions. An opportunity arises therefore in Buru where rare earth minerals found in

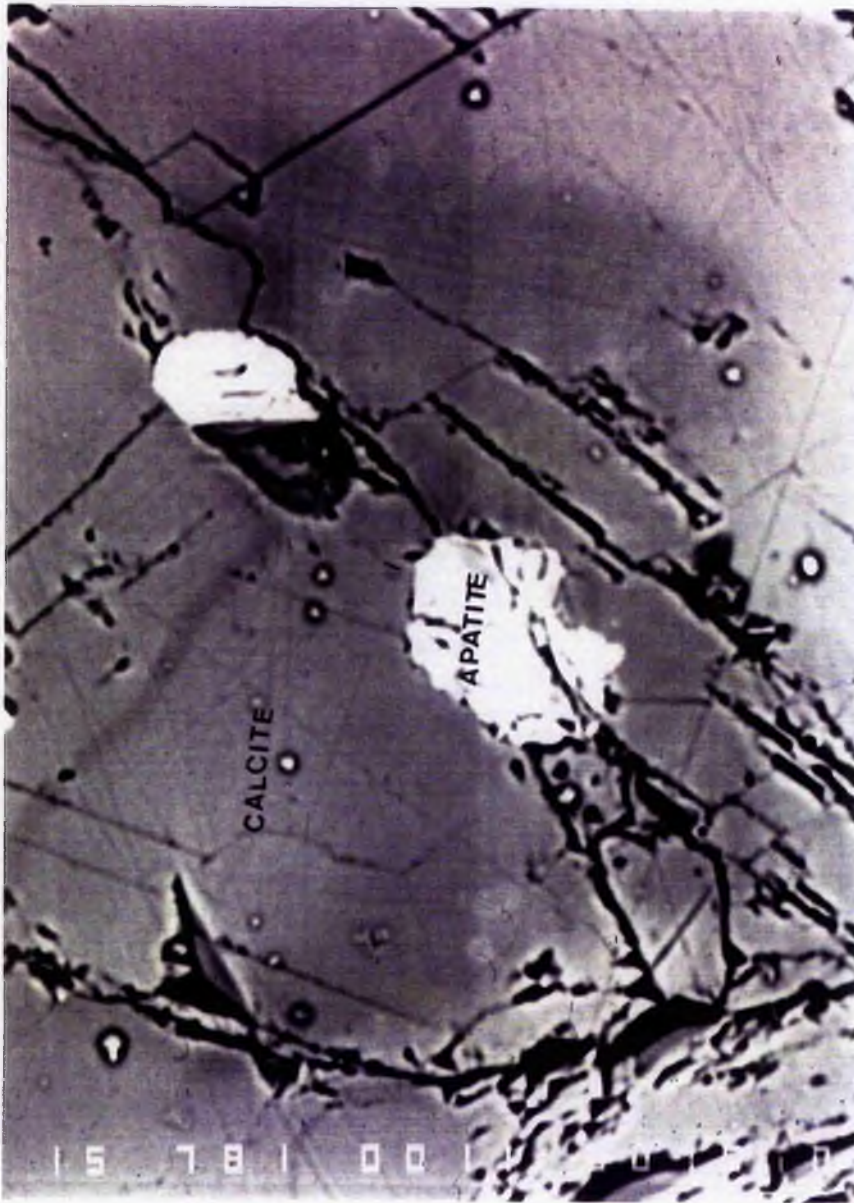


Plate 8-1 Backscattered electron (BSE) image showing rare earth containing apatite crystals from North Ruri carbonatite centre.  
Scale bar = 10  $\mu$  m.

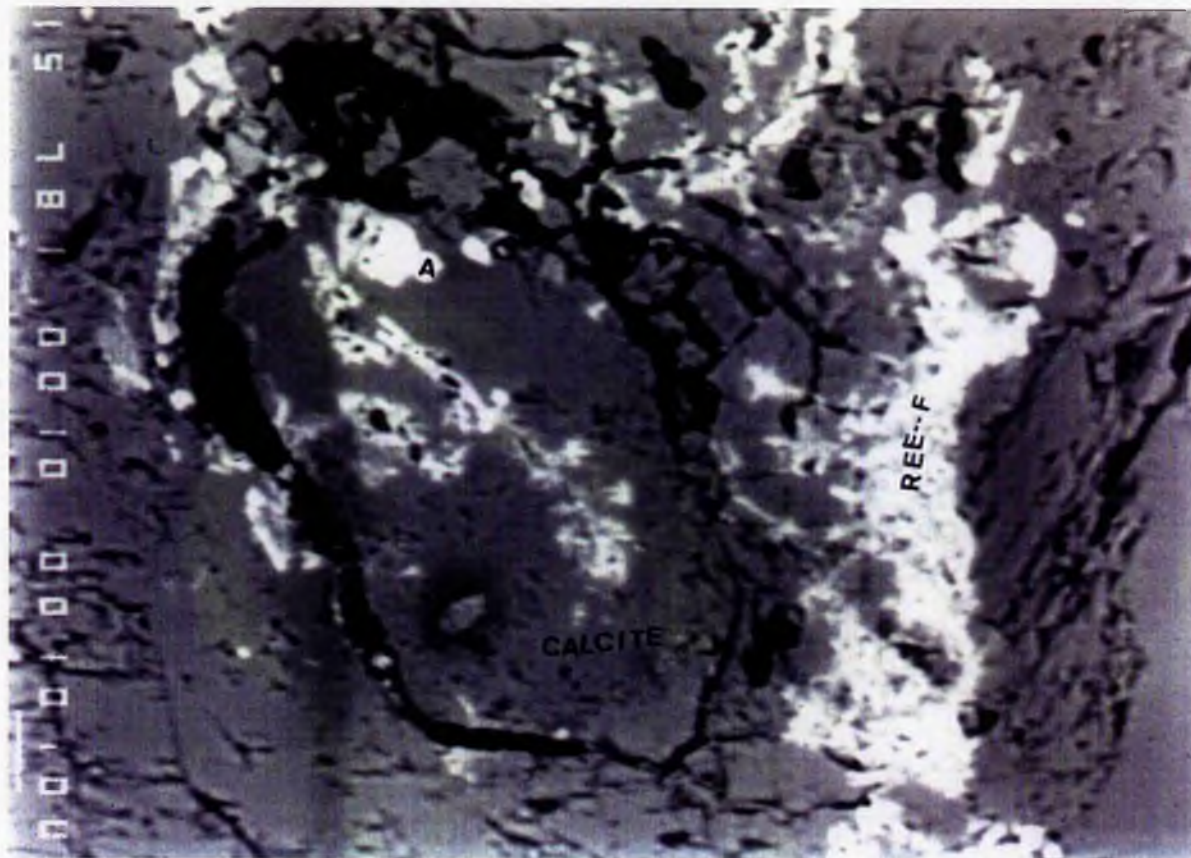


Plate 8-2 Backscattered electron image of calcite-carbonatite from North Ruri carbonatite centre with apatite (A) and RE - fluorocarbonate. Scale bar = 10  $\mu\text{m}$ .

both supergene and hydrothermal settings in the same deposit can be studied.

The back scattered electron (BSE) images of rare earth minerals within and below the weathering profile in Buru reveal interesting clues with respect to distribution, textural and age relationships. The fluorocarbonates in the supergene zone are mainly acicular in texture (Plate 8-3) or fibrous along the existing cavities, voids, fillings or fractures. These rare earth minerals commonly occur in association with complex Ba-Mn-Fe compounds, goethite, barite and fluorite. The fibrous texture is however the most common in both the laterite and fresh carbonatite (Plate 8-4). Monazite was detected occurring as euhedral grains in association with the same minerals as the fluorocarbonates. Both these minerals appear to occur as independent rare earth minerals. Below the weathering zone, where the hydrothermal processes dominate, the rare earth minerals (particularly the fluorocarbonates) are predominantly fibrous in texture and are observed exploiting the existing cavities within the earlier carbonate phases (Plate 8-5). The rare earth minerals are sometimes seen occurring as disseminated aggregates within either the calcite or siderite carbonate phases (Plate 8-6). Most of the rare earth minerals examined in the Buru carbonatite centre are secondary in origin, as observed from the cross-cutting relationships shown in Plate 8-7.

In Kuge, the monazite which is the most abundant rare earth mineral, occurs in clusters of euhedral, rounded grains, which often appear to be embedded in calcite (Plate 8-8) or is sometimes seen to occur as clusters within the existing cavities in association with calcite, barite and Ba-Mn compounds. The fluorocarbonates in Kuge are noted to occur as thin laths in some of the BSE images studied.

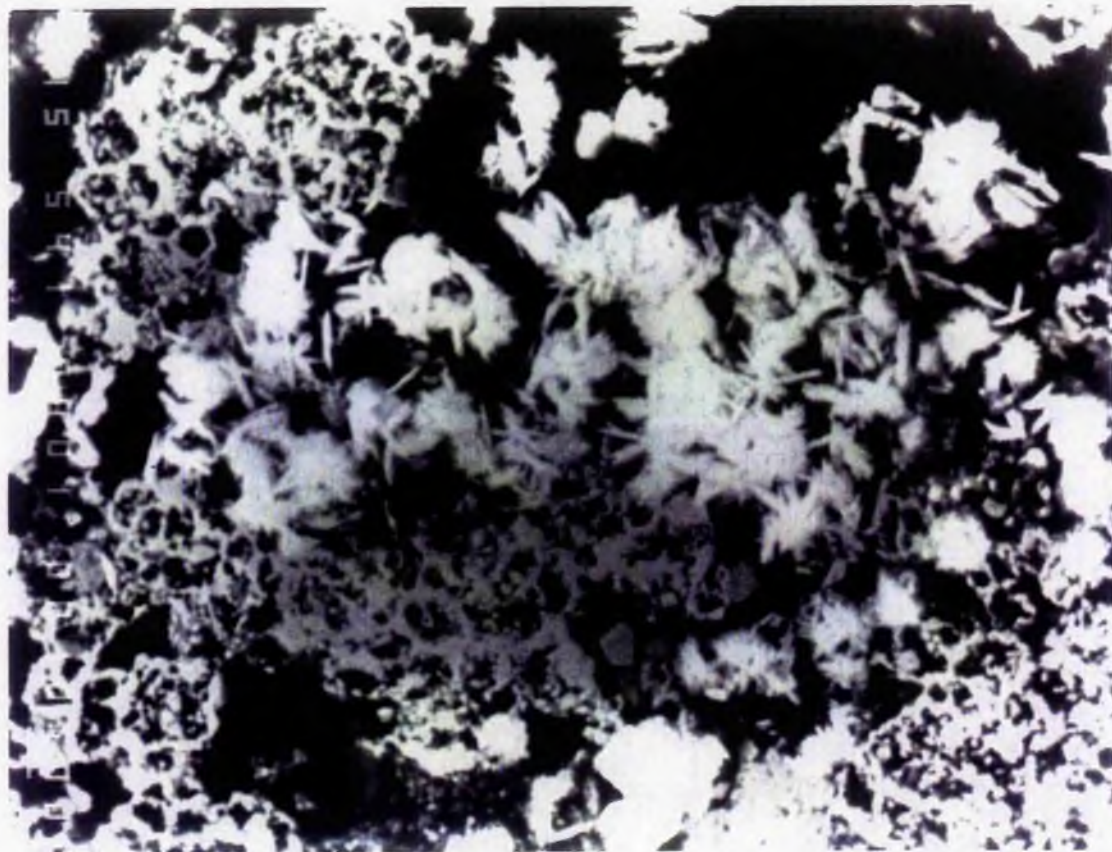


Plate 8-3 Backscattered electron image of acicular fluorocarbonates in lateritic zone - Buru carbonatite centre. Scale bar = 10  $\mu\text{m}$ .

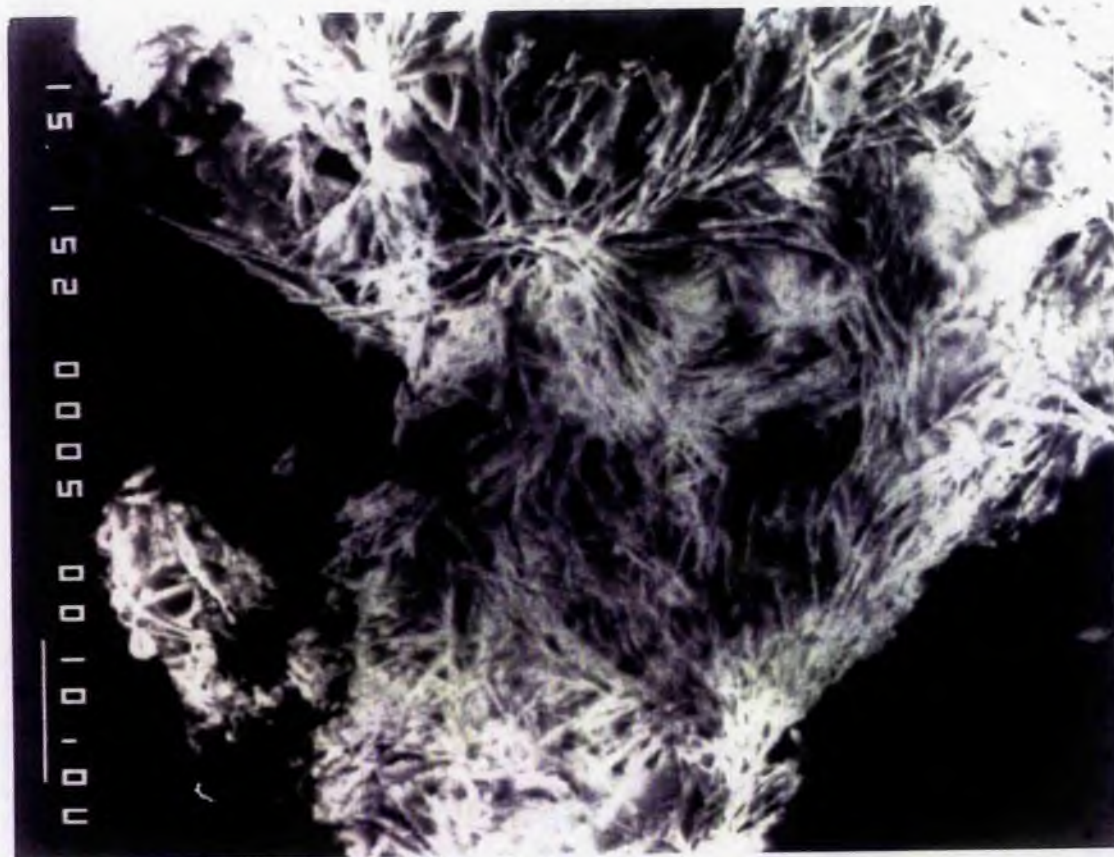


Plate 8-4 Backscattered electron image showing fibrous texture, the most common texture encountered in the fluorocarbonates.  
Scale bar = 10  $\mu\text{m}$ .

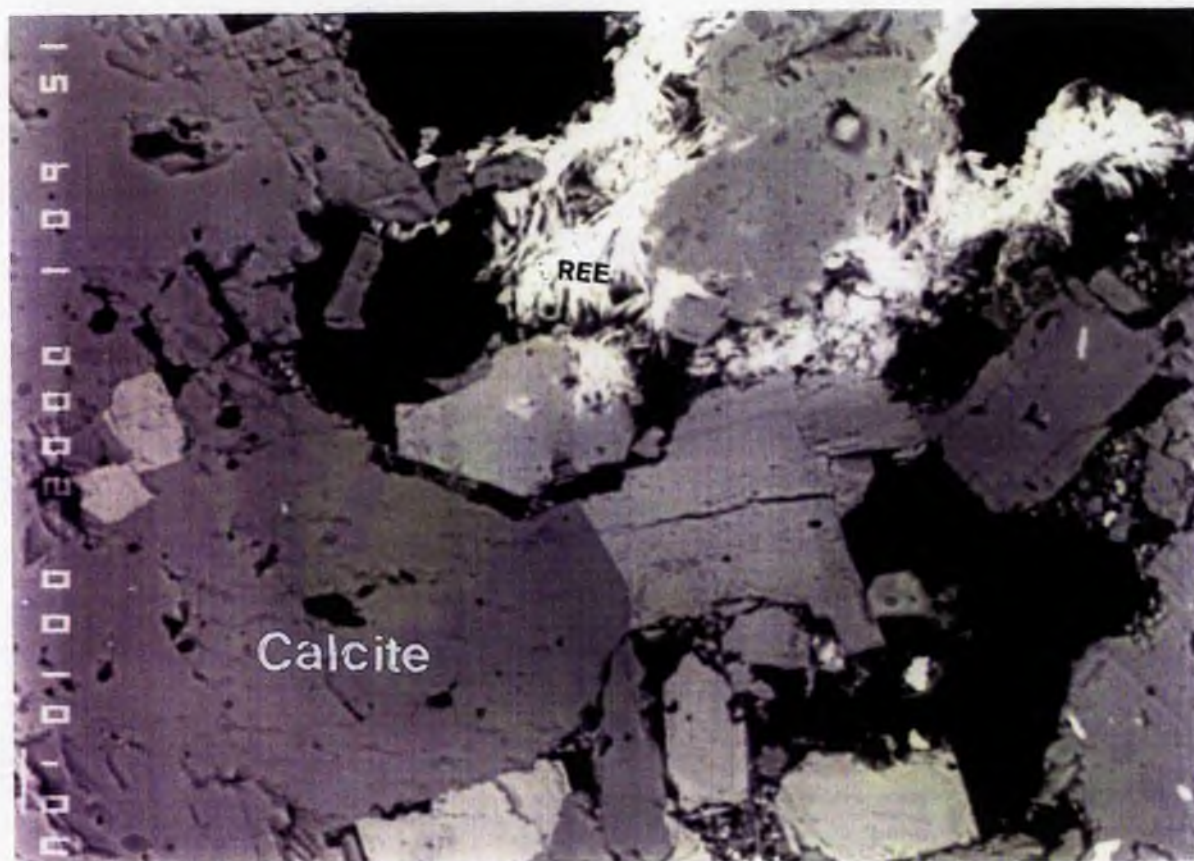


Plate 8-5 Backscattered electron image showing fibrous fluorocarbonates. The RE fluorocarbonates are seen exploiting earlier existing cavities within the carbonate phases - Buru carbonatite. Scale bar = 10  $\mu\text{m}$ .

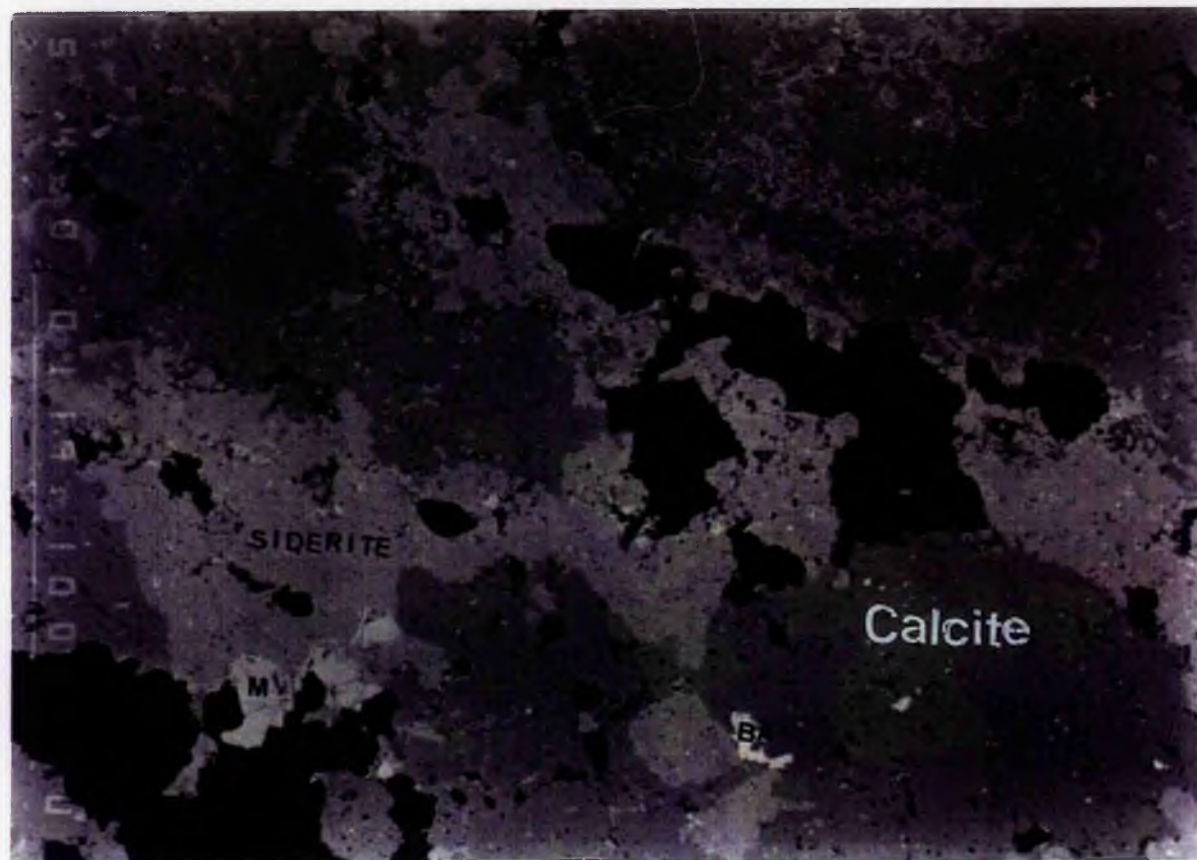


Plate 8-6 Backscattered electron image showing disseminated RE fluorocarbonates (white dots) in calcite and siderite carbonate phases at Buru hill. Magnetite (M) and barite (BA) are present. Scale bar = 1000  $\mu\text{m}$ .

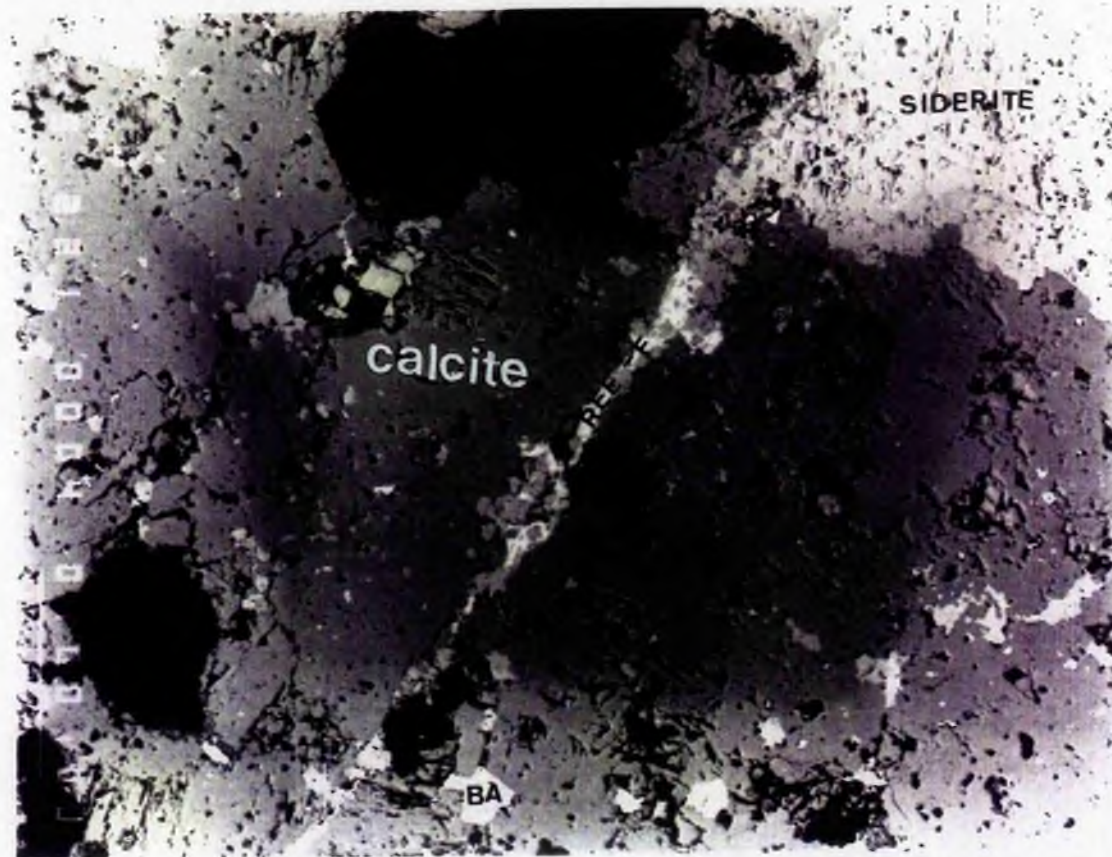


Plate 8-7 Backscattered electron image revealing the cross-cutting relationship of secondary fluorocarbonates from Buru carbonatite centre. Barite (BA) is also common in the micrograph. Scale bar = 100  $\mu\text{m}$ .

Scanning electron microscope (SEM) studies on both the Buru and Kuge carbonatite centres also indicates the presence of REE minerals. The main minerals identified by scanning a number of samples from the laterite of the Buru carbonatite are mainly fluorocarbonates (Plate 8-9 and Figure 8-6). Plate 8-9 also contains large areas of manganese mineral needles and goethite, which are characteristic of the carbonatite laterite in Buru, compared to Plate 8-10 selected from the lower sections of the Buru carbonatite, which shows rhombohedral calcite crystals. According to the energy-dispersive spectra, the rhombohedral calcite crystals are void of rare earth elements (Figure 8-7) Careful search for apatite or barite crystals during the SEM studies were not successful.

Supergene monazite was also identified in the Kuge carbonatite centre using SEM. The euhedral and globular monazite shown in Plate 8-11 reveals a complicated internal structure. The small rounded spheres on the monazite could possibly be cerianite. The corresponding energy dispersive X-ray (EDX) shown in Figure 8-8 shows that the monazite is cerium selective. The phosphate peak is blocked by sulphur.

#### 8.12 RARE EARTH MINERALS IN LATERITES OVERLYING CARBONATITE COMPLEXES.

Research on rare earth-bearing minerals in laterites overlying carbonatites has been investigated by various authors, including Mariano (1989a, b), Von Maravic et al. (1989), Lottomorser (1990, 1995), Walter et al. (1995) and Morteani and Preinfalk (1996). According to Mariano (1989b), the most important supergene rare earth mineral in carbonatites is monazite. Monazite is usually accompanied by bastnäesite, synchysite, pariste and the crandallite-group minerals, which includes florencite, gorceixite, goyazite and less commonly rhabdophane. In the Mt Weld carbonatite laterite, the

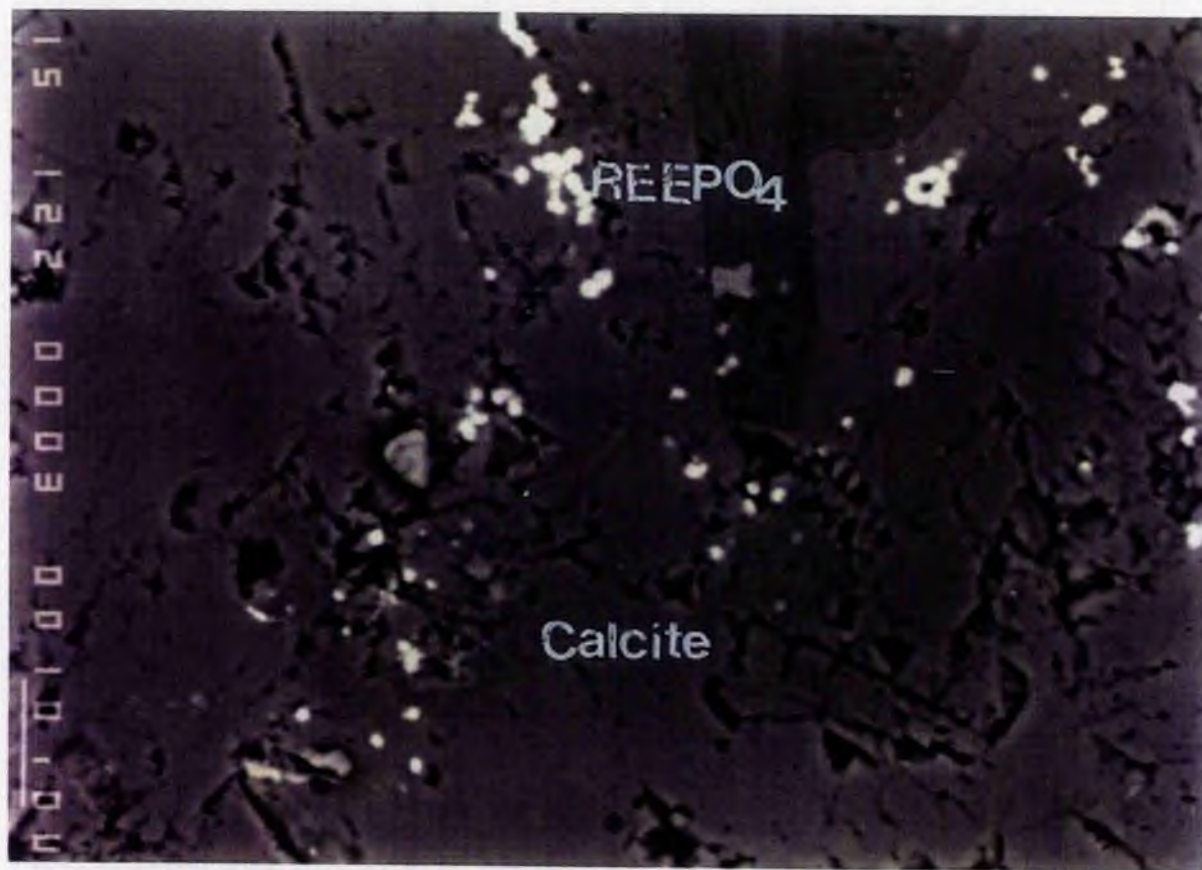


Plate 8-8 Backscattered electron image showing euhedral monazite (REEPO<sub>4</sub>) in calcite from Kuge carbonatite centre. Scale bar = 10  $\mu$ m.

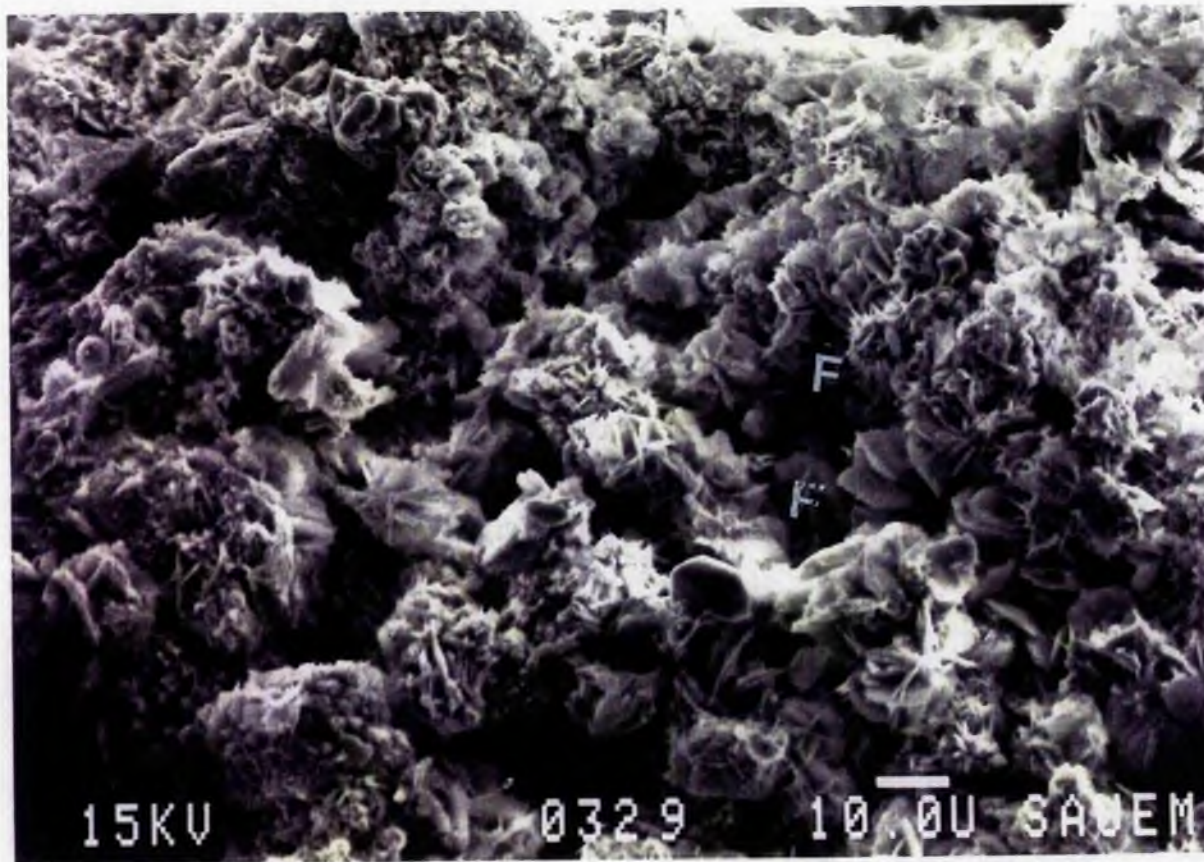


Plate 8-9 Scanning electron photomicrograph (SEM) of RE fluorocarbonate (F) from the laterite zone at Buru carbonatite centre. Note the common occurrence of manganese oxide needles. Scale bar = 10  $\mu\text{m}$ .

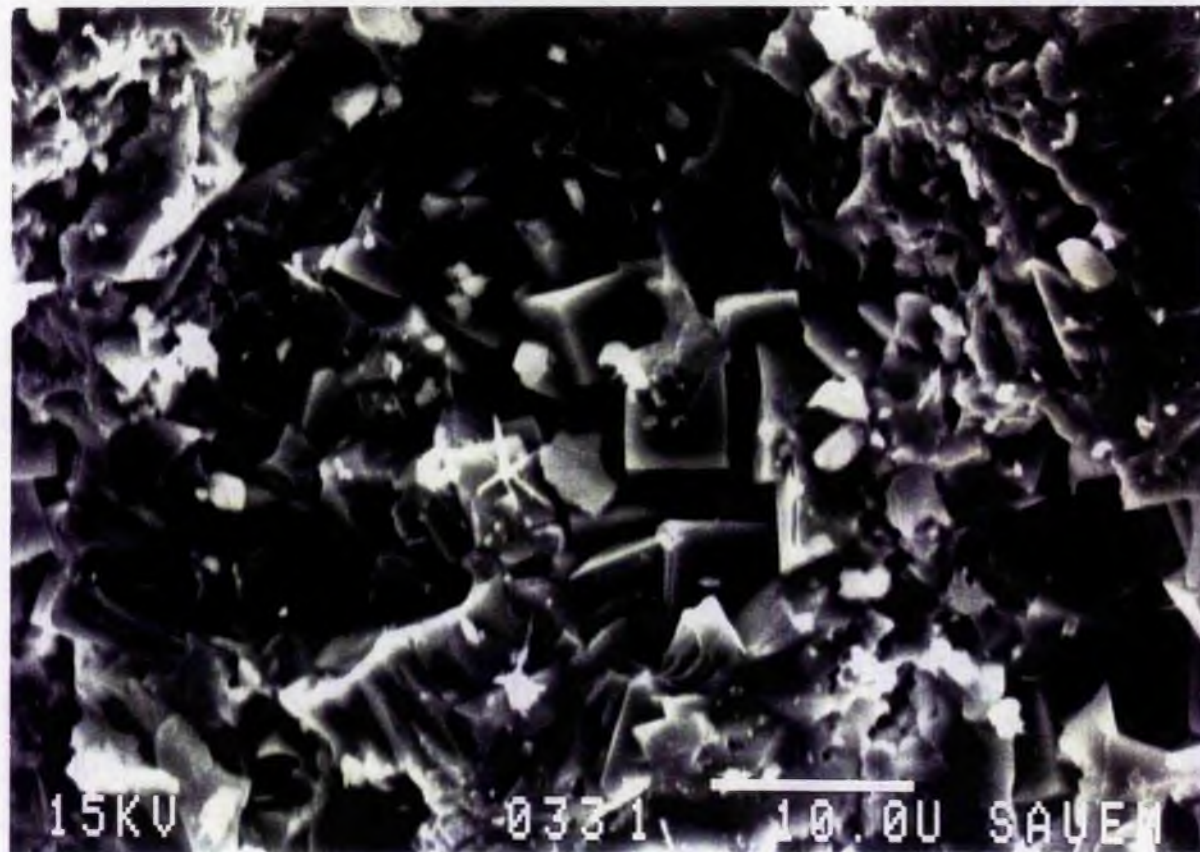


Plate 8-10 Scanning electron photomicrograph (SEM) of rhombohedral calcite crystals in carbonatite below the laterite at the Buru hill.  
Scale bar = 10  $\mu\text{m}$ .

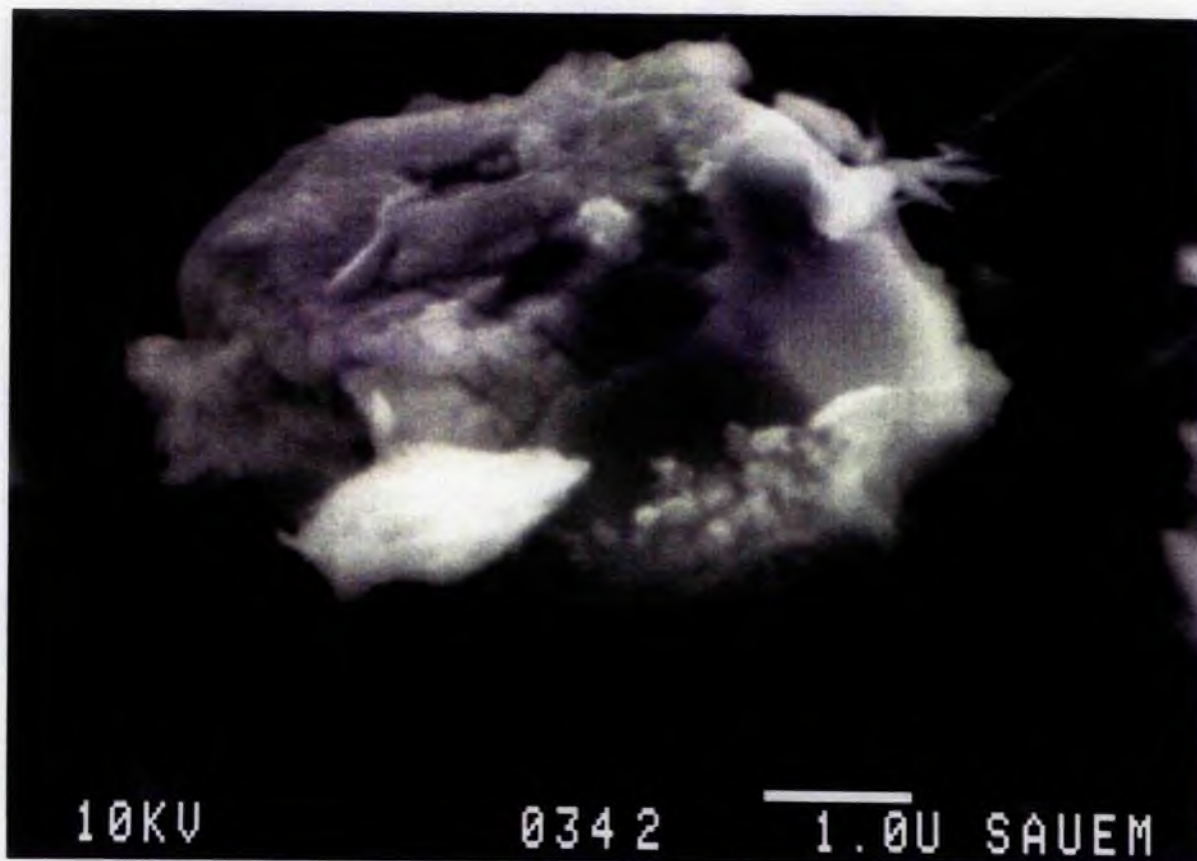
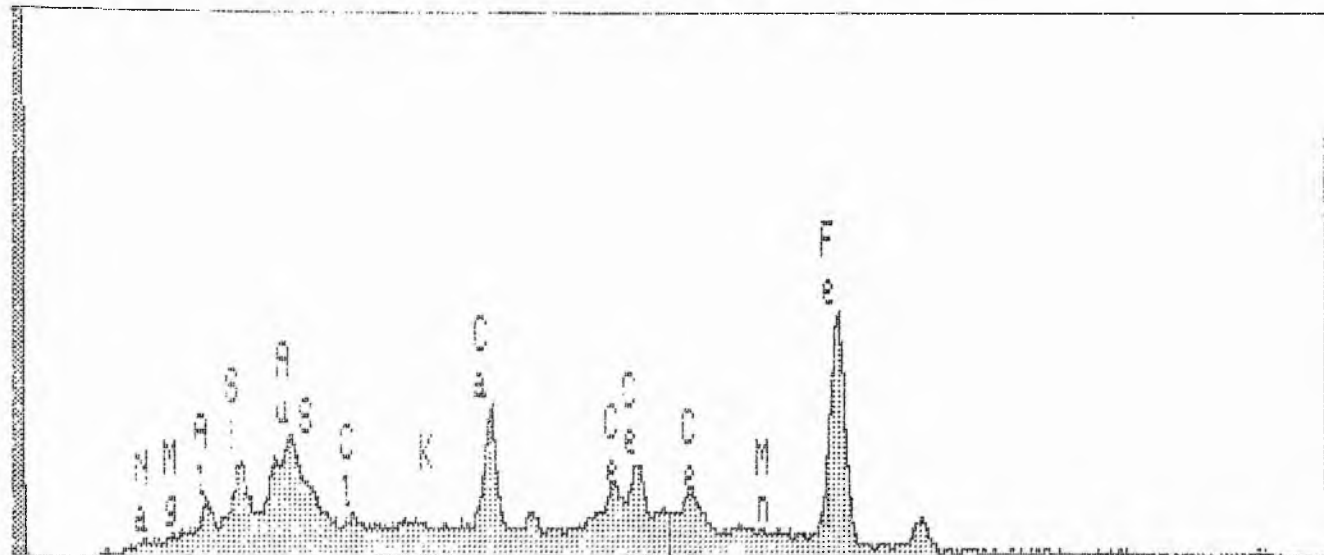


Plate 8-11 Scanning electron photomicrograph (SEM) of supergene monazite in ferrocarbonatite breccia at the Kuge carbonatite centre. Small rounded spheres could possibly be cerianite. Scale bar = 10  $\mu\text{m}$ .

X-RAY: 0 - 20 keV  
Live: 100s Preset: 100s Remaining: 0s  
Real: 122s 18% Dead



< - .0 5.100 keV 10.2 >  
FS= 8K ch 265= 398 cts  
MEM1:

Figure 8-6 Energy-dispersive X-ray (EDX) on a coated sample from the lateritic zone at Buru carbonatite showing the presence of rare earth elements.

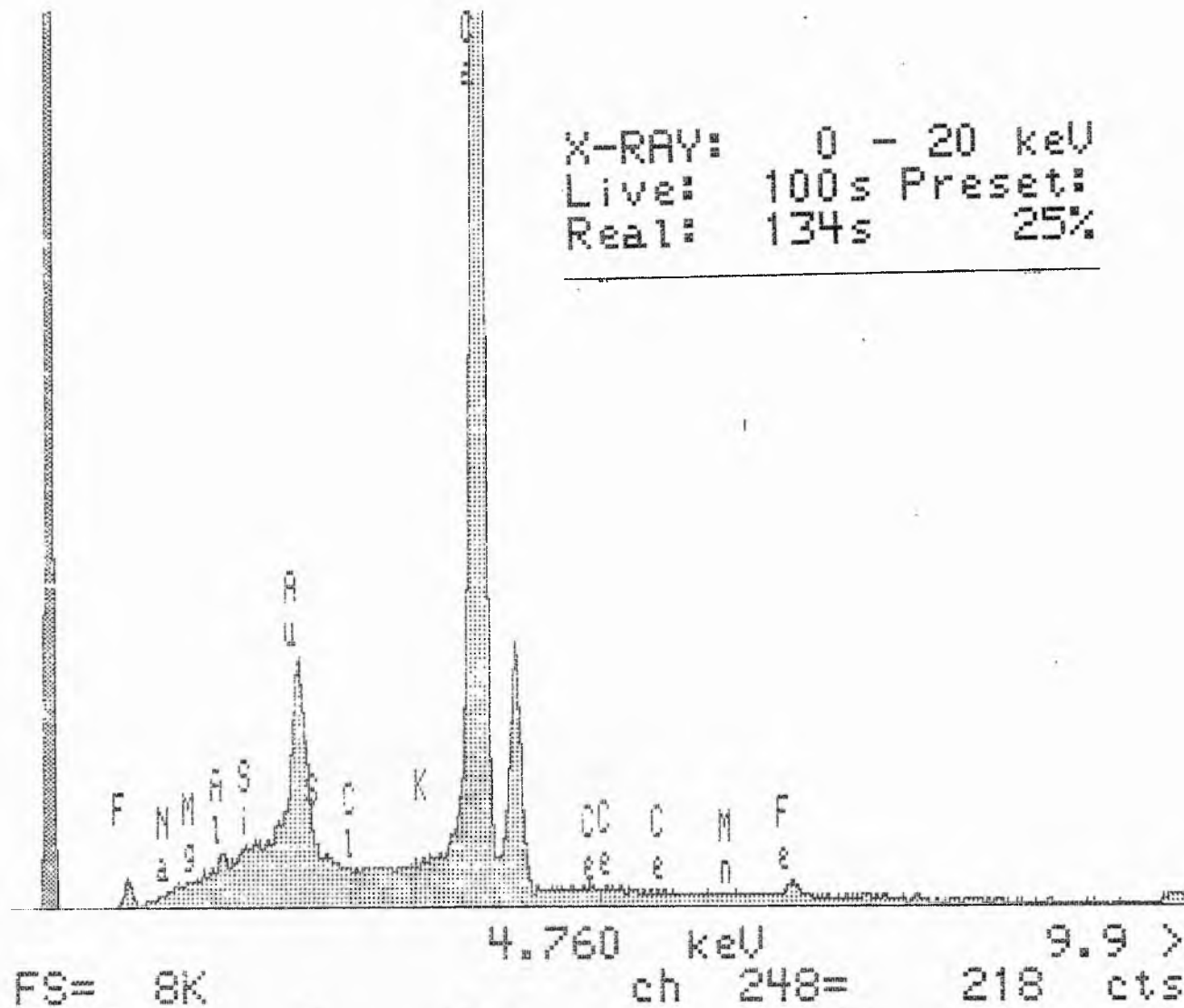


Figure 8-7 Energy-dispersive X-ray (EDX) on a coated sample corresponding to Plate 8-10. The spectrum reveals that the calcite does not contain rare earth elements.

---

X-RAY: 0 - 20 keV  
Live: 100s Preset: 100s Remaining: 0s  
Real: 120s 17% Dead

---

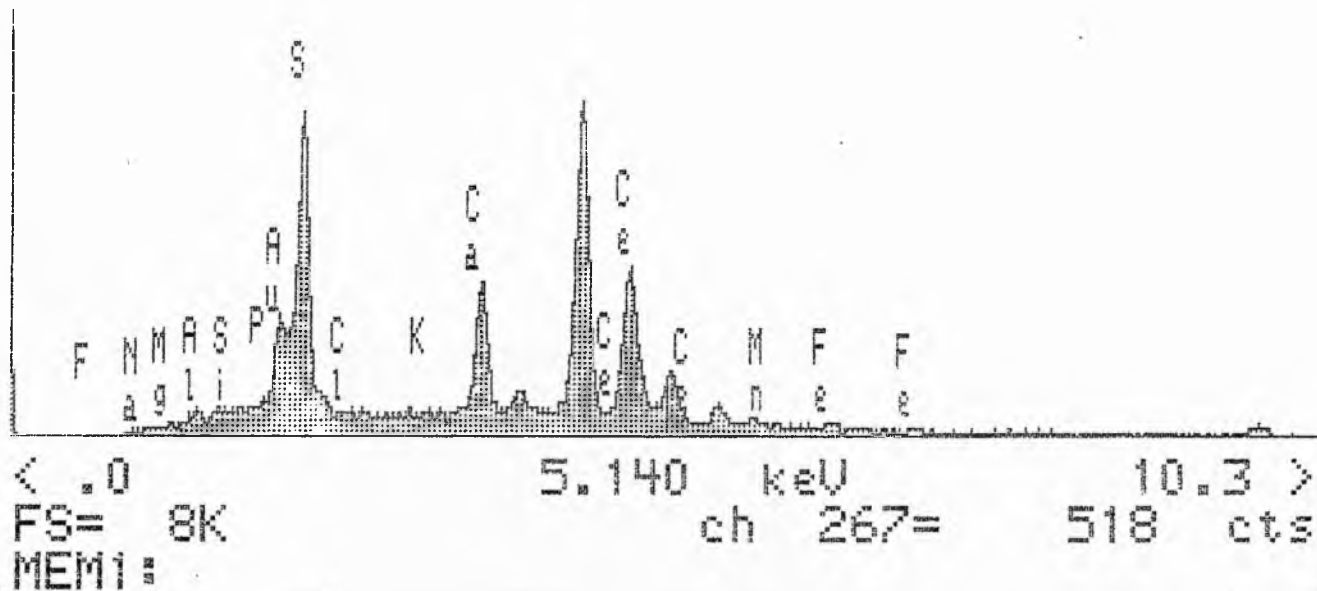


Figure 8-8 Energy-dispersive X-ray (EDX) of monazite from Kuge carbonatite centre. The spectrum shows monazite to be cerium selective.

bulk of the REEs and yttrium are accommodated in secondary minerals such as monazite, churchite, cerianite, apatite, carbonates and the plumbogummite-group minerals, together with small amounts of REEs which are incorporated in amorphous, poorly crystalline iron oxyhydroxides (Lottmoser, 1990, 1995).

The minerals of the plumbogummite group are the hydrated aluminophosphates with the general formula  $AB_3(XO_4)_2(OH, F)_5 \cdot H_2O$ , containing a wide range of possible A-site (Ca, Sr, Ba, Na, K, Y, LREE, Th and U), B-site (Al and  $Fe^{3+}$ ) and X-site cations (P, Si,  $S^{6+}$  and C). The commonest aluminophosphates are crandallite (Ca-rich), goyazite (Ba-rich), gorceixite (Sr-rich) and florencite (REE-rich). An important observation within the Mt Weld carbonatite laterite is the pronounced fractionation of REEs with depth noted by Lottermoser (1990).

In their petrographic and geochemical studies on the Lueshe carbonatite complex, Von Maravic et al. (1989) observed goethite, crandallite, goyazite and florencite as the major minerals in the weathering profile, together with minor occurrences of cryptomelane and psilomelane. Relics of the original alkaline rock mineral assemblages of pyrochlore, columbite and fluorapatite were also observed. The most important niobium-bearing mineral observed in this deposit was pyrochlore and notably monazite but the lanthanide fluorocarbonates were not observed.

In the extensive laterites of Araxá and Catalao (Brazil), the main REE carriers within the lateritic profiles of both complexes investigated by Morteani and Preinfalk (1996) were found to be secondary apatite and gorceixite. The iron hydroxides (goethite) were also considered by the authors to accommodate some REEs. Apatite and calcite were found to be

major REE carriers in the fresh alkaline carbonatites. Fractionation was not observed in both Araxá and Catalao and the REEs are believed to have behaved as immobile elements. The distribution patterns in the laterites mirror those of the underlying alkaline rocks. Unlike Mt Weld, cerianite and the fluorocarbonates were not observed in the Araxá and Catalao carbonatite complexes.

In the Buru laterite, the fluorocarbonates, the phosphates and accessory cerianite were found through combined petrography, electron probe microanalysis and scanning electron microscope studies. It was noted that the top sections of the laterite were dominated mainly by the lanthanide fluorocarbonates and minor cerianite. Monazite and especially apatite were recognized towards the lower sections of the laterite profile.

The other accessory minerals identified within the Buru laterite include, non-stoichiometric Mn-Ba-Fe compounds, goethite, hematite, barite and fluorite. These minerals were found to contain minimal detectable REEs. Pyrochlore and huanghoite [ $\text{BaCe}(\text{CO}_3)_2\text{F}$ ] were not found during the present study, but the two minerals were reported by previous workers (JICA Report, 1988-1990). The Buru carbonatite and its laterite, together with the Kuge carbonatite, are characterized by the absence of hydrated aluminium phosphates of the crandallite-group of minerals consisting of florencite, gorceixite and goyazite. These minerals are frequently reported in laterites overlying carbonatites, where they can be the major carriers of REEs.

The presence of aluminium is required for the formation and precipitation of crandallite-group of minerals. From the major element geochemistry, the Buru laterites have extremely low concentrations of aluminium (average of

<1.0 wt%), which suggests that aluminium was not readily available for the formation of the crandallite-group of minerals. The Proterozoic gneisses into which Buru is emplaced are rich in aluminium and it is surprising that the laterites developed adjacent to the gneisses are not enriched in the mineral. It is possible that the fluids derived from the parent carbonatite were not able to extract enough aluminium from the gneisses, or if they did, aluminium became mobile and was subsequently removed from the system.

### 8.13 SUMMARY.

Different laterites to a large extent seem to develop their own secondary rare earth minerals and associated accessory minerals, depending on the chemical and mineralogical composition of the protolith (parent), although the majority of the rare earth minerals tend to be phosphates such as monazite, churchite, apatite and the crandallite-group of minerals. The dominance of the phosphate minerals in lateritized profiles confirms the widespread occurrence of the mineral apatite in carbonatites or in related alkaline-silicate complexes. Lateritization processes tend to involve complete or partial removal of some elements such as aluminium, magnesium, iron and the REE from their parent rock minerals and become accumulated in the laterite weathering profile. There is no doubt therefore that the minerals found in various laterites are derived from the underlying parent rocks and, as is the case at Buru, from the underlying carbonatites.

The mineralogy and geochemistry of the carbonatite laterites are complex. Apart from the pre-lateritized parent rocks which largely determines the nature of the laterites, the other significant factor includes the extent and depth of weathering, which are also closely related to rainfall patterns, structure and age (Mariano, 1989b). The transformation of rare earth minerals has been observed in many hydrothermal systems (Gieré, 1996).

Mariano (1989b) described the transformation of bastnäesite to monazite at Karonge/Gakara (Burundi) by the interaction with late phosphate-bearing fluids, whereas Watson and Snyman (1975) reported that monazite was replaced by bastnäesite at Buffelsfontein (South Africa). According to Gieré (1996), the above transformations can schematically be represented by the reaction:



Accordingly, the transformation of rare earth minerals will be more pronounced in lateritized zones during supergene processes. A clear example in Buru and possibly Kuge is the transformation of  $\text{Ce}^{3+}$  to  $\text{Ce}^{4+}$  (cerianite), a process which will depend on the oxygen fugacity at the time of transformation. In some areas of severe chemical weathering, most minerals are totally destroyed and hence removed from the system. The presence of high concentrations of  $\text{H}_2\text{CO}_3$  from meteoric waters probably enhances the destruction and removal of some minerals from the laterites.

#### 8.14 CONCLUSION.

From the distribution of REEs and the occurrence of rare earth minerals in the Buru and Kuge carbonatite centres, in conjunction with major and trace geochemistry and stable isotope studies, the following summary is proposed for the REE mineralization.

Both the Buru and Kuge carbonatite centres are characterized by high contents of REEs and particularly LREEs. The REE distribution patterns portray steep LREE patterns that are almost identical in the two centres under study. There is clearly high  $(\text{La}/\text{Yb})_N$  ratios in samples selected from the top of the sampling profile (most oxidized samples) along different drill

cores and an indication of REE separation, where LREEs are deposited at the top of the sampling profile and the majority of the MREE towards the lower sections of the core. This separation of REEs indicates fractionation trends.

The minerals in both the Buru and Kuge carbonatite centres are secondary in origin. The secondary nature of the minerals is supported mainly by the cross-cutting relationships shown by various minerals in back-scattered electron (BSE) images and by elevated values of both  $\delta^{13}\text{C}$  and  $\delta^{18}\text{O}$  for the carbonatite carbonates from the Buru and Kuge hills. The minerals probably precipitated from hydrothermal fluids which were responsible for removing both the REEs and rare earth minerals contained in the primary carbonatites.

The observed REE abundance and their distribution patterns cannot be accounted for only in terms of one particular parameter but by an interplay of factors involving the effects of temperature of crystallization and chemistry of the various minerals, which is determined by the nature of the parent magma.

The REEs, together with some rare earth minerals, were assumed to be transported in the form of REE complexes with either carbonate, fluoride, sulphate and/or phosphate ligands. Because of a low temperature environment and near-neutral conditions, carbonate is suggested to be the likely ligand for complexing the REEs, however the existence of mixed ligand complexes such as fluorocarbonate were also involved. Precipitation of rare earth minerals from hydrothermal fluids took place in response to a number of factors, including changes in pressure and temperature, and/or crystallization of some minerals such as fluorite or calcite leading to the

breakdown of the inferred REE-complexes, which consequently initiated the precipitation of rare earth minerals, as explained by Gieré (1996).

The most common rare earth minerals in Buru and Kuge are the fluorocarbonates and the phosphates. Both types of mineral control the distribution and certainly the bulk of the REEs in the two areas under study. The Buru laterite is dominated mainly by the fluorocarbonates and less commonly by the phosphates. Both the monazite and apatite are not observed in the top upper sections of the laterite, suggesting that they may have been destroyed by severe supergene processes. In Kuge, monazite dominates over the fluorocarbonates in a number of polished thin-sections studied, indicating relatively higher concentrations of phosphate ions compared to those found in the Buru carbonatite centre.

It is considered that low temperature hydrothermal fluids introduced the rare earth minerals in the Buru and Kuge carbonatite centres. During the process of lateritization in Buru, the REEs as rare earth minerals contained in the carbonatites were released and became concentrated in the weathering profile. Thus supergene processes are critically important and are reflected by the stable isotope, major and trace element signatures.

## CHAPTER NINE

### CONCLUSION

This thesis has demonstrated the importance of secondary processes (meteoric-hydrothermal and supergene) during sub-solidus recrystallization and mineralization in carbonatites. It has been shown in this study that the geochemical characteristics of volcanic carbonatites, especially specific trace and major elements, the stable isotopic ratios and rare earth element distributions, are greatly influenced during sub-solidus re-equilibration. Fingerprinting the secondary stages and their geochemical evolution is the key to understanding the meteoric-hydrothermal, and supergene processes involved in lanthanide distribution and re-concentration in carbonatites.

In this thesis, the presence of goethite and hematite have been found to provide a useful criteria in distinguishing between hydrothermal and supergene alteration processes where the iron phases identified by X-ray diffraction studies, for example in Tables 5-1 and 5-2 indicate a distinct geochemical environment of deposition. The laterite, which is the most oxidized zone consists of iron goethite/hematite mixtures and is characterized by the absence of carbonates. The middle zone which reveal partial breakdown of carbonates is represented by calcite mixed with goethite. The lower zone which marks the first appearance of siderite is characterized by the absence of goethite. These zones are clearly depth related. It was therefore shown that low-temperature hydrothermal processes could be recognized by the presence of siderite, and supergene processes by the occurrence of goethite or hematite mineralization.

The presence of goethite/hematite is supported by the major element geochemistry, where higher values of  $\text{Fe}_2\text{O}_3$  contents noted in both Buru and Kuge carbonatite centres, particularly in their supergene zones were attributed to late-stage formation of these secondary minerals. High MnO contents are due to the presence of psilomelane [ $\text{Ba}(\text{H}_2\text{O})_2\text{Mn}_2\text{O}$ ], a secondary mineral usually found in association with manganese deposits due to weathering.

Meteoric-hydrothermal and supergene processes have been separately recognized particularly from the C-O stable isotope studies. The combined  $\delta^{13}\text{C}$  and  $\delta^{18}\text{O}$  isotopic composition for Buru and Kuge carbonatite centres (Figure 7-7) shows two distinct trends. The first trend, involving mainly the Buru calcite carbonates, is dominated by hydrothermal alteration through hot spring activity, followed by reprecipitation at surface temperatures with the introduction of atmospheric  $\text{CO}_2$ . The second trend for the Kuge carbonates involves low temperature recrystallization in a water-dominated environment without the influence of surface carbon.

The temperatures of the meteoric-hydrothermal and supergene processes have been estimated using isotope reference data from modern day geothermal systems from Kenya Rift Valley (Clarke et al., 1990). The estimated temperatures for calcite precipitation at Buru are  $100^\circ\text{C}$  (Figure 7-1; Group 1) and  $62^\circ\text{C}$  (Figure 7-1; Group 2) respectively. The precipitation of siderite at Buru yield an isotope equilibration temperature of  $144^\circ\text{C}$  (Figure 7-1). These estimated temperatures are consistent with hydrothermal alteration and isotopic exchange taking place during hot spring activity. The meteoric-hydrothermal processes are supported by the dominant occurrence of barite and fluorite observed in both the Buru and Kuge drill-cores. Barite and

fluorite are typical products of late-stage crystallization of carbonatites where they are deposited by circulating hydrothermal fluids.

Carbonates from the uppermost sections of the drill cores (Group 3) dominated by various compounds of iron (goethite and hematite) and calcite, are characterized by the lowest isotope equilibration temperature of 30°C. They are considered to have been reprecipitated by weathering (supergene) processes rather than by meteoric-hydrothermal fluids.

Low temperature meteoric-hydrothermal processes recognized in this investigation considerably enhance the recrystallization of lanthanide minerals such as rare earth fluorocarbonates whereas further enrichment occurs during the supergene stage when the carbonatite becomes lateritized on weathering developing monazite and cerianite. It has been shown in this work that the rare earth fluorocarbonates are dominantly of meteoric-hydrothermal in origin whereas monazite and cerianite found in the upper lateritic profiles, especially in Buru carbonatite centre, are thought to be primarily concentrated by supergene processes. These rare earth minerals are mainly either bastnäesite, synchysite and parisite or monazite and their presence, particularly below the weathering zones, is in accord with the REEs being transported as either carbonate, fluoride or phosphate complexes. The absence of carbonates within the Buru lateritic profiles suggests phosphate and/or fluoride to be the dominant anionic species. In the Kuge carbonatite centre, it has been shown that the phosphate dominates over fluorite, a feature manifested by frequent occurrence of monazite than the rare earth fluorocarbonates. However, the particular RE-mineral that precipitates depends on the relative amounts of the cations and anions in solution and the temperatures of crystallization.

A significant contribution of this investigation with respect to lanthanide mineralization within the western Kenyan carbonatites is the demonstration that the mineralization is of low-temperature in origin. The evolution of the hydrothermal and supergene stages has successfully been distinguished by the stable isotope systematics where samples selected from the supergene zones show higher  $\delta^{18}\text{O}$  and  $\delta^{13}\text{C}$  isotopic values compared to those samples chosen below the weathering zone where hydrothermal activity prevails. Higher  $\delta^{13}\text{C}$  and  $\delta^{18}\text{O}$  isotopic values were shown to correspond to higher REE abundances, a major factor in lanthanide exploration in laterites overlying carbonatite complexes.

## CHAPTER 10.

### SUGGESTIONS FOR FURTHER WORK

#### 10.1 ISOTOPE STUDIES

Detailed age dating of the carbonatite centres and the various rock types associated with the carbonatites is needed for a clearer understanding of the evolution of the western Kenyan carbonatites. K-Ar dating of carbonatites and associated rock types including the fenites is recommended.

If the carbonatite intrudes country rocks such as limestone, the effect on isotopic composition will be recognized readily. In cases where the carbonatites intrude Proterozoic gneisses and/or Archaean basalts, as in the case of the Buru and Kuge centres, respectively, crustal contamination of the carbonatite will not be obvious. The writer suggests that further radiogenic analyses (Sm-Nd, U-Pb and Rb-Sr) be completed on all carbonatite centres, as well as on the fenites, to supplement the carbon and oxygen isotopic data obtained in this study.

It was not possible to determine precisely which of the two factors (namely redox processes or isotopic fractionation due to the loss of volatiles) were responsible for the variations in  $\delta^{34}\text{S}$  shown by the Buru and Kuge carbonatite centres. The writer suggests that further detailed work on sulphur isotope systematics is necessary in order to understand which of the two processes is involved.

#### 10.2 LANTHANIDE MINERALIZATION.

Complex mechanisms are involved in the formation of rare earth minerals particularly in post-magmatic environments. Understanding the nature of the

rare earth carrying minerals and the conditions of their formation is crucial in identifying other areas that might have possible economic REE accumulations. As mechanisms are not well understood, the writer suggests research to be concentrated on experimental work involving various aspects of REE geochemistry, especially the stability relationships of rare earth minerals.

### 10.3 INDUSTRIAL APPLICATIONS.

The ever increasing application of rare earths in industry have recently stimulated an increasing interest on the part of mining companies in the exploitation of the new resources of these elements, especially from weathered carbonatite crusts. In the near future, production of REEs from lateritic or regolithic deposits will successfully compete with operations based on more traditional sources of REE, such as beach sands and hard-rock carbonatite ores.

The major problem encountered in the beneficiation of lateritic ores is their small size and intimate relationship with other gangue minerals. If the beneficiation difficulties associated with REEs in carbonatite lateritic environments are solved through well coordinated research (involving industry and University research Institutes), ore deposits such as Mrima hill, a deeply weathered carbonatite located along the Kenyan coast, will be elevated to become one of the largest producers of REEs in the world. At present REE concentrations at Mrima hill have been estimated at 6,000,000t (bastnäesite/monazite) with a grade of 16.2% rare earth oxide. The same lanthanide potential could exist for the volcanic carbonatites of the Nyanza rift, western Kenya.

## REFERENCES

- Alderton, D. H. D., Pearce, J. A. and Potts, P. J. 1980. Rare earth element mobility during granite alteration: Evidence from SW England. *Earth Planetary Science Letters* **49**, 149-165.
- Alviola, R., Kortman, C. Githinji, I. Mulaha, T. and Nzau, K. 1985. Report on cement raw materials investigations in Koru and Songhor areas, western Kenya. Ministry of Environment and Natural Resources, Republic of Kenya, pp 205.
- Andersen, T. 1984. Secondary processes in carbonatites: Petrology of "rodberg" (hematite-calcite-dolomite carbonatite) in the Fen central complex, Telmark (southeast Norway). *Lithos* **17**, 227-245.
- Andersen, T. 1986. Compositional variation of some rare earth minerals from Fen complex (Telmark, southeast Norway): Implications for the mobility of rare earths in a carbonatite system. *Mineralogical Magazine* **50**, 503-509.
- Andersen, T. 1987. A model for the evolution of hematite carbonatites, based on whole rock major and trace element data from Fen complex, southeast Norway. *Applied Geochemistry* **2**, 163-180.
- Armitage, R. 1995. Geochemical study of the Koru carbonatite complex. Genetic and economic implications. *BSc (Hons) Geochemistry dissertation* 78pp. St Andrews University, U.K.
- Bailey, D. K. 1960. Carbonatites of the Rufunsa valley. *Bulletin* **5**. North Rhodesia geological Survey.
- Baker, B. H., Williams, L. A. and Fitch, F. J. 1971. Sequence and geochronology of Kenya rift volcanics. *Tectonophysics* **11**, 191-215.
- Balashov, Yu. A. and Pozharitskaya, L. K. 1968. Factors governing the behaviour of rare-earth elements in the carbonatite process. *Geochemistry International* **No.3**, 285-303
- Barber, C. 1974. The geochemistry of carbonatites and related rocks from two carbonatite complexes, south Nyanza, Kenya. *Lithos* **7**, 53-63.
- Barker, D. S. 1989. Field relations of carbonatites. In: *Carbonatites, Genesis and Evolution* (edited by Bell, K.) pp38-69. Unwin Hyman, London.

Barth, T. F. W. and Ramberg, I. B. 1966. The Fen circular complex. In: *Carbonatites* (edited by Tuttle, O. F. and Gittins, J.) pp225-257. Interscience, New York.

Bayliss, P. and Levinson, A. A. 1988. A system of nomenclature for rare earth-mineral species: revision and extension. *American Mineralogist* **73**, 422-423.

Bell, K. 1989. *Carbonatites, Genesis and Evolution*. Unwin Hyman, London.

Bell, K. and Blenkinsop, J. 1989. Neodymium and strontium isotope geochemistry of carbonatites, In: *Carbonatites, Genesis and Evolution* (edited by Bell, K.) pp278-297. Unwin Hyman, London.

Binge, F. W. 1962. Geology of Kericho area. *Report 50*, Geological Survey Kenya.

Bishop, W. W., Miller, J. A. and Fitch, F. J. 1969. New potassium-argon age determinations relevant to the Miocene fossil mammal sequence in East Africa. *American Journal Science* **267**, 669-699.

Bottinga, Y. 1968. Calculation of fractionation factors for carbon and oxygen isotopic exchange in the system calcite-carbon dioxide-water. *Journal Chemistry Physics* **72**, 800-808.

Braun, J. J., Pagel, M., Muller, J. P., Bilong, J. P., Michard, A. and Guillet, B. 1990. Cerium anomalies in lateritic profiles. *Geochimica Cosmochimica Acta* **54**, 781-795.

Buckley, H. A. and Woolley, A. R. 1990. Carbonatites of the magnesite-siderite series from four carbonatite complexes. *Mineralogical Magazine* **50**, 503-509.

Burt, D. M. 1989. Compositional and phase relations among rare earth element minerals. In: *Geochemistry and Mineralogy of Rare Earth Elements, Reviews in Mineralogy*, **21** (edited by Lipin, B. R. and MacKay, G. A.) pp259-307. Mineralogical Society America.

Cantrell, K. J. and Byrne, R. H. 1987. Rare earth element complexation by carbonate and oxalate ions. *Geochimica Cosmochimica Acta* **51**, 597-606.

Carothers, W. W., Adami, L. H. and Rosenbauer, R. J. 1988. Experimental oxygen isotope fractionation between siderite-water and phosphoric acid liberated CO<sub>2</sub>-siderite. *Geochimica Cosmochimica Acta* **52**, 2445-2450.

Chacko, T., Mayeda, T. K., Clayton, R. N. and Goldsmith, J. R. 1991. Oxygen and carbon isotope fractionation between CO<sub>2</sub> and calcite. *Geochimica Cosmochimica Acta* **55**, 2867-2882.

Chaussidon, M., Albarede, F. and Sheppard, S. M. F. 1989. Sulphur isotope variations in the mantle from ion microprobe analyses of micro-sulphide inclusions. *Earth Planetary Science Letters* **92**, 144-156.

Church, A. and Jones, A. P. 1995. Silicate-carbonate immiscibility at Oldoinyo Lengai. *Journal Petrology* **36**, 869-889.

Clarke, M. G. C. and Roberts, B. 1986. Carbonated melilitites and calcitized alkali carbonatites from Homa Mountain, western Kenya: A reinterpretation. *Geological Magazine* **123**, 683-692.

Clarke, M. C. G., Woodhall, D. G., Allen, D. and Darling, D. 1990. Geological, volcanological and hydrogeological controls on the occurrence of geothermal activity in the area surrounding Lake Naivasha, Kenya. Ministry of Energy, Nairobi, Kenya 138p.

Cluver, A. F. 1958. Buru Hill: Exclusive Prospecting Licence, Kericho District, Kenya. *Unpublished Internal Report*. New Consolidated Gold Fields, Johannesburg, South Africa.

Coleman, M. L. and Moore, M. P. 1978. Direct reduction of sulphates to sulphur dioxide for isotopic analysis. *Analytical chemistry* **50**, 1594-1595.

Cooper, A. F., Gittins, J. and Tuttle, O. F. 1975. The system Na<sub>2</sub>CO<sub>3</sub> - K<sub>2</sub>CO<sub>3</sub> - CaCO<sub>3</sub> at 1kb and its significance in carbonatite petrogenesis. *American Journal Science* **275**, 534-560.

Cooper, A. F. and Paterson, L. A. 1995. Lithium in carbonatites - consequence of an enriched mantle source. *Mineralogical Magazine* **59**, 401-408.

Dalton, J. A. and Wood, B. J. 1993. The compositions of primary melts and their evolution through wall-rock reaction in the mantle. *Earth Planetary Science Letters* **119**, 511-525.

Daly, R. A. 1933. *Igneous Rocks and Depths of the Earth*. McGraw-Hill, New York.

Dawson, J. B. 1962. The geology of Oldoinyo Lengai. *Bulletin Volcanology* **24**, 349-387.

Dawson, J. B., Garson, M. S. and Roberts, B. 1987. Altered former alkalic carbonatite lava from Oldoinyo Lengai, Tanzania: Inferences for calcite carbonatite lavas. *Geology* **15**, 756-768.

Dawson, J. B. 1993. A supposed sövite from Oldoinyo Lengai, Tanzania: Result of extreme alteration of alkali carbonatite lava. *Mineralogical Magazine* **57**, 93-101.

Dawson, J. B., Pinkerton, H., Norton, G. E., Pyle, D. M., Browning, P., Jackson, D. and Fallick, A. E. 1995. Petrology and geochemistry of Oldoinyo Lengai Lavas extruded in November 1988: Magma Source, ascent and crystallization. In: *Oldoinyo Lengai and petrogenesis of natrocarbonatite* (edited by Bell, K. and Keller, J.) pp49-69.

Deans, T. 1966. Economic mineralogy of African carbonatites. In: *Carbonatites* (edited by Tuttle, O. F. and Gittins, J.) pp385-413. Interscience.

Deans, T. and Roberts, B. 1984. Carbonatite tuffs and lava clasts of the Tinderet foothills, western Kenya: A study of calcified natrocarbonatites. *Journal of the Geological Society London* **141**, 563-580.

Deer, W. A., Howie, R. A. and Zussman, J. 1992. *An introduction to Rock Forming Minerals*. 2nd edition. Longman, Scientific and Technical.

Deines, P. 1970. The carbon and oxygen isotopic composition of carbonates from Oka carbonatite, Quebec, Canada. *Geochimica Cosmochimica Acta* **34**, 1199-1225.

Deines, P. and Gold, D. P. 1973. The isotopic composition of carbonatite and kimberlite carbonates and their bearing on the isotopic composition of deep-seated carbon. *Geochimica Cosmochimica Acta* **37**, 1709-1733.

Deines, P. 1989. Stable isotope variations in carbonatites. In: *Carbonatites, Genesis and Evolution* ( edited by Bell, K.) pp301-359. Unwin Hyman, London.

Dixon, J. A. 1968. The structure and petrology of the carbonatite complexes of North Ruri and Kuge, Kenya. *Ph.D. dissertation*. University of Leicester, U.K.

Dodson, M. H., Bell, K. and Shackleton, R. M. 1973. Archaean geochronology of East Africa. *Fortschritte Mineralogie* **50**, 67-68.

Duddy, I. R. 1980. Redistribution and fractionation of rare earth and other elements in a weathering profile. *Chemical Geology* **30**, 363-381.

Eby, G. N. 1975. Abundance and distribution of the rare earth elements and yttrium in the rocks of the Oka carbonatite complex, Quebec. *Geochimica Cosmochimica Acta* **39**, 597-620.

Eckermann, H. V. 1966. Progress of research on the Alnö carbonatite. In: *Carbonatites* (edited by Tuttle, O. F. and Gittins, J.) pp3-32. Interscience, New York.

Eggler, D. H. 1989. Carbonatites, primary melts and mantle dynamics. In: *Carbonatites, Genesis and Evolution* (edited by Bell, K.) pp561-579. Unwin Hyman, London.

Emrich, K., Ehhalt, D. H. and Vogel, J. C. 1970. Carbon isotope fractionation during precipitation of calcium carbonate. *Earth Planetary Science Letters* **8**, 363-371.

Faure, G. 1992. *Principles and Applications of Inorganic Chemistry*. 626p. Maxwell Macmillan International Editions.

Fleischer, M. 1960. Studies of the manganese oxide minerals. III. Psilomelane. *American Mineralogist* **45**, 176-187.

Freestone, I. C. and Hamilton, D. L. 1980. The role of liquid immiscibility in the genesis of carbonatites. *Contributions Mineralogical Petrology* **73**, 105-117.

Garson, M. S. and Campbell Smith, W. 1958. The geology of Chilwa Island, Nyasaland. *Memoir 1*, Geological Survey, Malawi.

Garson, M. S. 1965. Carbonatites in Southern Malawi. *Bulletin 15*. Geological Survey, Malawi.

Gieré, R. 1996. Formation of rare earth minerals in hydrothermal systems. In: *Rare Earth Minerals - Chemistry, origin and ore deposits* (edited by Jones, A., Wall, F. and Williams, T.) pp105-150. Chapman & Hall, London.

Gittins, J. 1989. The origin and evolution of carbonatite magmas. In: *Carbonatites, Genesis and Evolution* (edited by Bell, K.) pp580-600. Unwin Hyman, London.

Gittins, J. and Jago, B. C. 1991. Extrusive carbonatites: their origins reappraised in the light of new experimental data. *Geological Magazine* **128**, 301-305.

Gold, D. P. 1963. Average chemical composition of carbonatites. *Economic Geology* **58**, 988-991.

Grauch, R. I. 1989. Rare earth elements in metamorphic rocks. In: *Geochemistry and Mineralogy of Rare Earth Elements, Reviews in Mineralogy* **21** (edited by Lipin, B. R. and McKay, G. A.) pp147-167. Mineralogical Society America, Washington, DC.

Grinenko, L. N. Kononova, V. A. and Grinenko, V. A. 1970. Isotopic composition of sulphide sulphur in carbonatites. *Geochemistry International* **6**, 45-53.

Haas, J. R. Shock, E. R. and Sassani, D. C. 1995. Rare earth elements in hydrothermal systems: Estimates of standard partial molal thermodynamic properties of aqueous complexes of the rare earth elements at high pressures and temperatures. *Geochimica Cosmochimica Acta* **59**, 4329-4350.

Haggerty, S. E. 1989. Mantle metasomes and the kinship between carbonatites and kimberlites. In: *Carbonatites, Genesis and Evolution* (edited by Bell, K.) pp546-560. Unwin Hyman, London.

Hamilton, E. I. and Deans, T. 1963. Isotopic composition of strontium in some African carbonatites and limestones and in strontium minerals. *Nature* **198**, 776-777.

Harmer, R. E. and Gittins, J. 1995. Carbonatites: primary or secondary magma types? In: GSA'95 International Conference, Nairobi. Abstract Volume. pp110.

Hay, R. L. and O'Neil, J. R. 1983. Carbonatite tuffs in the Laetolil beds of Tanzania and the Kaiserstuhl in Germany. *Contributions Mineralogy and Petrology* **82**, 403-406.

Heinrich, E. 1966. *The Geology of Carbonatites*. 555p. Rand McNally, Chicago.

Henderson, P. 1996. The rare earth elements. Introduction and review. In: *Rare Earth Minerals - Chemistry, origin and ore-deposits* (edited by Jones, A. P., Wall, F. and Williams, C. T.) pp1-19. Chapman & Hall, London.

Hogarth, D. D. 1989. Pyrochlore, apatite, and amphibole: Distinctive minerals in carbonatites. In: *Carbonatites, Genesis and Evolution* (edited by Bell, K.) pp105-148. Unwin Hyman, London.

Hoefs, J. 1987. *Stable Isotope Geochemistry*, 3<sup>rd</sup> edition. 236p. Springer-Verlag, Berlin.

Huang, Y. -M., Hawkesworth, C. J., van Calsteren, P. and McDermott, F. 1995. Geochemical characteristics and origin of the Jacupiranga carbonatites, Brazil. *Chemical Geology* **119**, 79-99.

Hubberten, H. W., Katz-Lehnert, K. and Keller, J. 1988. Carbon and oxygen isotope investigations in carbonatites and related rocks from the Kaiserstuhl, Germany. *Chemical Geology* **70**, 257-274.

Javoy, M., Pineau, F., Staudacher, T., Cheminée, J. L. and Krafft, M. 1989. Mantle volatiles sampled from a continental rift: the 1988 eruption of Oldoinyo Lengai. *TERRA abstract* **1**, pp324.

J.I.C.A. Reports. 1988-1990. Report on the mineral exploration in the HomaBay area, Republic of Kenya. *Unpublished confidential Reports* **1**, **2** and **3**.

Jones, A. P. 1989. Upper-mantle enrichment by kimberlitic or carbonatitic magmatism. In: *Carbonatites, Genesis and Evolution* (edited by Bell, K.) pp448-463. Unwin Hyman, London.

Jones, W. B. and Lippard, S. J. 1979. New age determinations of the Kenya rift-Kavirondo rift junction, western Kenya. *Journal Geological Society London* **136**, 693-704.

Kamitani, M. and Hirano, H. 1987. Araxa carbonatite deposit and its lateritization. In: *Research on mineral deposits associated with carbonatite in Brazil. Geological Survey Japan* 56-73.

Kapustin, Y. L. 1980. *Mineralogy of Carbonatites*. 259p. Amerind Publishing Company, New Delhi.

Keller, J. 1989. Extrusive carbonatites and their significance. In: *Carbonatites, Genesis and Evolution* (edited by Bell, K.) pp70-88. Unwin Hyman, London.

Keller, J. and Hoefs, J. 1995. Stable isotope characteristics of recent natrocarbonatites from Oldoinyo Lengai. In: *Carbonatite volcanism, Oldoinyo Lengai and the Petrogenesis of Natrocarbonatites* (edited by Bell, K. and Keller, J.) pp113-123. IAVCEI Proceedings in Volcanology.

Kent, P. E. 1944. The Miocene beds of Kavirondo, Kenya. *Quarterly Journal Geological Society London* **100**, 85-118.

King, B. C. 1949. The Napak area of south Karamoja, Uganda. *Memoir* **5** Geological Survey of Uganda.

King, B. C. 1960. Alkaline rocks of eastern and southern Africa. *Science Progress* **48**, 298-321, 504-524 and 709-720.

King, B. C. and Sutherland, D. S. 1966. The carbonatite complexes of eastern Uganda. In: *Carbonatites* (edited by Tuttle, O. F. and Gittins, J.) pp73-126. Interscience, New York.

King, B. C., Le Bas, M. J. and Sutherland, D. S. 1972. The history of the alkaline volcanoes and intrusive complexes of eastern Uganda and western Kenya. *Journal Geological Society London* **128**, 173-205.

Kjarsgaard, B. A. and Hamilton, D. L. 1988. Liquid immiscibility and the origin of alkali-poor carbonatites. *Mineralogical magazine* **52**, 43-55.

Kjarsgaard, B. A. and Hamilton, D. L. 1989. The genesis of carbonatites by immiscibility. In: *Carbonatites, Genesis and Evolution* (edited by Bell, K.) pp338-404. Unwin Hyman, London.

Kjarsgaard, B. A. and Peterson, T. D. 1991. Nephelinite-carbonatite liquid immiscibility at Shomhole volcano, East Africa: petrographic and experimental evidence. *Mineralogy and Petrology* **43**, 293-314.

Kjarsgaard, B. A., Hamilton, D. L. and Peterson, T. D. 1995. Peralkaline nephelinite/carbonatite liquid immiscibility: Comparison of phase compositions in experiments and natural lavas from Oldoinyo Lengai. In: *Carbonatite volcanism of Oldoinyo Lengai and petrogenesis of natrocarbonatite* (edited by Bell, K. and Keller, K.) pp163-190 IAVCEI Proceedings in volcanology, Berlin, Springer.

Koster van Groos, A. F. and Wyllie, P. J. 1966. Liquid immiscibility in the system  $\text{Na}_2\text{O} - \text{Al}_2\text{O}_3 - \text{SiO}_2 - \text{CO}_2$  at pressures up to 1 Kb. *American Journal Science* **264**, 234-255.

Koster van Groos, A. F. and Wyllie, P. J. 1968. Liquid immiscibility in the join  $\text{NaAlSi}_3\text{O}_8 - \text{Na}_2\text{CO}_3 - \text{H}_2\text{O}$  and its bearing on the origin of carbonatites. *American Journal Science* **266**, 932-967.

Knudsen, C. and Buchardt, B. 1991. Carbon and oxygen isotope composition of carbonates from Qaqassuk carbonatite complex, southern west Greenland. *Chemical Geology* **86**, 263-274.

Kresten, P. and Morogan, V. 1986. Fenitization at the Fen complex, southern Norway. *Lithos* **19**, 27-42.

Kuellermer, F. J., Visocky, A. P. and Tuttle, O. F. 1966. Preliminary survey of the system barite-calcite-fluorite at 500 bars. In: *Carbonatites* (edited by Tuttle, O. F. and Gittins, J.) pp353-364. Interscience, New York.

Lapin, A. V. 1990. Carbonatite weathering crusts: Geochemical types and mineralization. *Geochemistry International* **29**, 72-83.

Lapin, A. V. 1994. The rare earth elements in carbonatite weathering crusts: distribution, fractionation and mineral forms. *Geochemistry International* **31**, 34-49.

Le Bas, M. J. 1977. *Carbonatite-Nephelinite volcanism*. 347p. John Wiley & Sons, London.

Le Bas, M. J. 1981. Carbonatite magmas. *Mineralogical Magazine* **44**, 133-140.

Le Bas, M. J. and Aspden, J. A. 1981. The comparability of carbonatitic fluid inclusions in ijolites with natrocarbonatite lava. *Bulletin Volcanology* **44**, 429-438.

Le Bas, M. J. 1987. Nephelinites and Carbonatites. In: *Alkaline Igneous Rocks* (edited by Fitton, J. G. and Upton, B. G. J.) Geological Society Special Publication, No. 30.

Le Bas, M. J. 1989. Diversification of carbonatites. In: *Carbonatites, Genesis and Evolution* (edited by Bell, K.) pp428-447. Unwin Hyman, London.

Le Maitre, R. W., Bateman, P., Dukek, A., Keller, J., Lameyre, J., Le Bas M. J., Sabine, P. A., Schmid, R., Sørensen, H., Streckeisen, A., Woolley, A. R. and Zanettin, B. 1989. A classification of Igneous Rocks and Glossary of Terms. *Recommendations of the International Union of Geological Sciences Subcommission on the Systematic of Igneous Rocks*. Oxford, Blackwell.

Lee, J. H. and Byrne, R. H. 1992. Examination of comparative rare earth element complexation behaviour using linear free-energy relationships. *Geochimica Cosmochimica Acta* **56**, 1127-1137.

Lee, J. H. and Byrne, R. H. 1993. Complexion of trivalent rare earth elements (Ce, Eu, Gd, Tb and Yb) by carbonate ions. *Geochimica Cosmochimica Acta* **57**, 295-302.

Lottermoser, B. 1990. Rare earth element mineralization within the Mt Weld carbonatite laterite, Western Australia. *Lithos* **24**, 151-167.

Lottermoser, B. 1995. Ore minerals of Mt Weld rare earth element deposit, Western Australia. *Transactions Institution Mining Metallurgy* (Section B: Applied Earth Science) **104**, B203-B209.

Loubet, M., Bernat, M., Javoy, M. and Allegre, C. J. 1972. Rare earth contents in carbonatites, *Earth Planetary Science Letters* **14**, 226-232.

Lippard, S. J. 1973. The petrology of phonolites from the Kenya rift. *Lithos* **6**, 217-234.

McCall, G. J. H. 1958. Geology of Gwasi area. *Report* **45**, 88p. Geological Survey, Kenya.

McCrea, J. M. 1950. On the isotopic chemistry of carbonates and a paleotemperature scale. *Journal Chemistry Physics* **18**, 849-857.

Macdonald, R., Kjarsgaard, B. A., Skilling, I. P., Davies, G. R., Hamilton, D. L. and Black, S. 1993. Liquid immiscibility between trachyte and carbonate in ash flow tuffs from Kenya. *Contributions Mineralogy Petrology* **114**, 276-287.

McKie, D. 1966. Fenitization. In: *Carbonatites* (edited by Tuttle, O. F. and Gittins, J.) pp261-294. Interscience, New York.

Mäkelä, M. and Vartiainen, H. 1978. A study of sulphur isotopes in the Sokli multi stage carbonatite (Finland). *Chemical Geology* **21**, 257-265.

Mariano, A. N. 1989a. Economic geology of rare earth elements. In: *Geochemistry and Mineralogy of Rare Earth Elements* (edited by Lipin, B. R. and McKay, G. A.) pp309-337. *Reviews in mineralogy* **21**, Mineralogical Society of America, Washington, D.C.

Mariano, A. N. 1989b. Nature of economic mineralization in carbonatites and related rocks. In: *Carbonatites, Genesis and Evolution* (edited by Bell, K.) pp149-176. Unwin Hyman, London.

Marsh, J. S. 1991. REE fractionation and Ce anomalies in weathered Karoo dolerite. *Chemical Geology* **90**, 189-194.

Matsuhisa, Y. 1979. Oxygen isotopic composition of volcanic rocks from the East Japan island Arcs and their bearing on petrogenesis. *Journal Volcanology Geothermal Research* **5**, 271-296.

Mattey, D. P., Taylor, W. R., Green, D. H. and Pillinger, C. T. 1990. Carbon isotopic fractionation between CO<sub>2</sub> vapour, silicate and carbonate melts: An experimental study to 30kbar. *Contributions Mineralogy Petrology* **104**, 492-505.

- Michard, A. 1989. Rare earth element systematics in hydrothermal fluids. *Geochimica Cosmochimica Acta* **53**, 745-750.
- Millero, F. J. 1992. Stability constants for formation of rare earth inorganic complexes as a function of ionic strength. *Geochimica Cosmochimica Acta* **56**, 3123-3132.
- Mitchell, R. H. and Krouse, H. R. 1971. Isotopic composition of sulphur in carbonatite at Mountain Pass, California. *Nature* **231**, 182.
- Mitchell, R. H. and Krouse, H. R. 1975. Isotopic composition of sulphur in carbonatites. *Geochimica Cosmochimica Acta* **39**, 1505-1513.
- Möller, P., Morteani, G. and Schley, F. 1980. Discussion of REE distribution patterns of carbonatites and alkalic rocks. *Lithos* **13**, 171-179.
- Mongelli, G. 1993. REE and other trace elements in granitic weathering profile from Serre, southern Italy. *Chemical Geology* **103**, 17-25.
- Morogan, V. and Woolley, A. R. 1988. Fenitization in the Alnö complex, Sweden: Distribution, mineralogy, and genesis. *Contributions Mineralogy Petrology* **100**, 169-182.
- Morogan, V. 1994. Ijolite versus carbonatite as sources of fenitization. *Terra Nova* **6** (2), 166-176.
- Morteani, G. and Preinfalk, C. 1996. REE distribution and REE carriers in laterites formed on the alkaline complexes of Araxá and Catalao (Brazil). In: *Rare Earth Minerals - Chemistry, origin and ore deposits* (edited by Jones, A., Wall, F. and William, T.) pp222-255. Chapman & Hall, London.
- Nakamura, N. 1974. Determination of REE, Ba, Fe, Mg, Na, and K in carbonaceous and ordinary chondrites. *Geochimica Cosmochimica Acta* **38**, 757-775.
- Nash, W. P. 1972. Mineralogy and petrology of Iron Hill carbonatite complex, Colorado. *Geological Society America Bulletin* **83**, 1361-1382.
- Nearly, C. R. and Highly, D. E. 1984. The economic importance of rare earth elements. In: *Rare Earth Element Geochemistry, Developments in Geochemistry*, 2 (edited by Henderson, P.) pp423-466. Elsevier, Amsterdam.
- Nelson, D. R., Chivas, A. R., Chappel, B. W. and McCulloch, M. T. 1988. Geochemical and isotopic systematics in carbonatites and implications for

the evolution of ocean-island sources. *Geochimica Cosmochimica Acta* **52**, 1-17.

Nesbit, H. W. 1979. Mobility and fractionation of rare earth elements during weathering of a granodiorite. *Nature* **279**, 206-210.

Notholt, A. J. G., Highley, D. E. and Deans, T. 1990. Economic minerals in carbonatites and associated alkaline rocks. *Transaction Institution Mining Metallurgy* (Section B: Applied earth science), B59 - B79.

Ngwenya, B. T. 1994. Hydrothermal rare earth mineralization in carbonatites of the Tundulu complex, Malawi: processes at the fluid/wall interface. *Geochimica Cosmochimica Acta* **58**, 2061-2072.

Ohmoto, H. 1972. Systematics of sulphur and carbon isotopes in hydrothermal ore deposits. *Economic Geology* **67**, 551-579.

Ohmoto, H. and Rye, R. O. 1979. Isotopes of sulphur and carbon. In: *Geochemistry of Hydrothermal Ore Deposits* (edited by Barnes, H. L.) pp509-567. Wiley, New York.

Onuong'a, I. O. 1983. The Geology and Geochemistry of Macalder Mine, Kenya. *MSc. dissertation*, 118p. Carleton University, Ottawa, Canada.

O'Neil, J. R., Clayton, R. N. and Mayeda, T. K. 1969. Oxygen isotope fractionations in divalent carbonates. *Journal Chemistry Physics* **51**, 5547-5558.

Overstreet, W. C. 1967. The geologic occurrence of monazite. *U.S. Geological Survey Professional Paper* **530**, 327p.

Pecora, W. P. 1956. Carbonatites: A review. *Geological Society of America Bulletin* **67**, 1537-1556.

Peseil, E. A. and Pinet, M. 1976. Contribution à la connaissance des romanéchites et des cryptomèlanes - coronadites - hollandites. Traits essentiels et paragenèses. *Contributions Mineralogy Petrology* **55**, 191-204.

Peterson, T. D. 1989a. Peralkaline nephelinites: I. Comparative petrology of Shombole and Oldoinyo Lengai, East africa. *Contributions Mineralogy Petrology* **101**, 458-478.

Peterson, T. D. 1989b. Peralkaline nephelinites: II. Low pressure fractionation and the hypersodic lavas of Oldoinyo Lengai. *Contributions Mineralogy Petrology* **102**, 336-346.

Peterson, T. D. 1990. Petrology and genesis of natrocarbonatite. *Contributions Mineralogy Petrology* **105**, 143-155.

Pineau, F., Javoy, M. and Allègre, C. J. 1973. Etude systématique des isotopes de l'oxygène du carbon et du strontium dans les carbonatites. *Geochimica Cosmochimica Acta* **51**, 2363-2377.

Platt, R. G. and Woolley, A. R. 1990. The carbonatites and fenites of Chipman Lake, Ontario. *Canadian Mineralogist* **28**, 241-250.

Powell, J. L., Hurley, P. M. and Fairbairn, H. W. 1962. Isotopic composition of strontium in carbonatites. *Nature* **196**, 1085.

Reid, D. L. and Cooper, A. F. 1992. Oxygen and carbon isotope patterns in the Dicker Willem carbonatite complex, southern Namibia. *Chemical Geology* **94**, 293-305.

Richens, D. T. (*in press*). *The chemistry of aqua ions*. Wiley, Chichester, U.K.

Robinson, B. W. 1975. Carbon and oxygen isotopic equilibria in hydrothermal calcites. *Geochemical Journal* **9**, 43-46.

Roedder, E. 1973. Fluid inclusion from fluorite deposits associated with carbonatite of Amba Dongar, India and Okorusu, South West Africa. *Transactions Institute Mining Metallurgy (Section B)* B35-B39.

Rosenbaum, J. and Sheppard, S. M. F. 1986. An isotopic study of siderites, dolomites and ankerites at high temperatures. *Geochimica Cosmochimica Acta* **50**, 1147-1150.

Rosenberg, P. E. 1967. Subsolidus studies in the system  $\text{CaCO}_3 - \text{MgCO}_3 - \text{FeCO}_3$  between 350 and 550°C. *American Mineralogist* **52**, 787-797.

Santos, R. V. and Clayton, R. B. 1995. Variations of oxygen and carbon isotopes in carbonatites: A study of Brazilian alkaline complexes. *Geochimica Cosmochimica Acta* **59**, 1339-1352.

Shackleton, R. M. 1951. A contribution to the geology of Kavirondo Rift Valley. *Quarterly Journal Geological Society London* **106**, 345-392.

Shand, S. J. 1943. *Eruptive Rocks*. 2nd edition. Thomas Murby, London.  
Sheppard, S. M. F. and Dawson, J. B. 1975. Hydrogen, carbon, and oxygen isotopes studies of megacrysts and matrix minerals from Lesothan and South African kimberlites. *Physics and Chemistry of the Earth* **9**, 747-763.

Sheppard, S. M. F. 1986. Characterization and isotopic variations in Natural Waters. In: *Stable Isotopes in High Temperature Geological Processes* (edited Valley, J. W., Taylor, H. P. and O'Neil, J. R.) pp165-183 *Reviews in Mineralogy* **16**, Mineralogical Society America.

Silva, L. C., Le Bas, M. J. and Robertson, A. H. F. 1981. An oceanic carbonatite volcano on Santiago, Cape Verde Islands. *Nature* **294**, 644-645.

Simonetti, A. and Bell, K. 1994. Isotopic and geochemical investigation of the Chilwa Island carbonatite complex, Malawi: Evidence for a depleted mantle source region, liquid immiscibility, and open-system behaviour. *Journal Petrology* **35**, 1597-1621.

Simonetti, A., Bell, K. and Viladkar, S. G. 1995. Isotopic data from the Amba Dongar carbonatite Complex, west-central India: Evidence for an enriched mantle source. *Chemical Geology (Isotope Geoscience Section)* **122**, 185-198.

Smith, W. C. 1956. A review of some problems of African carbonatites. *Quarterly Journal Geological Society London* **112**, 189-220.

Sokolov, S. V. 1985. Carbonates in ultramafic alkali-rock, and carbonatite intrusions. *Geochemistry International* **22**, 150-166.

Streckeisen, A. 1980. Classification and nomenclature of volcanic rocks, lamprophyres, carbonatites and melilitic rocks. IUGS Subcommittee on the Systematics of Igneous Rocks. *Geologische Rundschau* **69**, 194-207.

Sutherland, D. S. 1969. Sodic amphiboles and pyroxenes from fenites in East Africa. *Contributions Mineralogy Petrology* **24**, 114-135.

Suwa, K., Oana, S., Wada, H. and Osaki, S. 1975. Isotope geochemistry and petrology of African carbonatites. *Physics Chemistry Earth* **9**, 735-745.

Sverjensky, D. A. 1984. Europium redox equilibria in aqueous solution. *Earth Planetary Science Letters* **67**, 70-78.

Sweeney, R. J. 1994. Carbonatite melt compositions in the earth's mantle. *Earth Planetary Science Letters* **128**, 259-270.

Taylor, B. E. 1986. Magmatic volatiles; Isotopic variation of C, H, and S. In: *Stable Isotopes in High Temperature Geological Processes* (edited by Valley, J. W., Taylor, H. P., Jr. and O'Neil, J. R.) pp185-225. *Reviews in Mineralogy* **16**, Mineralogical Society America.

Taylor, H. P., Frechen, J. and Degens, T. 1967. Oxygen and carbon isotope studies of carbonatites from the Laacher See district W.Germany and Alno district Sweden. *Geochimica Cosmochimica Acta* **31**, 407-430.

Taylor, S. R. and McLennan, S. M. 1985. *The continental crust: its composition and evolution*. Blackwell, Oxford.

Tazaki, K., Fyfe, W. S. and Dissanayake, C. B. 1987. Weathering of apatite under extreme conditions of leaching. *Chemical Geology* **60**, 151-162.

Twyman, J. D. and Gittins, J. 1987. Alkalic carbonatite magma: parental or derivative? In: *Alkaline Igneous Rocks* (edited by Fitton, J. G. and Upton, B. G. J.) pp85-94. *Geological Society Special Publication* **30**.

Van Couvering, J. A. and Miller, J. A. 1969. Miocene stratigraphy and age determinations, Rusinga Island, Kenya. *Nature* **221**, 628-632.

Varne, R. 1968. The petrology of Moroto Mountain, eastern Uganda, and the origin of nephelinites. *Journal Petrology* **9**, 169-190.

Von Gehlen, K. 1967. Sulphur isotopes from the sulphide bearing carbonatite of phalaborwa, South Africa. *Transaction Institute Mining Metallurgy* **76B**. Abstract.

Von Maravic, H., Morteani, G. and Roethe, G. 1989. The cancrinite-syenite/carbonatite complex of Lueshe, Kivu/NE-Zaire: petrographic and geochemical studies and its economic significance. *Journal African Earth Sciences* **9**, 341-355.

Wakita, H., Rey, P. and Schmitt, R. A. 1971. Abundances of the 14 rare earth elements and 12 other trace elements in Apollo 12 samples: five igneous and one breccia rocks and four soils. *Proceedings of the Second Lunar Science Conference* 1319-1329.

Wall, F., Le Bas, M. J. and Srivastava, R. K. 1993. Calcite and carbocernaite exsolution and coectic texture in Sr, REE-rich carbonatite dyke from Rajasthan, India. *Mineralogical Magazine* **57**, 495-513.

Wall, F. and Mariano, A. N. 1996. Rare earth minerals in carbonatites: a discussion centred on the Kangankunde Carbonatite, Malawi. In: *Rare Earth Minerals - Chemistry, origin and ore deposits* (edited by Jones, P., Wall, F. and Williams, C. T.) pp193-225. Chapman & Hall, London.

Wallace, M. E. and Green, D. H. 1988. An experimental determination of primary carbonatite magma composition. *Nature* **335**, 343-346.

Walter, A.-V., Nahon, D., Flicoteaux, R., Girard, J. P. and Melfi, A. 1995a. Behaviour of major and trace elements and fractionation of REE under tropical weathering of a typical apatite-rich carbonatite from Brazil. *Earth Planetary Science Letters* **136**, 591-602.

Walter, A.-V., Flicoteaux, R., Parron, C., Loubet, M. and Nahon, D. 1995b. Rare earth elements and isotopes (Sr, Nd, O and C) in minerals from Juquiá carbonatite (Brazil): Tracers of a multi-stage evolution, *Chemical Geology* **120**, 27-44.

Watkinson, D. H. and Wyllie, P. J. 1969. Phase equilibrium studies bearing on the limestone-assimilation hypothesis. *Geological Society America Bulletin* **80**, 1565-1576.

Watkinson, D. H. and Wyllie, P. J. 1971. Experimental study on the join  $\text{NaAlSiO}_4$  -  $\text{CaCO}_3$  -  $\text{H}_2\text{O}$  and the genesis of alkalic rock-carbonatite complexes. *Journal Petrology* **12**, 357-378.

Watson, M. D. and Snyman, C. P. 1975. The geology and mineralogy of the fluorite deposits at the Buffalo fluorspar mine on Buffelsfontein, 347KR, Naboomspruit District. *Transactions Geological Society South Africa* **78**, 137-151.

Wood, S. A. 1990a. The aqueous geochemistry of rare earth elements and yttrium 1. Review of available low-temperature data for inorganic complexes and the inorganic REE speciation of natural waters. *Chemical Geology* **89**, 99-125.

Wood, S. A. 1990b. The aqueous geochemistry of rare earth elements and yttrium 2. Theoretical predictions of speciation in hydrothermal solutions to 350°C at saturation water vapour pressure. *Chemical Geology* **89**, 99-125.

Wood, D. A., Joron, J. L. and Treuil, M. 1979. A reappraisal of the use of trace elements to classify and discriminate between magma series erupted in different tectonic settings. *Earth Planetary Science and Letters* **45**, 326-336.

Woolley, A. R. 1982. A discussion of carbonatite evolution and nomenclature, and the generation of sodic and potassic fenites. *Mineralogical Magazine* **46**, 13-17.

Woolley, A. R. and Kempe, D. R. C. 1989. Carbonatites: nomenclature, average chemical compositions and element distribution. In: *Carbonatites, Genesis and Evolution* (edited by Bell, K.) pp1-14. Unwin Hyman, London.

Woolley, A. R., Barr, M. W., Din, V. K., Jones, G. C., Wall, F. and Williams, C. T. 1991. Extrusive carbonatites from Uyaynah Area, United Arab Emirates. *Journal of Petrology* **32**, 1143-1167.

Wyllie, P. J. and Tuttle, O. F. 1960. The system CaO-CO<sub>2</sub>-H<sub>2</sub>O and the origin of carbonatites. *Journal of Geology* **1**, 1-96.

Wyllie, P. J. 1965. Melting relationships in the system CaO - MgO - CO<sub>2</sub> -H<sub>2</sub>O with petrological implications. *Journal of Geology* **6**, 101-123.

Wyllie, P. J. and Huang, W. L. 1975. Peridotite, kimberlite, and carbonatite explained in the system CaO-MgO-CO<sub>2</sub>. *Geology* **3**, 621-624.

Wyllie, P. J. 1989. Origin of carbonatites - Evidence from phase equilibrium studies. In: *Carbonatites: Genesis and Evolution* (edited by Bell, K.) pp500-545. Unwin Hyman, London.

Wyllie, P. J., Baker, M. B. and White, B. S. 1990. Experimental boundaries for the origin and evolution of carbonatites. *Lithos* **26**, 3-19.

Wyllie, P. J., Jones, A. P. and Deng, J. 1996. Rare earth elements in carbonate-rich melts from the mantle to crust. In: *Rare Earth Minerals - Chemistry, origin and ore-deposits* (edited by Jones, A. P., Wall, F. and Williams, C. T.) pp77-103. Interscience, New York.

Zheng, Y.-F. 1990. The selective flux of sulphur and implications for magmatic sulphur isotope fractionations. *Isotopenpraxis* **26**, 371-374.

Zheng, Y.-F. and Hoefs, J. 1993. Stable isotope geochemistry of hydrothermal mineralizations in Harz Mountains: I. Carbon and oxygen isotopes of carbonates and implications for the origin of hydrothermal fluids. In: *Formation of hydrothermal vein deposits*. (edited by Möller, P. and Lüders, V.) pp169-187. Monograph Series on Mineral Deposits **30**.

Zheng, Y.-F. and Hoefs, J. 1993. Stable isotope geochemistry of hydrothermal mineralizations in Harz Mountains: II. Sulphur and oxygen isotopes of sulphides and sulphates and constraints on metallogenetic models. In: *Formation of hydrothermal vein deposits*. (edited by Möller, P. and Lüders, V.) pp 211-229. Monograph Series on Mineral Deposits **30**.

**APPENDICES**

## APPENDIX 5-1

### X.RAY DIFFRACTION ANALYSIS (XRD)

#### SAMPLE PREPARATION.

##### 1. Whole rock or mineral separate.

The samples were crushed using a Tungsten carbide Tema mill or hand ground in an Agate and Pestle until the grain size of the powder was less than 200 mesh. The powdered sample was then packed into a sample holder and analyzed.

##### 2. Analysis.

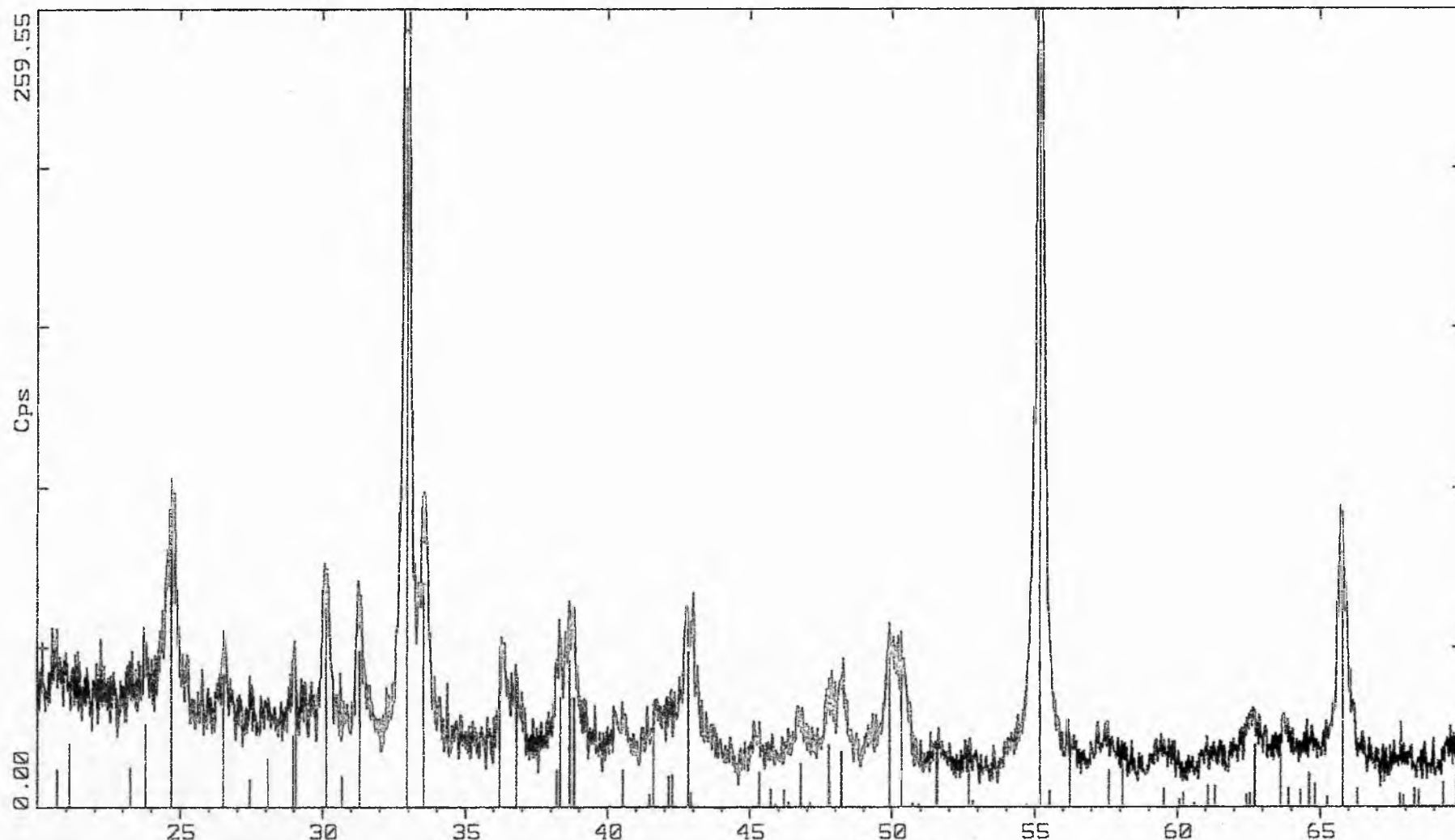
X-ray diffraction analysis was performed using a Philips PW1050 Goniometer-Hiltonbrooks Generator with a Cu or Co ( for Fe rich samples) X-ray tube for primary excitation. The machine is equipped with an automatic sample changer (36 sample capacity) and a PC controlled step motor drive. Typical conditions used for a 5° to 70° Two Theta scan were; 40Kv, 35mA, 1° divergence slit, 2 mm receiving slit. 0.02° theta/sec scan speed and a graphite monochrometer.

The resulting diffractograms were interpreted and printed using the Siemens DiFFRAC AT software package.

**APPENDIX 5-2****SELECTED DIFFRACTOGRAMS**

2-Theta - Scale

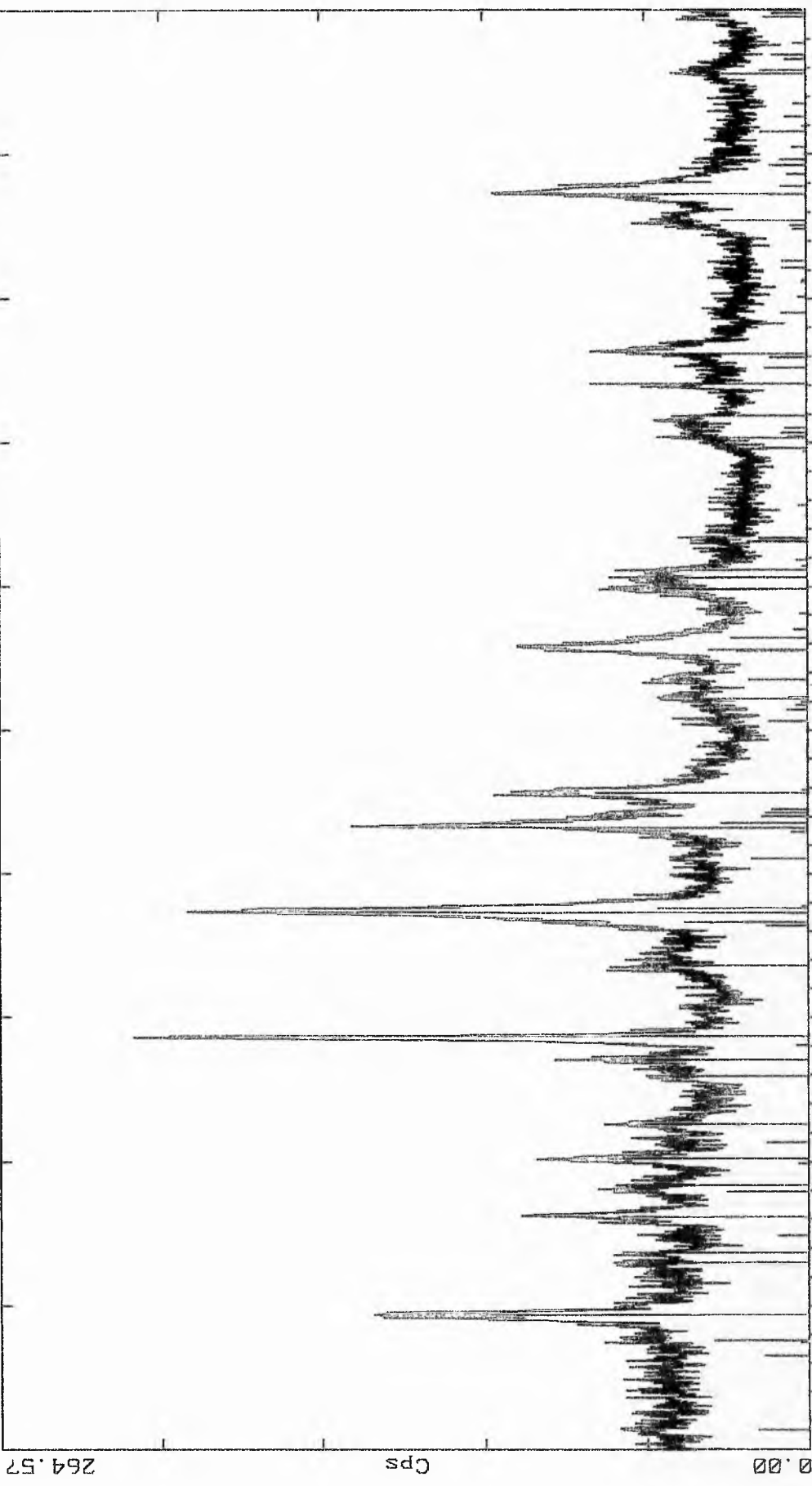
Dept of Geology, St Andrews University. 27-Oct-1994 10:59



C:\XRDUXD\ISAAC2\BR1.RAW WH ROCK (CT: 1.0s, SS:0.020dg, WL: 1.7890Ao, y : xxxxxxxx)  
5-0448 D BaSO4 Barite (WL: 1.7890Ao)  
29-0713 I FeO(OH) Goethite (WL: 1.7890Ao)  
24-0072 D Fe2O3 Hematite (WL: 1.7890Ao)  
4-0864 D CaF2 Fluorite, syn (WL: 1.7890Ao)  
11-0340 I CeCO3F Bastnaesite-(Ce) (WL: 1.7890Ao)

Dept of Geology, St Andrews University. 27-Oct-1994 11:27

2-Theta - Scale



C:\XRDUXD\ISAAC2\BR8.RAW WH ROCK (CT: 1.0s, SS:0.020ds, WL: 1.7890Ao, y : \*\*\*\*\*)

24-0027 D CaCO3 Calcite (WL: 1.7890Ao)

5-0448 D BaSO4 Barite (WL: 1.7890Ao)

29-0713 I FeO(OH) Goethite (WL: 1.7890Ao)

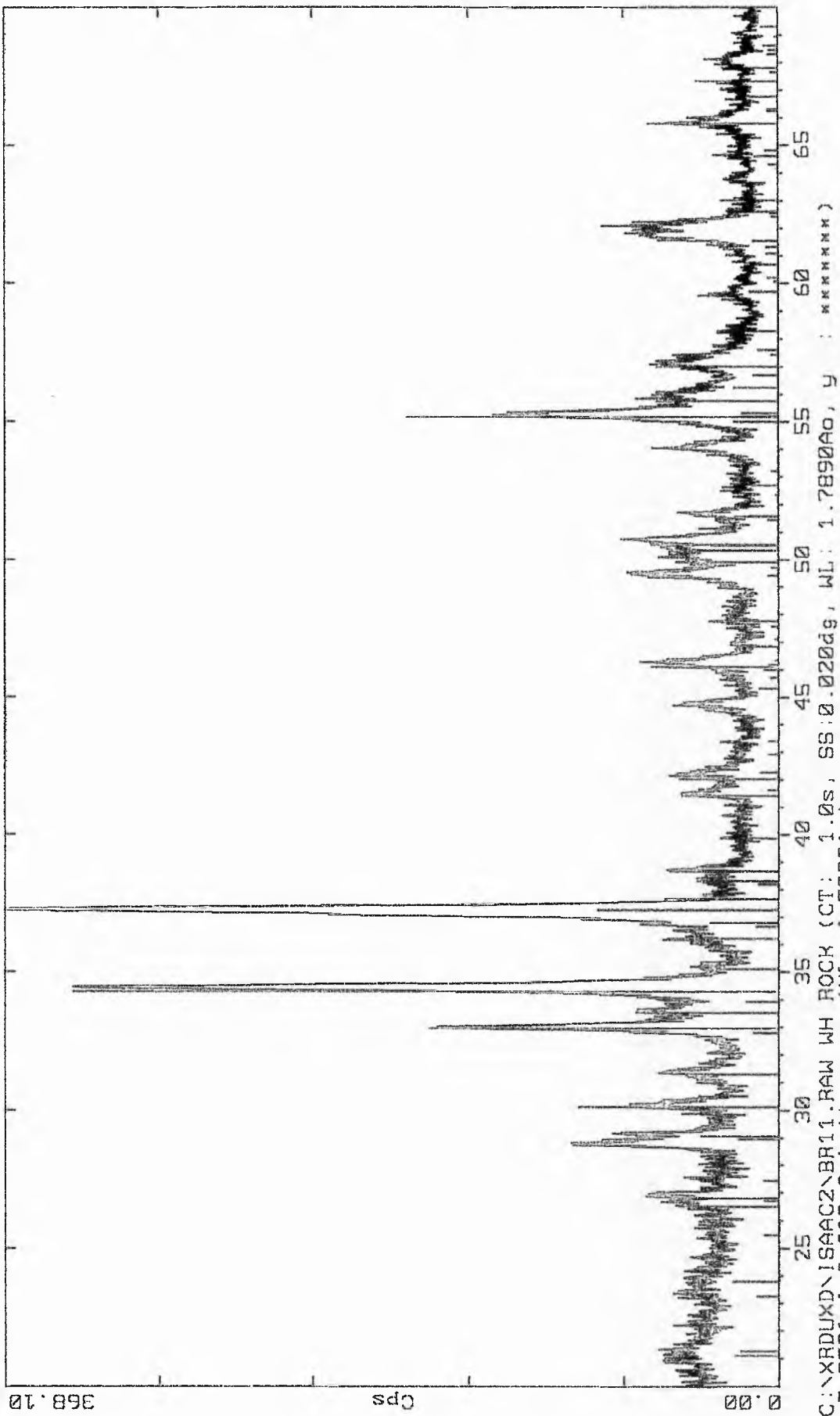
24-0072 D Fe2O3 Hematite (WL: 1.7890Ao)

4-0864 D CaF2 Fluorite, syn (WL: 1.7890Ao)

27-0032 I BaCa(CO3)2 Alstonite (WL: 1.7890Ao)

Dept of Geology, St Andrews University. 27-Oct-1994 11:44

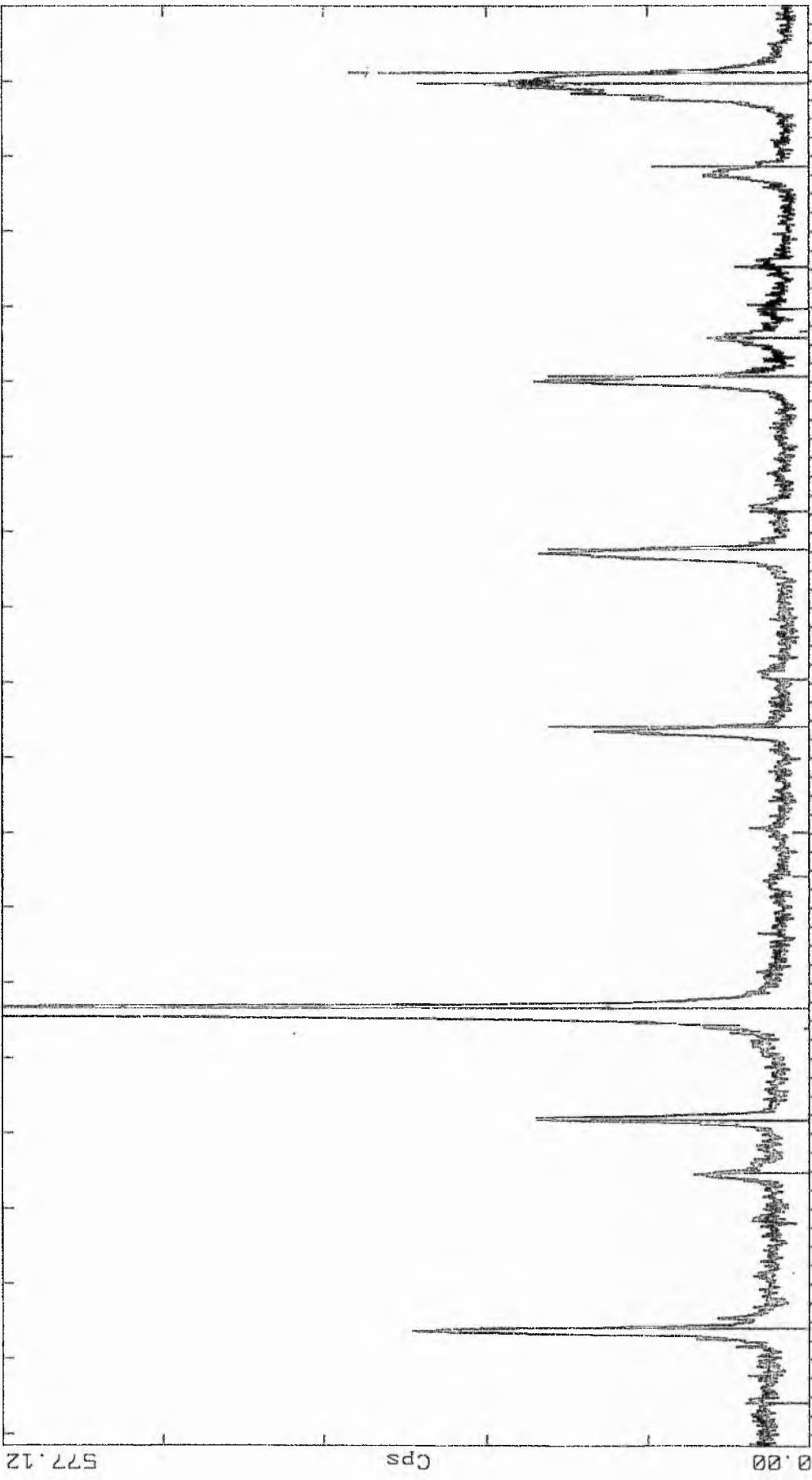
2-Theta - Scale



C:\XRD\UXD\ISAAC2\BR11.RAW WH ROCK (CT: 1.0s, SS:0.020ds, WL: 1.7890Ao, Y : \*\*\*\*\*)  
 5-0586 I CaCO3 Calcite, syn (WL: 1.7890Ao)  
 5-0448 D BaSO4 Barite (WL: 1.7890Ao)  
 4-0864 D CaF2 Fluorite, syn (WL: 1.7890Ao)  
 11-0340 I CeCO3F Bastnaesite-(Ce) (WL: 1.7890Ao)  
 11-0614 D Fe3O4 Magnetite (WL: 1.7890Ao)  
 15-0876 \* Ca(P04)3F Fluorapatite, syn (WL: 1.7890Ao)

Dept of Geology, St Andrews University, 25-Mar-1994 15:15

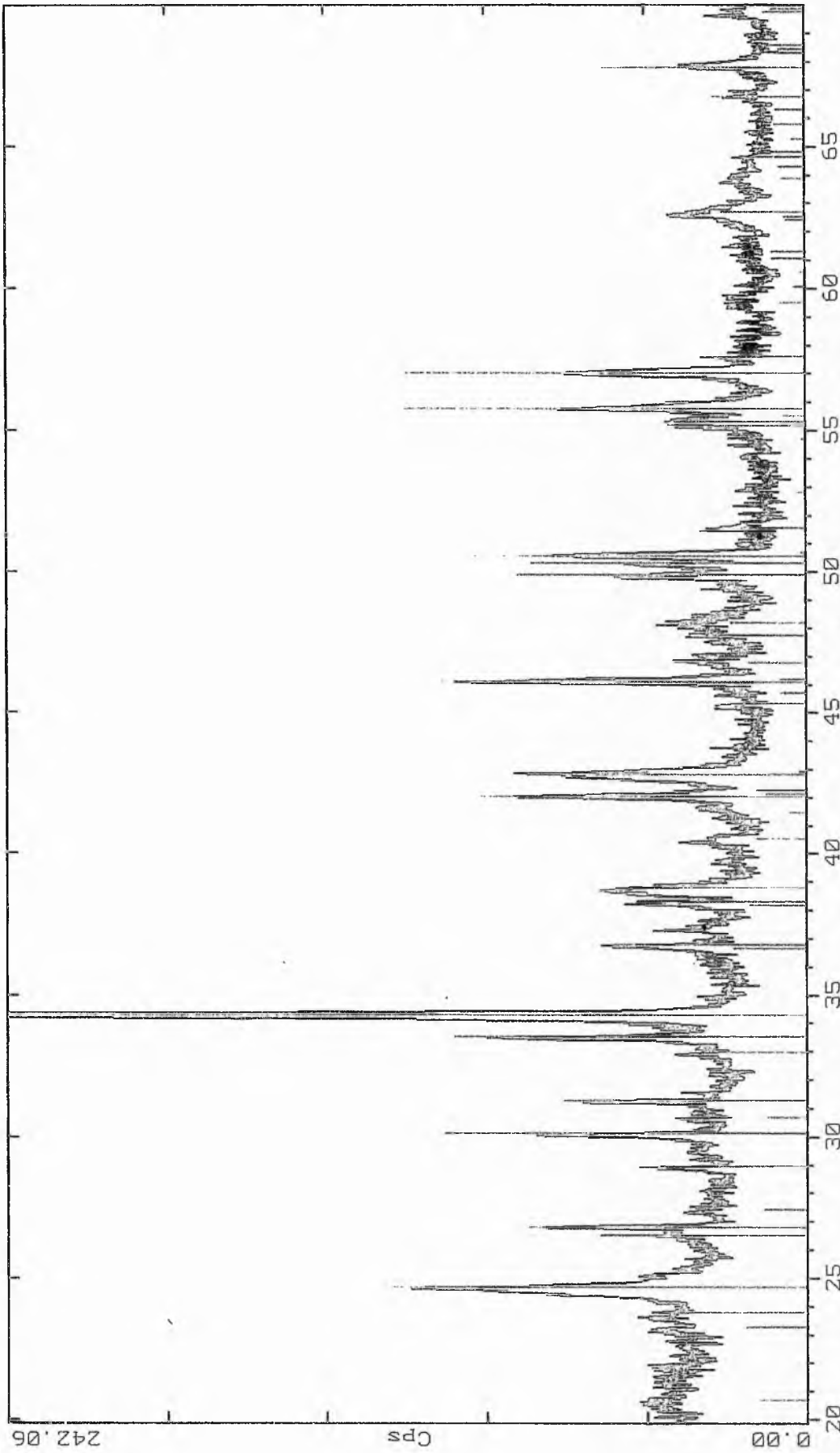
2-Theta - Scale



26 28 30 32 34 36 38 40 42 44 46 48 50 52 54 56 60 62  
 C:\UXD\ISAAC\BR183.RAW WH ROCK (CT: 1.0s, SS:0.020dg, WL: 1.7890Ao, X : \*\*\*\*\*)  
 29-0696 \* FeCO3 Siderite (WL: 1.7890Ao)  
 24-0027 D CaCO3 Calcite (WL: 1.7890Ao)  
 4-0864 D CaF2 Fluorite, syn (WL: 1.7890Ao)

Z-Theta - Scale

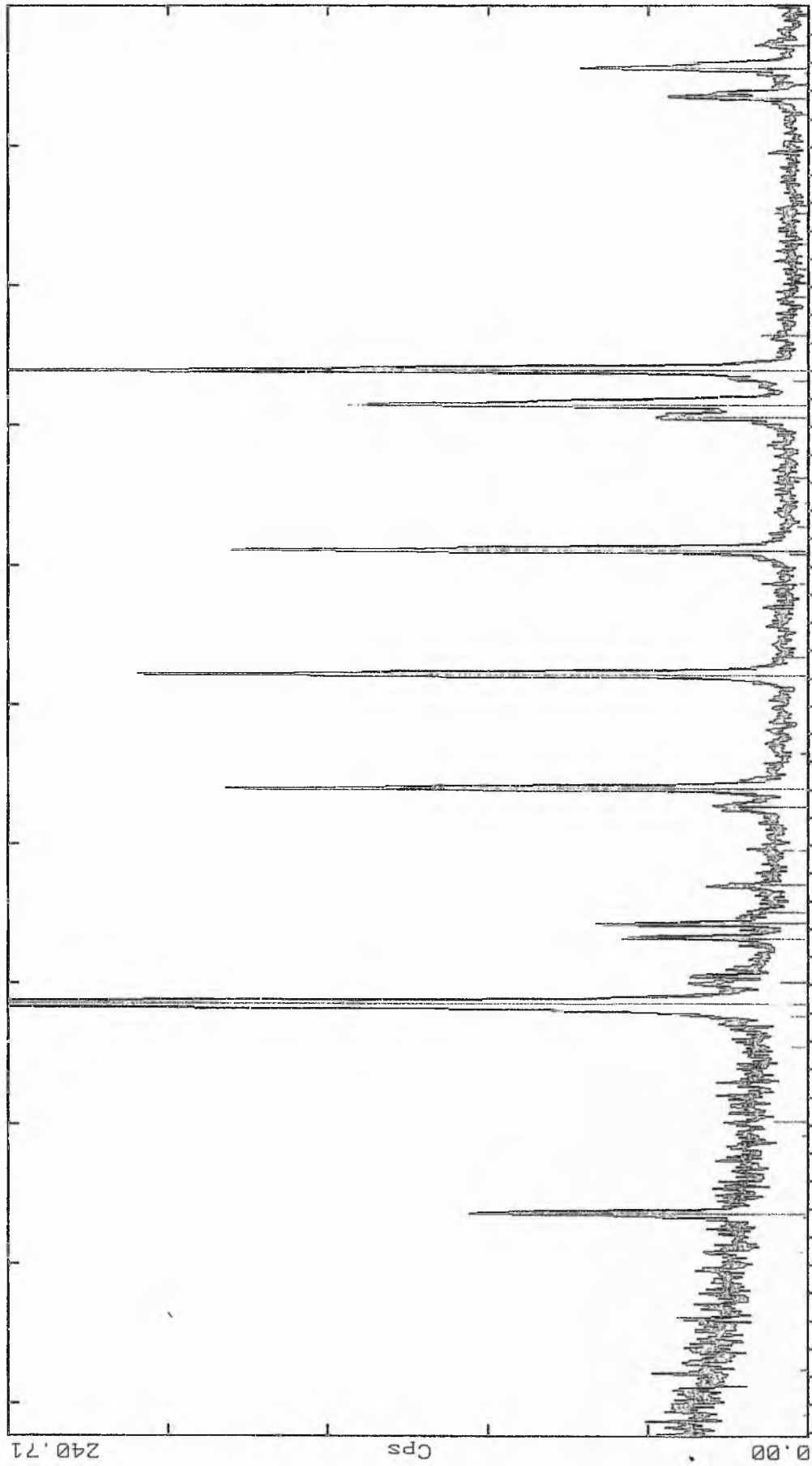
Dept of Geology, St Andrews University, 21-Mar-1994 13:15



C:\UXD\ISAAC\KG72.RAW MH ROCK (CT: 1.0s, SS:0.020dg, WL: 1.7890Ao, x : \*\*\*\*\*)  
 S-0385 CaSO<sub>4</sub> Barite (JCPDS 07-07-0500)  
 S-0448 BaSO<sub>4</sub> Barite (JCPDS 07-07-0500)  
 4-0864 CaSO<sub>4</sub> Barite (JCPDS 07-07-0500)

Dept of Geology, St Andrews University, 25-Mar-1994 12:54

Z-Theta - Scale



C:\UXD\ISAAC\NR280.RAW WH ROCK (CT: 1.0s, SS:0.020dg, WL: 1.7890Ao, X : \*\*\*\*\*)  
 5-0586 Calcite  
 19-0629 \* FeFe2O4 Magnetite, syn (WL 1.7890Ao)  
 19-0629 \* FeFe2O4 Magnetite, syn (WL 1.7890Ao)

## APPENDIX 6-1

### X-RAY FLUORESCENCE ANALYSIS

#### SAMPLE PREPARATION.

##### 1. Crushing.

The samples were crushed and split using a hydraulic splitter to approx 3-4 " blocks. These blocks were then fed into a jaw crusher to reduce the rock to small chips (approx 1-2 cm). The chips were ground in a Tungsten Carbide 'Tema' mill until the grain size of the powder was less than 200 mesh.

##### 2. Major elements - Fused glass discs.

666 g of Spectroflux 105 was added to a 95% Pt / 5% Au crucible and fused at 950°C for 15 minutes. 0.500 g of rock powder and 0.05 g of oxidant (ammonium nitrate) was then added to the fused flux, which was then re-fused at 950°C for 30 minutes. The resulting mix was re-heated and cast into 32 mm glass discs. This method is essentially that of Norrish and Hutton (1968).

##### 3. Trace elements - Pressed powder pellets.

7-8 g of rock powder was mixed thoroughly with 10-12 drops of polyvinyl alcohol binder (Movial). The rock and binder were compressed using a hydraulic press and a 32 mm die to 12 tons per square inch for 5 minutes. The pellets were then numbered and placed in an oven set at 80-100°C for 3-4 hours to dry.

Note: During the procedure for bead preparation it was found that the beads were not combining well with the carbonatite rock samples. A 50 % silica matrix was added to the carbonatite samples to allow the flux to form a bead.

A computer conversion equation was generated to remove the effects of adding the SiO<sub>2</sub> from the final analysis.

#### 4. Analysis.

X-ray analysis was performed using a Philips PW 1450/20 automatic sequential spectrometer with a Rh X-Ray tube for primary excitation. Calibration was done by reference to a monitor (H12), supplied by K. Norrish and using 25 international rock standards. The method uses a calculated regression line through apparent fluorescence values (AFV's) to calculate a value for H12.

Matrix corrections for the major elements were applied using coefficients for the Rh tube supplied by K. Norrish. Matrix corrections for the trace elements were applied using major element data. The methods and conditions were generally similar to those described by Norrish and Chappell (1977). All intensities were calculated in terms of a ratio to the monitor (H12), which was always in the first sample position to eliminate the effects of machine drift. For consistency, all calculations were performed by an on-line computer.

**APPENDIX 6-2 (1-4)**

	SiO <sub>2</sub>	TiO <sub>2</sub>	Al <sub>2</sub> O <sub>3</sub>	Fe <sub>2</sub> O <sub>3</sub>	MnO	MgO	CaO	Na <sub>2</sub> O	K <sub>2</sub> O	P <sub>2</sub> O <sub>5</sub>	P.LOSS
BR-1	0.10	0.46	0.50	27.52	6.90	0.46	25.36	0.10	0.08	1.66	7.20
BR-3	0.00	0.16	0.70	16.00	8.42	0.38	35.46	0.22	0.16	1.60	7.20
BR-4	1.42	0.44	0.74	40.50	8.18	0.68	11.86	0.26	0.38	2.32	10.80
BR-7	1.50	0.14	0.22	53.22	10.02	0.46	10.02	0.12	0.06	1.08	15.60
BR-8	0.86	0.54	0.27	55.17	9.14	0.35	8.08	0.10	0.07	0.49	12.60
BR-9	1.76	0.14	0.24	26.02	5.08	1.46	22.74	0.22	0.20	0.76	30.40
BR-10	1.80	0.48	0.22	16.14	3.50	1.14	33.16	0.46	0.26	1.18	23.60
BR-11	0.00	0.48	0.20	22.86	3.74	1.16	28.02	0.26	0.08	1.08	27.20
BR-12	0.00	0.20	0.38	11.04	3.46	1.62	34.58	0.28	0.20	4.10	30.00
BR-13	11.57	0.40	2.62	14.83	2.31	2.08	25.77	0.71	1.52	1.38	25.40
BR-15	0.00	0.20	0.22	12.68	4.78	0.92	33.82	0.30	0.10	0.44	27.60
BR-16	1.29	0.25	0.49	20.69	2.64	1.44	31.90	0.48	0.27	0.15	33.40
BR-17	1.18	0.66	0.36	23.38	3.88	1.38	24.08	0.30	0.16	0.90	24.80
BR-19	2.24	0.84	0.96	29.00	5.60	1.68	16.64	0.52	0.24	2.72	23.20
BR-20	0.00	0.12	0.16	46.52	10.20	1.10	1.02	0.20	0.04	0.02	28.40
BR-27	2.70	0.42	0.35	14.20	4.52	4.14	30.08	0.18	0.30	0.76	28.80
BR-28	2.59	0.19	0.22	19.94	4.51	2.66	24.92	0.53	0.32	4.53	26.00
BR-46	0.82	0.62	0.49	24.00	4.78	0.62	35.80	0.24	0.27	2.98	23.00
BR-49	1.96	0.93	0.56	47.07	5.99	0.61	15.37	0.14	0.26	0.98	16.00
BR-50	0.56	0.49	0.49	28.03	5.63	0.68	24.4	0.20	0.21	3.16	18.60
BR-51	1.96	0.42	0.62	33.65	6.19	0.73	20.87	0.21	0.34	2.54	18.80
BR-53	0.47	0.22	0.32	15.56	2.73	0.85	39.75	0.15	0.16	1.64	31.20
BR-54	2.72	0.29	0.56	42.94	5.61	0.80	19.04	0.28	0.27	1.32	17.60
BR-56	2.35	0.24	0.63	46.12	9.50	0.69	6.35	0.15	0.38	0.17	15.6
BR-58	3.18	0.33	1.04	18.64	4.09	1.96	22.88	0.31	0.94	2.35	24.4
BR-59	1.69	0.41	0.85	17.73	3.58	2.61	27.83	0.38	0.78	1.22	32.00

Major elements in wt %; P.Loss = Powder loss.

1. Major elements from the Buru carbonatite centre. Analyses by XRF.

	Nb	Zr	Y	Sr	U	Pb	Th	Pb	Zn	Cu	Ni	Ce	Ba	La
Selected samples from BRL-1														
BR-1	678	197	464	2214	201	5	413	1300	2642	19	38	>10000	>10000	7800
BR-3	195	119	612	1928	162	4	574	437	1712	10	49	>10000	>10000	9200
BR-4	848	139	1368	1665	4	20	1487	1248	2895	0	114	8500	>10000	5300
BR-7	492	38	513	789	9	1	1239	701	1456	2	56	5000	>10000	2600
BR-8	765	122	547	999	5	2	1155	1502	2347	8	50	2986	>10000	1494
BR-9	251	105	882	1508	0	10	970	568	1865	0	58	4564	>10000	2980
BR-10	849	99	426	2205	8	12	261	518	947	8	28	8000	>10000	7200
BR-12	679	72	363	2830	28	9	344	809	1343	2	27	5800	>10000	6000
BR-15	434	136	169	2550	0	3	264	849	1760	5	18	>10000	>10000	7200
BR-16	921	98	548	2681	0	6	658	531	1700	5	51	3200	>10000	1800
BR-17	998	172	516	7967	0	61	380	373	1100	5	69	6100	>10000	2200
BR-19	1612	179	893	10120	0	17	819	747	1425	5	68	6100	>10000	2200
BR-20	210	278	888	2600	0	0	988	102	516	0		844	>10000	154
BR-27	873	153	163	19451	0	15	248	927	1666	26	14	>10000	>10000	>10000
BR-28	202	142	320	33000	0	8	314	613	1390	40	27	4750	9000	1850
Selected samples from BRL-3														
BR-46	743	58	497	2003	7	21	549	1173	1933	5	40	33	>10000	>10000
BR-49	1320	58	299	1019	4	15	651	929	2011	15	24	18	>10000	3500
BR-50	934	116	567	1893	10	8	885	802	2100	0	49	22	>10000	8200
BR-51	1035	92	662	1737	7	21	773	980	3487	5	52	19	>10000	4950
BR-53	467	41	257	2148	9	13	266	768	1286	8	19	13	>10000	400
BR-54	716	57	535	1640	5	16	1015	1134	2581	0	45	21	>10000	3700
BR-56	379	71	303	1047	0	18	756	959	1971	15	33	6	>10000	1200
BR-58	577	134	436	11000	0	42	653	566	1436	6	31	14	>10000	4200
BR-59	1332	75	374	1877	10	36	609	767	1200	0	26	12	>10000	3300

Trace elements in ppm

2. Trace elements from the Buru carbonatite centre. Analyses by XRF.

3) Major elements from the ferrocarbonatite breccia, Kuge carbonatite centre.

	KG-66	KG-69	KG-71	KG-76	KG-80	KG-94
SiO <sub>2</sub>	1.54	0.00	1.40	3.50	12.22	2.46
TiO <sub>2</sub>	0.26	0.12	0.04	0.06	0.56	0.50
Al <sub>2</sub> O <sub>3</sub>	0.62	0.34	0.60	1.42	4.48	0.82
Fe <sub>2</sub> O <sub>3</sub>	27.64	11.28	16.18	35.86	20.66	9.76
MnO	3.94	3.58	7.42	9.38	2.64	2.12
MgO	0.68	0.62	0.66	0.66	2.82	1.00
CaO	30.64	23.36	26.40	18.08	22.52	41.0
Na <sub>2</sub> O	0.42	0.51	0.40	0.28	0.28	0.30
K <sub>2</sub> O	0.16	0.08	0.08	0.06	1.76	0.36
P <sub>2</sub> O <sub>5</sub>	0.50	0.24	2.58	3.40	0.34	0.14
P.LOSS.	29.20	22.40	25.20	21.60	22.80	34.0

Trace elements from the ferrocarbonatite breccia, Kuge carbonatite.

La	8200	5600	6100	237	3600	5000
Ce	8000	4200	>10000	1877	4300	10000
Sr	1540	844	1613	2657	1245	761
Ba	>10000	>10000	>10000	>10000	>10000	10000
Nb	65	38	45	914	411	132
Zn	2850	1042	1640	1285	1746	1600
Y	103	50	191	699	113	151
Rb	3	0	1	1	31	1
Pb	160	118	877	1407	576	1038
Th	113	108	334	677	158	242
U	20	2	0	3	0	0
Cu	27	7	14	20	125	1
Ni	19	2	14	55	55	14
Cr	34	0	6	39	94	30
V	256	57	73	174	283	234
Zr	103	50	191	61	70	34

Note: KG-66 to KG-76 obtained from drill hole KG-2  
 KG-80 - drill hole KG-4  
 KG-94 - drill hole KG-3

Oxides in wt %, trace elements in ppm  
 P. Loss = Powder loss.

Sample	SiO <sub>2</sub>	TiO <sub>2</sub>	Al <sub>2</sub> O <sub>3</sub>	Fe <sub>2</sub> O <sub>3</sub>	MnO	MgO	CaO	Na <sub>2</sub> O	K <sub>2</sub> O	P <sub>2</sub> O <sub>5</sub>	LOSS
Drill hole BR-16											
BR-29	43.25	0.43	8.56	14.9	2.99	2.71	7.02	2.09	5.81	0.06	8.8
BR-31	49.04	0.8	14.72	6.28	0.23	2.44	7.39	3.05	5.14	0.05	7.8
BR-32	53.35	0.76	14.89	9.31	0.78	2.5	4.53	3.48	3.62	0.1	5.4
BR-33	62.23	0.57	15.65	4.99	0.09	2.41	3.89	3.97	3.25	0.12	2.8
BR-34	54.06	0.75	16.09	6.7	0.43	2.84	6.45	3.88	3.1	0.17	5
Drill hole BR-17											
BR-101	45.93	0.85	14.65	12.74	1.88	0.94	1.64	0.37	10.52	0.02	5
BR-102	53.05	0.71	16.27	9.14	1.26	1.01	0.48	0.41	12.46	0.05	3.2
BR-106	55.1	0.57	19.63	5.69	0.42	0.7	0.99	1.11	10.56	0.04	4.8
BR-107	23.84	0.79	6.2	26.22	4.31	2.11	11.68	0.18	5.03	0.21	7.2
Drill hole BR-20											
BR-108	59.43	0.58	12.98	9.42	0.53	0.67	0.63	2.26	9.45	0.03	1.6
BR-109	58.78	0.52	11.7	11.36	1.04	0.74	1.07	3	7.97	0.02	2.8
BR-110	41.84	0.59	6.58	15.32	1.82	2.61	5.15	1.99	6	0.02	12.4
BR-111	52.64	0.57	10.68	11.1	1.3	1.24	2.18	2.75	7.96	0.01	6.8
BR-112	56.12	0.27	12.06	9.88	0.79	1.15	1.52	3.36	5.95	0.04	7.2
Drill hole BR-23											
BR-113	68.16	0.33	18.2	1.09	0.09	0.53	0.16	5.37	4.83	0.04	1.8
BR-114	74.46	0.24	13.53	1.79	0.02	0.34	0.13	4.32	3.89	0.02	1.8
BR-115	72.79	0.25	14.29	1.7	0.21	0.46	0.13	4.2	4.02	0.03	2.4
BR-116	71.78	0.22	14.24	1.83	0.19	0.41	0.42	4.36	4.27	0.03	2.2
BR-117	71.95	0.24	13.55	1.99	0.04	0.28	1.07	3.69	5.09	0.03	2

4) Major element analysis of the fenitized gneisses from the Buru carbonatite centre.

## APPENDIX 7-1

### SAMPLE PREPARATION AND STABLE ISOTOPE EXPERIMENTAL PROCEDURES

#### Sample preparation.

Samples were crushed and sieved to 125 microns. They were then washed in cold water and dried before being separated into lighter and heavier phases using Tetrabromoethane of specific gravity 2.96.

Clean grains of calcite and siderite were separated from the other phases by hand-picking beneath a binocular microscope and checked for purity by XRD. The relative abundances of calcite and siderite in the samples were estimated on the basis of the intensity of the X ray diffraction peaks. Some of the calcite and siderite concentrates, however, contained up to 10-15% grains of mainly fluorite, barite and iron hydroxides/oxides.

For barite, the heavy fraction was washed with hydrochloric acid to remove carbonates attached to the barite or iron hydroxides/oxides. X-ray analysis of the concentrate showed goethite, hematite and fluorite to be present in varying amounts. No attempt was made to separate the oxides, which are considered not to affect the carbon dioxide extraction procedure.

#### Experimental procedures.

Carbon dioxide from the calcites was released by the action of 103% phosphoric acid of specific gravity >1.92 in a vacuum at 25°C following the method of McCrea (1950). About 30 mg of siderite/calcite was reacted with phosphoric acid at 25°C for 24 hours in order to remove CO<sub>2</sub> produced from calcite. The released carbon dioxide was collected and discarded. Siderite

was then reacted at 100°C for 12 hours according to Rosenbaum and Sheppard (1986). The evolved CO<sub>2</sub> was then purified according to McCrea (1950). Isotopic measurements were made on a VG SIRA 10 mass spectrometer at the Scottish Universities Research and Reactor Centre (SRRC) with  $\delta^{13}\text{C}$  reported relative to PDB and  $\delta^{18}\text{O}$  reported relative to SMOW. The precision for both the  $\delta^{13}\text{C}$  and  $\delta^{18}\text{O}$  was better than  $\pm 0.2\%$ . Because of oxygen isotope fractionation during CO<sub>2</sub> release, calcite and siderite values were corrected using the oxygen fractionation factor of  $10^3 \ln \alpha = 10.25$  for calcite at 25°C and  $10^3 \ln \alpha = 8.77$  for siderite at 100°C, according to Rosenbaum and Sheppard (1986).

Approximately 50-80 mg of barite concentrate was mixed and ground with 200 mg of Cu<sub>2</sub>O and 600 mg of silica. The mixture was reduced quantitatively in a vacuum at 1120°C according to Coleman and Moore (1978). The addition of fine silica sand to the sample Cu<sub>2</sub>O mixture and the higher combustion temperature ensured maximum conversion to SO<sub>2</sub>. The evolved gases were passed over Cu at 600°C to reduce any SO<sub>3</sub> to SO<sub>2</sub>. The yield was measured on a capacitance manometer. The isotope composition of sulphur in the SO<sub>2</sub> was determined by a VG SIRA II mass spectrometer at the Scottish Universities Reactor Centre (SURRC) with isotopic composition reported as conventional  $\delta$  values relative to CDT. The precision was better than  $\pm 0.2\%$ .

## APPENDIX 8.

## LIST OF SPECIMENS

## A) DRILL CORE SPECIMENS - Buru carbonatite centre.

Drill Hole BRL-1.

<b>Sample No.</b>	<b>Depth (m)</b>	<b>Rock type</b>
BR-1	5	Laterite
BR-201	11	Laterite
BR-203	16	Laterite
BR-206	23	Laterite
BR-3	31	Laterite
BR-4	58	Laterite
BR-5	65	Laterite
BR-6	66	Calcite carbonatite
BR-7	71	Calcite carbonatite
BR-8	75	Calcite carbonatite
BR-9	79	Calcite carbonatite
BR-10	85	Calcite carbonatite
BR-11	92	Calcite carbonatite
BR-12	101	Calcite carbonatite
BR-13	108	Calcite carbonatite
BR-14	114	Calcite carbonatite
BR-15	116	Calcite carbonatite
BR-16	130	Calcite carbonatite
BR-17	138	Calcite carbonatite
BR-187	142	Calcite carbonatite
BR-19	144	Calcite carbonatite
BR-27	197	Calcite carbonatite
BR-28	200	Calcite carbonatite
BR-162	82	Siderite carbonatite
BR-158	89	Siderite carbonatite
BR-175	92	Siderite carbonatite
BR-177	98	Siderite carbonatite
BR-14b	114	Siderite carbonatite
BR-183	118	Siderite carbonatite
BR-186	142	Siderite carbonatite
BR-192	172	Siderite carbonatite
BR-194	187	Siderite carbonatite
BR-22	170	Ijolite

## Appendix 8 contd.

## Drill Hole BRL-2.

<b>Sample No.</b>	<b>Depth (m)</b>	<b>Rock type</b>
BR-210	11	Laterite
BR-212	23	Laterite
BR-214	37	Laterite
BR-217	51	Laterite
BR-218	71	Calcite carbonatite
BR-219	74	Calcite carbonatite
BR-222	82	Calcite carbonatite
BR-223	86	Calcite carbonatite
BR-224	89	Calcite carbonatite
BR-221	77	Ijolite

## Drill Hole BRL-3.

BR-46	6	Calcite carbonatite
BR-118	8	Calcite carbonatite
BR-126	10	Calcite carbonatite
BR-49	14	Calcite carbonatite
BR-50	15	Calcite carbonatite
BR-131	23	Calcite carbonatite
BR-133	25	Calcite carbonatite
BR-53	26	Calcite carbonatite
BR-54	30	Calcite carbonatite
BR-56	41	Calcite carbonatite
BR-143	46	calcite carbonatite
BR-147	57	Calcite carbonatite
BR-149	60	Calcite carbonatite
BR-151	61	Calcite carbonatite
BR-58	63	Calcite carbonatite
BR-59	78	Calcite carbonatite
BR-144	54	Siderite carbonatite
BR-146	57	Siderite carbonatite
BR-148	60	Siderite carbonatite
BR-150	61	Siderite carbonatite
BR-152	68	Siderite carbonatite
BR-59b	78	Siderite carbonatite

## Drill Hole BR-4

BR-235	41	Calcite carbonatite
BR-236	44	Calcite carbonatite
BR-237	46	Calcite carbonatite

## Appendix 8 contd.

<b>Drill Hole BR-9</b>		
<b>Sample No.</b>	<b>Depth (m)</b>	<b>Rock type</b>
BR-245	29	Calcite carbonatite
BR-247a	47	calcite carbonatite
BR-247b	47	Siderite carbonatite
<b>Drill Hole BR-10</b>		
BR-262	26	Calcite carbonatite
<b>Drill Hole BR-16</b>		
BR-29	13	Basement gneiss
BR-31	18	Basement gneiss
BR-32	20	Basement gneiss
BR-33	38	Basement gneiss
BR-34	41	Basement gneiss
<b>Drill Hole BR-17</b>		
BR-101	4	Basement gneiss
BR-102	12	Basement gneiss
BR-106	25	Basement gneiss
BR-107	41	Limonitic vein
<b>Drill Hole BR-20</b>		
BR-108	5	Basement gneiss
BR-109	13	Basement gneiss
BR-110	26	Basement gneiss
BR-111	37	Basement gneiss
<b>Drill Hole BR-23</b>		
BR-113	5	Basement gneiss
BR-114	11	Basement gneiss
BR-115	15	Basement gneiss
BR-116	28	Basement gneiss
BR-117	34	Basement gneiss

**B) DRILL HOLE SPECIMENS - Kuge carbonatite centre**

<b>Drill Hole KG-2</b>		
KG-64	5	Ferrocronatite
KG-66	15	Ferrocronatite
KG-69	22	Ferrocronatite
KG-72	36	Ferrocronatite
KG-76	44	Ferrocronatite

## Appendix 8 contd.

Drill Hole KG-3		
Sample No	Depth (m)	Rock type
KG-94	14	Ferrocarbonatite
KG-99	35	Ferrocarbonatite

Drill Hole KG-5		
KG-249	4	Ferrocarbonatite
KG-252	35	Ferrocarbonatite

Drill Hole KG-6		
KG-253	5	Ferrocarbonatite
KG-254	8	Ferrocarbonatite
KG-255	10	Ferrocarbonatite
KG-256	12	Ferrocarbonatite

## C) SURFACE SAMPLES - Kuge carbonatite centre

KG-119	-	Calcite carbonatite
KG-120	-	Calcite carbonatite
KG-122	-	Calcite carbonatite
KG-122	-	Calcite carbonatite
KG-124	-	Calcite carbonatite
KG-275	-	Calcite carbonatite
KG-125	-	Nyanzian metabasalt
KG-126	-	Nyanzian metabasalt
KG-127	-	Nyanzian metabasalt
KG-269	-	Calcrete
KG-279	-	Phonolite
KG-280	-	Phonolite
KG-281	-	Nephelinite
KG-282	-	Nephelinite

## D) SURFACE SAMPLES - North Ruri carbonatite centre

NR-271	-	Calcite carbonatite
NR-278	-	Calcite carbonatite